CROSSLINKED AND THERMALLY TREATED ULTRA-HIGH MOLECULAR WEIGHT POLYETHYLENE FOR joint replacements

STP 1445

EDITORS:
Steven M. Kurtz,
Ray A. Gsell, John Martell

ASTM
INTERNATIONAL
Standards Worldwide

STP 1445

Crosslinked and Thermally Treated Ultra-High Molecular Weight Polyethylene for Joint Replacements

Steven M. Kurtz, Ray A. Gsell, and John Martell, editors

ASTM Stock Number: STP1445

ASTM International
100 Barr Harbor Drive
PO Box C700
West Conshohocken, PA 19428-2959

Printed in the U.S.A.

Photocopy Rights

Peer Review Policy

Foreword

The Symposium on Crosslinked and Thermally Treated Ultra-High Molecular Weight Polyethylene (UHMWPE) for Joint Replacements was held in Miami Beach, Florida on 5–6 November, 2002. ASTM International Committee F04 on Medical and Surgical Materials and Devices served as the sponsor. Symposium co-chairmen and co-editors of this publication were Steven Kurtz, Exponent, Inc., Philadelphia, PA; Ray Gsell, Zimmer, Inc., Warsaw, IN; and John Martell, University of Chicago, Chicago, IL.

Contents

Quantifying Clinical Response

Christoph M. Sprecher,[1] *Erich Schneider,*[1] *and Markus A. Wimmer*[2]

Generalized Size and Shape Description of UHMWPE Wear Debris – A Comparison of Cross-Linked, Enhanced Fused, and Standard Polyethylene Particles

ABSTRACT: Released wear debris of implants causes local inflammation of the host tissue if it is in a phagocytosable size. The purpose of this study was to compare particle size, shape, and number of three different types of UHMWPE. After wear testing, particles were isolated from the serum and analyzed using SEM. The parameters 'equivalent circle diameter' (ECD) and 'equivalent shape ratio' (ESR) were determined. Most of the generated debris was sub-micron in size. Classifying the particles into size groups demonstrated a non-linear correlation between size and shape for all three types of polyethylene: small particles were more round, large particles were more elongated. Based on this relationship, the generated number of particles and their total surface area were estimated and compared with calculations based on size alone.

KEYWORDS: wear, particle characterization, polyethylene, hip prostheses

Nomenclature

l	theoretical particle length over all
l_o	length between the two half circles of the theoretical particle
r	theoretical particle radius
w	theoretical particle width
A	particle area
ECD	Equivalent Circle Diameter

[1] Student and Professor, respectively, AO-Research Institute, 1 Clavadelerstrasse, Davos, GR 7270, Switzerland.
[2] Assistant Professor, Department of Orthopedic Surgery, Rush Presbyterian St. Luke's Medical Center, 1653 West Congress Parkway, Chicago, IL 60612.

3

ESR	Equivalent Shape Ratio
N	particle number
N_{ECD}	calculated particle number based on the ECD
N_{ESR}	calculated particle number based on the ESR
P	particle perimeter
S_{ECD}	calculated particle surface based on the ECD
S_{ESR}	calculated particle surface based on the ESR
S_{ECD-T}	total surface of all particles based on the ECD
S_{ESR-T}	total surface of all particles based on the ESR
V_{ECD}	calculated particle volume based on the ECD
V_{ESR}	calculated particle volume based on the ESR
W_V	wear volume

Introduction

Conventional, ultra-high molecular weight polyethylene (UHMWPE), generally used as a biomedical implant articulation material during the last few decades, produces large quantities (on the scale of several thousand million per year) of submicrometer sized particles during wear [1]. These particles, which are released into the surrounding tissue, are phagocytosed by macrophages, a cell line responsible for host defense. During this process, the foreign material is engulfed by the cell and a series of intra- and inter-cellular signals are generated that produce inflammatory substances (proteins known as cytokines) mediating the clearance of the foreign body. However, in contrast to microorganisms (e.g. bacteria and viruses) debris generated from orthopaedic implant devices is generally not biodegradable. Thus, in response to wear debris, the inflammatory cascade is in a perpetual state of activation, leading to localized chronic inflammation and bone loss, known as osteolysis [2]. It has been demonstrated that particles small enough to undergo phagocytosis (less than 8 – 10 micrometers) are the most bioreactive in cell culture and are the most numerous in tissues adjacent to the implants [3]. Further, it has been shown that the cellular response to particulate debris is a function of the size, composition and dose of the particles [4,5]. In particular, 'surface area' of the wear debris has been suggested to be a determining factor in the onset of osteolysis [3].

In an effort to extend the longevity of contemporary joint replacements, highly crosslinked and thermally treated UHMWPE materials have been developed. Although the wear volume of these implant materials has been greatly reduced [6,7], wear debris is still generated. The morphological characteristics of the particulates differ from those of conventional polyethylene [8-11]. Besides radiation crosslinking, several other factors influence particle size and morphology, including type of nascent powder and processing route [12], contact stress [13,14], and the characteristic kinematics of the joint [15-17]. The necessity of suitably descriptive tools for particle characterization has been reflected by the activity of several normative bodies providing standards for this task [e.g., ASTM: Standard Practice for Characterization of Particles (F 1877-98)]. Based on these sugges-

tions and initiating scientific papers [e.g., 1], polyethylene wear particles are typically grouped into 'granules', 'fibrils' and 'shreds' based on their appearance, and are then analyzed by size. Studying the above-cited literature [8-17], it appeared that size and shape are not independent descriptors but, in fact, might be related in the case of polyethylene. Therefore the aim of this study was to investigate the size/shape relationship of all particles without previous grouping. Based on the results a new particle volume model is presented to better approximate the generated particle amount and surface area from differently processed UHMWPE materials.

Theoretical Considerations
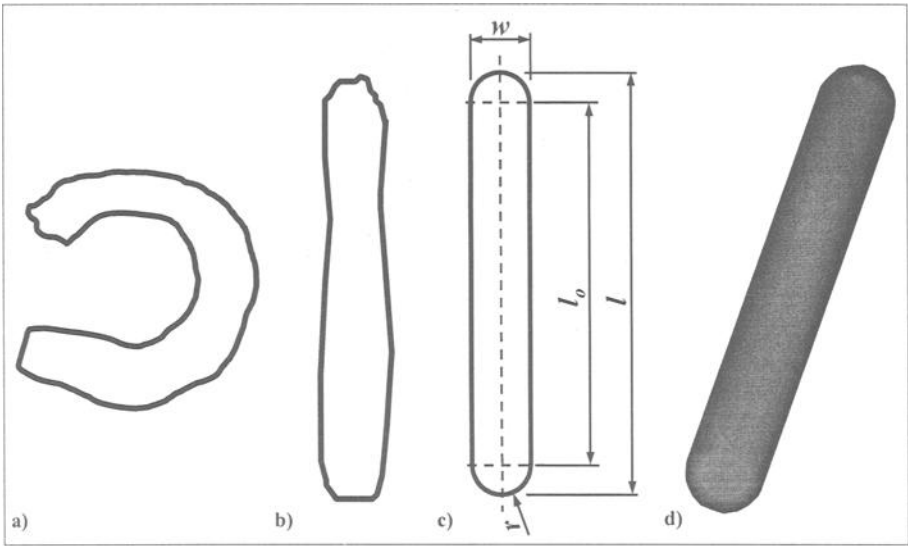
Figure 1 – *Particle in its prepared shape (a), in its "stretched" shape (b), in its 2D-model shape (c), and as a volumetric body (d)*

Material properties and tribological conditions are primarily responsible for the characteristics of the generated particles. In addition, the preparation technique may be influential. For example, fibrils of polyethylene may be preserved elongated or twisted (compare with Figure 2), which can persuade certain shape factors (e.g. feret ratio). Therefore, a shape factor independent of the twisting phenomenon shall be introduced. From the two-dimensional projection of the particle (Figure 1), area (A) and perimeter (P) are useful measures in this context and are used to build-up a 'model particle' having an overall width (w) and length (l). The two-dimensional projection of the model particle is approximated with two half-circles at its ends, such that

$$w = 2\,r \tag{1}$$

which are connected by a rectangle of the length l_0. Hence, perimeter and area are

$$P = 2\,l_o + w\,\pi \qquad (2)$$

$$A = l_o\,w + w^2\,\pi\,/\,4 \qquad (3)$$

Assuming $l \geq w$ (and $w > 0$), w and l are

$$w = P\,/\,\pi - (\,(P/\pi)^{\frac{1}{2}} - (4\,A\,/\,\pi)\,)^{\frac{1}{2}} \qquad (4)$$

$$l = (P - w\,\pi)\,/\,2 + w \qquad (5)$$

Finally, the *"Equivalent Shape Ratio (ESR)"* is defined by

$$ESR = w\,/\,l \qquad (6)$$

Similarly to other shape factors, the ESR ranges from 0 (needle shape) to 1 (perfectly round). The three-dimensional model of the particle, which is based on the assumption that its height equals its width, is shown in Figure 1d. It has a 'cigar-like' shape with half-spherical caps connected by a cylinder with the diameter w. Its volume and surface are

$$V_{ESR} = w^2\,\pi\,/\,4\,(l - w) + w^3\,\pi\,/\,6 \qquad (7)$$

$$S_{ESR} = w\,\pi\,l_o + w^2\,\pi \qquad (8)$$

The *'Equivalent Circle Diameter" (ECD)*, a measure of particle size, is defined according to ASTM F1877-98

$$ECD = (4\,A\,/\,\pi)^{\frac{1}{2}} \qquad (9)$$

Scott et al. [18] developed a particle volume model based on ECD, which will be used for comparison. In his model, particle volume and surface are defined by

$$V_{ECD} = ECD^3\,\pi\,/\,6 \qquad (10)$$

$$S_{ECD} = ECD^2\,\pi \qquad (11)$$

If the wear volume W_V is known, the total number of particles can be calculated according to

$$N_{ESR} = W_V\,/\,V_{ESR} \qquad (12)$$

$$N_{ECD} = W_V\,/\,V_{ECD} \qquad (13)$$

with V_{ESR} and V_{ECD} as the mean particle volume determined by the ESR and ECD-approach, respectively. Once the particle number is known, the free surface of all parti-

cles can be determined

$$S_{ESR-T} = S_{ESR} \; N_{ESR} \qquad (15)$$

$$S_{ECD-T} = S_{ECD} \; N_{ECD} \qquad (16)$$

where again the subscripts ESR and ECD refer to the approach taken.

Materials and Methods

Three different types of polyethylene were used: (1) Ref-PE: ram extruded GUR 4150 UHMWPE (so-called 'HSS reference polyethylene'), (2) Cross-PE: electron beam irradiated, melt annealed, highly crosslinked UHMWPE (commercially available under the trademark DURASUL®[3],), and (3) Hex-PE: via the meta-stable hexagonal phase processed UHMWPE. According to Rastogi et al. [20], the latter produces a completely fused polyethylene without grain boundaries. From each material, 12 pins were manufactured. The pins were cylindrical in shape (diameter 12 mm, height 7 mm) with a concave, cuplike bearing surface. The latter exhibited a radial clearance of 0.1 mm when paired with cobalt-chromium balls of 28 mm in diameter.

Wear debris was generated on a six-station Pin-on-Ball testing machine, which mimics the specific hip joint contact kinematics [21]. The interface is comprised of a pair of pins that are pressed orthogonally onto a ball. The two-dimensional interface motion is generated by axial oscillation of the pins and ball. By adjusting a 90°-phase shift between both amplitudes (30° each), elliptical displacement trajectories are generated. A constant compressive load of 1000N (nominal contact pressure 8.8 MPa) was applied, which is about the wear equivalent of a physiological gait profile with approximately 2kN peak magnitude [22]. The wear tests were carried out in diluted (33%) bovine serum at 1.8 Hz bi-axial oscillations for 5 million cycles. The generated wear particles were separated from the serum according to a method published by Scott et al. [19]. Briefly, 10 mL of the lubricant containing wear debris were mixed with 40 mL of 37% HCl and stirred at 350 rpm at 50°C for one hour. Using a pipette, 1 mL of the solution was drawn and added to 100 mL of methanol. This solution was then filtered through a polycarbonate filter with 0.1 μm pore size (Millipore, Bedford, MA) using a water jet pump to generate the necessary vacuum.

For size and shape analysis, the filters (coated with 10 nanometers Gold/Palladium (Au/Pd 80/20%)) were examined using a low-voltage scanning electron microscope (SEM, Hitachi FESEM S-4100, Kyoto, Japan). Images up to 5000X were taken in the secondary electron mode at 3-5 kV acceleration voltages. The area and perimeter of approximately 500 particles from each polyethylene were measured using PC-Image (Version 2.2.03, Foster Findlay Associates Ltd, Newcastle upon Tyne, United Kingdom). Particles were classified according to their size, i.e. equivalent circle diameter (ECD). For example, the class '0.15 μm' contains particles with 0.10 μm ≤ ECD < 0.15 μm.

---

[3] Centerpulse Orthopedics Ltd., Winterthur, Switzerland

In order to correlate ECD and ESR of the three different types of polyethylene, non-linear regression analyses, ANOVA and Tukey's post hoc tests were performed (SPSS Version 10, SPSS Inc., Chicago IL, USA). After finding the logarithms, all data were normally distributed. The level of significance was set to $p = 0.05$. Based on previously published volumetric wear rates [21], the particle amounts and total free surface areas were calculated. As outlined in the previous section, two models based on either ESR or ECD were employed. All data are plotted normalized to Ref-PE.

Results

The SEM images of Ref- and Hex-PE showed particles in a variety of sizes and shapes (Figures 2 R and H). Larger particles appeared elongated and often twisted, while small particles were typically round. The wear debris of Cross-PE looked different. It did not exhibit fibrillar particles but mostly particles small in size and spherical to ovoid in shape (Figure 2 C). The vast majority of all analyzed particles were smaller than 1 μm (Ref-PE 96.4 %, Hex-PE 93.8 %, Cross-PE 99.4 %), and the average particle size (based on ECD) was 0.39, 0.41, and 0.19 μm for Ref-, Hex- and Cross-PE, respectively (Table 1). Cross-PE had the least variation in particle size, followed by similar values for Ref- and Hex-PE (Table 1). A size histogram of all three types of polyethylene is shown in Figure 3.
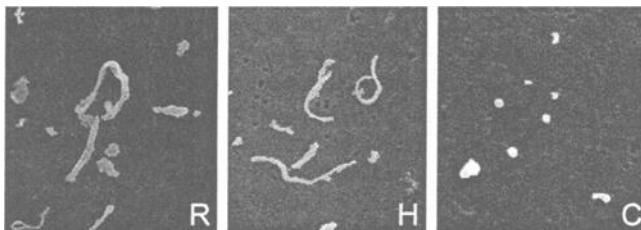
Figure 2 – *Polyethylene particles on a polycarbonate filter with 0.1 μm pore size: Ref-PE (left), Hex-PE (middle), Cross-PE (right)*

With ESR equal to 0.38 and 0.32, Ref- and Hex-PE displayed similar mean shape values, while the ESR of Cross-PE was two times higher (0.69, Table 1). All three materials correlated regarding size and shape (Figure 4). An exponential equation approximated the relationship best

$$ESR = 0.105477 \cdot ECD^{-1.014511}; \ R^2 = 0.565, \ p < 0.001 \tag{17}$$

This correlation indicates that particles are becoming more elongated with increasing size, independent of material type. At least four homogenous subgroups (classified according to increasing particle size; each group containing an equal amount of particles)

were found which differed significantly from each other regarding the mean ESR. This is illustrated in Figure 5 for Ref-PE.

Table 1 – *Numerical results of the particle characterization (ECD < 1μm)*

	Ref-PE	Hex-PE	Cross-PE
ECD ± SD [μm] (Range)	0.39 ± 0.19 (0.09 – 1.00)	0.41 ± 0.20 (0.06 – 0.98)	0.21 ± 0.10 (0.06 – 0.80)
ESR ± SD [-] (Range)	0.38 ± 0.23 (0.04 – 1.00)	0.32 ± 0.22 (0.05 – 1.00)	0.69 ± 0.27 (0.11 – 1.00)
V_{ESR} ± SD [μm³] (Range)	0.0193 ± 0.0198 (0.0003 – 0.1170)	0.0182 ± 0.0181 (0.0011 – 0.1146)	0.0043 ± 0.0048 (0.0001 – 0.0337)
V_{ECD} ± SD [μm³] (Range)	0.0384 ± 0.0448 (0.0004 – 0.2118)	0.0393 ± 0.0428 (0.0019 – 0.1776)	0.0058 ± 0.0070 (0.0001 – 0.0413)
S_{ESR} ± SD [μm²] (Range)	0.40 ± 0.31 (0.02 – 1.41)	0.41 ± 0.30 (0.06 – 1.30)	0.12 ± 0.09 (0.01 – 0.52)
S_{ECD} ± SD [μm²] (Range)	0.48 ± 0.38 (0.03 – 1.72)	0.50 ± 0.37 (0.07 – 1.53)	0.14 ± 0.11 (0.01 – 0.58)
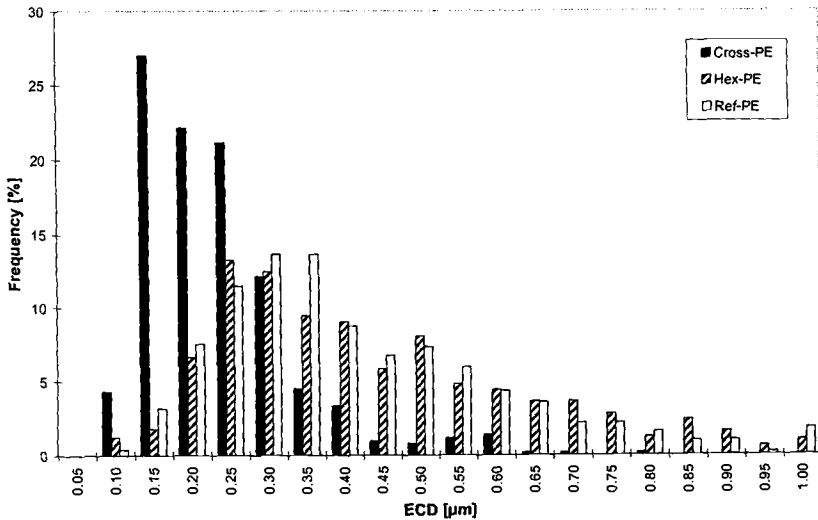
Figure 3 – *Histogram of the ECD from all three polyethylenes*
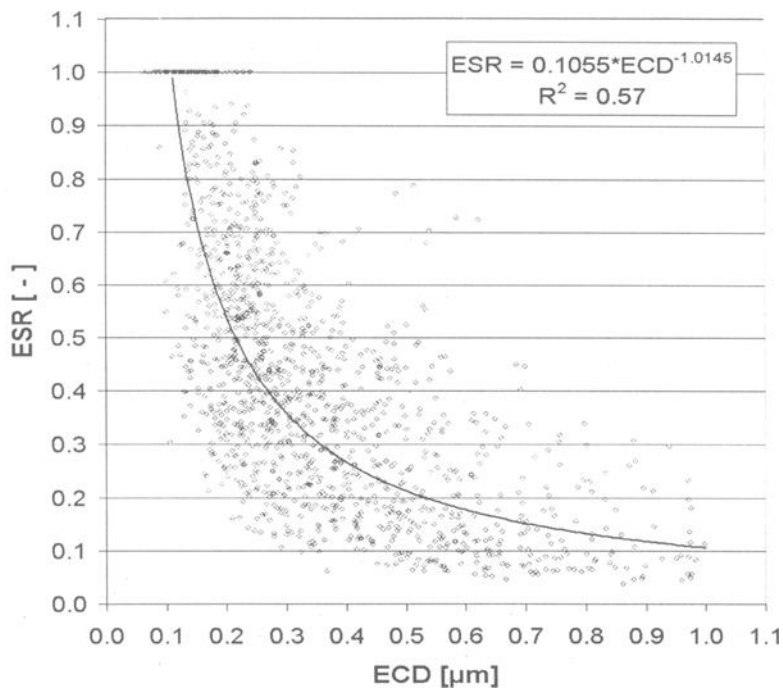
Figure 4 – *Scatter plots from the ECD versus ESR of all polyethylene's particles*
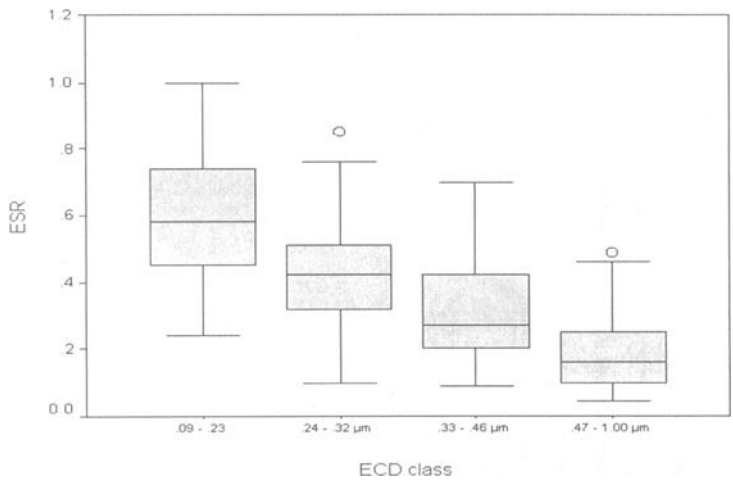
Figure 5 – *Homogenous subgroups of Ref-PE containing 121 particles each*

Although in previously published data [23], Cross-PE demonstrated the least amount of volumetric wear (approx. one-third of Ref-PE), in this study, it produced more particles than Ref-PE. Depending on the model used, the calculated values varied between 1.6 (ESR-model) and 2.3 (ECD-model) times more volumetric wear. Also, the particle number of Hex-PE was slightly higher for both models. These data are summarized in Table 2. Interestingly, despite the higher particle count, the total free surface of Cross-PE is only one-half that of Ref-PE (Table 2). This effect can be attributed to the more round and, hence, "surface-optimized" wear debris of Cross-PE.

Table 2 – *Particle amount and total surface area calculated from published vol. wear*

		Ratios		
		Ref-PE	Hex-PE	Cross-PE
Wear Volume [23]		1.00	1.07	0.35
Particle Number	N_{ESR}	1.00	1.13	1.59
	N_{ECD}	1.00	1.05	2.31
Particle Surface	S_{ESR-T}	1.00	1.15	0.49
	S_{ECD-T}	1.00	1.08	0.66

Discussion

The calculation of the 'Equivalent Shape Ratio' (ESR) is based on area and perimeter of the 2D-projection of the particle. Both area and perimeter are typical measures for image analysis software packages. The advantage is grounded in the availability size *and* shape information, since each particle is identified by its width and "stretched" length. That way, the ESR is a practical as well as easily understandable shape descriptor as shown in Table 3. Twisting and folding of particles, which might be introduced by the applied preparation technique, is no longer a matter of concern. Therefore, ESR might have its advantage over other shape factors commonly used for particle characterization, as, for example, the 'feret ratio' (definitions see ASTM F 1877-98). As shown in Table 3, the 'feret ratio' has its problems with folded and twisted polyethylene debris. Once width and "stretched" length of the particle have been determined, the ESR method allows a more precise description of particle volume and surface compared to the ECD method.

As has been shown in the results the latter methodology can easily overestimate the relative number of generated particles.

Table 3 – *Different form factors (ESR, Feret Ratio), volume (V_{ECD}, V_{ESR}) and free surface models (S_{ECD}, S_{ESR}) are calculated on a selection of commensurate particles from 'granules' till 'fibrils'*

Particle	1	2	3	4	5	6
ECD	------------------------------ 0.52 ------------------------------					
Area	0.22	0.22	0.22	0.22	0.22	0.22
Perimeter	1.67	2.32	3.16	3.44	4.39	3.92
Feret Ratio	0.92	0.63	0.36	0.92	0.54	0.12
ESR	*0.75*	*0.21*	*0.10*	*0.08*	*0.05*	*0.05*
V_{ECD}	------------------------------ 0.076 ------------------------------					
V_{ESR}	*0.048*	*0.016*	*0.013*	*0.012*	*0.012*	*0.012*
S_{ECD}	------------------------------ 0.86 ------------------------------					
S_{ESR}	*0.808*	*0.711*	*0.693*	*0.691*	*0.686*	*0.688*

The most exciting finding of this study, however, was the revelation of a non-linear size-shape relationship of UHMWPE wear debris. Statistically, smaller particles are rounder and larger particles are more elongated. While this finding is in agreement with common observation [1, 8-9], to the authors' knowledge it has never been mathematically formulated. It is further interesting to note that a general correlation of size and shape could be plotted for *all* three types of polyethylene. At first, this seemed astonishing since the processing histories of all three UHMWPE materials were very different. Hex-PE for example has not only a completely new processing route but its nascent powder displays a unique morphology[4] [20]. It is therefore suggested that size and shape of UHMWPE wear debris are primarily a result of the acting wear mechanism(s) and the material's microstructure at the bearing surface. The mechanical properties of the bulk material may indirectly influence the wear outcome.

---

[4] the powder has been manufactured by DSM, Eindhoven, The Netherlands

Care must be taken when extrapolating the ratio of particle amount to a clinical setting. The calculation of particles has been based on the wear rates of polyethylene pins rather than clinically utilized polyethylene cups. In the latter, the ball and socket joint, the rigid ball will penetrate into the polyethylene cup and increase the contact area between the two contacting bodies. This will result in a higher wear rate of polyethylene [24]. Since crosslinked polyethylene is penetrated less than conventional poly, the expected wear volume ratio should be smaller than the one presented herein.

Conclusion

There is a non-linear relationship between the size and the shape of polyethylene wear debris. Smaller particles tend to be spherical, while larger particles have an elongated appearance as suggested by the newly introduced shape factor 'equivalent shape ratio' (ESR). This relationship holds for different types of polyethylene, even though the generated sizes of particles may differ. Since width and length of the particles are determined when calculating ESR, a precise description of particle amount and total surface area of the wear debris may be extracted. This approach seems to be advantageous when working with UHMWPE particles.

Acknowledgments

References

[1]   McKellop, H. A., Campbell, P., Park, S.-H., Schmalzried, T. P., Grigoris P., Amstutz, H. C. and Sarmiento, A., "The Origin of Submicron Polyethylene Wear Debris in Total Hip Arthroplasty", *Clinical Orthopaedics and Related Research*, Vol. 311, 1995, pp. 3-20.

[2]   Glant, T.T., Jacobs, J.J., Molnar, G., Shanbhag, A.S., Valyon, M., and Galante, J.O., "Bone Resorption Activity of Particulate stimulated Macrophages," *Journal of Bone and Mineral Research,* Vol 8, 1993, pp. 1071-1079.

[3]   Shanbhag, A. S., Jacobs, J. J., Black, J., Galante, J. O., and Glant, T. T., "Macrophage/particle interactions: effect of size, composition and surface area", *Journal of Biomedical Material Research,* Vol. 28, 1994, pp. 81-90.

[4]   Ingham, E., and Fisher, J., "Biological reactions to wear debris in total joint re-
        placement", *Proceedings of the Institution of Mechanical Engineers. Part H, Jour-
        nal of Engineering in Medicine*, Vol. 214, 2000, pp. 21-37.
[5]   Jacobs, J. J., Shanbhag, A. S., Glant, T. T., Black, J., and Galante, J. O., "Wear De-
        bris in Total Joint Replacements," *Journal of the American Academy of Orthopedic
        Surgery*, Vol. 2, 1994, pp. 212-220.
[6]   McKellop, H., Shen, F. W., Lu, B., Campbell, P., and Salovey, R., "Development
        of an extremely wear-resistant ultra high molecular weight polyethylene for total
        hip replacements," *Journal of Orthopedic Research*, Vol. 17(2), 1999, pp.157-167.
[7]   Muratoglu, O. K., Bragdon, C. R., O'Connor, D. O., Jasty, M., Harris, W. H., Gul,
        R., and McGarry, F., "Unified wear model for highly crosslinked ultra-high mo-
        lecular weight polyethylenes (UHMWPE)," *Biomaterials*, Vol. 20, 1999, pp.1463-
        1470.
[8]   Shanbhag, A. S., Vai, C. W., Qureshi, S. A., and Rubsh, H. E., "Characteristics of
        Cross-Linked UHMWPE Wear Debris" *Proceedings 47th ORS Annual Meeting*,
        2001, p. 2.
[9]   Scott, M., Widding, K., Ries, M., and Shanbhag, A., "Wear Particle Analyses of
        Conventional and Crosslinked UHMWPE Tested in an Anatomic Hip Simulator",
        Proceedings 47th ORS Annual Meeting, 2001, p. 1.
[10]   Sprecher, C., Owen, G. R., and Wimmer, M. A., "Comparison of crosslinked and
        conventional polyethylene wear particles: A scanning electron microscopy study",
        Proceedings European Society for Biomaterials Conference, 2001, p. 54.
[11]   Endo, M. M., Barbour, P. S., Barton, D. C., Fisher, J., Tipper, J. L., Ingham,E., and
        Stone, M. H., "Comparative wear and wear debris under three different counterface
        conditions of crosslinked and non-crosslinked ultra high molecular weight polyeth-
        ylene", *Bio-Medical Materials and Engineering*, Vol. 11, 2001, pp. 23-35.
[12]   Endo, M. M., Barbour, P. S., Barton, D. C., Wroblewski, B. M., Fisher, J., Tipper,
        J. L., Ingham, E., and Stone, M. H., "A comparison of the wear and debris genera-
        tion of GUR 1120 (compression moulded) and GUR 4150HP (ram extruded) ultra
        high molecular weight polyethylene", *Bio-Medical Materials and Engineering*,
        Vol. 9, 1999, pp.113-124.
[13]   Landry, M. E., Blanchard, C., Mabrey, J. D., and Agrawal, C. M., "Wear Condi-
        tions Affecting Particle Size and Morphology", *Proceedings 43rd ORS Annual
        Meeting*, 1997, p. 69.
[14]   Landry, M. E., Mabrey, J. D., Blanchard, C., and Agrawal, C. M., "Effect of Wear
        Testing Parameters on UHMWPE Particle Morphology", *Proceedings 23rd Annual
        Meeting of the Society for Biomaterials*, 1997, p. 193.
[15]   Kobayashi, A., Freeman, M. A., Bonfield, W., Kadoya, Y., Yamac, T., Al Saffar,
        N., Scott, G., and Revell, P.A., "Number of polyethylene particles and osteolysis in
        total joint replacements. A quantitative study using a tissue-digestion method," *The
        Journal of Bone and Joint Surgery (British Vol.)*, Vol. 79, 1997, pp. 844-848.
[16]   Howling, G. I., Barnett, P. I., Tipper, J. L., Stone, M. H., Fisher, J., and Ingham, E.,
        "Quantitative characterization of polyethylene debris isolated from periprosthetic
        tissue in early failure knee implants and early and late failure Charnley hip im-
        plants", *Journal of Biomedical Materials Research*, Vol. 58, 2001, pp. 415-420.

[17] Schmalzried, T. P., Campbell, P., Schmitt, A. K., and Brown, I. C., Amstutz, H. C., "Shapes and dimensional characteristics of polyethylene wear particles generated in vivo by total knee replacements compared to total hip replacements", *Journal of Biomedical Materials Research*, Vol. 38, 1997, pp. 203-210.

[18] Scott, M., Wedding, K., Ries, M. and Shanbhag, A " Wear Particle Analysis of Conventional and Crosslinked UHMWPE Tested in an Anatomic Hip Simulator", Proceedings 47th Orthopaedic Research Society, 2001, p. 1.

[19] Scott, M., Forster, H., Vadodaria, K., Sauer, W., and Anthony, M., "Validation of an Alternative Method for Isolating UHMWPE Wear Debris from Joint Simulator Serum", Proceedings 6th World Biomaterials Congress, 2000, p. 177.

[20] Rastogi, S., Kurelec, L., and Lemstra, P. J., "Chain Mobility in Polymer Systems: On the Borderline between Solid and Melt. 2. Crystal Size Influence in Phase Transition and Sintering of Ultrahigh Molecular Weight Polyethylene via the Mobile Hexagonal Phase", *Macromolecules*, Vol. 31, 1998, pp. 5022-5031.

[21] Wimmer, M. A., Nassutt, R., Lampe, F., Schneider, E., and Morlock, M. M., "A new screening method designed for wear analysis of bearing surfaces used in total hip arthroplasty", *Alternative bearing surfaces in total joint replacement, ASTM STP 1346*, J.J. Jacobs and T. L. Craig, Eds., ASTM International, West Conshohocken, PA, 1998, pp. 30–43.

[22] Clarke, I. C., Johnson, S., Phipatanakul, W., and Good, V., Effects of hip-loading input on simulated wear of Al2O3-PTFE materials, *Wear*, Vol. 250, 2001, pp. 159-166.

[23] Wimmer, M. A., Kurelec, L., Sprecher, C., Engel, K., Hausam, V., and Rastogi, S., "Enhanced fusion of UHMWPE: A concept to improve wear resistance and mechanical properties of polyethylene?", Proceedings 28th Annual Meeting Society for Biomaterials, 2002, p. 536.

[24] Saikko, V., Ahlroos, T.," Wear simulation of UHMWPE for total hip replacement with a multidirectional motion pin-on-disk device: effects of counterface material, contact area, and lubricant", *Journal of Biomedical Materials Research*, Vol. 49, 2000, pp. 147-154.

Short-Term Retrievals

Claude B. Rieker,[1] *Reto Konrad,*[1] *Rolf Schön,*[1] *Werner Schneider,*[1] *and Niels A. Abt*[1]

Microscopy of Highly Cross-Linked UHMWPE Wear Surfaces

ABSTRACT: Highly cross-linked ultra high molecular weight polyethylenes (UHMWPEs) were developed to reduce UHMWPE wear in arthroplasty. These UHMWPEs have manifested a significant improvement in the in-vitro adhesive - abrasive wear resistance of total joint prostheses.

Examination of the first clinically retrieved liners revealed surface features not usually observed on previous retrievals. A flattening of the machining marks is evident, together with the presence of ripples with micro-fissures. To evaluate these features, examinations were performed on a cup-on-ball device, an AMTI hip simulator, and a Stanmore knee simulator, as well as on retrieved components with a maximum follow-up of 15 months. The surface features of the components were investigated with light microscopy, by scanning electron microscopy (SEM), and also by transmission electron microscopy (TEM).

Ripples with micro-fissures were observed on the loaded areas perpendicular to the principal directions of motion. The transverse examinations of all sections of these specimens, which were made with optical microscopy and by TEM, showed that the ripples with micro-fissures may be described as folds. With all the investigated samples, the depth of the micro-cracks at the tip of the folds extended to a maximum of 5 µm below the surface. The folds experienced with UHMWPE were already described in the late 1970s.

Due to the extreme wear resistance of highly cross-linked UHMWPEs, these folds accumulate on the surface of components manufactured in this new generation of UHMWPEs. In view of their depth stability with the number of cycles, we believe that these folds have no influence on the fatigue behavior of such components.

KEYWORDS: hip prosthesis, cross-linked UHMWPE, wear mechanisms, surface modifications

[1]Research Scientists, Centerpulse Orthopedics, PO Box 65, CH-8404 Winterthur, Switzerland.

Introduction

Total joint arthroplasty is one of the most successful surgical interventions, with more than 90% of "good" results with a follow-up of ten years [1]. The results after more than ten years degrade steadily, mainly as a result of the aseptic loosening induced by the particles disease, as described already by Willert in the 1970s [2].

Low wear solutions were developed to solve the problem of aseptic loosening. Ceramic-on-ceramic and metal-on-metal are two historic, low-wear solutions, with more than 30 years' clinical use in Europe. Following the pioneer work of Grobbelaar [3], Oonishi [4] and Wroblewski [5] with highly cross-linked UHMWPEs in the 1970s - 1980s, a second generation of highly cross-linked UHMWPEs was developed in the mid-1990s. These produced remarkable in-vitro results, with hardly or no measurable wear in hip simulator studies [6]. Following extensive in-vitro investigations, these highly cross-linked UHMWPEs were subsequently implanted in the late 1990s.

The examination of the clinically retrieved components manufactured in these highly cross-linked UHMWPEs revealed different surface features not usually observed on retrievals manufactured with moderately cross-linked UHMWPEs gamma sterilized under a protective atmosphere.

- A flattening of the machining marks is seen with the presence of ripples with micro-fissures [7]. A remelting technique, developed [8] to recover the flattening of the machining marks, showed that these components exhibited a minimum amount of in-vivo wear.
- A yellowing of these components is also apparent. This coloration is attributable to the diffusion of lipids into the UHMWPE [9].

The object of this study was to examine the ripples with micro-fissures observed on the surface of clinically retrieved components and to compare these features with those found on in-vitro tested components.

Experimental Methods

Materials

The raw material used in this study was GUR 1050 compression molded sheet of UHMWPE. The highly cross-linked UHMWPE was prepared by irradiation at 120°C using a 10-MeV electron-beam accelerator. The total irradiation level was 95 kGy. Following the irradiation, the samples were melt-annealed above 130°C for 5 hours to substantially reduce the concentration of the residual free radicals (DURASUL™ - Centerpulse Orthopedics Ltd.[2]).

---

[2]DURASUL™ is a trademark of Centerpulse Orthopedics Ltd., PO Box 65, CH-8404 Winterthur, Switzerland

Cup-on-Ball (up to 1 Million Cycles) with Reciprocating Motions

A cup-on-ball screening test [10] was performed with two DURASUL™ cups articulating on a CoCr alloy head with the following parameters (Table 1).

Table 1 – *Parameters of the cup-on-ball*

Parameters	
Static load	2 060 N
Motion of the head	Reciprocating motion - sinusoidal wave form - 90° - 1 Hz
Motion of the cup	No motion
Specimens	2
Temperature	37°C
Cycles	100,000 - 250,000 - 500,000 - 1,000,000

The wear tests were lubricated with a stabilized mixture of Ringer's solution having 33 % calf serum, and buffered to a pH of 7.2. The protein (20 g/l) content of this lubricant was almost the same as that of healthy human synovial fluid. The lubricant was filtered before testing with a 0.2 µm filter.

AMTI Hip Simulator

An AMTI hip simulator [11] was used with following parameters (Table 2).

Table 2 – *Parameters of the AMTI hip simulator*

Parameters	-
Dynamic load	3 250 N
Flexion - extension	23° - 23°
Abduction - adduction	8.5° - 8.5°
Internal rotation - external rotation	10° - 10°
Temperature	37°C
Specimens	6
Frequency	2 Hz
Cycles	27 million

DURASUL™ inserts with diameters of 22.2 mm and 28.0 mm were tested. All tests were conducted in a lubricant containing 100% bovine serum, which was stabilized by adding 0.2% sodium azide as an antibacterial agent and 20 mmol of ethylene-diamine-tetra-acetic acid (EDTA) to bind the calcium in the lubricant.

Stanmore Knee Simulator

A Stanmore load-controlled knee simulator KC [12] according to the ISO 14243-1 standard was used. The knee prostheses tested were of a highly congruent mobile bearing

design with a DURASUL™ insert. This test was conducted on four specimens up to 5 million cycles.

The wear tests were lubricated with the same lubricant as employed for the cup-on-ball test.

Retrievals (Acetabular Liners) with a Maximum Follow-Up of 15 Months

Five DURASUL™ retrieved cups (Alpha inserts - Centerpulse Orthopedics Ltd., PO Box 65, CH-8404 Winterthur, Switzerland) were collected for reasons not related with wear problems.

Table 3 provides an overview of these five retrievals.

Table 3 – *Reasons for the re-operation*

Reasons	Time in-vivo
Infection	5 months
Dislocation	7 months
Infection	7 months
Pain	14 months
Ossification	15 months

Surface Investigations with Scanning Electron Microscopy (SEM)

After a physical vapor deposition (PVD) gold sputtering having a thickness of 10 nm, all the samples were examined by SEM (JEOL JSM-840).

Transverse Investigations by Light Microscopy and Transmission Electron Microscopy (TEM)

The samples were embedded in an epoxy resin (Araldite D, Ciba Speciality Chemicals Inc., Switzerland) at room temperature. The surfaces were prepared close to the regions of interest with a diamond saw and the resulting blocks trimmed with a glass knife and then with a diamond knife at room temperature. The final surfaces, which intersected the regions of interest, were located at an angle of about 20° to the direction of motion, corresponding to the coarse surface markings on the samples, and perpendicular to the plane of the sample. The cut was made slightly oblique to the direction of motion in order to maximize the probability of sectioning surface ripples. After trimming, the surfaces were exposed to RuO_4 vapor for about an hour, and a further 1 μm was removed with a diamond knife. They were stained again in RuO_4 vapor for 12 hours and thin sections (100 to 200 nm) taken to a depth of about 2 μm with a diamond knife at room temperature for bright field observation with reflected light microscopy and TEM (Philips EM 430 ST).

Results

Cup-on-Ball Screening Test

Figure 1 shows the surface (SEM) on the loaded area (polar region) of one DURASUL™ specimen tested on the cup-on-ball screening test after 250,000 cycles. Ripples with micro-fissures were observed.
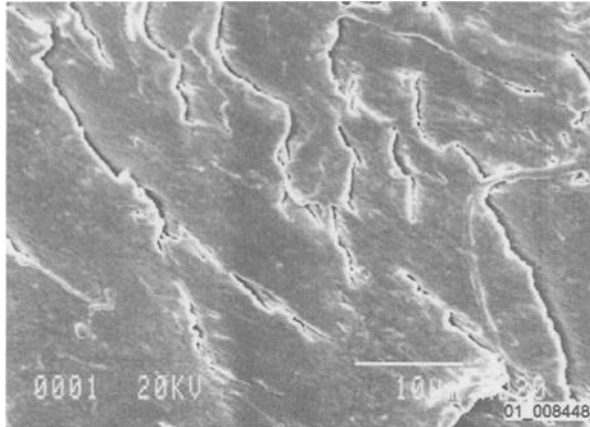
Figure 1 - *Surface on the loaded area of a DURASUL™ specimen with the cup-on-ball screening test - ¼ million - SEM*

These ripples are already visible after 100,000 cycles on all the tested components. The same ripples are also seen on all the components tested up to 1,000,000 cycles.

Figure 2 shows a transverse section of the surface depicted in Figure 1 and observed by means of reflected light microscopy. This figure shows quite clearly that the ripples with micro-fissures may be better described as folds.
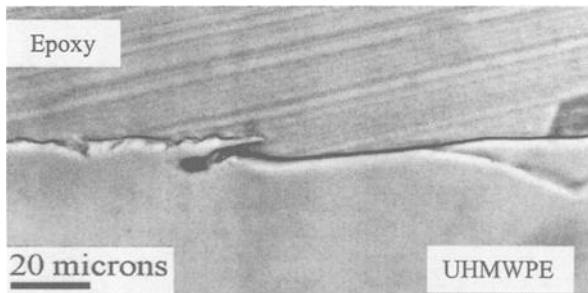
Figure 2 - *Transverse section on the loaded area of a DURASUL™ specimen tested with the cup-on-ball screening test - ¼ million cycles - Light microscopy*

AMTI Hip Simulator

Figures 3 and 4 show the surface (SEM) on the loaded area (polar region) of the DURASUL™ liners tested with the AMTI hip simulator (27 million cycles). Figure 3 shows the surface of a 22.2 mm liner, and Figure 4 that of a 28.0 mm liner.
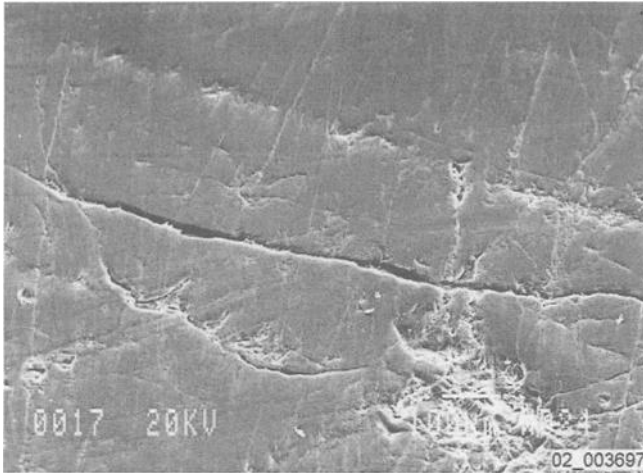
Figure 3 - *Surface on the loaded area of a DURASUL™ liner (22.2 mm) tested with the AMTI hip simulator - 27 million cycles - SEM*
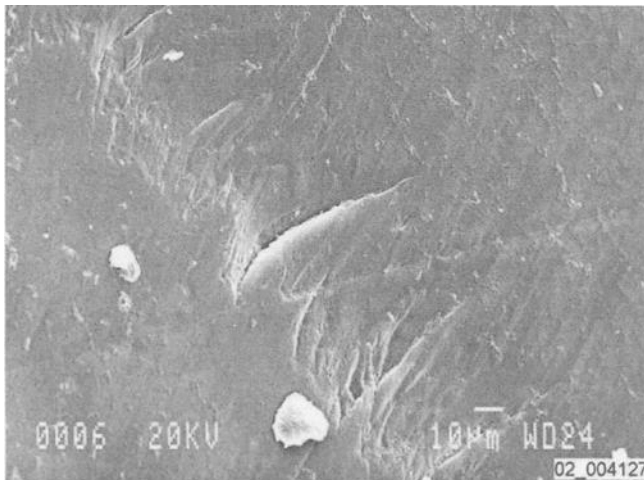
Figure 4 - *Surface on the loaded area of a DURASUL™ liner (28.0 mm) tested with the AMTI hip simulator - 27 million cycles - SEM*

Figure 5 shows a transverse section of the surface depicted in Figure 3 and observed by TEM. The depth of the micro-crack at the tip of the fold shown here is approximately 5 μm after 27 million cycles.
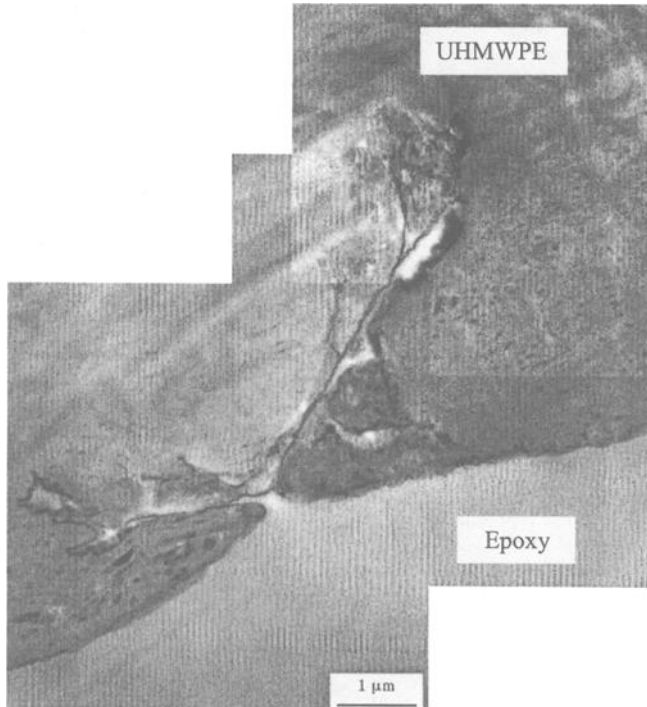
Figure 5 - *Transverse section on the loaded area of a DURASUL™ liner (22.2 mm) tested with the AMTI hip simulator - 27 million cycles - TEM*

Stanmore Knee Simulator

Figures 6 and 7 show the surface (SEM) on the loaded area of the liners tested with the Stanmore knee simulator (5 million cycles). Figure 6 depicts the proximal (femoral articulation) surface of the liner, and Figure 7 its distal (tibial articulation) surface.
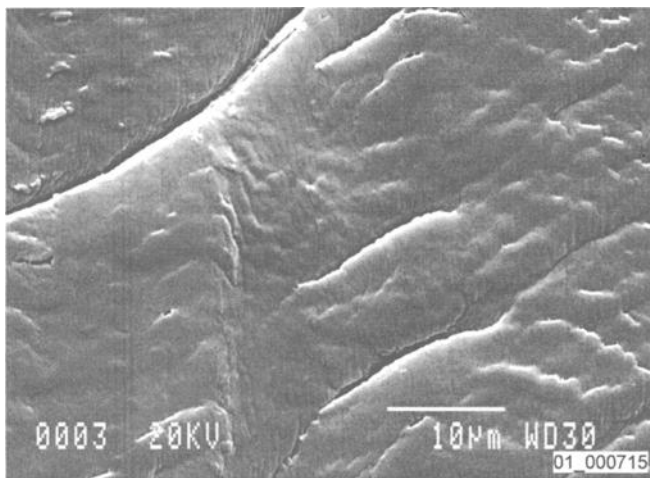
Figure 6 - *Surface on the loaded area of a DURASUL™ liner (proximal interface) tested with the Stanmore knee simulator - 5 million cycles - SEM*
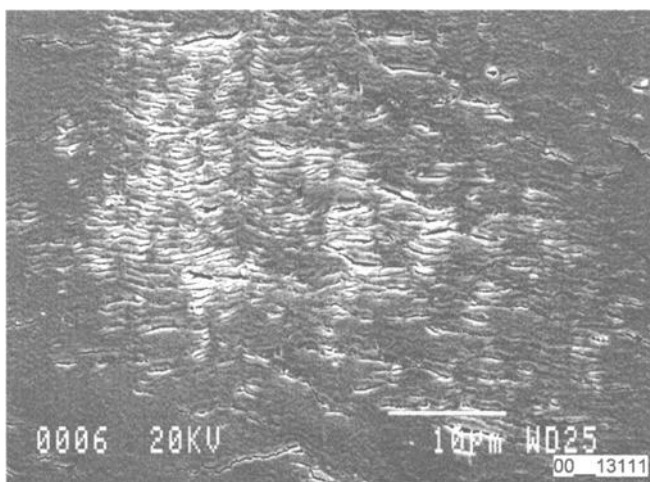
Figure 7 - *Surface on the loaded area of a DURASUL™ liner (distal interface) tested with the Stanmore knee simulator - 5 million cycles - SEM*

Figure 8 shows a TEM transverse section of the distal surface depicted in Figure 7. The depth of the micro-crack at the tip of the fold shown here is approximately 1 μm after 5 million cycles.
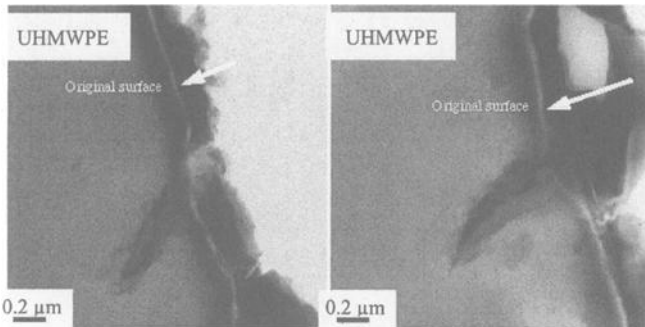
Figure 8 - *Transverse section on the loaded area of the liner (distal interface) tested with the Stanmore knee simulator - 5 million cycles - TEM*

Retrievals (Acetabular Liners) with a Maximum Follow-Up of 15 Months

Figure 9 shows the surface (SEM) on the loaded area of a retrieved DURASUL™ insert with a follow-up of 15 months.
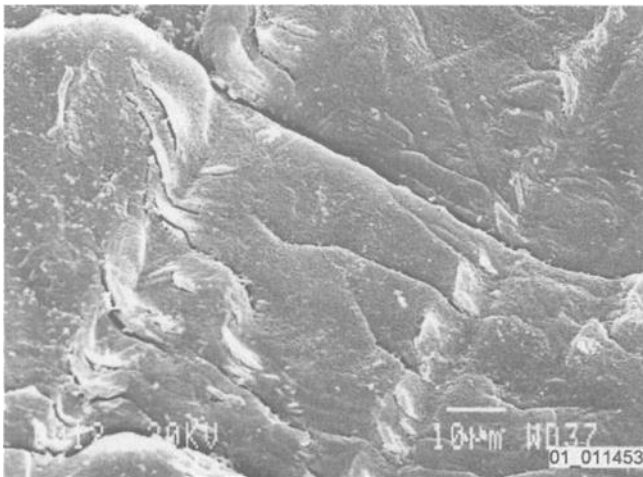
Figure 9 - *Surface on the loaded area of a retrieved DURASUL™ liner - 15 months - SEM*

Figure 10 shows a transverse section of the distal surface depicted in Figure 9 and observed by TEM. The depth of the micro-crack at the tip of the fold shown here is approximately 2 µm after 15 months in-vivo.
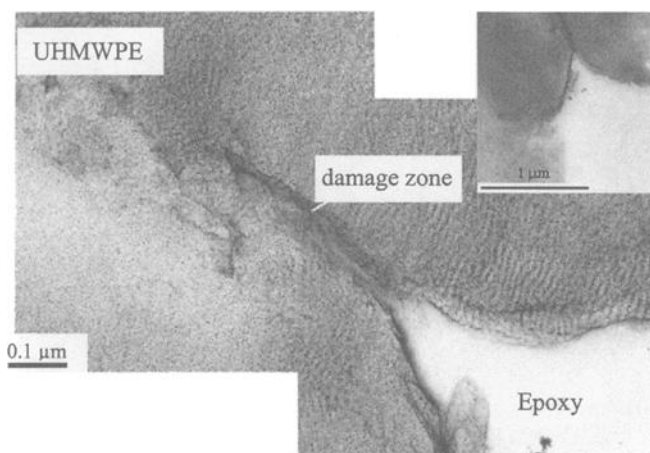
Figure 10 - *Transverse sections on the loaded area of a retrieved DURASUL™ liner - 15 months - TEM*

The ripples with micro-fissures are located on the loaded zone and mainly perpendicular to the main directions of motion. The transverse examinations of all sections of these DURASUL™ specimens by means of optical microscopy and TEM confirmed that these ripples with micro-fissures may be described as folds with micro-cracks at their tip. The TEM examinations of all the investigated samples tested up to 27 million cycles demonstrate that the maximum observed depth of these micro-cracks is 5 μm.

Discussion

The microscopy in-vitro investigations of these folds with micro-cracks and the observations made on retrieved components show that the maximum depth of these micro-cracks is less than 5 μm. The depth of all the micro-cracks investigated in this study is not influenced by the number of loading cycles. Furthermore, the depth of these micro-cracks is not influenced by the type of solicitation (cup-on-ball, AMTI hip simulator, Stanmore knee simulator, and retrieved cups).

The first folds were observed after only approximately 100,000 cycles with the cup-on-ball device. Folds were also observed after 27 million cycles with the AMTI hip simulator. Although the component tested on the AMTI hip simulator endured 270 - times as many cycles as its counterpart on the cup-on-ball device, both components exhibit similar folds on their surface.

Since the depth of all the observed micro-cracks is less than 5 μm and the fact that we were unable to detect any influence of the number of cycles (up to 27 million) on their depth, we describe these folds as stable systemic surface features. The stability of these micro-cracks with the number of cycles is an indication that the stress intensity factor K_1 endured by all the investigated probes (cup-on-ball, AMTI hip simulator, Stanmore knee

simulator, and retrieved cups) is below the fatigue threshold, where no detectable crack growth rate was observed. Such a stability of the micro-cracks suggests that there is no risk of crack propagation and fatigue failure in components manufactured in DURASUL™ for the investigated conditions.

This study also shows that the type of lubricant (100% bovine serum or 33% calf serum - 67% Ringer's solution or synovial fluid) has no influence on the morphology of these folds.

These folds with micro-cracks were experienced with moderately cross-linked UHMWPEs gamma sterilized under air and already described in the late seventies [13 and 14]. They were defined as a common feature, which is induced by the normal adhesive-abrasive wear behavior of the UHMWPE. Figure 11 presents Figure 10 of Rostoker's publication [13], which provides an idealized description of the fold formation. Figure 12 shows the ripples with micro-fissures observed on Charnley acetabular cups (Figure 11 of Dowling's publication [14]).

ELASTIC INDENT   COLD FLOW   FOLD THINNING   TORN DEBRIS
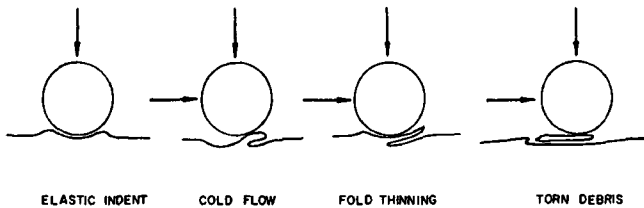
Figure 11 - *Idealized description of fold formation - Rostoker [13]*

5 μm
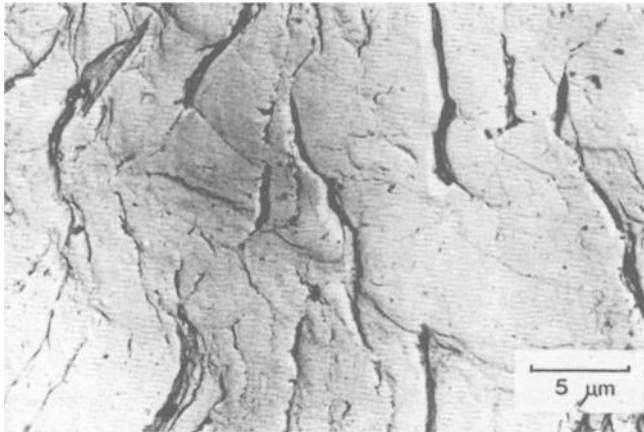
Figure 12 - *Ripples with micro-fissures on standard polyethylene - Dowling [14]*

With moderately cross-linked UHMWPEs gamma sterilized under air, these folds are likely to be worn rapidly away through the normal adhesive-abrasive wear mechanism. Since the usual range of the wear rate of this type of UHMWPE is typically 50 - 300 μm

per year [15], the common wear mechanisms will continuously erase these folds formed on the surface of components manufactured in this type of UHMWPE.

On the other hand, the extreme wear resistance of this type of highly cross-linked material (DURASUL™) will cause these folds to accumulate simply on the surface of components manufactured in this manner.

Conclusions

The folds with micro-cracks at their tip are a direct consequence of loading the DURASUL™ material under the test conditions described. Retrieved acetabular cup liners (implanted up to 15 months and manufactured from the same material) exhibit similar features. Since we did not find any micro-cracks larger than 5 μm, it is our belief that there is no risk of fatigue failure.

Acknowledgments

References

[1]   Herberts, P., Malchau, H., "Long-Term Registration has Improved the Quality of Hip Replacement: a Review of the Swedish THR Register Comparing 160,000 Cases," *Acta Orthop Scand*, Vol. 71, 2000, pp. 111 - 121.

[2]   Willert, H. G., "Reactions of the Articular Capsule to Wear Products of Artificial Joint Prostheses," *J Biomed Mater Res*, Vol. 11, 1977, pp. 157 - 164.

[3]   Grobbelaar C. J., du Plessis T. A., Marais F., "The Radiation Improvement of Polyethylene Prostheses," *J Bone Joint Surg Br*, Vol. 60-B, 1978, pp. 370 - 374.

[4]   Oonishi H., Takayama Y., Tsuji E. "Improvement of Polyethylene by Irradiation in Artificial Joints," *Radiat Phys Chem*, Vol. 39, 1992, pp. 495.

[5]   Wroblewski B. M., Siney P. D., Dowson D., Collins S. N., "Prospective Clinical and Joint Simulator Studies of a New Total Hip Arthroplasty using Alumina Ceramic Heads and Cross-Linked Polyethylene Cups," *J Bone Joint Surg Br*, Vol. 78-B, 1996, pp. 280 - 285.

[6]   Muratoglu O. K., Bragdon C. R., O'Connor D. O., Jasty M., Harris W. H., "A Novel Method of Cross-Linking Ultra-High-Molecular-Weight Polyethylene to

Improve Wear, Reduce Oxidation, and Retain Mechanical Properties," *J Arthroplasty*, Vol. 16, 2001, pp. 149 - 160.

[7]   Greenwald A. S., Bauer T. W., Ries M. D., "New Polys for Old: Contribution or Caveat?," *AAOS - Scientific Exhibit SE13*, Dallas, 2002.

[8]   Muratoglu O.K. et al., "Surface Analysis of Early Retrieved Acetabular Polyethylenes Liners: a Comparison of Standard and Highly Crosslinked Polyethylenes," *ORS - Poster 1029*, Dallas, 2002.

[9]   Costa L., Bracco P., del Prever E. B., Luda M. P., Trossarelli L., "Analysis of Products Diffused into UHMWPE Prosthetic Components in vivo," *Biomaterials*, Vol. 22, 2001, pp. 307 - 315.

[10]   Wimmer M. A. and al., "A New Screening Method Designed for Wear Analysis of Bearing Surfaces Used in Total Hip Arthroplasty," *Alternative Bearing Surfaces in Total Joint Replacement, ASTM, STP 1346*, J.J. Jacobs and T.L. Craig, Eds., American Society for Testing and Materials, 1998.

[11]   Bragdon C. R., O'Connor D. O., Lowenstein J. D., Jasty M., Syniuta W. D., "The Importance of Multidirectional Motion on the Wear of Polyethylene," *Proc Inst Mech Eng [H]*, Vol. 201, 1996, pp. 157 - 165.

[12]   DesJardins J. D., Walker P. S., Haider H., Perry J., "The Use of a Force-Controlled Dynamic Knee Simulator to Quantify the Mechanical Performance of Total Knee Replacement Designs during Functional Activity," *J Biomech*, Vol. 33, 2000, pp. 1231 - 1242.

[13]   Rostoker W., Chao E. Y. S., Galante J. O., "The Appearances of Wear on Polyethylene - a Comparison of in vivo and in vitro Wear Surfaces," J Biomed Mater Res, Vol. 12, 1978, pp. 317 - 335.

[14]   Dowling J. M., Atkinson J. R., Dowson D., Charnley J., "The Characteristics of Acetabular Cups Worn in the Human Body," *J Bone Joint Surg Br*, Vol. 60-B, 1978, pp. 375 - 382.

[15]   Semlitsch M., Willert H. G., "Clinical Wear Behaviour of Ultra-High Molecular Weight Polyethylene Cups Paired with Metal and Ceramic Ball Heads in Comparison to Metal-on-Metal Pairings of Hip Joint Replacements," *Proc Inst Mech Eng [H]*, Vol. 211, 1997, pp. 73 - 88.

John P. Collier,[1] *Michael B. Mayor,*[2] *Barbara H. Currier,*[1] *and Markus W. Wittmann*[1]

Retrieval Analysis of Cross-linked Acetabular Bearings

ABSTRACT: Polyethylene acetabular bearings which have been purposely cross-linked with doses of radiation above the 2.5-4 Mrads historically used for sterilization are now being implanted clinically. While there are considerable data from hip simulators that suggest that the wear rate of these new, cross-linked materials may be lower than their predecessors [1], there are little clinical data available. This study provides the results of the analysis of six retrieved cross-linked acetabular bearings, all with implantation durations of less than two years.

KEYWORDS: cross-link, polyethylene, acetabular, wear

Experimental Methods

All 6 retrieved bearings were photographed and examined visually using a Nikon Binocular Dissecting Microscope (Nikon Corporation, Tokyo, Japan) with a magnification factor of 10. The bearings were evaluated for wear using the techniques described by Hood [2]. To evaluate the material of the polyethylene bearings, each bearing was cut with a band saw through the center of the cup exposing a vertical cross section of the polyethylene. Thin slices (approximately 200 µm thick) were removed parallel to the exposed cross section using a Jung microtome (Jung, Heidelberg, Germany) (Figure 1). Fourier Transform Infrared spectroscopy (FTIR) was used to determine the level of oxidation in each bearing. FTIR absorbance spectra were obtained using a Perkin Elmer AutoImage Infrared Microscope (Norwalk, CT). Oxidation measurements were made versus depth on a vertical cross section of each bearing using the infrared microscope. The incorporation of oxygen into the polyethylene was evaluated by examining the carbonyl region of the FTIR spectra, wave numbers between 1800 and 1660 cm⁻¹. The carbonyl region, measuring carbon-oxygen double bonds, indicates the presence of ester, ketone, aldehyde, and carboxylic acid. The oxidation

---

[1] Professor, Research Engineer, and Research Associate, respectively, Dartmouth Biomedical Engineering Center, Thayer School of Engineering, Dartmouth College, Hanover, NH, 03755.
[2] Attending Orthopaedist DHMC, Professor of Surgery in Orthopaedics DMS, Department of Orthopaedics Dartmouth Hitchcock Medical Center, 1 Medical Center Drive, Lebanon, NH, 03756.

level of the bearing thin section was defined as the measured ketone (1718 cm^{-1}) peak height normalized to the 1368 cm^{-1} peak height.

Band saw   Microtome
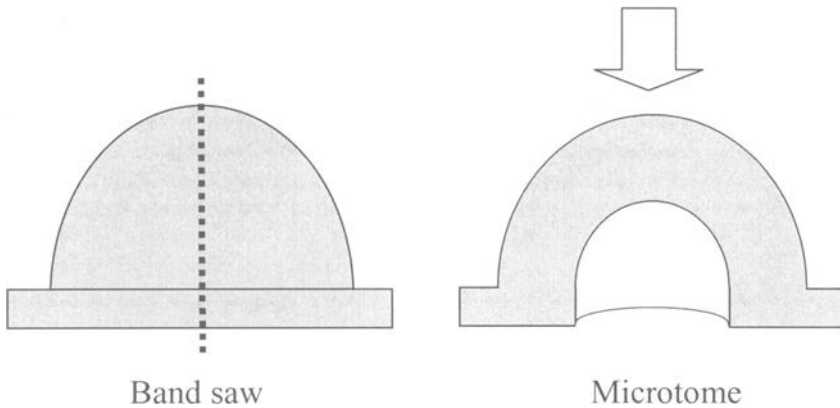
Figure 1- *Schematic showing how thin sections used for oxidation measurements were obtained from an acetabular bearing.*

Only one retrieved bearing had a flange region large enough for tensile specimens to be stamped out from thin sections (approximately 200-μm thick) cut parallel to the surface of the flange portion of the bearing. A sequence of thin sections representing a depth to approximately 2 mm (10 sections) was taken from this flange sample. The horizontal thin sections taken from each bearing flange were stamped, using a metal die, into a dumbbell configuration suitable for mechanical testing, in accordance with the ASTM Test Method for Tensile Properties of Plastics (D#638-99). The gauge length was that of an ASTM standard (D#638-99) Type V sample (7.62 mm), but with smaller gripping zones, again because of bearing geometry limitations. Uniaxial tension tests were done using these dumbbell-shaped horizontal thin sections. Ultimate tensile strength, elongation at break, and tensile stress at yield point were measured for each thin section. The tensile stress at yield point is the first point on the stress-strain curve at which an increase in strain occurs without an increase in stress (D#638-99).

The apparatus used for the tensile testing consisted of a load frame (Model 8501 Instron Corp, Canton, MA), with a servohydraulic actuator (Model 3398-341), and a 200-lb load cell (Model 2518-806). The thin sections were gripped by Instron Series 2712 pneumatic action grips. Specimen elongation was measured using an Instron noncontacting video extensometer (Model 2663-304) for accurate measurement of specimen strain. Instron Series IX Automated Materials Testing System software

(Version 7.26) controlled testing and recorded output. The samples were loaded at a testing speed of 25 mm / minute.

Results

All of the acetabular bearings demonstrated considerable evidence of scratching even at short duration. Some of the original machining marks were no longer visible. The amount of material loss (if any) could not be measured. There was no evidence of gross cracking or delamination, although micro damage to the raised portion of the machining marks was not uncommon. A new type of surface damage, not previously observed on more than 1000 retrieved polyethylene acetabular bearings was identified. This feature was termed 'furrows' due to the appearance of irregular, smooth-bottomed grooving of the surface in a random pattern (Figure 2). This phenomenon appears primarily in the worn regions of the cup.

The oxidation levels of the bearings were low (Table 1), most an order of magnitude less than the ketone oxidation measured in a never-implanted, gamma radiation in air sterilized bearing with a shelf life of 2 months. The five bearings that were melt annealed after radiation cross-linking and sterilized by non-gamma techniques showed minimal oxidation with a maximum at the surface. The one bearing that was annealed below the melt point and gamma radiation sterilized demonstrated a subsurface oxidation peak similar to other gamma radiation in air sterilized, retrieved bearings. Mechanical testing of five tensile specimens obtained from this latter bearing resulted in an average elongation, ultimate tensile strength and yield stress of 250%, 52 MPA and 23 MPA respectively. These values are in accordance with the ASTM Specification for Ultrahigh Molecular Weight Polyethylene Powder and Fabricated Form for Surgical Implants (F#648-00) of 250%, 27 MPA, and 19 MPA for the respective mechanical properties.
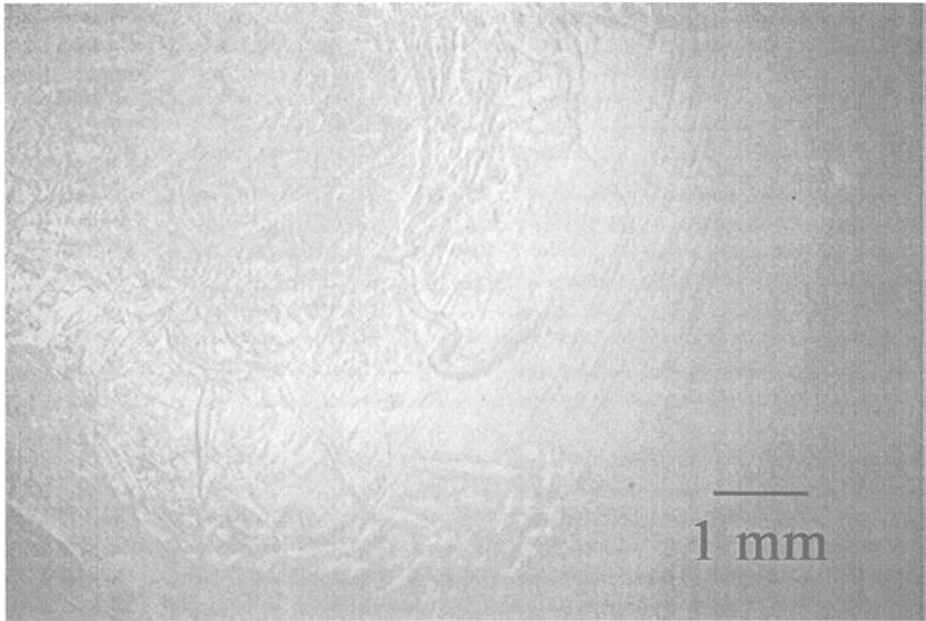
Figure 2 – *Image of unique surface damage seen in cross-linked acetabular bearings.*

Table 1 – *Oxidation levels for 6 retrieved, cross-linked, acetabular bearings.*

Annealing Temperature	Duration (months)	Average Ketone Oxidation
Melt	unknown	0.000
Melt	5.7	0.008
Melt	1.7	0.009
Melt	2.8	0.000
Melt	14	0.004
Below Melt	1.5	0.050
Non-cross-linked	2[#]	0.28

Duration on shelf. Non-cross-linked liner was never implanted and is included for comparison.

Discussion

The retrieved bearings, which were cross-linked at 7.5-10 Mrad, were quite scratched and demonstrated a mode of damage that has not been observed in polyethylene bearings which were either 1) EtO or gas plasma sterilized and not cross-linked or 2) cross-linked only by the gamma radiation sterilization dose of 2.5-4 Mrad. It is unclear what the source of the 'furrowing' is. The features are similar to what one might expect from round, third-body debris caught between the head and cup; yet it has not been observed in non-cross-linked cups. Five of the cups were made by processes that utilize a melting anneal between the radiation cross-linking step and the machining of the bearing with the goal of eliminating free radicals that can lead to later oxidation. One of the cups was

annealed at a temperature below the melting point. The 'furrows' were observed in both types of cups with no apparent difference in features. It is unclear whether this phenomenon is of importance or simply the response of a more cross-linked material to clinical wear. However, the phenomenon has not been reported by those carrying out simulator testing, or in the very much larger set of retrieved bearings that were not intentionally cross-linked at higher irradiation dosage. Figure 3 highlights the complex and random nature of the tracks and clearly demonstrates a variation in size and depth of the 'furrows' across the surface.

This appearance can be compared to the typical surface of a retrieved, gamma radiation sterilized bearing which was not cross-linked at high dosage (Figure 4). The surface shown in Figure 4 is partitioned into three zones that show A) an area where the femoral head did not seat and no wear occurred, B) where the femoral head seated briefly resulting in some burnishing, and C) the area where the femoral head finally seated and substantial wear occurred. Scratching can clearly be seen in zones A and C, with retrieval artifacts in zones B and C, but there is no evidence of furrows in any of the three zones.

Attempts were made to recreate the 'furrows' under the hypothesis that the phenomenon was a result of contact of an aspiration tube with the articular surface. The appearance of damage generated by this contact, recreated in the laboratory, can be seen in Figure 5. There was little similarity in the appearances suggesting that this was not the origin of the 'furrows'.
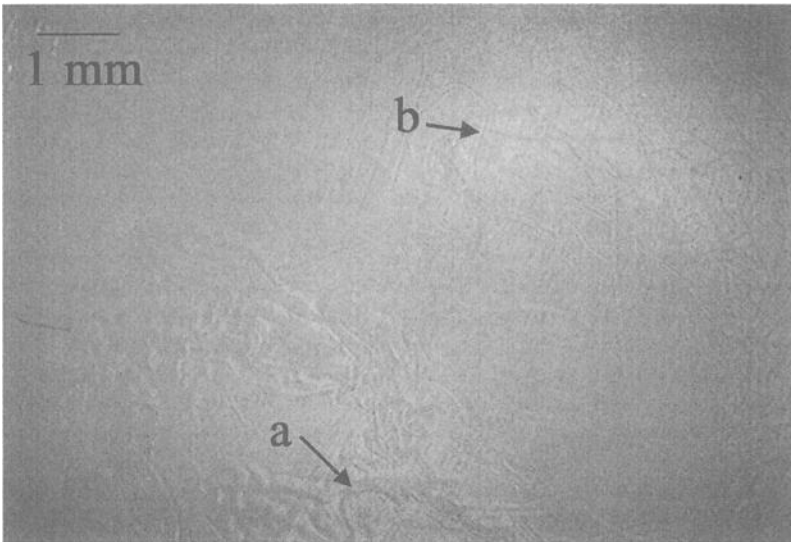
Figure 3 – *Surface of cross-linked acetabular bearing demonstrating a clear variation in size of observed 'furrows'. Larger, more pronounced deformations occur at 'a', as opposed to smaller 'furrows' seen at 'b'.*
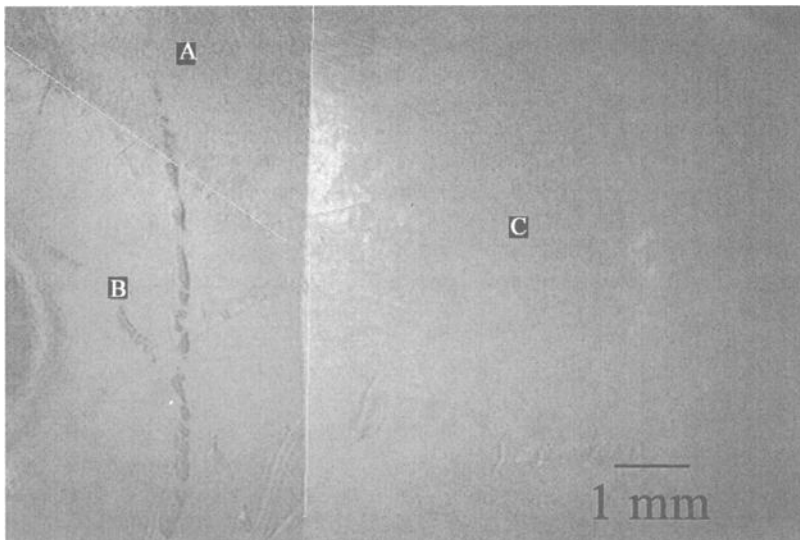
Figure 4 – *Surface of non-cross-linked acetabular bearing showing three distinct zones with varying amounts of wear. A) No wear from the femoral head, B) Some initial wear from the femoral head, and C) final seating place of the femoral head with substantial wear. Note the lack of 'furrows' across all three zones.*
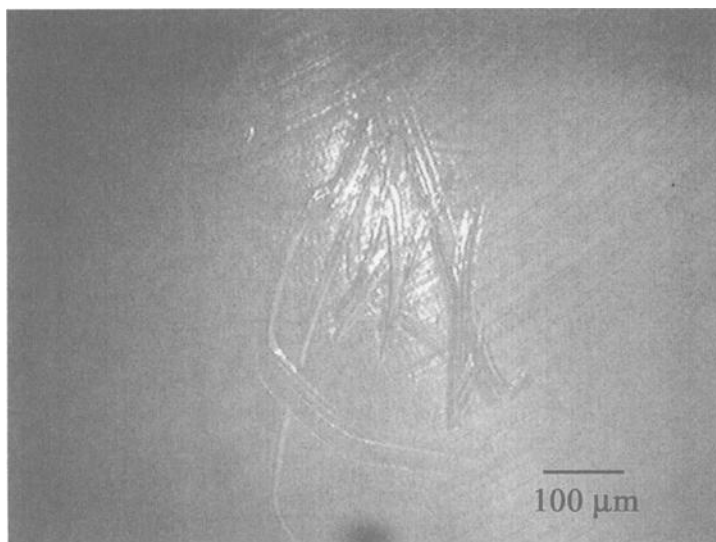
Figure 5 – *Image of articular surface of cross-linked acetabular cup after simulating aspiration technique likely to be encountered during surgery. The appearance of the resulting artifact is markedly different from 'furrows' observed in retrievals.*

Similar markings of cross-linked acetabular bearings have been reported by Muratoglu et al [3], and were referred to as multidirectional scratches rather than 'furrows'. The scratches were attributed to plastic deformation resulting from third body wear (possibly pieces of bone or bone cement). Qualitative support for this interpretation was obtained by heating the retrievals to the melting temperature at which point, due to the "memory effect", the surface scratches disappeared and the original machining marks reappeared. Based on these findings they concluded that no material wear had occurred and as a result these markings were not of clinical significance. As previously mentioned, the markings seen in this study are also suggestive of plastic deformation resulting from a third body, however no imbedded material could be found which might give rise to these 'furrows' and these markings could not be found on non-cross-linked retrievals of similar in vivo duration. One possible explanation for their absence is that cross-linked polyethylene has improved wear and creep properties which preserve markings resulting from third body wear, while in non-cross-linked polyethylene these markings are quickly worn away, or obscured by creep. Without more quantitative techniques for determining in vivo wear and material loss of polyethylene the clinical relevance of these markings will not be known. However, in examining early retrievals of cross-linked polyethylene it is worth noting that cross-linked bearings repeatedly show a distinct wear feature on the articular surface that is not seen in non-cross-linked bearings.

The oxidation of the five cups that were melt-annealed and subsequently sterilized with non-gamma radiation techniques were all low with the maximum oxidation occurring at the surface (suggesting that the oxidation is due to absorbed species). Similar observations have been made on EtO or gas plasma sterilized bearings. This

suggests that the future oxidation of these bearings may parallel those of other, non-gamma radiation sterilized bearings that have demonstrated low oxidation over periods in excess of 15 years [4].

The one cup that underwent a below melt temperature anneal following cross-linking, and a subsequent gamma radiation sterilization, demonstrated a subsurface oxidation peak similar to that observed in retrieved bearings which were gamma radiation sterilized in air (Figure 6) [5]. While the oxidation level was low at this short duration, a second oxidation measurement made after the bearing had sat on the shelf for 4 months demonstrated a much higher oxidation level. This indicates that the free radicals were still active and suggests that the long-term oxidation levels of these bearings in vivo cannot be predicted.
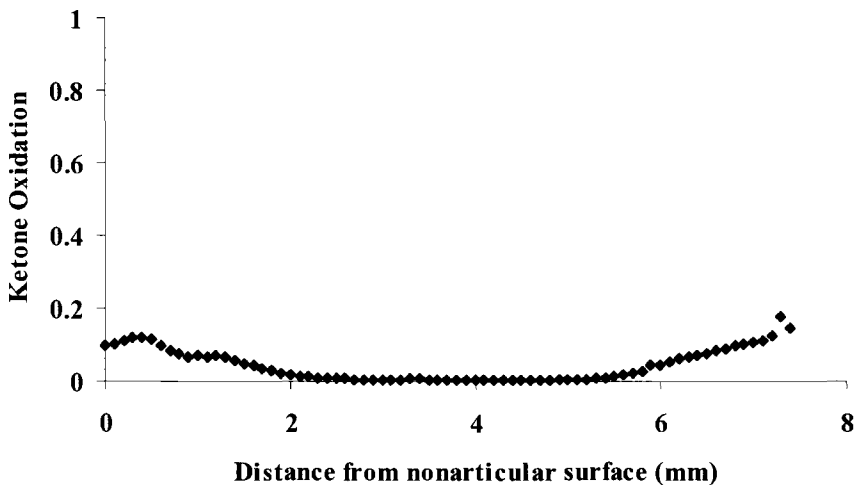
Figure 6 – *Plot of ketone oxidation versus depth for cross-linked acetabular cup that did not receive a melt anneal.*

Conclusions

The retrieved acetabular bearings did not reveal measurable wear, but at the short durations of use, non-cross-linked bearings would not be likely to demonstrate measurable wear either. The low oxidation in the melt-annealed and non-gamma radiation sterilized bearings indicates that long-term stability may be possible in a cross-linked material. The subsurface oxidation peak in the non-melt-annealed cup suggests a material that may oxidize to some extent in the body. No satisfactory technique of estimating the in vivo oxidation rate of this material, or any other, is currently accepted.

The 'furrows' on the surface of these cross-linked bearings appear to be unique to these materials and have not been observed in lower-dose gamma radiation sterilized

polyethylene bearings. No satisfactory mechanism for this wear artifact was determined and the importance of this phenomenon is unknown.

References

[1] McKellop, H., Shen, F., Lu, B., Campbell, P., and Salovey, R, "Development of an Extremely Wear-Resistant Ultra High Molecular Weight Polyethylene for Total Hip Replacements," *Journal of Orthopaedic Research*, Vol. 17, 1999, pp. 157-167.

[2] Hood RW, Wright TM, Burstein AH, "Retrieval Analysis of Total Knee Prostheses: A Method and its Application to 48 Total Condylar Prostheses," *Journal of Biomedical Materials Research, Vol.* 17, 1983, pp. 829-842.

[3] Muratoglu, O.K., Greenbaum, E., Larson, S., Jasty, M., Freiberg, A.A., Burke, D., Harris, W.H., "Surface Analysis of Early Retrieved Acetabular Polyethylene Liners: A Comparison of Standard and Highly Cross-linked Polyethylenes." *Transactions of the Orthopaedic Research Society*, Vol.27, 2002, 48th Annual Meeting, Dallas, Texas, Poster 1029.

[4] Williams, I.R., Mayor, M.B., and Collier, J.P., "The Impact of Sterilization Method on Wear in Knee Arthroplasty," *Clinical Orthopaedics and Related Research*, Vol. 356, 1998, pp. 170-180.

[5] Sutula, L.C., Collier J.P., Saum K.A., Currier, B.H., Currier J.H., Sanford, W.M., Mayor, M.B., Wooding R.E., Sperling D.K., Williams, I.R., Kasprzak, D.J., Surprenant, V.A., "Impact of Sterilization on Clinical Performance of Polyethylene in the Hip," *Clinical Orthopaedics*, Vol. 319, 1995, pp. 28-40.

Steven M. Kurtz,[1,2] *Joseph Turner,*[2] *Michael Herr,*[1] *Avram A. Edidin,*[2] *and Clare M. Rimnac*[3]

Assessment of Surface Roughness and Waviness Using White Light Interferometry for Short-Term Implanted, Highly Crosslinked Acetabular Components

ABSTRACT: The reduction of volumetric wear continues to be one of the imminent challenges for the orthopaedic research community in the area of ultra-high molecular weight polyethylene (UHMWPE) joint replacement components. Retrieval analyses are necessary to determine the relationship between in vitro hip simulator predictions and actual wear performance *in vivo*. To quantify short term wear in retrieved highly crosslinked acetabular components it is necessary to differentiate between the initial surface morphology (dominated by manufacturer's machining marks) and the smaller scale surface features associated with *in vivo* adhesive/abrasive wear mechanisms. We have developed and validated a technique for deconvolution of as-manufactured versus *in vivo* generated surface topology from retrieved, highly crosslinked polyethylene acetabular inserts. Surface topology was characterized by white light interferometry with advanced texture analysis software. A Fourier transform algorithm was used to deconvolve the low-frequency features (i.e., waviness) such as machining marks, from the high-frequency features (i.e., roughness). Twenty-one (21) short-term (less than 24 months) conventional and highly crosslinked retrievals from different manufacturers were evaluated in this study. The wear surfaces in the short-term retrievals were deconvolved using the cut-off frequencies from the new inserts. The frequency distribution and magnitude of the machining marks were found to be material and manufacturer specific. This study highlights the importance of quantitative techniques, such as white light interferometry for distinguishing between initial and *in vivo* generated surface morphology. The topology observed in the crosslinked retrievals was consistent with the surface damage mechanisms previously observed in conventional UHMWPE

---

[1] Principal Engineer and Senior Engineer, respectively, Exponent, Inc., 3401 Market St, Suite 300, Philadelphia PA, 19104;

[2] Assistant Research Engineer and Research Associate Professors, respectively, School of Biomedical Engineering, Science, and Health Systems, Drexel University, 3141 Chestnut St, Philadelphia PA, 19104;

[3] Associate Professor and Director, Musculoskeletal Mechanics and Materials Laboratories, Departments of Mechanical and Aerospace Engineering and Orthopaedics, Case Western Reserve University, Cleveland, OH 44106

components, namely macroscopic and microscopic adhesive/abrasive wear.

KEYWORDS: Ultra-high molecular weight polyethylene, UHMWPE, wear, surface topology, waviness, roughness, crosslinking, acetabular component, total hip replacement, white light interferometry

Introduction

Since the introduction of highly crosslinked and thermally treated UHMWPE for total hip arthroplasty during the late 1990s, there has been keen interest among members of the orthopedic community in the clinical wear performance of these new UHMWPE materials. (Throughout this paper, "highly crosslinked" will refer to UHMWPE that was irradiated with a total dose above 40 kGy, which is the upper limit of the dose typically used for sterilization [1]). Conventional UHMWPE used in contemporary clinical practice in the United States is also crosslinked (to a lesser extent), as a by-product of when it is gamma radiation sterilized in an inert environment with a dose of 25 to 40 kGy [1, 2]. Unirradiated UHMWPE sterilized by ethylene oxide or gas plasma is clinically used in the United States, but is not crosslinked [1]. As this paper deals only with radiation crosslinked UHMWPE materials, "conventional" UHMWPE in the context of our current work will refer to radiation sterilized material.

The clinical performance of both conventional and highly crosslinked UHMWPE can be assessed radiographically, using the methods established by Martell, Devane, and others [3-5]. Wear measurement studies based on radiographic techniques provide quantification of femoral head penetration into the acetabular liner. Radiographic wear assessments are also useful to quantify the time course during which femoral head penetration (assumed to be the wear rate) takes place during implantation; thus, hypotheses related to an accelerating (or decelerating) wear rate can be investigated. However, radiographic wear methods provide little information regarding the *mechanisms* of *in vivo* wear of orthopedic bearing materials. Therefore, for mechanistic studies of *in vivo* wear, direct examination of retrieved components is necessary.

Although the new highly crosslinked bearing materials are intended for long-term implantation, it is nonetheless important to examine components that have been retrieved after short-term *in vivo* service for two main reasons. First, retrieval studies of short-term retrieved components can potentially identify early warning signs of clinical wear or surface damage mechanisms that were unanticipated when the materials were developed. Second, the assessment of short-term retrievals provides an opportunity to provide additional validation of the hip simulator testing that was used in the development of the new materials. Because several different formulations of highly crosslinked and thermally treated UHMWPE have been developed by orthopedic manufacturers and introduced into clinical practice [2], each formulation of highly crosslinked UHMWPE should be validated independently, until unifying trends for *in vivo* performance have been established.

Several studies describing the characterization of short-term retrieved highly crosslinked UHMWPE has been reported thus far as abstracts at national meetings [6-10]. In all five of these studies, the implantation times were less than two years, and the reasons for revision were unrelated to wear of the components. Researchers have documented a range of wear mechanisms on the surface of short-term retrieved highly

crosslinked components, including scratching [6-8], abrasion [7], third body wear [9], pitting [7], surface cracking [7, 8], and plastic deformation of machining marks [7].

The methods used by researchers to examine the wear surface of highly crosslinked retrievals have varied. In four of the five previous studies [6-9], optical microscopy and scanning electron microscopy have been employed. However, in only two of the four previous studies using microscopy was quantification of the wear surface reported using a damage scoring technique [7, 9]. In a fifth study, reported by our institution, white light interferometry was used to measure surface topology of 11 new (never implanted) and 3 retrieved acetabular components [10]. We have since expanded our study of new and retrieved highly crosslinked components for the purpose of establishing a consistent and repeatable methodology for quantifying the wear surface features of short-term retrieved acetabular components using white light interferometry.

Because retrieval studies of highly crosslinked UHMWPE components are under way at multiple institutions, the extent to which wear surface assessment can be standardized will be beneficial to the orthopedic community. Surface damage scoring, such as the method developed by Hood and colleagues [11], provides quantification of the extent but not severity of wear in retrieved components. On the other hand, white light interferometry quantifies the surface height for a 640 by 480 pixel field of view (corresponding to 307 200 individual data points) of the articulating surface. In contrast with other surface measurement technologies (e.g., laser profilometry or atomic force microscopy), white light interferometry is relatively time-efficient, enabling the capture of surface data for a field of view within minutes.

White light interferometry is suitable for characterizing the surface of UHMWPE components after removal from a hip simulator [12] as well as after long-term implantation [13, 14]. Within a particular surface region of interest, it is helpful to distinguish between high-frequency (roughness) and low-frequency (waviness) features on the articulating surface [13, 15]. When considering long-term implanted components, the low-frequency surface features may include micropitting or other forms of micro-fatigue damage, which can take place on the length scale of a resin particle, with an approximate radius of 50 μm [13, 14]. For short-term retrievals, machining marks are the principal landmarks of the unworn surface, and the discrimination between roughness and waviness should be based on the surface amplitude spectrum of the machining marks rather than the dimensions of microfatigue damage observed in long-term retrievals.

In a previous study, we examined the surface morphology of three groups of new (as-manufactured) never implanted acetabular liners produced by two manufacturers to develop a guide for deconvolving the roughness from the waviness of the articulating surface [15]. The machined surfaces of five unirradiated GUR 1050 (control) and five gamma-crosslinked UHMWPE liners were obtained from Stryker Howmedica Osteonics; three electron beam crosslinked liners were also obtained from Sulzer Orthopedics. Significant differences in the morphology of the machining marks were observed between the two manufacturers. A low frequency cutoff of 0.08 1/μm was found to be an effective threshold for discriminating between roughness and waviness; using this threshold, the machining marks of the new components were consistently captured in the waviness, as opposed to the roughness, surface descriptions for all three groups of liners.

The primary objective of our current study was to develop a strategy for characterizing the wear surface of short-term implanted highly crosslinked acetabular

liners using white light interferometry. A secondary goal was to examine the effectiveness of our previously determined surface deconvolution threshold for a range of clinical retrievals. We hypothesized that *in vivo* wear damage would significantly alter the surface roughness and waviness of conventional and highly crosslinked UHMWPE liners after short-term implantation. We further hypothesized that, for a particular type of surface morphology (e.g., machining marks, or adhesive/abrasive wear), the surface roughness and waviness was material-specific. The direct measurement of surface roughness and waviness of highly crosslinked UHMWPE liners from retrievals will useful for the validation of hip simulator studies for these types of polymeric materials. Ultimately, our long-term goal is to compile a database of surface roughness and waviness measurements for all types of highly crosslinked UHMWPEs after short-term, intermediate-term, and long-term implantation to facilitate ongoing hip simulator development and validation.

Methods and Materials

For the present study, the surface topology of 21 retrieved acetabular inserts was analyzed by white light interferometry using a NewView 5000 Model 5032 equipped with advanced texture analysis software (Zygo, Middlefield, CT). The interferometer had an out-of-plane resolution of 0.1 nm in a field of view of 0.3 by 0.4 mm. Using a 10× objective lens, the field of view was sampled in a 640 by 480 array of data points. The instrument was calibrated using a step-height reference standard traceable back to the National Institute of Standards and Technology (Gaithersburg, MD).

Articulating surface topology was measured in 10 conventional and 11 highly crosslinked acetabular components. The components were all implanted for less than two years and revised for reasons other than wear (e.g., instability, fracture, infection, or loosening). The liners were also all originally manufactured out of GUR 1050 resin, which has a viscosity average molecular weight of 5 to 6 million g/mol [1].

The retrieved liners were categorized into conventional, Crossfire, or Durasul groups, each produced by a different manufacturer. The first group consisted of 10 conventional liners that were fabricated by Zimmer, Inc. (Warsaw, IN) and gamma radiation sterilized in nitrogen. The second, electron beam-irradiated (hereafter, Durasul) group consisted of four liners which were crosslinked with a 105 kGy dose of electron beam irradiation and thermally processed by remelting above the melt transition. The second group was machined by Sulzer Orthopedics (Austin, TX). The third, gamma-crosslinked (hereafter, Crossfire) group, produced by Stryker Howmedica Osteonics (Mahwah, NJ) included seven components that were crosslinked by a 75 kGy dose of gamma radiation, thermally processed by annealing below the melt transition, and radiation sterilized in nitrogen. In addition, we had previously characterized the surface morphology of five new gamma-crosslinked components (equivalent to Crossfire) and three new Durasul components, produced by Howmedica Osteonics and Sulzer Orthopedics, respectively [15]. These new components, which were never implanted, provided as-machined controls for comparison with the results from the short-term retrievals.

Nine to twelve nonadjacent regions were randomly sampled from the articulating surface of each retrieved insert, corresponding to a total of 269 independent observations for the study. An additional 48 independent observations collected from the articulating surface of new (never implanted) liners, sampled during our previous research, were also
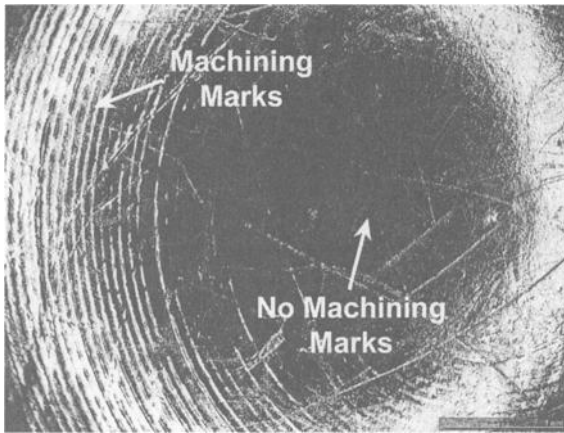
Figure 1—*Optical micrograph of the articulating surface of a short-term retrieved Durasul liner (implanted 17 months). The scale bar is 1 mm.*

included in the present study. During our preliminary analyses of three short-term highly crosslinked retrievals [8, 15], we observed considerable variation in the surface morphology of individual liners. As illustrated in Figure 1, the articulating surface of a short-term retrieval might include regions of pristine machining marks, regions of partially worn machining marks, as well as regions of burnishing.

In addition, regions of microplasticity or articulating surface microcracking have been observed on short-term crosslinked retrievals, as indicated previously [7, 8]. Based on these observations, we judged that classification of the field of view sampled by the interferometer would facilitate interpretation of the surface roughness and waviness data during subsequent statistical analysis. Consequently, surface regions were classified into one of the following three general categories:

- **Machining Marks.** All fields of view that contained evidence of machining marks were placed into this general category. Rather than developing further categories for partially worn machining marks, we assumed that the magnitude of the average surface waviness would more appropriately quantify changes in the morphology of surface regions in this category.
- **Adhesive/Abrasive Wear.** Surface regions with no evidence of machining marks in the waviness profile were considered worn if they appeared burnished. Typical surface features for these regions included multidirectional scratches associated with the adhesive/abrasive wear mechanism for UHMWPE [16-19]. These worn regions were relatively smooth as compared with the other two surface categories.
- **Plastic Deformation.** Surface regions with no evidence of machining marks in the waviness profile were considered plastically deformed if they appeared irregular and were not burnished. It was not possible to analyze further the mechanism producing the irregular morphology based on white light interferometry alone.

A baseline (least-squares) spherical surface was first mathematically subtracted from each field of view collected by the interferometer. The surface data were then Fourier transformed to deconvolve the low-frequency features (i.e., the *waviness*), which were intended to encompass the machining marks, from the high-frequency features (i.e., the *roughness*). A cut-off of 0.08 1/μm, which was associated with a spatial wavelength of

12.5 μm, was used to discriminate between the waviness and roughness of the articulating surface, as described previously [15].

For each field of view, standard surface roughness and waviness metrics were computed. Specifically, we examined the arithmetic mean roughness (R_a) and arithmetic mean waviness (W_a). The arithmetic mean roughness is calculated using the following equation [13, 20]

$$R_a = \frac{1}{l_x l_y} \int_0^{l_x} \int_0^{l_y} |n(x, y)| dxdy \tag{1}$$

where $n(x,y)$ is the surface roughness profile. W_a is also calculated using equation (1), with the exception that the waviness profile is substituted for the surface roughness profile, $n(x,y)$.

Unlike new components, in which the surface features are normally distributed [15], the surface features of retrieved components generally do not conform to a normal or Gaussian distribution [13]. Hence, nonparametric statistical methods are necessary, as opposed to parametric statistical tests, such as the t-test or ANOVA, which apply only to normally distributed data. In the present study, the Kruskal-Wallis test was used compare the ranking of surface roughness and waviness data between different material groups and surface region categories. Statistical analyses were performed using Staview 5.01 Software (SAS Institute, Cary, NC), and p-values of less than 0.05 were interpreted as statistically significant.

Results

Machining marks, adhesive/abrasive wear, and plastic deformation were identified in surface regions of liners fabricated from all three UHMWPE materials (Figures 2 to 4). However, it was rare to observe all three categories of surface regions in an individual component. Evidence of machining marks was most commonly encountered in the surface regions sampled from the highly crosslinked retrievals, as opposed to the conventional retrievals. Specifically, 28 of the 120 (23.3%) surface regions sampled from the conventional retrievals had evidence of machining marks, whereas 86/130 (66.1%) of the surface regions sampled from the highly crosslinked retrievals had evidence of machining marks. In regions observed with machining marks, the difference in the average surface waviness among the three groups of highly crosslinked liners was statistically significant beyond the 0.0001 level (Table 1). However, no significant difference among the groups of liners was noted in the average surface roughness of regions identified with machining marks (Table 1).

The surface filtering threshold of 0.08 1/mm was found to capture the geometry of the machining marks in the waviness, as opposed to the roughness plot of the conventional, Crossfire, and Durasul retrievals effectively (Figure 2). The filtering threshold was effective on pristine, as well as partially worn, machining marks for all three materials. These observations confirmed our assumption that the average surface waviness could be used to quantify the initial wear of machining marks in the retrievals.

Figure 2—*Surface roughness and waviness oblique plots for regions classified as machining marks in short-term conventional (A, B), Durasul, (C, D) and Crossfire (E, F) retrievals. In these surface regions, the machining marks were moderately worn to approximately 50% of their original height. (A) Conventional, R_a = 0.183 μm; (B) Conventional, W_a = 0.583 μm; (C) Durasul, R_a = 0.167 μm; (D) Durasul, W_a = 0.453 μm; (E) Crossfire, R_a = 0.134 μm; (F) Crossfire, W_a = 0.586 μm.*

Table 1—*Summary of average surface roughness (R_a) and waviness (W_a) for surface regions classified with machining marks from the three groups of short-term retrieved acetabular liners. The mean rank calculated from the Kruskal-Wallis test is also reported when significant (p < 0.0001).*

Roughness (R_a)	No. Observations	Median (μm)	IQR (μm)	Mean Rank (Kruskal-Wallis)
Conventional	28	0.171	0.048	66.2 (NS)
Crossfire	52	0.154	0.040	53.1 (NS)
Durasul	34	0.165	0.067	57.0 (NS)
Waviness (W_a)				
Conventional	28	0.221	0.175	26.3
Crossfire	52	0.554	0.404	59.7
Durasul	34	0.698	0.445	79.9

NS-Not Significant (p = 0.24). IQR = Interquartile Range.

Table 2—*Summary of average surface roughness (R_a) and waviness (W_a) for surface regions classified with adhesive/abrasive wear from the three groups of short-term retrieved acetabular liners. The mean rank calculated from the Kruskal-Wallis test is also reported when significant (p < 0.0001).*

Roughness (R_a)	No. Observations	Median (μm)	IQR (μm)	Mean Rank (Kruskal-Wallis)
Conventional	70	0.193	0.053	57.7
Crossfire	23	0.134	0.066	27.3
Durasul	4	0.123	0.065	21.4
Waviness (W_a)				
Conventional	70	0.168	0.196	51.7 (NS)
Crossfire	23	0.121	0.118	41.8 (NS)
Durasul	4	0.145	0.103	43.8 (NS)

NS-Not Significant (p = 0.32). IQR = Interquartile Range.

Burnished regions consistent with adhesive/abrasive wear were identified in retrievals from all three materials (Figure 3). The surface filtering strategy adopted for regions with machining marks proved to be equally applicable for the burnished or worn regions of the conventional and highly crosslinked liners, in terms of discriminating between waviness and roughness of the articulating surface (Figure 3).

Evidence of burnishing was most commonly observed with the conventional UHMWPE surface regions (70/120, 58.3%) rather than with the surfaces regions analyzed from the highly crosslinked retrievals (27/130, or 20.8%). Significant differences were noted in the average surface roughness—but not the waviness—of regions consistent with adhesive/abrasive type wear among the three groups of retrieved liners (Table 2).

Irregular surface regions, consistent with microscopic, plastic deformation, were also observed in surface regions of the conventional and highly crosslinked retrievals (Figure 4). Among the conventional UHMWPE retrievals, 22/120 (18.3%) of the surface regions had evidence of microplasticity; among the highly crosslinked UHMWPE retrievals, 17/130 (13.1%) of the surface regions had evidence of microplasticity. The morphologies of the plastically deformed regions were effectively captured in the waviness descriptions of the surface plots for all three materials (Figure 4). Among the three groups of retrieved liners, significant differences were noted in the average surface waviness—but not the roughness—of regions classified with microplasticity (Table 3).

The three classifications of surface regions (i.e., machining marks, adhesive/abrasive wear, plastic deformation) were also associated with significant differences in roughness and waviness, whether interpreted based on individual box plots for each UHMWPE material (Figures 5ABC) or based on the computed rankings from Kruskal-Wallis analyses. For example, in regions with plastic deformation, the median and interquartile ranges of roughness and waviness data for sampled regions in the conventional UHMWPE (Figure 5A), Durasul (Figure 5B) and Crossfire components (Figure 5C), were consistently higher than among the regions sampled with evidence of machining marks or adhesive/abrasive wear. Similarly, the regions classified as adhesive/abrasive wear on the retrievals were consistently ranked as having the lowest roughness and waviness as compared with regions containing machining marks or plastic deformation. The differences in roughness and waviness between the three classifications of surface regions were statistically significant, based on the Kruskal-Wallis analyses conducted for each type of UHMWPE material ($p < 0.05$).

Table 3—*Summary of average surface roughness (R_a) and waviness (W_a) for surface regions classified with plastic deformation from the three groups of short-term retrieved acetabular liners. The mean rank calculated from the Kruskal-Wallis test is also reported when significant ($p = 0.001$).*

Roughness (R_a)	No. Observations	Median (μm)	IQR (μm)	Mean Rank (Kruskal-Wallis)
Conventional	22	0.207	0.046	16.9 (NS)
Crossfire	10	0.235	0.091	25.0 (NS)
Durasul	7	0.259	0.169	22.8 (NS)
Waviness (W_a)				
Conventional	22	0.712	0.274	14.2
Crossfire	10	1.189	0.762	26.9
Durasul	7	1.787	1.083	28.4

NS-Not Significant *(p = 0.14)*. IQR = Interquartile Range.
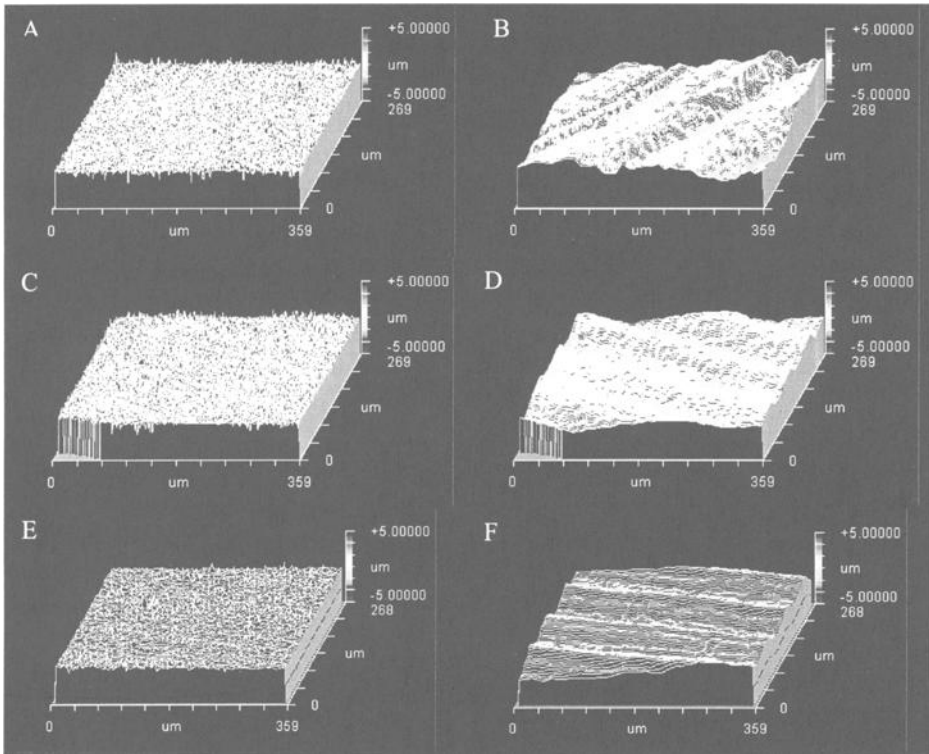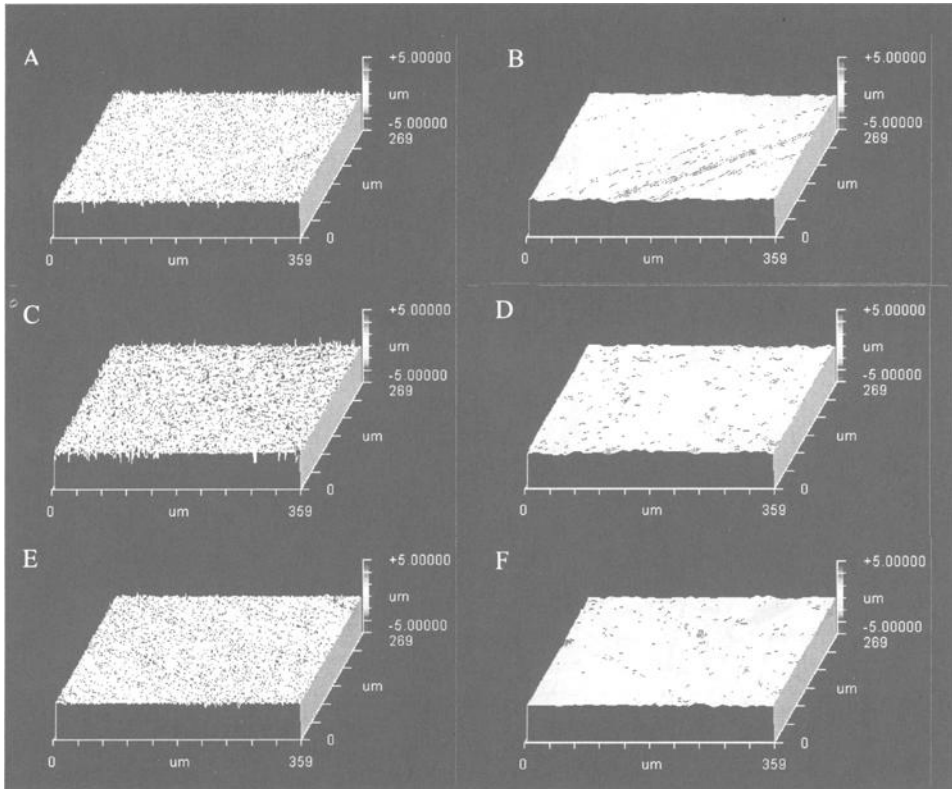
Figure 3—*Surface roughness and waviness oblique plots for regions classified as adhesive/abrasive wear in short-term conventional (A, B), Durasul, (C, D) and Crossfire (E, F) retrievals. In these surface regions, no evidence of machining marks was observed. (A) Conventional, $R_a = 0.126$ µm; (B) Conventional, $W_a = 0.124$ µm; (C) Durasul, $R_a = 0.113$ µm; (D) Durasul, $W_a = 0.108$ µm; (E) Crossfire, $R_a = 0.093$ µm; (F) Crossfire, $W_a = 0.105$ µm.*
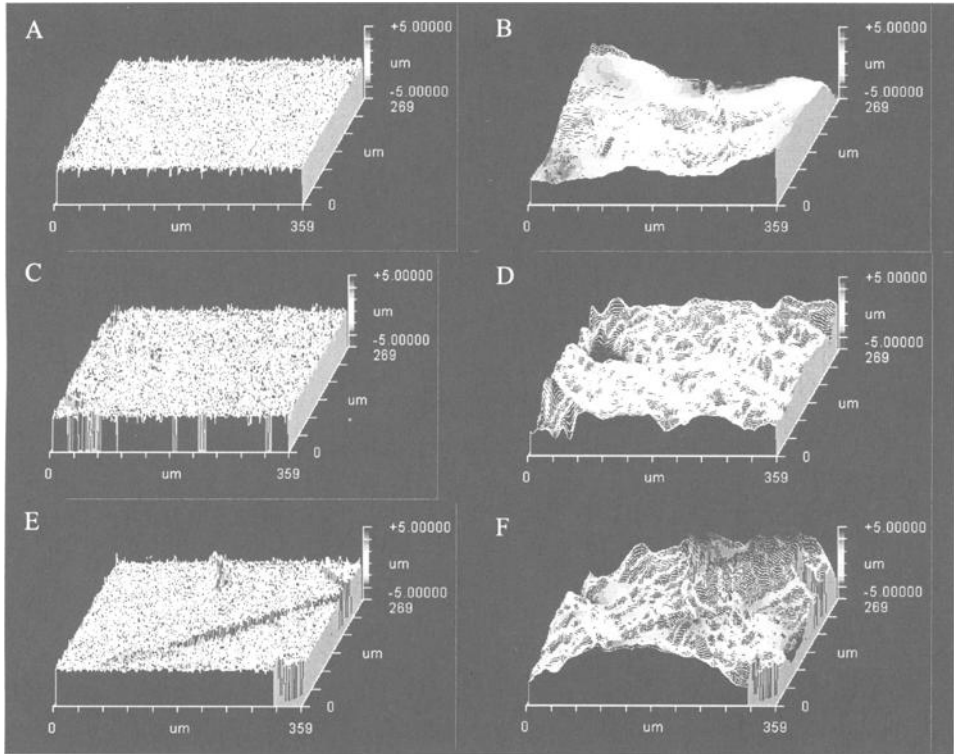
Figure 4—*Surface roughness and waviness oblique plots for regions classified as plastic deformation in short-term conventional (A, B), Durasul, (C, D) and Crossfire (E, F) retrievals. In these surface regions, no evidence of machining marks was observed, and the surface morphology was highly irregular. (A) Conventional, $R_a = 0.162$ μm; (B) Conventional, $W_a = 1.140$ μm; (C) Durasul, $R_a = 0.208$ μm; (D) Durasul, $W_a = 0.787$ μm; (E) Crossfire, $R_a = 0.210$ μm; (F) Crossfire, $W_a = 1.302$ μm.*

Discussion

The broad range in surface morphologies observed for highly crosslinked UHMWPE acetabular liners was consistent with the adhesive/abrasive wear mechanism attributed to conventional UHMWPE. We saw evidence of erosion or flattening of machining marks in the highly crosslinked retrievals, leading to burnishing or polishing of localized surface regions. In addition, irregular surface morphologies, consistent with microplasticity, were observed in both conventional as well as highly crosslinked retrievals. Taken together, these observations suggest that conventional and highly crosslinked UHMWPE components exhibit similar *in vivo* wear mechanisms. However, we detected significant differences between the conventional and highly crosslinked retrievals in the surface roughness or the waviness after short-term implantation. For instance, regions of adhesive/abrasive wear in the highly crosslinked retrievals were associated with significantly lower surface roughness as compared with similarly classified regions on the conventional UHMWPE liners. It remains to be seen in future research whether the surface roughness and waviness of highly crosslinked UHMWPE is material-dependent and whether the surface morphologies vary as a function of implantation time. Nevertheless, the methodology established in the present study will provide the foundation for classifying and measuring the surface morphology in not only short-term but also long-term implanted acetabular components, whether manufactured from conventional or highly crosslinked UHMWPE.

Our observations of surface morphology in the highly crosslinked UHMWPE are consistent with the macroscopic and microscopic wear mechanisms proposed by Cooper, Fisher, and others [21, 22]. In the unworn, or undeformed configuration, the surface of the component is covered by machining marks with a characteristic waviness that is manufacturer- and material-specific [15]. Based on our earlier measurements, it also appears that the surface waviness of machining marks is normally distributed in new components [15]. During the initial wear-in of the hip bearing, the machining marks become progressively eroded, resulting in a reduction of the median waviness and a broadening of the distribution by a "macroscopic" wear mechanism, as described by Cooper and Fisher [21].

The reduction in median waviness of the machining marks, when compared with as-manufactured control liners, is observed in the Crossfire and Durasul liners in Figures 5 B and C (no control liners were available for comparison with the conventional retrievals in the present study). After removal of the machining marks, wear proceeds by a "microscopic" process [21], captured in the present study by changes to the surface roughness (Table 2), not the waviness. Thus, for both conventional and highly crosslinked UHMWPE liners, the wavelength cutoff of 12.5 μm (corresponding to a spatial frequency of 0.08 1/μm) provides an effective distinction between "macroscopic" wear, with surface features on the same length scale as machining marks, and "microscopic" wear associated with polishing or burnishing of the articulating surface.

Muratoglu et al. [6] have advocated remelting the surface of highly crosslinked retrievals to discriminate between plastic deformation and wear. Upon remelting highly crosslinked liners after short-term implantation, Muratolgu et al. [6] have observed the apparent recovery of surface features resembling machining marks, attributed to the "memory effect" of the crosslinked polymers. We did not remelt the liners from our short-term retrieval collection, because it remains unclear what irreversible effect
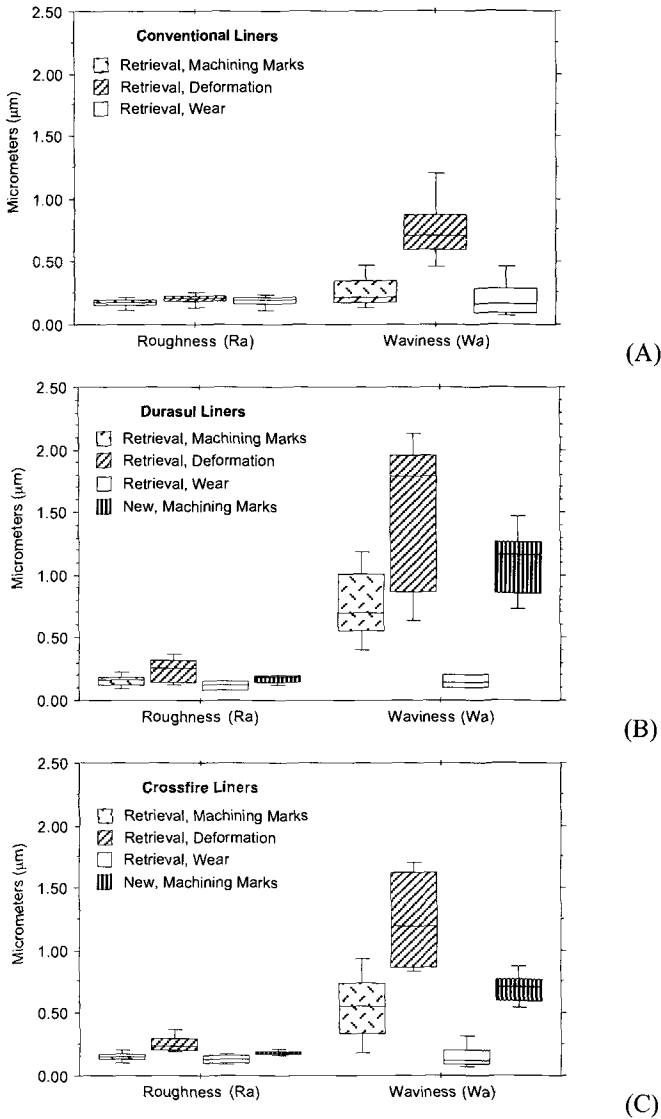
Figure 5—*Box plot comparison of average surface roughness and waviness for (A) n=120 observations from ten short-term retrieved conventional liners; (B) n=45 observations from four short-term retrieved Durasul liners, with data also shown for n=18 observations collected from three new (never implanted) control liners; and (C) n=85 observations from seven short-term retrieved Crossfire liners, with data also shown for n=30 observations collected from five new (never implanted) control liners.*

remelting may have on changes to the physical, chemical, and mechanical behavior that may occur during implantation.

Based on the recovery of machining marks following remelting, Muratoglu and coworkers have concluded that highly crosslinked acetabular components exhibit "essentially no wear" during short term implantation of up to 18 months [6]. In our study, the increased prevalence of machining marks and irregular surface topology, relative to conventional liners, is consistent with a wear-resistant material. However, several limitations of this study preclude the determination of a reliable wear rate from these retrievals, including the short implantation time and the small numbers of the retrievals for each UHMWPE material. Furthermore, the reasons for revision (e.g., loosening, instability, and fracture), while not related to wear of the liners, may nonetheless have led to reduced activity for these patients and contributed to lower wear than may be occurring in the general population. For these reasons, the measurements performed in the current study on short-term retrieved components should serve as a useful quantitative reference for the various wear mechanisms in crosslinked UHMWPE, against which the results from hip simulator studies, as well as future, longer-term retrieval studies, can be compared.

Acknowledgments

References

[1]   Kurtz, S. M., Muratoglu, O. K., Evans, M., and Edidin, A. A., "Advances in the processing, sterilization, and crosslinking of ultra- high molecular weight polyethylene for total joint arthroplasty," *Biomaterials,* 1999, Vol. 20, pp. 1659-88.

[2]   Muratoglu, O. K., and Kurtz, S. M., "Alternative bearing surfaces in hip replacement." *Hip Replacement: Current Trends and Controversies*, R. Sinha, Eds., New York, Marcel Dekker, 2002, pp. 1-46.

[3]   Martell, J. M., and Berdia, S., "Determination of polyethylene wear in total hip replacements with use of digital radiographs," *J Bone Joint Surg Am,* 1997, Vol. 79, pp. 1635-41.

[4]   Devane, P. A., Bourne, R. B., Rorabeck, C. H., Hardie, R. M., and Horne, J. G., "Measurement of polyethylene wear in metal-backed acetabular cups. I. Three-dimensional technique," *Clin Orthop,* 1995, Vol. 319, pp. 303-16.

[5]   Bragdon, C. R., Malchau, H., Larson, S. L., Borlin, N., Karrholm, J., and Harris, W. H., "Validation of digital radiography, for use with radiosteriometric analysis (RSA) using a dynamic phantom wear model," *Transactions of the 48th Orthopedic*

Research Society, 2002, Vol. 27, pp. 1020.

[6]   Muratoglu, O. K., Greenbaum, E. S., Larson, S., Jasty, M., Freiberg, A. A., Burke, D. W., and Harris, W. H., "Surface analysis of early retrieved acetabular polyethylene liners: A comparison of conventional and highly crosslinked polyethylenes.," *Transactions of the 28th Society for Biomaterials,* 2002, Vol. 25, pp. 62.

[7]   Bradford-Collons, L., Baker, D., Graham, J., Chawan, A., Ries, M. D., and Pruitt, L., "Crosslinked polyethylene shows evidence of wear and fatigue: A retrieval study of Durasul liners," *Transactions of the 28th Society for Biomaterials,* 2002, Vol. 25, pp. 609.

[8]   Edidin, A. A., Hozack, W. J., Villarraga, M. L., Ciccarelli, L., and Kurtz, S. M., "Evaluation of wear in short-term retrieved highly crosslinked acetabular liners," *Transactions of the 28th Society for Biomaterials,* 2002, Vol. 25, pp. 27.

[9]   Willie, B. M., Foot, L. J., Le, D., Bloebaum, R. D., and Hoffmann, A. A., "Assessment of oxidation resistance using FTIR in a series of thirty retrieved Durasul crosslinked acetabular liners," *Transactions of the 28th Society for Biomaterials,* 2002, Vol. 25, pp. 608.

[10]   Kurtz, S. M., Turner, J., Herr, M., Hozack, W. J., and Edidin, A. A., "Wear characterization in short term highly crosslinked UHMWPE liners using surface morphology," *Transactions of the 28th Society for Biomaterials,* 2002, Vol. 25, pp. 184.

[11]   Hood, R. W., Wright, T. M., and Burstein, A. H., "Retrieval analysis of total knee prostheses: a method and its application to 48 total condylar prostheses," *J Biomed Mater Res,* 1983, Vol. 17, pp. 829-42.

[12]   Kurtz, S. M., Muhlstein, C., and Edidin, A. A., "Surface morphology and wear mechanisms of four clinically relevant biomaterials after hip simulator testing," *J Biomed Mater Res,* 2000, Vol. 52, pp. 447-459.

[13]   Elfick, A. P. D., Hall, R. M., Pinder, I. M., and Unsworth, A., "The influence of femoral head surface roughness on the wear of ultrahigh molecular weight polyethylene sockets in cementless total hip replacement," *J. Biomed. Mater. Res. (Appl. Biomat.),* 1999, Vol. 48, pp. 712-718.

[14]   Edidin, A. A., Rimnac, C. M., Goldberg, V., and Kurtz, S. M., "Mechanical behavior, wear surface morphology, and clinical performance of UHMWPE acetabular components after 10 Years of implantation," *Wear,* 2001, Vol. 250, pp. 152-158.

[15]   Kurtz, S. M., Turner, J. L., Herr, M., and Edidin, A. A., "Deconvolution of surface topology for quantification of initial wear in highly cross-linked acetabular components for THA," *J Biomed Mater Res,* 2002, Vol. 63, pp. 492-500.

[16]   Wang, A., Stark, C., and Dumbleton, J. H., "Mechanistic and morphological origins of ultra-high molecular weight polyethylene wear debris in total joint prostheses," *Proc. Instn. Mech. Engrs.,* 1996, Vol. 210, pp. 141-155.

[17]   Wang, A., Essner, A., Polineni, V. K., Stark, C., and Dumbleton, J. H., "Lubrication and wear of ultra-high molecular weight polyethylene in total joint replacements," *Tribology International,* 1998, Vol. 31, pp. 17-33.

[18]   McKellop, H. A., Campbell, P., Park, S. H., Schmalzried, T. P., Grigoris, P., Amstutz, H. C., and Sarmiento, A., "The origin of submicron polyethylene wear

debris in total hip arthroplasty," *Clin Orthop,* 1995, Vol. 311, pp. 3-20.

[19] Jasty, M., Goetz, D. D., Bragdon, C. R., Lee, K. R., Hanson, A. E., Elder, J. R., and Harris, W. H., "Wear of polyethylene acetabular components in total hip arthroplasty. An analysis of one hundred and twenty-eight components retrieved at autopsy or revision operations," *J Bone Joint Surg Am,* 1997, Vol. 79, pp. 349-58.

[20] Bhushan, B., "Solid state surface characterization." *Principles and Applications of Tribology,* Eds., New York, John Wiley & Sons, Inc., 1999, pp. 99-197.

[21] Cooper, J. R., Dowson, D., and Fisher, J., "Macroscopic and microscopic wear mechanisms in ultra-high molecular weight polyethylene," *Wear,* 1993, Vol. 162-164, pp. 378-384.

[22] Wang, A., Stark, C., and Dumbleton, J. H., "Role of cyclic plastic deformation in the wear of UHMWPE acetabular cups," *J Biomed Mater Res,* 1995, Vol. 29, pp. 619-26.

Crosslinked PE in Knees: Is It Safe?

Jian Q. Yao,[1] *Cheryl R. Blanchard,*[1] *Xin Lu,*[1] *Michel P. Laurent,*[1] *Todd S. Johnson,*[1]
Leslie N. Gilbertson,[1] *Dale F. Swarts,*[1] *and Roy D. Crowninshield*[1]

Improved Resistance to Wear, Delamination and Posterior Loading Fatigue Damage of Electron Beam Irradiated, Melt-Annealed, Highly Crosslinked UHMWPE Knee Inserts

---

ABSTRACT: Recently, a knee prosthesis containing an electron beam irradiated (58 – 72 kGy, nominal dose of 65 kGy), melt-annealed, highly crosslinked UHMWPE (HXPE) tibial insert has been developed. In the present study, the wear and delamination resistance of the HXPE tibial insert and its fatigue performance under a posterior loading condition have been evaluated against its conventional gamma-sterilized UHMWPE counterpart (37kGy, in nitrogen). The test methodologies used were newly developed with the aim to evaluate this new material under severe testing conditions.

In comparison to the gamma controls, the HXPE inserts: (a) wore significantly less (achieving wear reductions of 81% and 73% over 5 and 20 million cycles, respectively); (b) exhibited significantly improved delamination resistance; and (c) exhibited significantly improved posterior loading fatigue resistance.

KEYWORDS: wear, delamination, fatigue, knee, UHMWPE, crosslinked polyethylene

Introduction

Significant advances in total knee arthroplasty (TKA) technology have taken place over the past three decades. Modern TKAs have successfully relieved the pain and

---

[1] Principal Engineer, Vice President of Research and Biologics, Senior Engineer, Principal Engineer, Director of Analytical and Experimental Mechanics, Director of Research Processes, Director of Process Technology, and Chief Scientific Officer/Senior Vice President, respectively, Research Department, Zimmer, Inc., P.O. Box 708, Warsaw, IN, 46581-0708.

restored ambulatory functions of millions of patients with degenerative joint diseases or traumatic injuries. Among many important developments, improved mechanical designs of implants and the associated surgical instruments, innovative materials and enhanced surgical techniques have all contributed greatly to the success of TKA. Indeed, the total number of TKA procedures per annum is now about the same as that of total hip arthroplasty (THA) procedures [1]. However, surface wear and, more prevalently, subsurface fatigue damage of ultra-high molecular weight polyethylene (UHMWPE) tibial inserts may limit the longevity of TKAs. Improved resistance to surface wear and subsurface fatigue damage is therefore desirable.

Active efforts have been made to reduce wear of UHMWPE in both total hip and knee replacements. Among several wear reduction technologies, highly crosslinked UHMWPE, made by exposure to irradiation or chemical agents, has been shown to reduce significantly the wear of total hip arthroplasty (THA) in both *in vitro* simulator tests [2-5] and *in vivo* clinical studies [6-8]. The significant wear reduction has been attributed to the positive effect of crosslinking of UHWMPE on reducing its strain softening, which arises from multi-directional shear stresses acting on linear polymers [9, 10]. Recently, it has been shown that tibial inserts are also subjected to multi-directional shear stresses due to internal/external rotation and anterior/posterior translation of knee joints, albeit with a lower extent of cross-motion than in THA [11, 12]. Hence, the strain softening due to multi-directional shear stresses may be as important a factor in the wear of UHMWPE tibial inserts of TKAs as that of THAs. It therefore appears that highly crosslinked UHMWPE may also effectively reduce wear in TKAs.

On the other hand, it has been observed that subsurface fatigue damage of tibial inserts may be mitigated by minimizing the degradation of mechanical properties of UHMWPE over time [13, 14]. Examples are UHMWPE tibial inserts which are either machined and subsequently gamma sterilized in an inert environment or net-shape molded [13,14]. These inserts often do not develop fatigue damage, nor undergo significant mechanical degradation. Recently, a melt-annealing process has been developed to reduce free radicals to an undetectably low level [3] and has a much improved stability in its mechanical properties [15]. It would therefore be reasonable to expect that the melt-annealed UHMWPE may be more resistant to fatigue damage such as delamination.

The objective of the present study is to investigate whether electron-beam irradiated and subsequently melt-annealed highly crosslinked UHMWPE tibial inserts indeed possess improved resistance to both surface wear and subsurface fatigue damage, in comparison with the currently widely-used conventional UHMWPE tibial inserts sterilized with gamma irradiation. Three sets of experiments were conducted: a knee wear simulator test, a delamination test of the central condylar areas; and a posterior loading fatigue test of the posterior edges of the tibial inserts.

Materials and Methods

Machined highly crosslinked UHMWPE (HXPE) and conventional gamma irradiated UHMWPE (gamma controls) tibial inserts of the NexGen® Complete Knee Solution Cruciate Retaining (CR) knee joints (Zimmer Inc., Warsaw, IN) were tested. All were manufactured from the same lot of GUR1050 compression molded slabs. The high crosslink density of HXPE was achieved by exposure to electron-beam (e-beam)

irradiation at 58 - 72 kGy. Subsequently, a proprietary melt-annealing process was applied to HXPE, where the material was held in an oven at elevated temperatures, in order to reduce free radicals to an undetectably low level. The cooling rate was controlled in order to produce appropriate crystallinity levels. The HXPE components were then machined and gas plasma sterilized. The gamma control samples were machined directly from GUR1050 compression molded slabs. Subsequently, they were packaged in nitrogen pouches and then sterilized by gamma irradiation at 37 kGy.

Before wear, delamination and posterior fatigue loading tests, all of the tibial inserts were accelerated aged per ASTM Guide for Accelerated Aging of Ultra-High Molecular Weight Polyethylene (F2003: Method B), i.e., 70 ^{0}C in pure oxygen at 5 atm (73 psi) for 2 weeks. The extent of oxidation was estimated by calculating the surface oxidation index (SOI) per ASTM Guide for Evaluating the Extent of Oxidation in Ultra-High-Molecular-Weight Polyethylene Fabricated Forms Intended for Surgical Implants (F2102). The SOI was defined as the average of the FTIR 1720/1369 cm^{-1} oxidation indices from the surface to a depth of 3 mm subsurface.

Wear Test

A group of 12 HXPE tibial inserts (six each at 58 kGy and 72 kGy e-beam irradiation doses) and a group of six conventional UHMWPE inserts (gamma irradiated in nitrogen at 37 kGy) were wear tested to five million cycles (Mc). Subsequently, in order to assess the wear performance and mechanical durability of the inserts, a subset of 12 samples (n=4, HXPE at 58 kGy; n=4, HXPE at 72 kGy; n=4, conventional gamma control) were wear tested to 20 million cycles.

The knee wear tests were performed in three 6-station knee wear simulators (Advanced Mechanical Technology Incorporation, Watertown, MA) (Figure 1). Dynamic loading and motion representative of those during level walking were applied onto the joints [16] (Figure 2). The peak applied load during the stance phase was 3200 N and a minimum applied load during the swing phase was 50 N. The ranges of motions were: femoral extension from 0 to -58 degrees, internal tibial rotation from 1.9 to -5.7 degrees and femoral posterior translation from 0 to 5.2 mm. The knees were articulated at the physiological frequency of 1.1 Hz. Each joint was tested in a sealed chamber in which 250 mL of undiluted bovine calf serum lubricant (JRH Bioscience, Lenexa, KS), containing 0.75 g sodium azide and 2.25 g disodium EDTA, was recirculated and maintained at 37 ± 3° C. The lubricant was replaced every 0.5 million cycles. Gravimetric wear measurements were made at intervals of one million cycles. Because the tibial inserts changed weights during wear testing not only due to wear losses, but also weight gains through fluid absorption, the net wear loss must take into account the fluid absorption. Therefore, "load-soak" tibial inserts were used, onto which dynamic loading identical to the wear samples was applied but no motion was imparted.

a. Overall view   b. Close-up view of a wear station
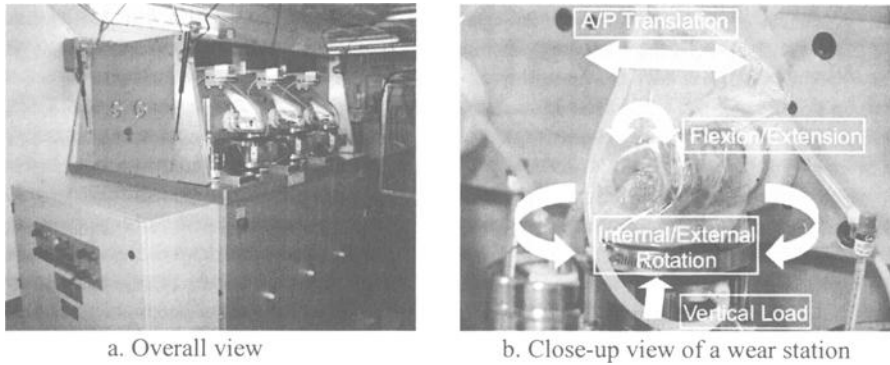
Figure 1 – *AMTI knee simulator*
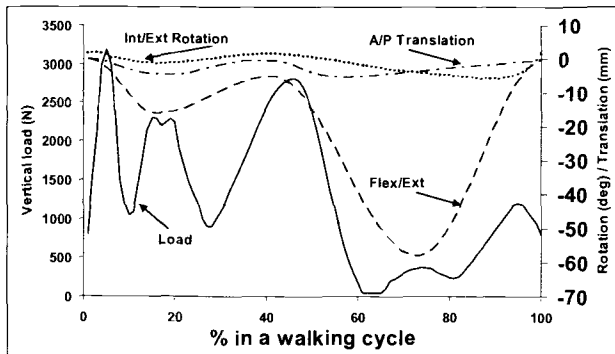
Figure 2 – *Load/motion inputs for the knee wear simulator*

Delamination Test

Six HXPE (72 kGy) and six conventional UHMWPE tibial inserts were articulated against spherical CoCr counterfaces with a 16 mm radius under a constant load in a 12-station delamination tester built in-house (Figure 3). The 16 mm radius was in the smaller size range of the radii of femoral condyles in the sagittal plane (15.6 – 65 mm, significantly smaller than those in the frontal plane). As the radii of curvature of the tibial inserts were about 80 mm, the radial clearances were about 64 mm. The constant applied load was 1779 N (400 lbs). This load and radial clearance combination led to a contact area of 63 mm^2 as measured with a Fuji pressure sensitive film. The corresponding *average* contact stress was approximately 28 MPa. Assuming an elliptical contact pressure distribution, the corresponding maximum contact pressure was approximately 42 MPa, which is at the high end of the normal range of contact stresses expected for tibiofemoral contact at flexion [16]. The spherical counterface slid against the UHMWPE sample reciprocating with a 20 mm stroke. The sliding waveform was sinusoidal at 1 Hz. This resulted in a maximum sliding speed of 63 mm/s, within the range of the physiological sliding speed in the tibiofemoral joint during the heavily loaded stance phase of the gait cycle [17]. During the testing period, undiluted bovine calf serum (JRH

Bioscience, Lenexa, KS) was used as the lubricant. The temperature of the lubricant was maintained at $37 \pm 3\ ^0C$.
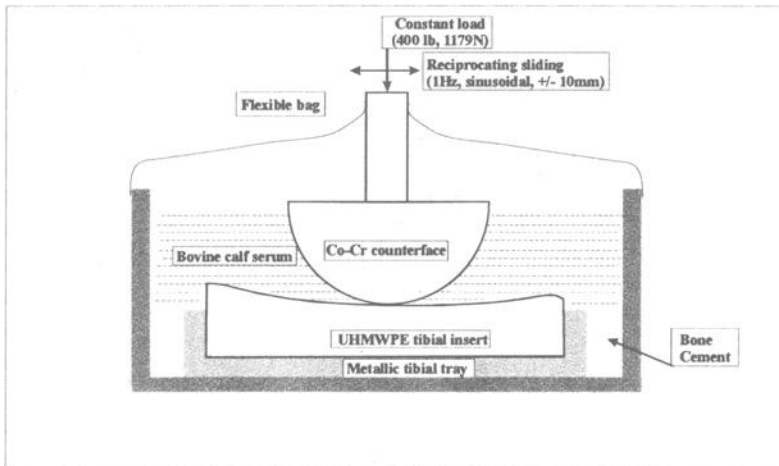
Figure 3 – *Schematics of the delamination tester*
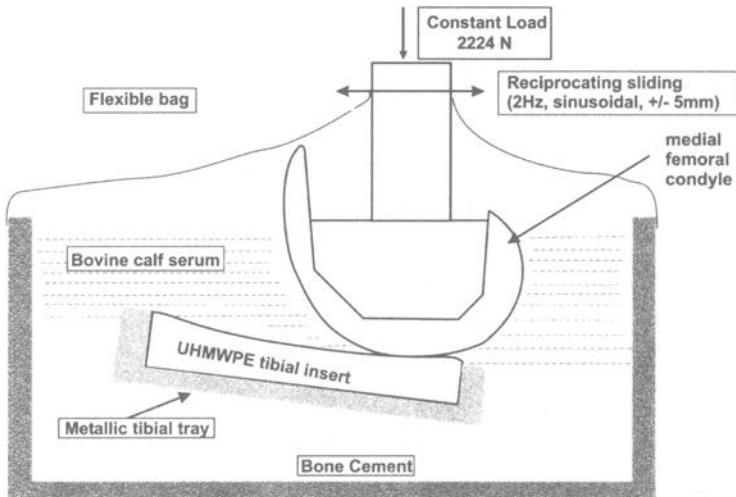
Figure 4 – *Schematics of the posterior loading fatigue tester*

Posterior Loading Fatigue Test

Five HXPE (72 kGy) and five conventional UHMWPE inserts were articulated against matching CoCr femoral condyles (Figure 4). The sliding motion was controlled such that the apex (the most distal point at full extension) of each femoral condyle was 2 mm from the posterior edge of the opposing tibial insert when the femur was at its most posterior

position. Eight tibial inserts were tested on two 4-station reciprocating testers built in-house and two more on two single-station biaxial material testers (MTS Systems Corp., Eden Prairie, MN). The knee joint samples were all set up in the full extension position, with the tibial component set at a posterior slope of 7 °, as recommended for surgical implantation. A 2224 N (500 lbs) constant load was applied vertically on the medial condyle of each insert through the medial femoral condyle. The contact area was 139.5 mm^2 as measured with a Fuji pressure sensitive film. The corresponding *average* contact stress was approximately 16 MPa. Assuming an elliptical contact pressure distribution, the corresponding maximum contact pressure was approximately 24 MPa, which is at the high end of contact stresses expected for the tibiofemoral contact at full extension [16]. The lateral femoral condyle was machined off so that the lateral tibiofemoral compartment was not loaded. A 2 Hz, sinusoidal sliding motion of the femoral components relative to the tibial inserts was applied. The stroke of the reciprocating sliding motion was 10 mm, resulting in a peak sliding speed of 63 mm/s. The tibial inserts were immersed in bovine calf serum at 37 ± 3 °C throughout the test in individual sealed environmental chambers. Tibial inserts were visually examined periodically for signs of fatigue damage.

Results

Wear Test
    The HXPE tibial inserts were found to wear significantly less than the conventional gamma controls (Figure 5). After 5 Mc of wear testing, the group-averaged cumulative wear rates were 14.4 ± 2.8 mg/Mc for the gamma controls, 3.7 ± 1.1 mg/Mc for the 58 kGy HXPE tibial inserts, and 1.7 ± 0.6 mg/Mc for the 72 kGy HXPE tibial inserts (± standard deviations). The average wear rate reductions achieved over the gamma controls were 71% and 88% for the 58 kGy and 72 kGy HXPE tibial inserts, respectively, for an aggregate wear reduction of 81% (representing an average radiation level of 65 kGy). After 20 Mc of wear testing, the group-averaged cumulative wear rates became 13.3 ± 3.0 mg/Mc for the gamma controls, 4.4 ± 0.5 mg/Mc for the 58 kGy HXPE tibial inserts and 2.9 ± 0.7 mg/Mc for the 72 kGy HXPE tibial inserts (Figure 7). There was not a statistically significant change in the wear rates of gamma controls from 5 Mc to 20 Mc, but there was a statistically significant increase in the wear rates of HXPE inserts from 5 Mc to 20 Mc. Despite that, after 20 Mc wear testing, HXPE inserts still wore significantly less than the gamma controls (achieving wear reductions of 67% and 78% for the 58 kGy and 72 kGy HXPE inserts, respectively, for an aggregate wear reduction of 73% for an average radiation level of 65 kGy).
    It was also observed that one of the four gamma control inserts tested to 20 Mc underwent extensive delamination damage (Figure 6). The onset of delamination was observed visually starting at 12 Mc. In contrast, none of the HXPE inserts exhibited signs of delamination at the completion of 20 Mc of wear testing.

Delamination Test
    It was found that all six gamma control tibial inserts delaminated within 5.8 Mc of delamination testing (average 2.9 Mc, ranging from 1.5 to 5.8 Mc) (Table 1 and Figure 7). Once a loose UHMWPE fragment was detached from the insert, the test for this particular insert was terminated. In contrast, none of the melt-annealed HXPE inserts

exhibited delamination even after 8 million cycles. The test for HXPE inserts was terminated at 8 Mc, as at this point the relative delamination resistance of HXPE and gamma control inserts had been well established. A subsurface white patch was visible at the onset of delamination, indicating the subsurface initiation of delamination. This corresponded to the subsurface location of the maximum von Mises stress [16]. The white patch progressively propagated to the surface and eventually led to the detachment of loose fragments of UHMWPE. It was also noted that the delaminated area showed a slope of around 45 degrees to the horizontal plane, indicating the slope along which the delamination process progressed. This suggested a shear fatigue failure mechanism.
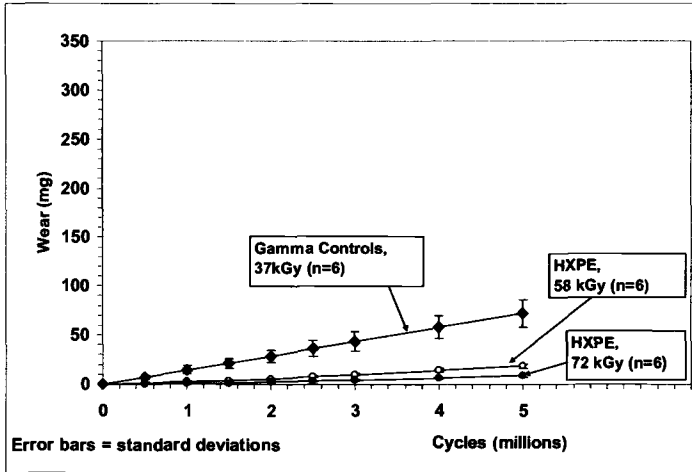
(a) 5 Mc
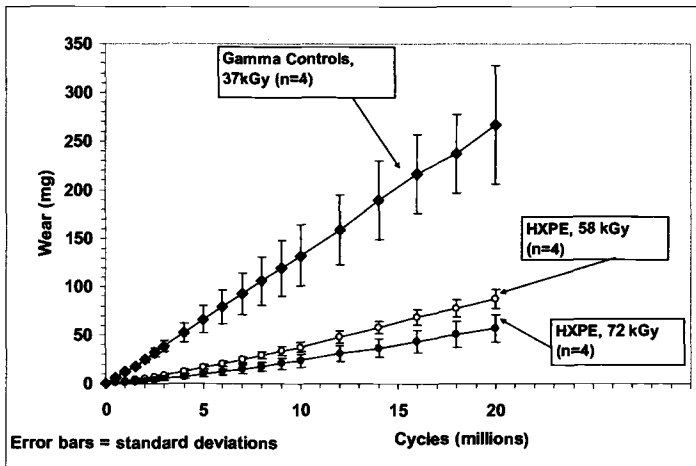
(b) 20 Mc

Figure 5 – *Wear of HXPE and conventional UHMWPE tibial inserts*
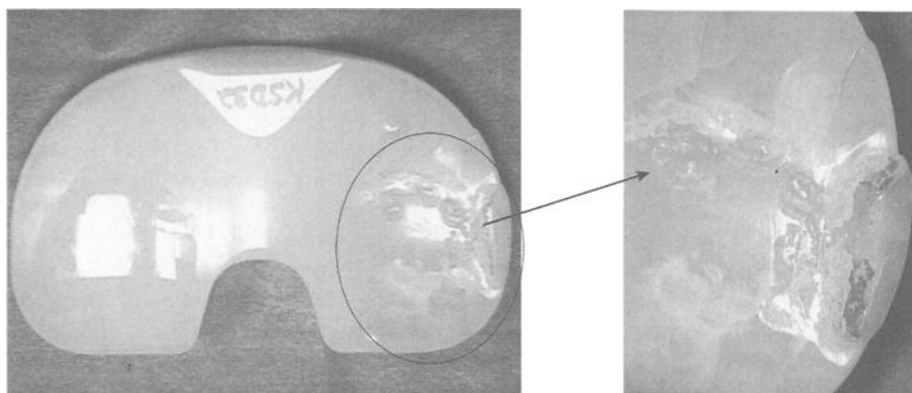
Figure 6 – *Delamination of one gamma control insert observed during wear testing*

Table 1 – *Delamination resistance of HXPE vs. conventional UHMWPE tibial inserts*

Sample ID	Insert Material	Delamination Initiation	Delamination Detachment of loose fragments	End of the Test Outcome
KD 155	Gamma Control 37kGy	1.0 - 1.8 Mc	1.8 Mc	Delaminated (1.8 Mc)
KD 156	Gamma Control 37kGy	5.3 Mc	5.8 Mc	Delaminated (5.8 Mc)
KD 157	Gamma Control 37kGy	1.8 Mc	1.9 Mc	Delaminated (1.9 Mc)
KD 158	Gamma Control 37kGy	3.7 Mc	4.2 Mc	Delaminated (4.2 Mc)
KD 159	Gamma Control 37kGy	1.8 Mc	2.2 Mc	Delaminated (2.2 Mc)
KD 160	Gamma Control 37kGy	1.0 Mc	1.5 Mc	Delaminated (1.5 Mc)
KD 161	HXPE 72 kGy	-	-	Not Delaminated (8.0 Mc)
KD 162	HXPE 72 kGy	-	-	Not Delaminated (8.0 Mc)
KD 163	HXPE 72 kGy	-	-	Not Delaminated (8.0 Mc)
KD 164	HXPE 72 kGy	-	-	Not Delaminated (8.0 Mc)
KD 165	HXPE 72 kGy	-	-	Not Delaminated (8.0 Mc)
KD 166	HXPE 72 kGy	-	-	Not Delaminated (8.0 Mc)
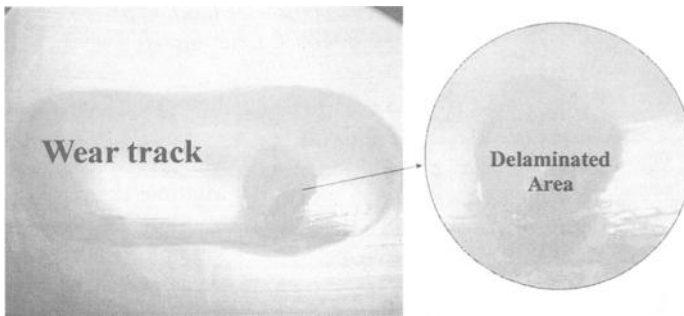
Figure 7 – *A typical example of a delaminated area in the wear track*
(gamma control insert)

Posterior Loading Fatigue Test

   It was found that all five gamma irradiated control inserts developed visible fatigue damage within 2.8 Mc of posterior loading fatigue testing (average 2.2 Mc, ranging from 1.3 to 2.8 Mc) (Table 2). Similar to the onset of delamination, the posterior edge fatigue damage was initiated below the superior surfaces of the inserts in the form of multiple subsurface cracks (Figure 8). The cracks ran predominantly perpendicular to the direction of the sliding motion. Upon further fatigue loading, the subsurface cracks grew in size and propagated towards the superior surface. Indeed, a large fragment of UHMWPE was removed from the posterior edge of one of the gamma control inserts. The test for gamma controls was terminated once fatigue damage has been well developed (3.5 Mc). On the other hand, it was found that none of the five HXPE inserts showed any fatigue damage even after 5 million test cycles. The test for HXPE was terminated at 5 Mc, since at this point the relative resistance to fatigue damage of HXPE and gamma control inserts had been well established.

Subsurface crack as seen
against a back light source
(first observed at 2.8Mc)
(pictured at 3.5 Mc)
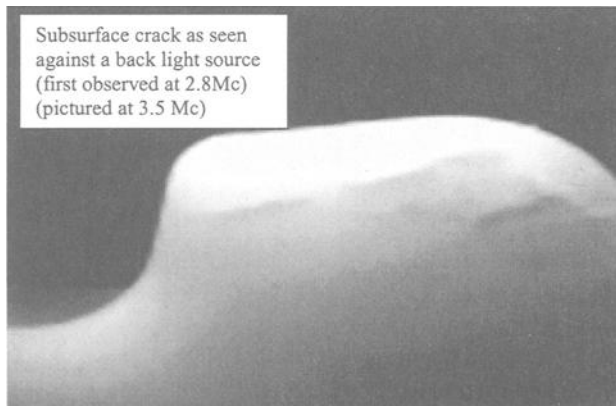
Figure 8 – *A Typical example of posterior edge subsurface fatigue damage*
(gamma control)

Table 2 – *Fatigue resistance to posterior loading of*
HXPE vs. conventional UHMWPE tibial inserts

Sample ID	Insert Material	Fatigue Damage Initiation	End of the Test Outcome
2	Gamma Control 37kGy	2.8 Mc	Multiple Cracks (2.8 Mc)
4	Gamma Control 37kGy	1.3 Mc	Multiple Cracks (3.5 Mc)
6	Gamma Control 37kGy	2.8 Mc	Multiple Cracks (3.5 Mc)
8	Gamma Control 37kGy	2.8 Mc	Multiple Cracks (3.5 Mc)
10	Gamma Control 37kGy	1.3 Mc	Detachment of A Large Fragment (1.3 Mc)
1	HXPE 72 kGy	-	No damage seen (5.0 Mc)
3	HXPE 72 kGy	-	No damage seen (5.0 Mc)
5	HXPE 72 kGy	-	No damage seen (5.0 Mc)
7	HXPE 72 kGy	-	No damage seen (5.0 Mc)
9	HXPE 72 kGy	-	No damage seen (5.0 Mc)

Oxidative Degradation

Oxidation measurements showed that the melt-annealed HXPE and conventional UHMWPE gamma control inserts responded very differently to accelerated oxidative challenge. Their surface oxidation indices were 0.054 ± 0.041 and 0.294 ± 0.024, respectively (Figure 9). Therefore, HXPE was significantly more resistant to oxidation than conventional UHMWPE ($p<0.0001$). This indicates that the melt-annealed HXPE has a significantly lower propensity to become oxidized than the conventional UHMWPE in an oxidative environment, such as that during the accelerated aging in this study.
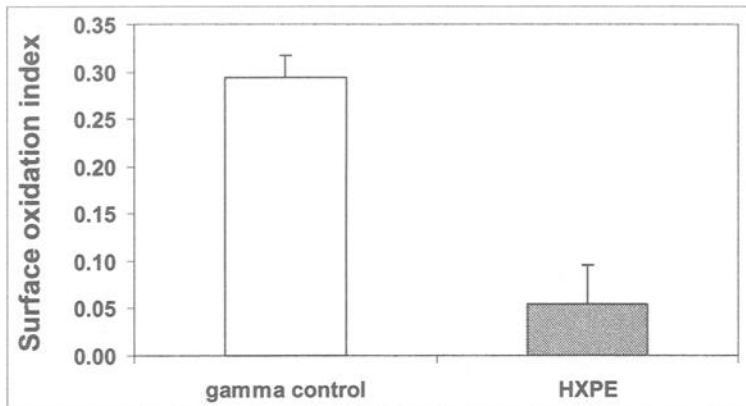
Figure 9 – *SOI of HXPE vs. conventional UHMWPE tibial inserts*

Discussion

Cross-Motion in the Knee Joint

While cross-motion in hip joint kinematics is a well established phenomenon, cross-motion in the knee joint is less well characterized. By using physiological kinematics data

(Figure 2) and a CAD model of the NexGen CR knee joint, the cyclic cross-motion path at any point on the UHMWPE tibial articulating surface can be determined analytically. At any specific time instance during a gait cycle, a specific point on the medial femoral condylar surface is in contact with a corresponding point on the opposing medial tibial condylar surface. Therefore, throughout the whole gait cycle, a fixed point on the superior surface of the UHMWPE tibial insert experiences sequential contacts with a series of points on the opposing femoral condylar surface. The profile formed by this series of points represents the path of cross-motion at this fixed point on the tibial articulating surface. For example, at the lowest point on each of the medial and lateral tibial condylar surfaces, the cross-motion path exhibits an approximate teardrop shape (Figure 10). While the aspect ratio of the cross-motion path, defined as the ratio of its width over its length (1), is less than that for the hip during the gait cycle [10, 18], it is sufficient to cause the molecular re-orientation and, consequently, strain softening of UHMWPE [10]. Consequently, enhanced crosslinking with electron beam irradiation has been shown in this study to reduce significantly the wear of UHMWPE.
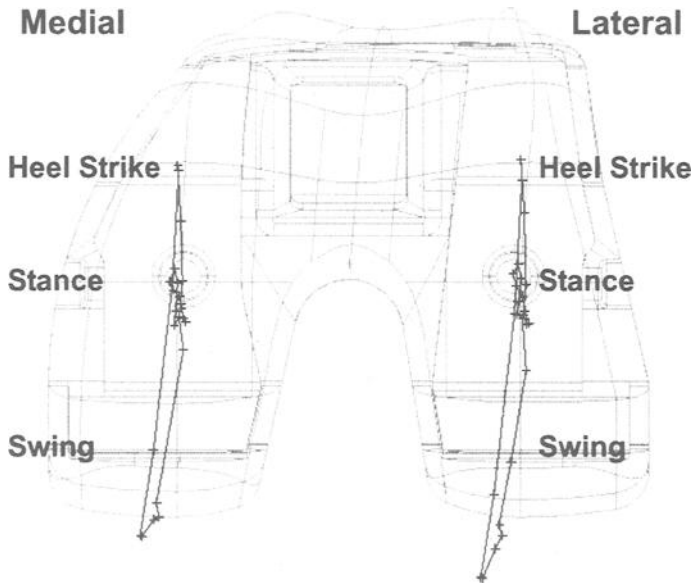
Figure 10 – *Cross-motion paths at one fixed point on each of the femoral condylar surfaces*

Balance between Wear and Mechanical Properties
It is known that, while the wear resistance of UHMWPE increases with the irradiation dose, some mechanical properties decrease concomitantly [2]. On the other hand, it is intuitive that higher mechanical properties are desired for tibial inserts than for acetabular cup liners, because of the higher mechanical stresses generated in the knee joint [16]. Therefore, the electron beam irradiation dose (65 ± 7 kGy) chosen for HXPE NexGen CR

tibial inserts was lower than that chosen for highly crosslinked UHMWPE cup liners (100 ± 10 kGy).

In Vitro and In Vivo Aging

In vitro aging may occur during the storage of UHMWPE components pre-implantation. *In vivo* aging may also take place post-implantation. To minimize the *in vitro* oxidative aging, improved packaging techniques have been introduced where UHMWPE components are enclosed in low oxygen environments (vacuum or inert gases). For instance, UHMWPE cup liners and tibial inserts that were gamma irradiated in nitrogen and stored in nitrogen packages have shown significantly reduced rates of *in vitro* oxidation [19]. However, *in vivo* degradation of conventional gamma irradiated UHMWPE after exposure to the body environment may occur, as shown in its reduced mechanical properties over time *in vivo* [20, 21]. Therefore, the improved oxidation resistance of the melt-annealed HXPE will likely significantly reduce its *in vivo* oxidative degradation potential and preserve its mechanical properties. While UHMWPE components gamma irradiated in nitrogen and packaged in nitrogen pouches have excellent clinical performance so far, melt-annealed HXPE tibial inserts are expected to improve even further the long term performance of TKA. Therefore, HXPE tibial inserts have not only lower wear due to higher crosslink densities, but also improved resistance to delamination and posterior loading fatigue damage relative to conventional UHMWPE when accelerated aged.

Conclusions

A series of newly developed tests have demonstrated that accelerated aged electron-beam irradiated and melt-annealed highly crosslinked UHMWPE has markedly improved resistance to wear, delamination and posterior loading fatigue damage compared to conventional gamma irradiated UHMWPE when accelerated aged. The melt-annealing process largely eradicates the free radicals generated during the irradiation process, resulting in a significantly enhanced oxidation resistant material.

Acknowledgement

References

[1] Horev, A.D. and Weinstein, M., "Orthopaedic Industry Update," *J. P. Mogan Securities Industry Update*, June 28th, 2002, N.Y.

[2] McKellop, H.A., Shen, F.W., Bin, L., Campbell, P. and Salovey, R., "Development of an Extremely Wear-Resistant Ultra-High Molecular Weight Polyethylene for Total Hip Replacements," *Journal of Orthopedic Research, vol. 17*, 1999, pp. 157-167.

[3] Muratoglu, O.K., Bragdon, C.R., O'Connor, D.O., Jasty, M. and Harris, W.H., "A Novel Method of Cross-Linking Ultra-High Molecular Weight Polyethylene to Improve Wear, Reduce Oxidation and Retain Mechanical Properties," *Journal of Arthroplasty, vol. 16,* 2001, pp. 149-160.

[4] Wang, A., Polineni, V.K, Essner, A., Sun, D.C., Stark, C. and Dumbleton, J.H., "Effect of Radiation Dosage on the Wear of Stabilized UHMWPE Evaluated by Hip and Knee Joint Simulators," *Transactions of the 23rd Society Congress on Biomaterials,* 1997, p. 394.

[5] Laurent, M.P., Yao, J.Q., Bhambri, S.K., Gsell, R.A., Gilbertson, L.N., Swarts, D.F. and Crowninshield, R.D., "High Cycle Wear of Highly Crosslinked UHMWPE Acetabular Liners Evaluated in a Hip Simulator," *Transaction of the 46th Annual Meeting of Orthopaedic Research Society,* 2000, p. 567.

[6] Oonishi, H., Saito, M. and Kadoya, Y., "Wear of High Dose Gamma Irradiated Polyethylene in Total Joint Replacement - Long-Term Radiological Evaluation," *Transaction of the 44th Annual Meeting of Orthopaedic Research Society,* 1998, p. 97.

[7] Wroblewski, B.M., Siney, P.D. and Fleming, P.A., "Low-Friction Arthroplasty of the Hip Using Alumina Ceramic and Crosslinked Polyethylene," *Journal of Bone and Joint Surgery (Br),* vol.81(B), 1991, pp. 54-55.

[8] Grobbelaar, C.J., Du Plessis, T.A. and Marais, F., "The Radiation Improvement of Polyethylene Prosthesis," *Journal of Bone and Joint Surgery (Br),* vol.60(B), 1978, pp.370-374.

[9] Pooley, C.M. and Tabor, D., "Friction and Molecular Structure: The Behaviour of Some Thermoplastics," *Proceedings of the Royal Society of London,* vol. 329, 1972, pp.251-258.

[10] Wang, A., Sun, D.C., Edwards, B., Sokol, M., Essner, A., Polineni, V.K., Stark, C. and Dumbleton, J.H., "Orientation Softening in the Deformation and Wear of Ultra-High Polyethylene," *Wear,* vol. 203/204, 1997, pp. 230-241.

[11] Johnson, T.S., Laurent, M.P. and Yao, J.Q., "The Tibiofemoral Cross-Motion Pattern and Its Effect on the Wear of a Prosthetic Knee," *Transaction of the 28th Annual Meeting of Society for Biomaterials,* 2002, p. 191.

[12] Ramamurti, B., Estok, D.M., Muratoglu, O.K. and Harris, W.H., "Comparison of Paths Traced by Points on the Polyethylene Surface in THA and TKA," *Transaction of the 45th Annual Meeting of Orthopedic Research Society,* 1999, p. 823.

[13] Williams, I.R., Mayor,M.B. and Collier, J.P., "The Impact of Sterilization Method on Wear in Knee Arthroplasty," *Clinical Orthopedics and Related Research,* vol. 356, 1998, pp. 170-180.

[14] Won, C.H., Rimnac, C., Goldberg, V., Kraay, M. and Rohatgi, S., "Effect of Resin Type and Manufacturing Method on Wear Damage Modes in MG I and MG II UHMW Polyethylene Tibial Components," *Transaction of the 25th Annual Meeting of the Society for Biomaterials,* 1999, p.302.

[15] Bhambri, S., Gsell, R., Kirkpatrick, L., Gilbertson, L.N., Swarts, D.F., Blanchard, C.R. and Crowninshield, R.D., "The Effect of Aging on Melt-Annealed Cross-Linked Polyethylene," *Transaction of the 28th Annual Meeting of the Society for Biomaterials,* 2002, p.58.

[16] Bartel, D.L., Nicknell, V.L. and Wright, T.M., "The Effect of Conformity, Thickness and Material on Stresses in Ultra-High Molecular Weight Components for Total Joint Replacement," *Journal of Bone and Joint Surgery (Am),* vol. 68A, 1986, pp. 1041-1051.

[17] Johnson, T.S., Laurent, M.P., Yao, J.Q. and Gilbertson, L.N., "The Effect of Displacement Control Input Parameters on Tibiofemoral Prosthetic Knee Wear," *Wear,* vol. 250, 2001, pp.222-226.

[18] Ramamurti, B.S., Bragdon, C.R., O'Connor, D.O., Lowenstein, J.D., Jasty, M., Estok, D.M. and Harris, W.H., "Loci of Movement of Selected Points on The Femoral Head During Normal Gait: Three-Dimensional Computer Simulation," *Journal of Arthroplasty,* vol. 11, 1996, pp.845-852.

[19] Edidin, A.A., Muth, J., Spiegelberg, S. and Schaffner, S., "Sterilization of UHMWPE in Nitrogen Prevents Oxidative Degradation for More Than Ten Years," *Transaction of the 46th Annual Meeting of Orthopedic Research Society,* 2000, p. 1.

[20] Hardaker, C.S., Fisher, J., Issac, G., Stone, M. and Older, J., "Quantification of the Effect of Shelf and *In Vivo* Aging on the *In Vivo* and *In Vivo* Wear Rates of a Series of Retrieved Charnley Acetabular Cups," *European Society of Biomaterials,* 2000.

[21] Edidin, A.A., Villaraga, M.L., Herr, M.P., Ciccarelli, L., Hozack, W., Turner, W. and Kurtz, S.M., "Relationship between Clinical Performance and Mechanical Behavior of Retrieved UHMWPE Acetabular Liners," *Transactions of the 28th Annual Meeting of the Society for Biomaterials,* 2002, p. 25.

Donald E. McNulty, [1] *Stephen W. Swope,* [2] *Daniel D. Auger,* [3] *and Todd Smith* [4]

The Effect of Crosslinking UHMWPE on In Vitro Wear Rates of Fixed and Mobile Bearing Knees

ABSTRACT: This study evaluated the wear performance of conventional (gamma irradiation at 4Mrads in low oxygen) and moderately crosslinked (gamma irradiation at 5Mrads and melt-annealed) ultra high molecular weight polyethylene (UHMWPE) materials in fixed and mobile knee bearing designs. Kinematic and load inputs corresponding to the gait cycle outlined in the ISO displacement controlled knee simulation draft standard, ISO/CD 14243-3, were maintained in all simulations. Wear rates were determined gravimetrically. Surface finish changes and worn surface characteristics were also noted. Moderately crosslinked fixed bearing knee component wear rate was 74% lower than conventional fixed bearing components. There was no discernable difference in wear rate for the mobile bearing knee for the two materials. However, the mobile bearing knee wear rates were 94% and 79% lower than fixed bearing conventional and fixed bearing moderately crosslinked materials, respectively. In the fixed bearing knee, the majority of the wear reduction of the moderately crosslinked material compared to the conventional material was attributed to enhanced crosslinking due to the melt-annealing process rather than the dose difference. The reduction in wear rate of the mobile bearing knee compared to the fixed bearing was attributed to the reduced cross shear motion at the tibio-femoral articulation since mobile bearing wear was independent of material.
KEYWORDS: In Vitro Wear, Mobile Bearing Knee, Fixed Bearing Knee, Crosslinked UHMWPE

Introduction

A key factor to long-term success of total knee arthroplasty (TKA) is the ability of the polymeric bearing material to resist fatigue failure and excessive particulate debris generation linked to osteolysis [1]. These failure modes have been associated with shelf aged, gamma in air irradiated components that oxidized [2]. Since the introduction of

---

[1] Materials Research Fellow, [2] Senior Laboratory Technician, [3] Engineering Fellow, [4]Director of Materials Research, [1,2,4] Materials Research Department and [3]Product Development Department, DePuy Orthopaedics, Inc., 700 Orthopaedic Drive, Warsaw, IN, 46581.

73

TKA, technical developments in UHMWPE processing and terminal product sterilization has lead to improved clinical performance. Current UHMWPE sterilization-processing methods used for knee bearings include: sterilization by gas plasma or ETO with no resultant crosslinking; sterilization using gamma irradiation in a low oxygen environment that results in minor crosslinking and residual free radicals; and gamma or ebeam irradiation followed by a thermal treatment to promote crosslinking and reduce free radicals known to cause oxidation [3-5]. The extent of crosslinking for this latter approach can be modulated by the radiation dose, which has also been shown to effect mechanical properties [6]. A dose of 5 Mrads followed by melt-annealing is considered to result in a moderately crosslinked material. A dose of 10 Mrads with subsequent melt-annealing yields materials that are considered to be highly crosslinked because no further improvements in wear is achieved with additional irradiation.

Gamma irradiation in a low oxygen package represents the industry convention. Irradiated and melt-annealed crosslinked polyethylenes have recently been integrated into several existing fixed bearing total knee implant systems. Fixed bearing knee simulator testing has revealed appreciable wear improvement with crosslinked UHMWPE compared to conventional UHMWPE [3-5]. The purpose of this study was to compare the in vitro wear rates of conventional and moderately crosslinked UHMWPE bearings in both fixed and mobile knee bearing designs using standardized knee simulator inputs.

Materials and Experimental Methods

Tested Materials

Fixed knee bearing and mobile knee bearing components were selected from the P.F.C. ® Sigma Knee System (DePuy Orthopaedics, Inc., Warsaw, IN). The femoral component (size 3) was common to both the fixed and mobile systems and manufactured from cast CoCrMo alloy in accordance with the ASTM Specification for Cobalt-28 Chromum-6 Molybdenum Casting Alloy and Cast Products for Surgical Implants (F 75). Mobile bearing tibial components were machined from cast CoCr (F 75) and fixed bearing tibial tray components were machined from Ti–6AL-4V alloy in accordance with the ASTM Specification for Alpha Plus Beta Titanium Alloy Forgings for Surgical Implants (F 620).

Tibial insert bearings were produced from UHMWPE and were processed to result in either moderately crosslinked or conventional material. Conventional components were machined from 1020 compression molded sheet. These components were gamma sterilized in a foil bag that was initially evacuated and subsequently purged with inert gas and sealed. The components were gamma irradiated to a dose of 40±2 kGy. Moderately crosslinked components were machined from 1050 ram extruded bar and gamma irradiated to 50±5 kGy. After irradiation, the bar was heated to 155° C for 24 hours to promote enhanced crosslinking and extinguish free radicals formed during irradiation. A post annealing process was also employed. All bearing insert and tray combinations corresponded to the size 3, 10 mm composite thickness. The fixed bearing inserts were machined with the curved geometry, which includes a combination of tangent radii in the sagital plane resulting in anterior and posterior constraint. The mobile bearing inserts were machined with one continuous radius in the sagital plane. All inserts were considered to have high conformity with the femoral component in the coronal plane.

Simulation Inputs

Components were tested using six-station knee simulators (AMTI, Watertown, MA) with closed loop servo-hydraulic control. Compressive joint load, flexion-extension (F-E), internal-external rotation (I-E) and anterior-posterior displacement (A-P) were programmed for the gait cycle in accordance with the draft ISO displacement controlled knee simulation standard; Implants for surgery-Wear of total knee joint prostheses-Part 3: Loading and displacement parameters for wear testing machines with displacement control and corresponding environmental conditions for tests (ISO/CD 14243-3). Tested input profiles (Figure 1) and the resultant range of simulation inputs (Table 1) are provided.

It should be noted that the sagital conformity of both the fixed and mobile components required modification to the A-P displacement input profile. The draft standard specifies that the A-P displacement correspond to the femoral component displacement with the starting position at the low point of the tibial insert in the sagital plane. In low sagital conformity designs, this programmed input is feasible. However, the combination of the specified starting position and conformity of the tested components resulted in excessively posterior positioning of the femoral contact point. The ISO stipulated positioning permits the femoral component to contact the posterior ridge of the tibial insert for a substantial portion of the duty cycle. To alleviate this and to permit tibio-femoral contact typically encountered in the clinical setting, the A-P displacements were interpreted to correspond to the tibio-femoral contact point rather than the femoral component displacement. This was accomplished through the use of computer modeling that accounted for the tibial and femoral geometries as well as the fixturing of the femoral components on the F-E shafts.

It is recognized that the kinematics of mobile and fixed bearing devices may be different clinically. It must also be recognized that different kinematics may result from patient variation even with the same surgeon and same knee design due to surgical and anatomic variability. Both the fixed and mobile devices of this study are cruciate retaining designs. It therefore seemed reasonable to use the same kinematic movement for both devices as if they were implanted in the same patient with the same ligamentous stability and other soft tissue constraints. In this regard, the intentional use of common A-P tibio-femoral displacement was employed to elicit the effect of certain variables (fixed vs mobile and UHMWPE processing) by reducing the effect of the A-P sliding distance, a variable which has been shown to effect wear. [7]
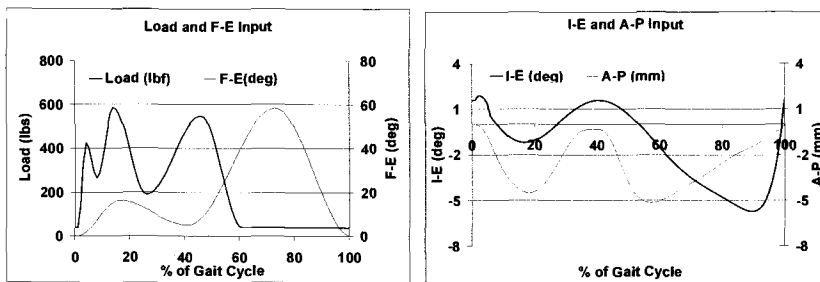
Figure 1- *Simulation input profiles*

Input Description	Load (Lbf)	Flexion/ Extension	Tibio-Femoral contact pt. Displacement	Internal(-) External(+) Tibial Rotation
ISO/CD 14243-3	40- 585 lbf	0°-58°	0-5.2 mm	+1.9° to −5.7°

Table 1– *Simulation Input Ranges and Magnitudes*

Component Fixturing

Tibial trays were secured to fixtures with acrylic cement (KERR self curing plastic-Romuls, MI) with 3 degree posterior slopes as prescribed in the surgical protocols. Positioning the medial-lateral centerline of the tibial tray component approximately 5mm medial relative to a pivot integral to the fixture retaining the tibial tray resulted in an approximate 60% medial - 40% lateral compartmental distribution of the compressive loads. The offset stipulated in the ISO draft standard is 0.07 times the medial-lateral width of the tray. For the components tested, this value is approximately 5mm.

Mobile bearing inserts readily assembled into tibial trays due to the insert taper-tray cone geometry. The fixed bearing inserts were locked into tibial trays fitted with modified locking mechanisms that permitted easy disassembly without affecting the integrity of the locking mechanism. Femoral implants were also cemented to F-E shaft assemblies of the simulator. A typical mobile bearing setup is depicted (Figure 2).
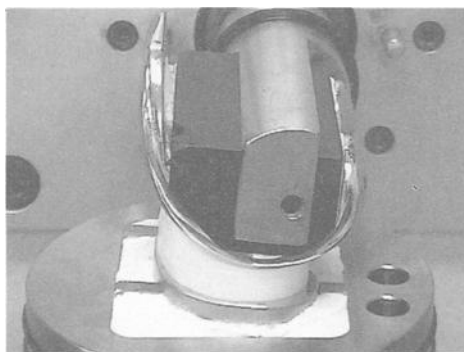
Figure 2 – *Typical fixturing setup of tibial and femoral components*

Simulation Protocol

Multiple wear simulations were conducted using a minimum of three replicates for each fixed and mobile knee variation. Test duration was 6M cycles run at 1Hz. Wear was measured gravametrically using a Satorius model R-200D digital microbalance (Long Island, NY) with 0.01 mg resolution and in accordance with the ASTM Test Method for Gravimetric Measurement of Polymeric Components for Wear Assessment (F 2025). Soak controls were used to account for wear specimen fluid absorption. Weight loss measurements were taken every 0.5M cycles which corresponded to the lubricant change

intervals. Tests used 90% bovine calf serum (Hyclone Laboratories, Logan, UT) maintained at $37° \pm 2°$ C via recirculation. The serum was treated with sodium azide at a concentration of 0.2 % mass fraction to retard bacterial growth and with ethylenediaminetetraacetate acid (EDTA) at a concentration of 20mM (7.45 g/L) to prevent calcium precipitates. Periodic data was accrued from six component force/torque cells fitted on each station which permitted monitoring moments and forces at the tibio-femoral articulation. Statistical analysis for wear rates was conducted using student t tests.

Articulating Surface Evaluation

The articular surfaces of the femoral and tibial tray components were evaluated at 1M cycle increments visually, photographically (Sony DCR-PC1 digital camera), and with profilometry. Tibial inserts were examined using a stereomicroscope (Wild Heerbrugg) for burnished and scratched regions. Image documentation of the tibial inserts was made with a digital camera (DXM 1200 Nikon) fitted onto an available aperture of the stereomicroscope.

Profilometry

Profilometry was conducted on the tibial trays and femoral components at consistent locations every 1M cycles using a Rank Form Talysurf Series 2 contact profilometer (Taylor Hobson, Liecester, UK). Trays were evaluated at posterior locations in the medial and lateral compartments beneath the high load area of the tibio-femoral articulation. Traces on the mobile bearing trays were oriented radially from the central cone and medial to lateral on the fixed bearing trays (Figures 3a and 3b). Femoral components were assessed on each condyle with stylus traces directed medial-lateral at femoral contact locations corresponding to the stance phase of gait (Figure 3c). Accrued surface finish parameters included Ra and Rpm, which were evaluated for wear rate effect. Surface profilometer settings were: gaussian filter, cutoff .25mm, trace length 4mm, stylus radius 1.5um, 100:1 low pass cutoff and bandwidth.
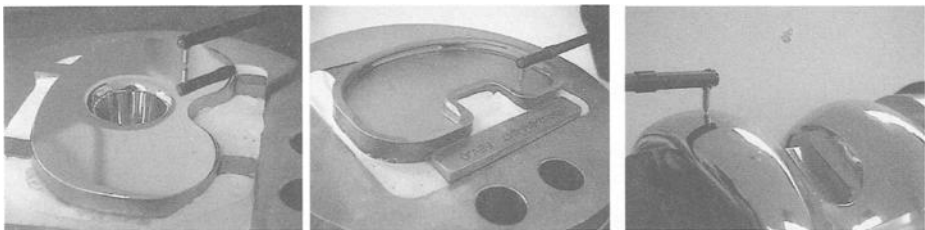
3a. *Mobile bearing tibial tray*   3b. *Fixed bearing tibial tray*   3c. *Common femoral component*

Figure 3- *Profilometry trace orientation for tibial trays and femoral components*

Results and Discussion

Wear

The average wear versus test cycles of each implant design and material combination are reported (Figure 4). Average wear rates per million cycles of testing were calculated using linear regression for each specimen within an implant design and tibial insert material combination (Figure 5). Statistically significant differences in wear rate were found for the following comparisons:
a. Fixed bearing conventional to fixed bearing moderately crosslinked ($p<0.01$);
b. Fixed bearing conventional and moderately crosslinked to mobile bearing conventional ($p<0.01$ in both cases); and
c. Fixed bearing conventional and moderately crosslinked to mobile bearing moderately crosslinked ($p<0.01$ in both cases).
A statistically significant difference was not found between the mobile bearing conventional and moderately crosslinked wear rates ($p=0.458$).

Fixed Conventional to Fixed Moderate Crosslinked Comparison

The statistically significant difference in the wear rates between fixed bearing conventional material and moderately crosslinked material is consistent with the literature [4, 8, 9]. This difference corresponded to a 74% reduction in wear of the moderately crosslinked fixed bearing knee components compared to the conventional fixed bearing components. A postulated mechanism for the improved wear resistance with increased crosslinking relates to reduced mobility of molecular chains [10-12]. Increased
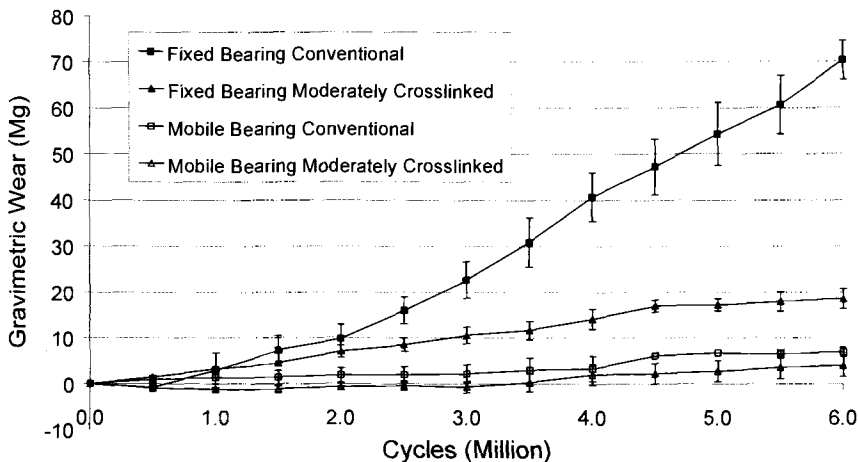
Figure 4 – *Wear vs Cycles*
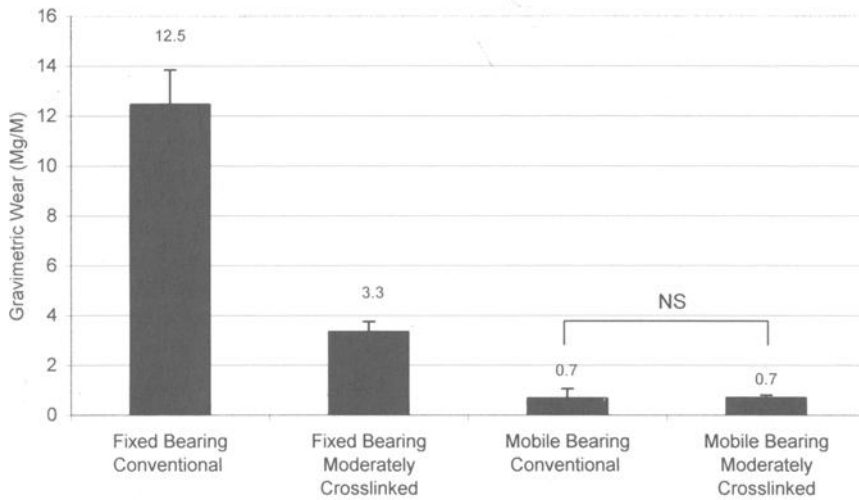
Figure 5- Wear Rates mg/M cycles

crosslinking increases bonds between adjacent chains in the polymer network that, in turn, resist strains that are imparted during articulation of the femoral component on the tibial insert [10]. These strains result from adhesive forces due to bonding of surface asperities and abrasion with the microroughened surface of the metal counterface that plow the softer UHMWPE [1]. With the repetitive motion, these adhesive and abrasive actions eventually generate a critical strain resulting in the release of wear particles [13]. Thus with increased crosslinking, a stronger molecular network results that reduces the accrued strain leading to a lower volume of particle generation.

The swell ratio correlates with the wear resistance of a polymer as it is a measure of the frequency of molecular bonds between adjacent chains and chain entanglement that resist external forces. The conventional material in this study typically has swell ratio values in the 5 to 7 range using the ASTM Test Method for Determination of Gel Content and Swell Ratio of Crosslinked Ethylene Plastics (D 2765). The moderately crosslinked material achieves swell ratios below 3.5. These values agree with the wear ranking of the polymers. Swell ratio may therefore be considered as the ability to resist movement of molecular chains, which is the precursor to accrual of the critical strains that result in the generation of wear debris.

Mobile Bearing Comparisons and Mobile to Fixed Bearing Comparisons

There was no discernable difference in wear rates between the two materials in the mobile bearing system. However, mobile bearing knee wear rates (both materials) were 94% and 79% lower than fixed bearing conventional and moderately crosslinked materials, respectively. The significant difference in the wear rates between the fixed bearing and mobile bearing materials has previously been demonstrated by McEwen under different input conditions [11, 12]. In this study, rotating platform mobile bearing

tibial inserts were manufactured from gas plasma sterilized (non crosslinked) 1050 REB UHMWPE and tested against sagitally curved fixed bearing insert designs manufactured with conventional 1020 CMS gamma vacuum foil (GVF) sterilized components. The design of the mobile bearing insert limited motion to rotation about a central taper, similar in concept to the components of the subject study. Compressive loads and F-E were maintained in simulation tests for both the fixed and mobile components. Inputs for the fixed bearing were displacement controlled for A-P and I-E, while these inputs for the mobile bearing were force controlled. The study demonstrated that the mobile bearing design wore at ~1/3 the rate of the fixed bearing design. The authors acknowledged that the different A-P and I-E inputs could have played a beneficial role in the mobile bearing wear rate. It was also noted that these wear rates were in lieu of greater tibio-femoral contact area for the mobile bearing and an additional tibial wear surface for the mobile bearing.

The mechanism for the reduced wear of the mobile bearing designs compared to the fixed bearing designs was discussed by McEwen and colleagues and applies to the tests that are the subject of this paper. It was proposed that the mobile bearing design reduces cross-shear motion at the tibio-femoral interface by decoupling the tibial insert from the tray. Less cross-shear, or motion transverse to the principal direction of motion at the tibio-femoral articulation, results in less transverse strain imparted to the UHMWPE (principal motion was considered as A-P from the F-E input). As previously discussed, less transverse strain reduces wear. The mobile bearing design converts cross-shear to reciprocating motion without cross-shear at the tray-insert interface. Reciprocating motion without cross-shear is recognized as exhibiting up to an order of magnitude lower wear compared to motions that have cross shear [10]. This mechanism also explains why there was no difference in wear rates for the conventional and moderately crosslinked bearing materials used in the mobile bearing components that are the subject of this paper.

In another study by Bell and colleagues, fixed and mobile bearing knee designs were produced from the same UHMWPE material (the sterilization process was not defined) [14]. The devices were subjected to identical gait cycle inputs for displacement and compressive load. The results after 5M cycles indicate the fixed bearing design exhibited ~ 40 % lower wear rates than the mobile bearing design. In an extension of the study, only the mobile bearing inputs for I-E and A-P translations were doubled. The reported basis for this was that a higher degree of mobility might be experienced in-vivo. Comparison of the fixed bearing and mobile bearing wear rates disclosed an ~ 70% reduction in the wear rate of the fixed bearing for these conditions. The contradictory findings of this study were puzzling but the following explanation is offered. Although not fully described in this paper, the mobile bearing device tested by Bell may have permitted rotational freedom of the tibial insert relative to the tray in addition to A-P translation at this interface. The combination of these two movements could generate motions at the tray-insert interface that are no longer limited to reciprocating rotation as in the present and McEwen studies. The added degree of freedom allows motion transverse to the principal A-P motion from F-E. This produces the cross-shear motion, that as previously discussed, is known to generate greater wear compared to reciprocating motion. The tray-insert interface can therefore generate wear comparable to the tibio-femoral articulation. It is therefore postulated that mobile bearing designs that permit

A-P and I-E movements can perform dramatically different than those that are restricted to I-E freedom by design.

Articulating Surface Examination

Examination of femoral components for both fixed and mobile knee bearing designs disclosed scratches consistently oriented in the A-P direction corresponding to the direction of principal motion due to F-E (Figures 6a and 6b). Fixed bearing tibial tray components showed occasional stippling on the proximal surface (Figure 7a). Mobile bearing knee tibial trays disclosed evidence of circumferential scratches consistent with the movement permitted between the tray and insert (Figure 7b). Both features are commonly found on retrieved bearing components.

Examination of tibial insert components disclosed features common to both UHMWPE materials. Wear scars consisting of burnished and scratched regions were present at the proximal tibio-femoral articulation surfaces for both fixed (Figure 8a) and mobile bearing inserts (Figure 8b). The distal surface (or backside) of the fixed bearing inserts display mild burnishing in the region corresponding to high loading. The distal surface of the mobile bearing inserts displayed circumferential scratches complementary to those on the tray (Figure 9).

6a. *Fixed bearing*   6b. *Mobile bearing*
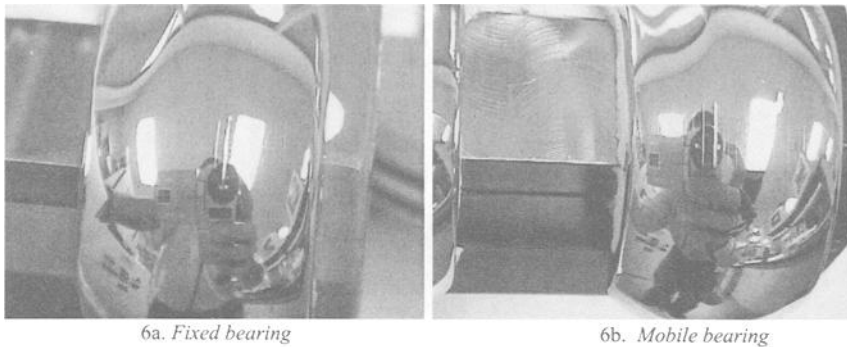
Figure 6 – *Typical A-P oriented scratches observed for femoral components used with fixed (6a) and mobile (6b) systems.*

7a. *Fixed bearing*   7b. *Mobile bearing*
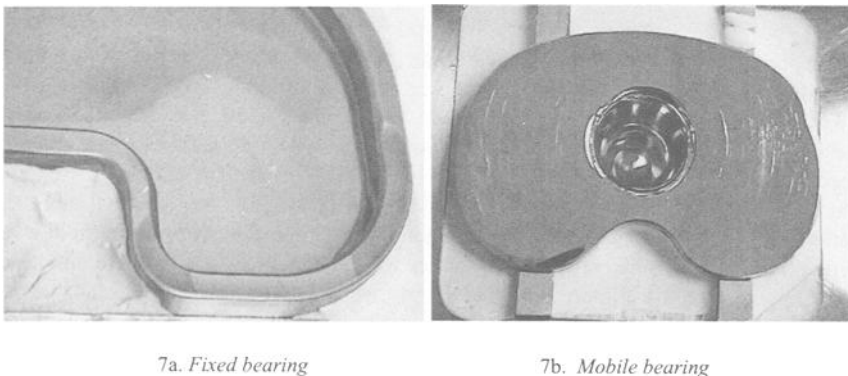
Figure 7- *Fixed and mobile bearing tibial trays*

8a. *Fixed bearing*   8b. *Mobile bearing*
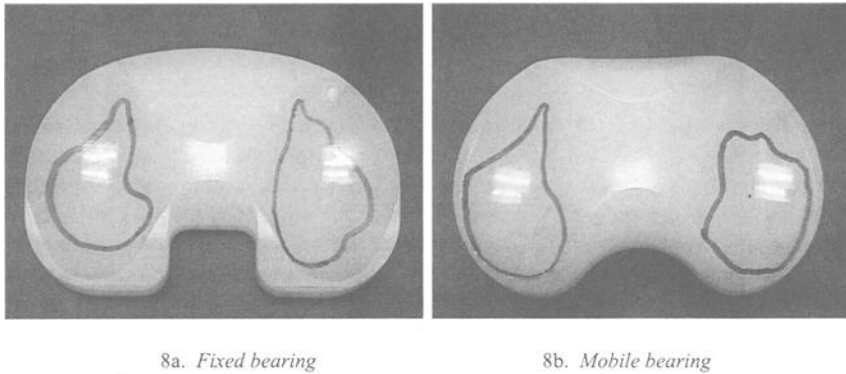
Figure 8- *Typical wear scars and burnishing on proximal surface of fixed and mobile bearing tibial inserts*
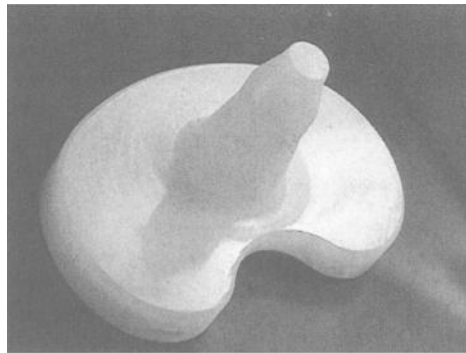
Figure 9- *Typical burnishing on distal surface of mobile bearing tibial inserts*

Profilometry

The pre- and post-test Ra and Rpm surface roughness values are provided for all test configurations for the femoral components (Figure 10) and tibial tray components (Figure 11). The difference of pre- and post-test values had no measurable effect on the wear rate in these tests (Figure 4). The literature often demonstrates an increase in wear rate as surface roughness increases [15]. The probable cause for the lack of effect in this study is that the surface finish irregularities ran in a direction parallel to the principal motion direction, that is, A-P for the femoral components and circumferential for the mobile bearing tibial inserts. Since profilometry traces were made transverse to these directions, the resulting surface finish increases were therefore strongly influenced by scratches that had minimal effect on wear rate.
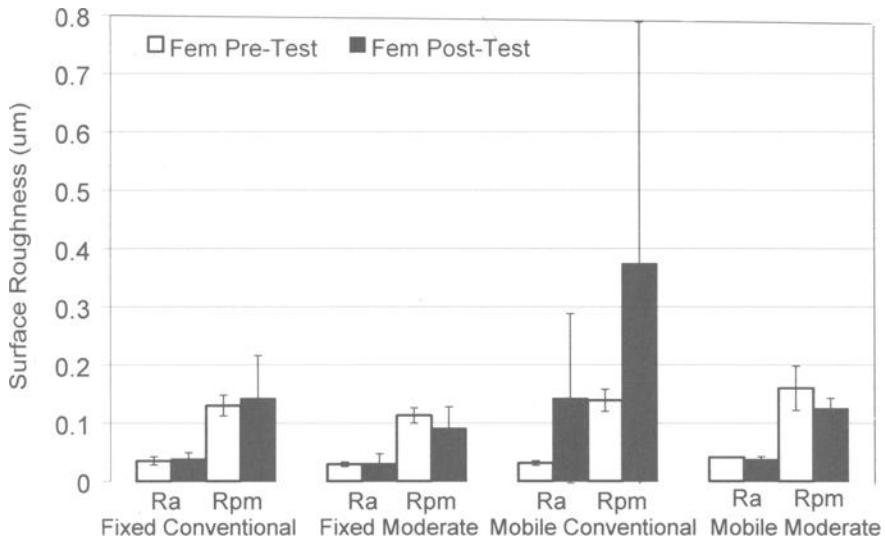
Figure 10 – *Pre- and Post-Test Femoral Component Ra and Rpm values (microns)*
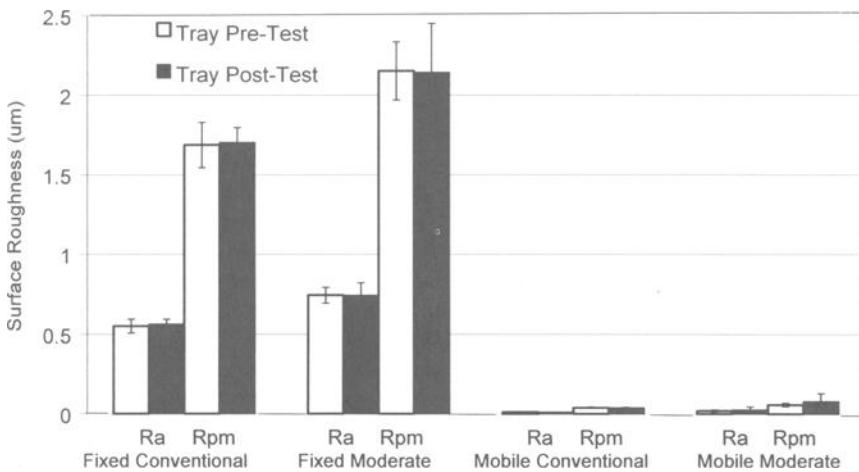
Figure 11 – *Pre- and Pos-Test Tibial Tray Component Ra and Rpm Balues (microns)*

Conclusions

The results of this wear simulation indicate that under identical kinematic inputs, a considerable wear reduction may be realized using moderately crosslinked materials in fixed bearing knee design compared to conventional materials. Additionally, the results

for the mobile bearing knee design used in this study suggest lower wear rates may be attained over fixed bearing designs independent of tibial insert material crosslinking status. It is recognized that the use of identical kinematic inputs for the fixed and mobile bearing tests can be challenged. However, the basic trend of wear reduction of the mobile bearing due to less cross-shear would be maintained due to decoupling the tibio-femoral motions resulting in the reduced wear mode of reciprocating motion compared to cross-shear motion. This conclusion is confirmed by the results of McEwen and colleagues who used A-P load control kinematics for mobile bearings yet obtained an approximate 2/3 reduction in wear rate for the mobile bearing. Additional testing using actual clinical motions from fluoroscopy studies as well as variations in the simulated duty cycle (stair climbing) and simulation parameters (serum concentration) would be beneficial to give a more comprehensive view of the relationships between these total knee designs and bearing materials.

Acknowledgments

References

[1]   Wright, T. M. and Goodman, S., *Implant Wear in Total Joint Replacement*. 1st ed. American Academy of Orthopaedic Surgeons, 2001, pp. 224.

[2]   Currier, B. H., Currier, J. H., Collier, J. P., and Mayor, M. B., "Shelf Life and In Vivo Duration-Impact on Performance of Tibial Bearings," *Clinical Orthopaedics and Related Research*, Vol. 342, 1997, pp. 111-122.

[3]   Yao, J. Q., Gsell, R., Laurent, M. P., Gilbertson, L. N., Swarts, D., Blanchard, C. R., and Crowinshield, R. D., "Improved Delamination Resistance of Melt-Annealed Electron-Beam Irradiated Highly Crosslinked UHMWPE Knee Inserts, *Society for Biomaterials-28th Annual Meeting*, Tampa, FL, 2002.

[4]   Muratoglu, O., Bragdon, C. R., O'Connor, D. O., Perinchief, R. S., Drevolin, J., Rubash, H. E., Jasty, M., and Harris, W. H., "The Extent of Damage Induced by Simulated Adverse Kinematics on Tibial Knee Inserts: Influence of Aging and Crosslinking on a Flat-on-Flat Design," *Society for Biomaterials-28th Annual Meeting*, Tampa, FL, 2002.

[5]   McNulty, D., Mabrey, J. D., Liao, Y. -S., Swope, S., Smith, T., and Agrawal, C. M., "UHMWPE Sterilization and Processing Effects on Wear Particles Morphology for In Vitro Testing of a Fixed Bearing Knee Design," *Society for Biomaterials*, 2001.

[6]   McKellop, H., Shen, F., Campell, P., and Salovey, R., "Development of an Extremely Wear-Resistant Ultra High Molecular Weight Polyethylene for Total Hip Replacement," *Journal of Orthopeadic Research*, Vol. 17, No. 2, 1999, pp. 157-167.

[7]   Johnson, T. S., Laurent, M. P., Yao, J. Q., and Gilbertson, L. N., "The Effect of Displacement Control Inputs on Tibiofemoral Prosthetic Knee Wear." *Society for Biomaterials-Sixth World Biomaterials Congress*, Kamuela, HI, 2000.

[8]   Walker, P., and Zhou, X. M., "The Dilema of Surface Design in Total Knee
        Replacement," *33rd Annual Meeting, Orthopaedic Research Society,* San
        Francisco, CA, 1987.
[9]   McNulty, D. E., King, R., Liao, Y. -S., Smith, T., Greer, K., and Hanes, M.,
        "Wear Rates for a Fixed Bearing Knee System using Crosslinked UHMWPE
        Materials," *Society for Biomaterials-28th Annual Meeting,* Tampa, FL, 2002.
[10]   Marrs, H., Barton, D. C., Jones, R. A., Ward, I. M., and Fisher, J., "Comparative
        Wear Under Four Different Tribological Conditions of Acetylene Enhanced
        Cross-Linked Ultra High Molecular Weight Polyethylene," *Journal of Materials
        Science: Materials in Medicine,* Vol. 10, 1999, pp. 333-342.
[11]   McEwen, H., Fisher, J., Goldsmith, A., Auger, D. D., Hardaker, C., and Stone,
        M., "Wear of Fixed Bearing and Rotating Platform Mobile Bearing Knees
        Subjected to High Levels of Internal and External Tibial Rotation," *Journal of
        Materials Science,* Vol. 12, 2001, pp. 1049-1052.
[12]   McEwen, H., Barnett, P., Farrar, R., Stone, M., and Fisher, J., "Reduction of TKR
        Wear Through The Use of The Rotating Platform Mobile Bearing Design," *48th
        Annual Meeting of the Orthopaedic Research Society,* 2002.
[13]   Wang, A., Stark, C., and Dumbleton, J. H., "Role of Cyclic Plastic Deformation in
        the Wear of UHMWPE Acetabular Cups," *Journal of Biomedical Materials
        Research,* Vol. 29, 1995, pp. 619-626.
[14]   Bell, C. J., Walker, P. S., Sathasivam, S., Campbell, P. A., and Blunn, G.,
        "Differences in Wear Between Fixed Bearing and Mobile Bearing Knees," *45th
        Annual Meeting of the Orthopaedic Research Society,* Anaheim, CA, 1999.
[15]   Dowson, D., Taheri, S., and Wallbridge, N. C., "The Role of Counterface
        Imperfections in the Wear of Polyethylene," *Wear,* Vol. 119, 1987, pp. 277-293.

Michel P. Laurent,[1] Cheryl R. Blanchard,[1] Jian Q. Yao,[1] Todd S. Johnson,[1] Leslie N. Gilbertson,[1] Dale F. Swarts,[1] and Roy D. Crowninshield[1]

The Wear of Highly Crosslinked UHMWPE in the Presence of Abrasive Particles: Hip and Knee Simulator Studies

ABSTRACT: The *in-vitro* wear behavior in the presence of abrasive particles was determined for two highly crosslinked ultrahigh molecular weight polyethylenes (HXPE), one in clinical application for hips and the other for knees. The wear studies were performed in joint simulators and were largely comparative, with conventional ultrahigh molecular weight polyethylene (UHMWPE) gamma irradiated 37 kGy in nitrogen used as the control. The test methodology used for these three-body wear tests was developed in-house. It was found that the wear advantage of the HXPEs relative to the conventional UHMWPE observed under clean conditions is largely preserved in the presence of the abrasive particles used (alumina and bone cement for hips, bone cement for knees) under the test conditions. These results suggest that the surface molecular chain orientation inhibition mechanism proposed to account for the increased wear resistance of highly crosslinked polyethylenes undergoing micro adhesive/abrasive wear is still operational even when a thicker surface layer is disturbed in the presence of abrasive particles. Therefore, the wear of the UHMWPE is not simply dependent on the bulk mechanical properties of the UHMWPE. The higher than expected wear of the 22 mm hip liners compared to the 32 mm liners in the presence of abrasive particles suggests that the wear rate of the UHMWPE becomes stress dependent rather than load dependent for sufficiently high stresses.

KEYWORDS: wear, three-body, hip, knee, UHMWPE, crosslinked polyethylene

---

[1] Principal Engineer, Vice President of Research and Biologics, Principal Engineer, Director of Analytical and Experimental Mechanics, Director of Research Processes, Director of Process Technology, and Chief Scientific Officer/Senior Vice President, respectively, Research Department, Zimmer, Inc., P.O. Box 708, Warsaw, IN, 46581-0708.

86

Introduction

The reduction in *in-vitro* wear achieved with highly crosslinked UHMWPE (HXPE) compared to conventional UHMWPEs has been well documented in recent years [1-4]. However, these data were mostly obtained under clean lubricant conditions. There is much less data pertaining to the wear behavior of HXPE under adverse three-body wear conditions that may also have clinical relevance. For example, Pizzoferrato et al. [5], report that cement wear fragments ranging from 10 to 100 µm are a frequent finding in the soft tissue membrane of failed prostheses, and that larger particles are also present. More recently, Muratoglu et al. [6] have observed substantial scratching on the articular surface of some explanted UHMWPE acetabular cup liners removed after only a few months of implantation for causes not related to the wear performance of the liner. This paper presents the results of hip wear tests performed with bone cement (BC) and alumina particles added to the lubricant and of knee wear tests performed with the addition of bone cement particles. The test methodologies were developed in house.

The objective of this study was to determine the effect of added abrasive on the wear rate of UHMWPE, comparing HXPE with conventional UHMWPE and knee with hip prostheses. In particular, it was desired to determine if the significant wear advantage of HXPE under clean conditions is maintained in the presence of added abrasive particles.

Materials and Methods

Hip Wear Tests

Longevity[®2] HXPE and conventional UHMWPE *Trilogy*[®] Acetabular System[2] liners with articular diameters of 22 and 32 mm were articulated against standard wrought Co-Cr-Mo heads. All the liners, conventional and HXPE, were machined from the same compression molded GUR 1050 UHMWPE lot. The HXPE liners were machined from bars of UHMWPE crosslinked by irradiation with an electron beam (e-beam) at a dose of 110 kGy and subsequently melt-annealed to reduce the free radical concentration to undetectable levels as measured by electron spin resonance. The dose of 110 kGy represents the upper extreme of the process control range (100 ± 10 kGy) for *Longevity* and is considered worst case under adverse mechanical conditions such as three-body wear. The control liners were sterilized by gamma radiation in nitrogen at 37 kGy, whereas the HXPE liners were gas plasma-sterilized two cycles. The liners were artificially aged under pressurized oxygen (73 psi) at 70°C for 14 days, according to Method B in ASTM Standard Guide for Accelerated Aging of Ultra-High Molecular Weight Polyethylene1 Standard (F 2003).

The hip wear tests were performed in a 12-station, biaxial rocking motion (23°) hip simulator (Shore Western Manufacturing, Inc., Monrovia, CA). The run configuration used was with the cup below the head, which was advantageous for the ingress and maintenance of particles into the articulating interface. A Paul-type loading curve [7], with a peak load of 2500 N and a minimum load of 250 N, was used. The lubricant was bovine calf serum (JRH Biosciences, Lenexa, Kansas) containing 3 g/L sodium azide (bactericide) and 9 g/L disodium EDTA and diluted with water to 25% of its original

concentration, resulting in a total protein concentration of 16 ± 2 g/L. The test chamber of each hip was cleaned and a fresh charge of lubricant (125 g) was introduced every half million cycles (Mc). A fresh charge of particulates was also introduced at that time, except that the addition of alumina was discontinued after 3 Mc because of the large number of particles cumulatively embedded in the liners.

The amount added and the nature of the particulates were as follows. For the alumina particles, 16 mg of 60-grit alumina (Washington Mills, Niagara Falls, New York) were added per 125 g charge of lubricant. The 60-grit rating corresponds to an average particle size of 300 to 400 µm, and the number of particles added per charge was on the order of 600. For the bone cement particles, 125 mg were added per 125 g charge of lubricant. The bone cement particles were made by pulverizing cured Osteobond[®]2 bone cement in a tumbler and sieving the resulting powder through a 250 µm screen. The alumina particles were used for a worst case scenario and because they are a possible implant contaminant from surface blasting processes [8]. The quantity of alumina particles added was sufficient to provide approximately equal ingress of particles in all the hip joints. The quantity of bone cement was somewhat arbitrary given the paucity of in vivo data. Pulse lavage irrigation studies by Sharley and McGuigan [9] for the removal of particulate debris after cemented total knee arthroplasty found an average of 150 mg of PMMA and other dichloromethane-soluble organics and 180 mg of bone particles, suggesting the quantity of 125 mg of bone cement particles used here per joint is reasonable. A greater mass of bone cement than alumina particles was used because, unlike alumina particles, bone cement particles are ubiquitous in vivo [5].

Two sets of hip wear tests or simulator runs were conducted, each involving 12 hips. Alumina particles were used in the first run and bone cement particles in the second run. The wear of the cup liners was determined gravimetrically by weighing them every half million cycles. The duration of the wear tests was 5 million cycles, except for one 22 mm conventional liner running in the presence of alumina particles, which had to be stopped after 4 Mc due to excessive wear.

To compensate for fluid absorption by the UHMWPE, three "load-soak" samples were also run for each liner group, along with the wear samples. The load-soak samples were loaded similarly to the wear samples but without the flexion-extension motion of the femoral component. The gain in weight of the load-soak samples was taken to be the amount of fluid absorbed by the wear samples. The load-soak controls are considered superior to simple soak controls because the cyclic load can have a significant effect on the amount of fluid uptake in UHMWPE [10].

Knee Wear Tests

NexGen[®] Complete Knee Solution Cruciate Retaining (*NexGen* CR) knees were used. Each knee consisted of a *NexGen* CR tibial articular surface, 9 mm thick, mounted on a Ti-6Al-4V alloy tibial baseplate, and articulating against a standard cast Co-Cr-Mo alloy femoral component of medium size.

All the tibial articular surfaces, conventional and HXPE, were machined from the same compression molded GUR 1050 UHMWPE lot. The HXPE articular surfaces were machined from bars of UHMWPE crosslinked by subjecting them to 72 kGy of e-beam radiation and subsequently melt-annealed to reduce the free radical concentration to

undetectable levels as measured by electron spin resonance (ESR). This material is available commercially as *Prolong®*. The dose of 72 kGy represents the upper extreme control range of the process and is considered worst case under adverse mechanical conditions such as three-body wear. The control articular surfaces were sterilized by gamma radiation in nitrogen at 37 kGy using current production processes, whereas the HXPE articular surfaces were gas plasma sterilized through two standard cycles. All the articular surfaces were artificially aged under pressurized oxygen (73 psi) at 70°C for 14 days, according to Method B in ASTM F 2003.

The design of experiment used is as follows: four groups of *NexGen* CR knees were wear tested, differing only in the material of the tibial articular surface (HXPE or conventional UHMWPE) and whether or not bone cement particles were added to the serum lubricant. The knee wear tests were performed on a six-station knee simulator built by Advanced Mechanical Technology, Inc. (AMTI, Watertown, Massachusetts). This type of knee simulator is now commercially available and has found widespread use. This simulator permits independent control of the axial load, femoral flexion-extension, tibial rotation, and anterior-posterior translation. The load is applied hydraulically in the vertical direction through the tibial baseplate-articular surface assembly, which is physically under the femoral component, as is the case during the normal walking cycle.

The wear test protocol was developed using physiological gait information obtained from the University of Minnesota and from Rush-Presbyterian Saint Luke's Medical Center in Chicago [11, 12]. The protocol simulates a walking gait, with femoral flexion-extension (F-E) motion from 0 to -58 degrees, internal-external (I-E) tibial rotation from 1.9 to –5.7 degrees, and an anterior-posterior (A-P) femoral translation amplitude of 5.2 mm. The peak load was 3200 N during the stance phase, and the minimum load was 50 N during the swing phase.
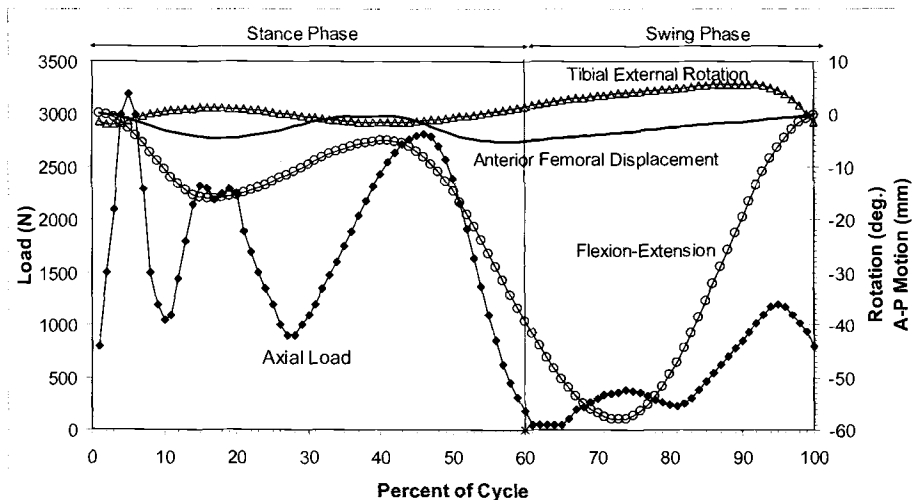
Figure 1 – *Load and motion curves for the knee wear tests.*

The knees were articulated at the physiological frequency of 1.1 Hz. The lubricant used was undiluted bovine calf serum (JRH Biosciences, Lenexa, Kansas) containing 3 g/L sodium azide (bactericide), 9 g/L disodium EDTA, and a total protein concentration of 64.5 ± 6.5 g/L 16. Each knee was run with 250 g of lubricant to which was added 250 ± 7 mg of bone cement particles prepared as described under *Hip Wear Tests*. The charge of particles consisted of 225 ± 5 mg of particles sieved through a 250 μm sieve and 25 ± 2 mg of particles sieved through a 600 μm sieve and retained by a 250 μm sieve, except from 2 to 3 million cycles when only the finer fraction was used. This particle size was chosen for clinical relevance based on the histological study reported by Pizzoferrato et al. [5]. No alumina particle simulations were conducted for the knee because they are less clinically significant than the bone cement particle simulations, and the effect of alumina particles on the wear of UHMWPE was already investigated using the hip joints. The serum lubricant was changed every half million cycles and a fresh charge of bone cement particles added to maintain a constant particulate level. Each joint was tested in an environmentally sealed chamber in which the serum lubricant was maintained at physiologic temperatures of $37 \pm 3°C$. During the test, the tibial baseplate and femoral components were mounted with bone cement on their respective simulator fixtures.

The wear of the articular surfaces was determined gravimetrically every half million cycles the first three million cycles and every million cycles thereafter. As in the hip wear tests, compensation for UHMWPE fluid uptake was effected by means of load-soak samples. Two load-soak articular surfaces were run for each knee group. The test duration was 5 million cycles.

Surface Roughness Measurements

The surface roughness measurements were performed with a S8P Perthometer profilometer (Mahr Federal Inc., Providence, Rhode Island). The metallic surfaces (hip heads and knee femoral components) were scanned with a laser noncontact probe (FOCODYN, Mahr Federal), whereas the UHMWPE articular surfaces were scanned with a 2 μm diamond probe. The noncontact probe was found to be unreliable on the UHMWPE surfaces, presumably due to surface reflectivity limitations. Typically, each measurement consisted of five parallel traces 0.56 mm in length in the area of interest, namely, the pole of the heads, the two distal condylar surfaces of the femoral components, and the two matching areas on the knee tibial articular surfaces. The cups were probed at approximately 30° from the pole to allow access of the diamond probe, the area probed being well within the wear scar. The cutoff length was 0.076 mm using a Gaussian filter.

Stastical Analyses

Design-Expert Version 6 (Stat-Ease, Inc., Minneapolis, Minnesota) was used to perform the multifactorial statistical analyses using standard analysis of variance (ANOVA) methods. Two-treatment comparisons were made with a Student t-test using Design-Expert or Microsoft®Excel (Microsoft Corporation, Redmond, Washington). A

model or difference was considered statistically significant at the 95% confidence level (p = 0.05).

Results

Hip Wear Tests

The average wear rates and the wear rate reductions measured on HXPE (110 kGy) relative to conventional liners are listed in Table 1, and the wear rates are compared graphically in Figure 1. The wear rate values with no particles added to the lubricant ("clean conditions") were obtained in another study, using an AMTI hip simulator, which under the test conditions used produces comparable UHMWPE wear rates to the Shore Western biaxial simulator [13]. A multifactorial analysis of the wear rate data indicates that both the abrasive particles and type of polyethylene have a highly statistically significant effect on the wear rates (p < 0.0001). The HXPE liners invariably wear much less than their conventional counterparts. Their average wear rates are only 7% to 31% that of the conventional liners, corresponding to wear rate reductions relative to the conventional liners of 69% to 93%. These wear rate reductions are statistically highly significant (p < 0.0001). The type of abrasive had an equally large effect. Relative to the clean conditions (no particles added), the average wear rates were 27- to 125-fold larger in the presence of alumina particles and 2- to 5-fold larger in the presence of bone cement particles. With no particles added, the 22 mm liners have lower wear rates than the 32 mm liners, whereas the opposite was found in the presence of abrasive particles. These differences are not, however, statistically significantly different (p ~ 0.25) due to the large scatter of the wear rate values, particularly in the presence of alumina particles (Table 1).

Table 1 - *Wear rates (mm^3/Mc) of conventional UHMWPE and HXPE in the presence of alumina and bone cement particles. The standard error is in parentheses.*

Abrasive	Alumina		Bone Cement		No Particles Added	
Liner Diameter	22 mm	32 mm	22 mm	32 mm	22 mm	32 mm
Conventional UHMWPE	348 (43)	359 (122)	38 (7.4)	31 (2)	8.0 (0.3)	13.3 (1.5)
HXPE	107 (22)	40 (8)	3.4 (3.4)	2.1 (2.1)	0.86 (0.11)	1.2 (0.12)
Wear Reduction*	69%	89%	92%	93%	89%	91%

*Wear reduction achieved with HXPE relative to the conventional UHMWPE.
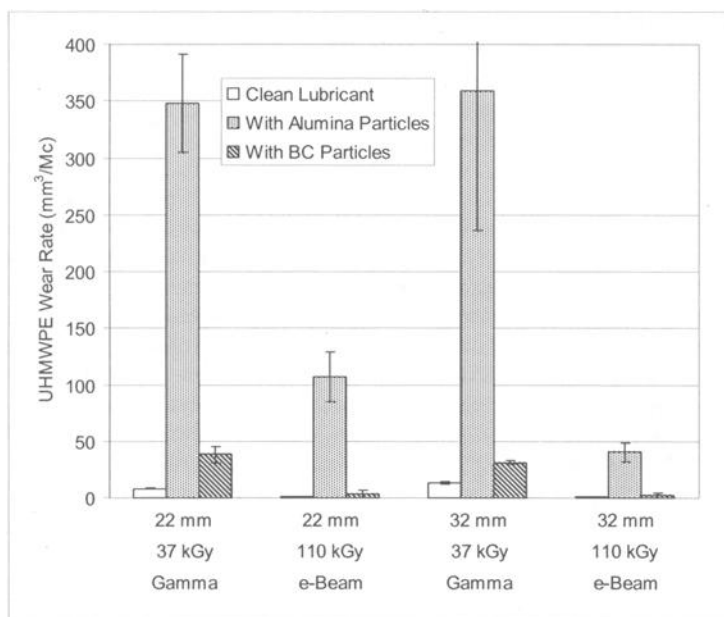
Figure 2 - *In vitro UHMWPE hip wear rates with and without added abrasive particles.*

The appearance of the articular surfaces was consistent with the abrasiveness of the particles added to the lubricant (Figure 3). The radial feature seen in the photograph of the HXPE liner with no particles added is a machining artifact. The articular surfaces subjected to the alumina particles were by far the most scratched. Those subjected to bone cement particles were nevertheless significantly more scratched than those tested with no particles added. These different levels of scratching are reflected in the surface roughness values of the articular surfaces. The average Ra (arithmetic mean surface roughness) values of the liner and head articular surfaces before testing, after five million cycles of wear testing in the presence of added abrasive particles or in their absence, are compared in bar charts in Figure 4 for alumina particles and in Figure 5 for bone cement particles.

The relative effect of the alumina particles is much greater on the heads than on the liners, with the Ra value increasing 14- to 39-fold for the heads and 1- to 5-fold for the liners after 5 million cycles. However, the effect of the alumina particles on the liners is more clearly seen by comparing the Ra values with and without added particles at the end of the test. Thus, whereas the surface roughness of the liners increases in the presence of alumina particles, it decreases under clean conditions, i.e., the articular surface of the liners are polished under clean conditions. As a result, the alumina/clean Ra value ratios range from 3 for the 32 mm HXPE liners to 17 for the 22 mm conventional liners at the end of the test. Similar but less pronounced effects were found after testing with bone cement particles. In this case head Ra values increased 1.2- to 2.8-fold for the heads and up to 1.9-fold for the liners. Because initial Ra value of the 22 mm conventional liners used in this test were unusually high, at 0.35 μm, their final Ra value actually decreased

after articulation for 5 million cycles in the presence of bone cement particles, to 0.096 µm, in line with the end of test values for the other liners, 0.062 to 0.144 µm.

A multifactorial ANOVA of the Ra values reveals similar trends for the heads and liners. For both, the abrasive type and polyethylene type have a significant effect on their surface roughness. On the other hand, the articular surface diameter was not found to have a statistically significant effect and there were no statistically significant interactions between the main factors (polyethylene, abrasive, and diameter), making the interpretation of the results straightforward. The surface roughness increases in going from no particles to bone cement particles to alumina particles added. As pointed out above, the effect is more pronounced for the heads than for the liners, particularly with alumina particles.

The extent of head roughening also increases in going from conventional to crosslinked UHMWPE. Thus, for the heads against conventional UHMWPE, the average Ra values are 0.0294, 0.0461, and 0.48 µm for no particles, bone cement, and alumina particles added, respectively. The corresponding values against HXPE are 0.0304, 0.0816, and 1.03 µm. A similar pattern is observed for the liners, with corresponding average Ra values of 0.0188, 0.0788, and 0.235 µm for conventional UHMWPE, versus 0.0318, 0.142, and 0.280 µm for HXPE. These trends may be seen graphically in Figure 4 for bone cement particles and Figure 5 for alumina particles. For the conventional UHMWPE liners, there is a good linear correlation ($R^2 = 0.99$) between the wear rate, normalized with respect to the liner ID, and the head Ra after 5 Mc, while for the HXPE liners, the corresponding linear correlation is rather weak ($R^2 = 0.563$) (Figure 6). The average HXPE 22 mm liner wear rate is higher than expected relative to the average HXPE 32 mm liner wear rate, given the average Ra values of the mating hip heads.
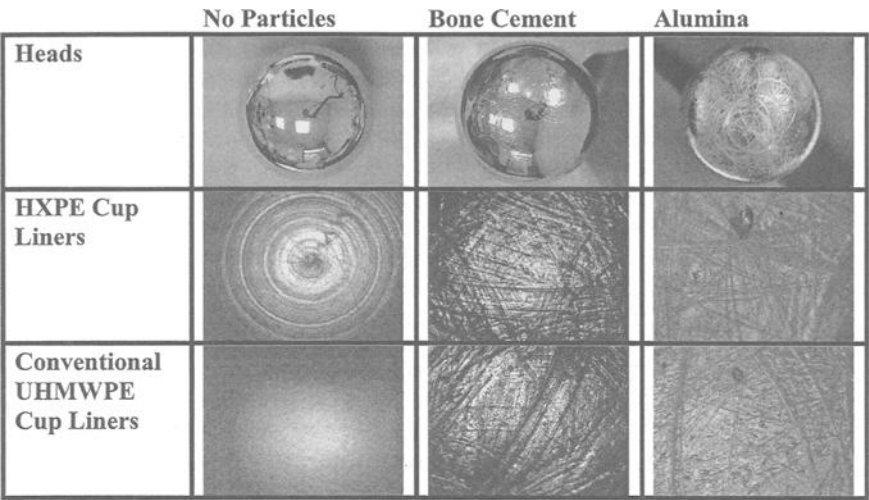
Figure 3 - *Representative photographs of articular surfaces after testing 5 million cycles with particles present as indicated on the header of each column. The heads shown are 32 mm in diameter. In the photographs of the cup liner surfaces, the horizontal length represents approximately 2.5 mm of actual length.*

(a) Liners   (b) Heads
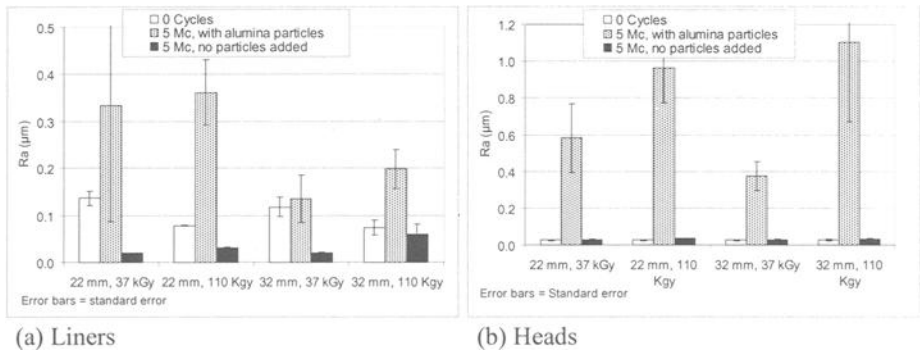
Figure 4 - *Ra surface roughness values of the liners and heads after articulation in the presence of alumina particles for five million cycles (5 Mc).*

(a) Liners   (b) Heads
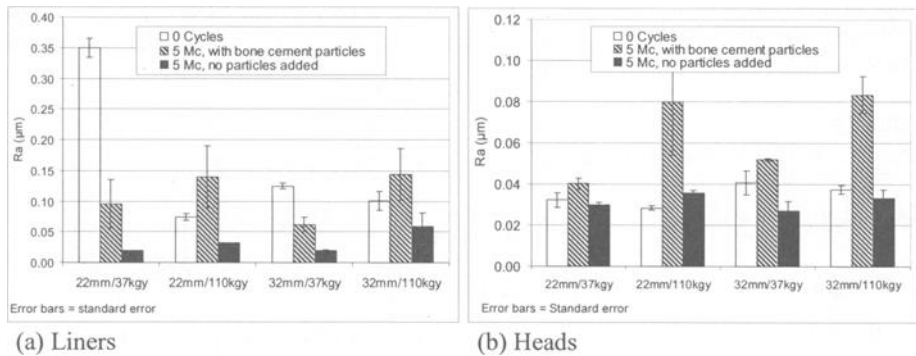
Figure 5 - *Ra surface roughness values of the liners and heads after articulation in the presence of bone cement particles for five million cycles (5 Mc).*
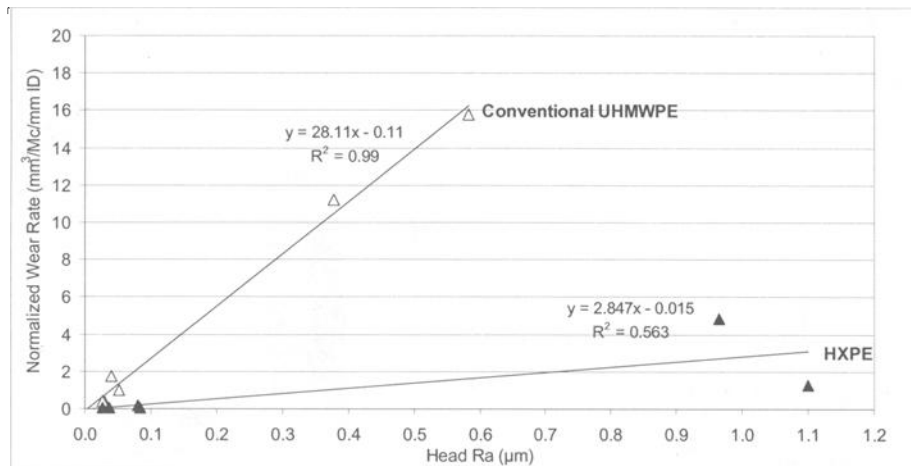
Figure 6 - *Wear rate versus head Ra. The wear rate is normalized with respect to the articular surface diameter.*

Knee Wear Test

The average gravimetric wear values versus the number of gait cycles are plotted in Figure 7 for the four groups tested: conventional UHMWPE (37 kGy gamma) and HXPE (72 kGy e-beam) with and without bone cement particles added. The corresponding average cumulative wear rates are given in Table 2 along with the relative wear rate increase in the presence of the bone cement particles and wear rate reduction achieved with HXPE relative to the conventional UHMWPE. Two salient points of these results are (1) the wear rate of the crosslinked polyethylene is significantly lower than that of the conventional UHMWPE, regardless of the test condition and (2) bone cement particles had a smaller effect on the wear rate of the crosslinked polyethylene relative to the

conventional UHMWPE. The wear rate reduction achieved with HXPE relative to the conventional UHMWPE is actually statistically the same at 88% with no particles added and 90% with particles added ($p \sim 0.6$).

Table 2 - *Cumulative wear rates (mm^3 /Mc) of conventional UHMWPE and HXPE in the presence of bone cement particles. The standard error is in parentheses.*

Abrasive Particles Added	Bone Cement	None	Wear Rate Increase with Bone Cement
Conventional UHMWPE	22.1 (0.7)	15.5 (1.2)	43%
HXPE	2.31 (0.67)	1.85 (0.27)	25%
Wear Reduction with HXPE Relative to the Conventional UHMWPE	90%	88%	
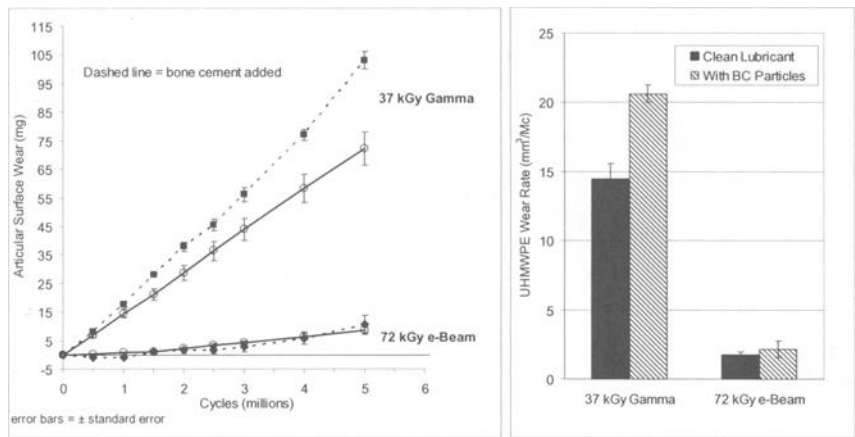
(a) Knee wear versus number of cycles   (b) Knee wear rates

Figure 7 - *Wear results for the HXPE (72 kGy e-beam) and conventional (37 kGy gamma) UHMWPE tibial inserts.*

As expected from the presence of bone cement particles in the serum lubricant, the articulating areas of the femoral components and tibial articular surfaces were markedly more scratched than is normally observed in a knee wear test. On the articular surfaces, the scratches and pitting were more pronounced on the periphery of the wear scars. The inferior aspect of all the articular surfaces was also scratched, particularly in the posterior lateral area. Burnishing and fading of inscribed numbers indicated some wear of this surface. The effect was more pronounced for the conventional UHMWPE inserts.

The average surface roughness values, Ra, of the articular surfaces before the test and after five million cycles with and without the addition of bone cement particles are

compared in Figure 8. Representative photographs of the tibial articular surfaces after 5 million cycles of testing are shown in Figure 9. With respect to the tibial articular surfaces, the HXPE and conventional UHMWPE follow the same patterns and there is no statistically significant difference between the Ra values of the two materials (p = 0.8). Compared to the conventional UHMWPE, there is a slight trend toward higher surface roughness with the HXPE in the presence of the particles. The wear test has a smoothing effect on the tibial articular surfaces, with or without added particles, although the effect is greater without the particles. Thus, the average Ra values change from 0.193 ± 0.008 μm to 0.039 ± 0.008 μm without particles and 0.103 ± 0.016 μm with added particles. These changes are statistically significant (p < 0.0001).

The changes in the surface roughness values of the femoral articular surfaces, like those of the tibial articular surfaces, exhibit no statistically significant dependence on the type of polyethylene (p = 0.7). However, a slight trend towards greater roughening with the HXPE under clean conditions was observed (Figure 8 (b)). The presence of the bone cement particles increased the average Ra surface roughness by 0.039 ± 0.008 μin relative to the initial average Ra value of 0.046 ± 0.002 μin. This 84% increase is statistically significant (p = 0.03).

(a) Tibial inserts   (b) Femoral components
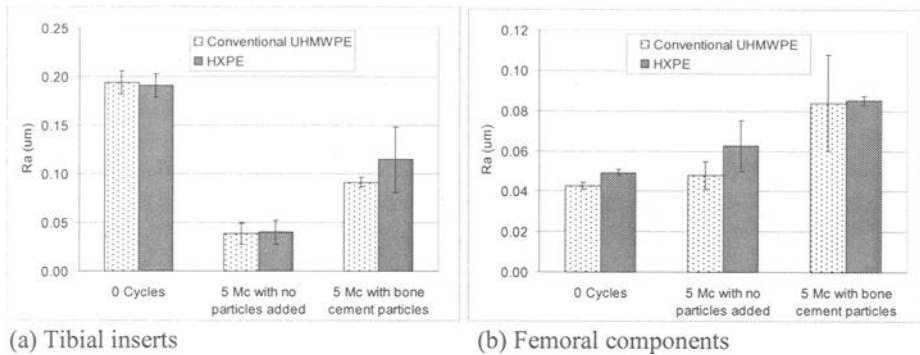
Figure 8 - *Ra surface roughness values of the articular surface of the tibial inserts and femoral components after articulation in the presence of bone cement particles for five million cycles (5 Mc). Error bars = ± standard error.*

(a) Conventional   (b) HXPE
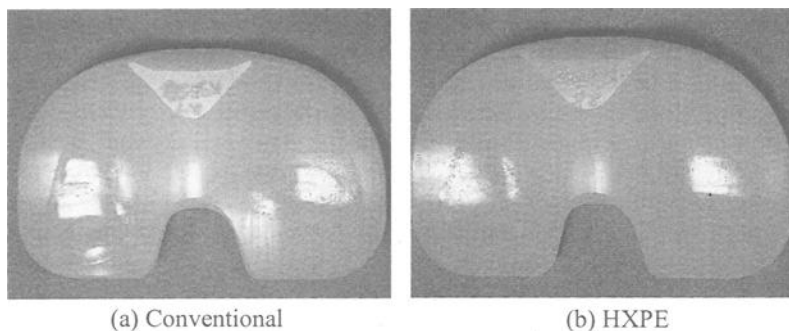
Figure 9 - *Tibial inserts articulated in the presence of bone cement particles for 5 million cycles. The medial-lateral (horizontal) length of the inserts is 74 mm.*

Discussion

Hip Wear Tests

Even in the presence of abrasive particles, the wear rates of the HXPE liners are markedly lower than those of the conventional liners, with average wear rate reductions relative to conventional liners of 69% to 93% (p < 0.0001). The largest wear rate reductions were achieved in the presence of bone cement particles, possibly the most clinically relevant three-body wear condition [5]. As a result, the average wear rates of the HXPE liners in the presence of bone cement particles are still much less than those of the corresponding conventional liners with no particles added (Table 1).

These findings mirror previous findings of wear reductions with highly crosslinked polyethylene's tested against roughened heads [14, 15]. It is of interest that the wear reductions in the presence of abrasive particles matched or exceeded the reductions achieved with clean serum lubricant, except for the 22 mm liner articulating in the presence of alumina particles. The latter represents the worst condition in terms of the articular stress and particle abrasiveness. Even though the wear reduction was still 69%, versus 89% under clean conditions, the relative increase in the wear rate may be related to the depth of the damage induced on the polythene surface by coarse scratching and plowing. Under macro-plowing conditions, the surface molecular chain orientation inhibition mechanism proposed to account for the increased wear resistance of highly crosslinked polyethylene's under micro adhesive/abrasive wear loses some effectiveness and the bulk mechanical properties of the material become a stronger factor.

The alumina particles have a far greater abrasive effect than the bone cement particles, as expected from their respective hardnesses (9 Mohs for alumina (corundum) versus 3.3 Mohs for the barium sulfate, the hardest component in bone cement). Relative to the clean conditions, the wear rates in the presence of bone cement increased from 1.7-fold (32 mm HXPE) to 4.8-fold (22 mm conventional UHMWPE), whereas in the presence of alumina, they increased from 27-fold (32 mm conventional UHMWPE) to 125-fold (22 mm HXPE). In particular, the bone cement particles did not act as an intermediate protective bearing surface that could have actually led to a decrease in the wear rate of the polyethylene. The increases in wear rates were approximately linearly correlated with the surface roughness of the hip heads after 5 million cycles, particularly for the conventional UHMWPE liners. The effect of the abrasive particles was relatively greater for the 22 mm liners than the 32 mm liners, probably due to the higher stresses in the 22 mm liners and the deeper plowing effected by the particles. As a result of this phenomenon, there was a wear rate reversal between the 22 and 32 mm liners for both types of polyethylene's in going from clean lubricant to lubricant with added alumina particles. Under clean conditions, the larger liners have higher wear rates in accordance with the correspondingly larger sliding distance.

The inverted (reverse-anatomic) configuration of the hip joint simulator may be advantageous because it facilitates the ingress of the abrasive particles, providing a worst case scenario. In addition, the fluid and particle transport properties in the actual joint are rather different from those in a hip simulator because of the presence of soft tissues. In a hip simulator with the anatomic configuration, the particles have to be carried up to the joint by fluid flow, limiting the amount and size of the particulates reaching the articular surfaces, whereas in vivo, the soft tissues could hold the particles in the vicinity of the joint, counteracting gravity. Therefore, in the inverted hip simulator configuration, gravity might roughly emulate the action of the soft tissues in vivo.

Knee Wear Tests

The wear and surface roughness results of the knee wear tests in the presence of bone cement particles follow the same trends as the corresponding hip wear test results. As with the hip liners, the wear rates of the HXPE tibial inserts were found to be markedly lower than those of the conventional inserts even in the presence of bone cement particles, with an average wear rate reduction with HXPE of 90%, versus 88% under clean conditions. The 25% increase in the average wear rate observed for the HXPE with the addition of bone cement particles is not statistically significant ($p = 0.6$), whereas the corresponding 40% increase for the conventional UHMWPE is statistically significant ($p = 0.002$). The similar wear reductions with and without added particles and the relatively modest increase in the wear rates suggest that the presence of the bone cement particles did not lead to a significant change in the wear mechanism.

A significant difference between the knee and hip wear results is the much lower wear rate increase induced by the presence of the particles in the knees relative to the hips. Thus the wear rate increases with bone cement particles were 25% to 40% for the knees, versus 70 % to 140% for the 32 mm liners and 300% to 380% for the 22 mm liners. The wear increase in the presence of particles therefore increases with the articular surface constraint, which permits better particle entrapment. Another important factor may be the difference in the shape of the paths of motion of the femoral component in knee and hips. In the knees, these paths are mostly in the anterior-posterior direction [16-18], with an estimated aspect ratio of approximately 20 in the present knee wear tests. In the hips, on the other hand, the paths of motion have a substantial component transverse to the flexion-extension direction [19-21]. In the biaxial hip simulator used in this study, the paths are circular in the polar area of the liner [21], and therefore have an aspect ratio of one. The narrower articular paths in the knees decrease the amount of motion transverse to a scratch previously generated by an abrasive particle on the femoral component. A scratch on the metal counterface is expected to be more abrasive when the direction of sliding is transverse rather than parallel to it. Furthermore, in hips the articular motion involves sliding exclusively, whereas the motion in knees is a combination of sliding and rolling, with the latter expected to contribute less to the generation of scratches and to their abrasiveness once formed.

As for the hips, there was a trend for the HXPE tibial articular surfaces to become rougher than the conventional UHMWPE articular surfaces in the presence of the bone cement particles. This trend may be attributed to the lower wear rate of the HXPE, which tends to preserve induced surface defects such as scratches.

Conclusions

The three-body wear behavior of two highly crosslinked UHMWPEs, one in clinical application for hips and the other for knees, was examined in joint simulator tests, with the following conclusions.

1. The highly crosslinked polyethylene acetabular liners and tibial articular inserts wore 69% to 90% less than their conventional, gamma-sterilized counterparts when third body particles were added to the test lubricant. These wear reductions matched those obtained in wear tests without added particles, except for the 22 mm acetabular cup liner articulated in the presence of alumina particles, which represents the most extreme case in this series of tests. Even in that case, a wear reduction of 69% was achieved with HXPE relative to the conventional UHMWPE.

2. The addition of bone cement particles did not have a statistically significant effect on the wear rate of the HXPE tibial articular inserts.

3. The effect of the alumina particles on acetabular liners was much greater than that of the bone cement particles with respect to wear and surface roughening. The average polyethylene wear rates in the presence of alumina particles were 9- to 31-fold those achieved in the presence of bone cement particles.

4. The wear rates for both acetabular liners and tibial inserts were approximately linearly correlated to the head Ra surface roughness, the correlation being better for the conventional UHMWPE than the HXPE.

5. Hips and knees followed the same trends with respect to wear and surface roughness, with the effect of the particles being more severe for hips. The latter is expected from the more constrained geometry in hips, which tends to trap particles better, and the greater amount of sliding transverse to a scratch in hips. In knees, the motion is more nearly unidirectional and includes rolling, which is expected to contribute less to abrasive wear.

6. For both the HXPE and the conventional UHMWPE, the 22 mm liners wore more than their 32 mm counterparts, the reverse of what happens under clean conditions (no particles added) and is expected from the sliding distance. This indicates that the compressive stresses, as opposed to the total load, become more important in the presence of particles, consistent with an abrasive plowing wear mechanism.

7. A trend was noted for the articular surfaces to be rougher with the HXPE than with the conventional UHMWPE, attributable to the much lower wear rate of the HXPE, which tends to preserve induced surface defects, such as scratches.

8. Given that wear testing in the presence of alumina particles represents conditions much more severe than expected clinically, the results of these tests suggest that the HXPE will outperform the conventional UHMWPE with respect to clinical wear under any foreseeable three-body wear conditions.

References

[1] Wang, A., Stark, C., Dumbleton, J., "Mechanistics and morphological origins of ultra-high molecular weight polyethylene wear debris in total joint replacement prostheses" , *Proceedings of the Institution of Mechanical Engineers*, Vol. 210, 1996, pp. 141-155.

[2] Jasty, M., Bragdon, C.R., O'Connor, D.O., Muratoglu, O.K., Premnath, V., Merrill, E., "Marked Improvement in the Wear Resistance of a New Form of UHMWPE in a Physiologic Hip Simulator", *Transactions of Society for Biomaterials*, Vol. 23, 1997, p. 157.

[3] McKellop, H., Shen, F-W., Salovey, R., Extremely Low Wear of Gamma-Crosslinked/Remelted UHMW Polyethylene Acetabular Cups", *Transactions of the Orthopedic Research Society*, Vol. 44, 1998, p. 98.

[4] Laurent, M.P., Yao, J.Q., Bhambri, S.K., Gsell, R.A., Gilbertson, L.N., Swarts, D.F., Crowninshield, R.D., "High Cycle Wear of Highly Crosslinked UHMWPE Acetabular Liners Evaluated in a Hip Simulator", *Sixth World Biomaterials Congress Transactions*, 2000, 851.

[5]   Pizzoferrato, A., Ciapetti, G., Stea, S., Toni, A., "Cellular Events in the Mechanisms of Prosthesis Loosening", *Clinical Materials*, Vol. 7, 1991, pp. 51-81.

[6]   Muratoglu, O.K., Greenbaum, E.S., Larson, S., Jasty, M., Freiberg, A.A., Burke, D., Harris, W.H., "Surface Analysis of Early Retrieved Acetabular Polyethylene Liners: A Comparison of Conventional and Highly Crosslinked Polyethylene's", *Transactions of Society for Biomaterials*, Vol. 28, 2002, 62.

[7]   Paul, J.P., "Forces Transmitted by Joints in the Human Body", *Proceedings of the Institution of Mechanical Engineers*, Vol. 181, Part 3J, 1967, pp. 8-15.

[8]   Merchant, K.K., Rohr, W.L., Lintner, W.P., Bhambri, S.K., "Orthopedic Implant Surface Debris", *Transactions of the 41st Annual Meeting of the Orthopedic Research Society*, 1995, p. 164.

[9]   Helmers, S., Sharkey, P.F., McGuigan, F.X., "Efficacy of irrigation for removal of particulate debris after cemented total knee arthroplasty", *Journal of Arthroplasty*, Vol. 14, 1999, pp. 549-552.

[10]   Yao, J.Q., Laurent, M.P., Gilbertson, L.N., Crowninshield, R.D., "The effect of minimum load on the fluid uptake and wear of highly crosslinked UHMWPE total hip acetabular components", *Wear*, Vol. 250, 2001, pp. 140-144.

[11]   Johnson, T.S., "In-Vivo Contact Kinematics of the Knee Joint: Advancing the Point-Cluster Technique", Ph.D. Dissertation, University of Minnesota, 1999.

[12]   Johnson, T.S., Laurent, M.P., Yao, J.Q., Gilbertson, L.N., "The effect of displacement control input parameters on tibiofemoral prosthetic knee wear", *Wear*, Vol. 250, 2001, pp. 222-226.

[13]   Laurent, M.P., Yao, J.Q., Gilbertson, L.N., Crowninshield, R.D., "Comparison of the AMTI and Shore Western Hip Simulators for Wear Testing UHMWPE Acetabular Liners", *Transactions of the 27th Annual Meeting of the Society for Biomaterials*, 2001, 358.

[14]   Essner, A., Polineni, V.K., Wang, A., Stark, C., Dumbleton, J.H., "Effect of Femoral Head Surface Roughness and Crosslinking on the Wear of UHMWPE Acetabular Inserts", *Transactions of the 24th Annual Meeting of the Society for Biomaterials*, 1998, 4.

[15]   McKellop, H., Shen, F-W., DiMaio, W., Lancaster, J., "Wear of Crosslinked UHMW Polyethylene under Adverse Conditions", *Transactions of the 25th Annual Meeting of the Society for Biomaterials*, 1999, 323.

[16]   Ramamurti, B., Estok, D.M., Muratoglu, O.K., Harris, W.H., "Comparison of Paths Traced by Points on the Polyethylene Surface in THA and TKA", *Transactions of the 45th Annual Meeting of the Orthopaedic Research Society*, 1999, 823.

[17]   Johnson, T.S., Laurent, M.P., Yao, J.Q., "The Tibiofemoral Cross-Motion Pattern and its Effect on the Wear of a Prosthetic Knee", *Transactions of the 28th Annual Meeting of the Society for Biomaterials*, 2002, 191.

[18]   Yao, J.Q., Lu, X., Laurent, M.P., Johnson, T.S., Gilbertson, L.N., Swarts, D.F., Blanchard, C.R., Crowninshield, R.D., "Improved Resistance to Wear, Delamination and Posterior Loading Fatigue Damage of Electron Beam Irradiated, Melt-Annealed, Highly Crosslinked UHMWPE Knee Inserts", *Crosslinked and Thermally Treated Ultra-High Molecular Weight Polyethylene for Joint Replacements*, in this *ASTM STP*.

[19]   Bradgon, C.R., O'Connor, D.O., Lowenstein, J.D., Jasty, M., Syniuta, W.D., "The importance of multidirectional motion on the wear of polyethylene", *Proceedings of the Institution of Mechanical Engineers*, Vol. 210, 1996, pp. 157-165.

[20]   Wang, A., Sun, D.C., Edwards, B., Sokol, M., Essner, A., Polineni, V.K., Stark, C., Dumbleton, J.H., "Orientation softening in the deformation and wear of ultra-high polyethylene", *Wear*, Vol. 203/204, 1997, pp. 230-241.

[21]   Ramamurti, B.S., Estok, D.M., Jasty, M., Harris, W.H., "Analysis of the Kinematics of Different Hip Simulators Used to Study Wear Candidate Materials for the Articulation of Total Hip Arthroplasties", *Journal of Orthopaedic Research*, Vol. 16, 1998, pp. 365-369.

Victoria D. Good,[1] *Kirstin Widding,*[2] *Marcus Scott,*[3] *and Shilesh Jani*[4]

The Sensitivity of Crosslinked UHMWPE to Abrasive Wear: Hips versus Knees

ABSTRACT: All formulations of commercially available highly crosslinked ultra-high molecular weight polyethylene (UHMWPE) have demonstrated dramatic reduction in wear compared to conventional UHMWPE. A majority of these demonstrations have been under "smooth," i.e., non-abrasive conditions. The question, therefore, remains: are contemporary highly crosslinked UHMWPE (XPE) materials suitable for both hips and knees under abrasive conditions in vivo? These studies examined both XPE (10Mrad, GUR1050) and non-irradiated UHMWPE (GUR1050) for hips and knees under smooth and abrasive conditions. Studies were conducted on a 12-station hip and 6-station knee simulator. The femoral components were left polished or tumbled with plastic cones and alumina powder to create uniform scratching with surface roughness similar to clinical retrievals. In smooth conditions, XPE wore significantly less than non-irradiated UHMWPE (CPE) for both hips and knees. In abrasive conditions, wear of XPE increased by at least 15 times in hip applications and at least 70 times in knee applications. Furthermore, XPE knees wore more than CPE knees in the abrasive condition. This study showed that both forms of UHMWPE were subject to accelerated wear under abrasive conditions; however, the sensitivity of XPE to abrasive wear was greater for knees than for hips. These findings need to be taken into consideration when developing materials for improved wear resistance in knees.

KEYWORDS: Crosslink, UHMWPE, wear, hip, knee, abrasive

Introduction

Various formulations of highly crosslinked polyethylene (XPE) have demonstrated dramatic reductions in hip simulator gravimetric wear [1-3]. In part due to these findings, XPE is currently being used clinically to help reduce wear in total hip arthroplasty (THA). Reductions in knee simulator gravimetric wear with the use of XPE have also been observed [4-8]. However, XPE has not found widespread clinical use in total knee arthroplasty (TKA), primarily because the crosslinking process inevitably leads to reductions in critical mechanical properties such as toughness and fatigue strength [9-11]. It had previously been common to find delamination and cracking, both of which are fatigue phenomena due to aging and oxidation, in some embrittled TKA inserts [12]. Contemporary XPE materials, however, are stabilized against oxidative aging [1]. Therefore, these mechanical property-related risks may be reduced enough to warrant use of XPE in TKA applications. An additional

---

[1] Manager, Tribology, Smith & Nephew, Memphis, TN 38116.
[2] Senior Research Engineer, Tribology, Smith & Nephew, Memphis, TN 38116.
[3] Senior Research Engineer, Smith & Nephew, Memphis, TN 38116.
[4] Manager, Advance Products, Smith & Nephew, Memphis, TN 38116.

104

consideration prior to widespread use of XPE in knees is abrasive wear, which has not been addressed adequately to date. This issue is the focus of this study.

Retrieval studies of CoCr femoral heads and knee components have shown evidence of scratching or abrasion to the surfaces [13-19]. The damage seen on retrievals was likely due to third body debris such as bone cement, bone chips or dislodged beads from porous coatings. In addition, carbides dislodged from the femoral component may cause damage to the surfaces. It has also been shown that the cannula from arthroscopy of the knee can cause scratching of the knee component [20]. These studies have indicated that damage to the femoral component leads to accelerated wear of the polyethylene component. Due to these findings, it is critical to test both hip and knee implants under simulated abrasive conditions in addition to the standard smooth conditions.

Different techniques have been developed to test the formulations of polyethylene under abrasive conditions. Two primary methods have been employed: 1) the addition of abrasives to the test serum and 2) pre-roughening of the CoCr femoral surface. These methods have only been used in hip wear simulation [21-28]. In experiments designed to examine the abrasive sensitivity of XPE where particles were added into the test serum, the results were more often than not inconclusive. However, studies examining pre-roughening of the femoral heads have consistently shown that abrasive conditions result in increased wear. Thus, roughening of the femoral surface creates a reliable method for simulating abrasive conditions.

All of the abrasive hip simulator studies showed that even with an increase in wear, XPE wear rates continued to be lower than CPE wear rates. However, the percent increase in wear from smooth to abraded of XPE was greater than it was for CPE, thus indicating that in the hip the wear of XPE was more sensitive to abrasive conditions. Previous knee simulator studies of XPE have been conducted only in smooth (non-abrasive) conditions. It is not known whether XPE in the knee will behave similarly to XPE in the hip under abrasive conditions. Thus, the current studies examined both XPE (10 Mrad, GUR1050) and C-PE (GUR1050) for hips and knees under smooth and abrasive conditions.

Materials and Methods

Tibial and acetabular liner test components were made from ram extruded GUR 1050 UHMWPE (Poly-Hi Solidur, Ft. Wayne, IN) and articulated on CoCr femoral components (Table 1). The UHMWPE was either untreated (no crosslinking) with EtO sterilization as the endpoint (CPE) or highly crosslinked by gamma irradiation at 10Mrad, melt annealed and then EtO sterilized (XPE). All simulator studies were run for a minimum of 5 million cycles (Mc). Wear was determined gravimetrically and corrected for fluid absorption. Weight measurements were converted to volumetric measurements using the UHWMPE density (0.93 g/cm^3).

TABLE 1 -*Test Matrix*

Identification	Type	N	Size	Crosslinking Treatment	Condition
H-CPE-S	Hip	3	32mm	None	Smooth
H-CPE-A	Hip	3	32mm	None	Abraded
H-XPE-S	Hip	3	32mm	10 Mrad	Smooth
H-XPE-A	Hip	3	32mm	10 Mrad	Abraded
K-CPE-S	Knee	3	5 Right	None	Smooth
K-CPE-A	Knee	3	5 Right	None	Abraded
K-XPE-S	Knee	3	5 Right	10 Mrad	Smooth
K-XPE-A	Knee	3	5 Right	10 Mrad	Abraded

Hips

The hips (Reflection, Smith and Nephew, Inc.) were tested on a 12-station hip simulator (AMTI, Boston, MA) using a combination of ISO test standard, Implants for surgery – Wear of total hip-joint prostheses (14242-1.2), and Bergman input profiles alternating every 10 000 cycles [29]. The ISO parameters were: 0.27 kN to 2.36 kN axial load, 23° flexion to 20° extension, 7° internal to 4° external rotation and 7° abduction to 5° adduction. The Bergman parameters were: 0.11 kN to 2.18 kN axial load, 23° each flexion/extension, 8.4° each internal/external rotation, 8.9° each abduction/adduction. Each hip replacement was immersed in 550 mL of 100% alpha calf serum (Hyclone, Logan, UT with ~22mg/mL protein) with additives of 20mM EDTA and 0.2% sodium azide, which was recirculated and kept at 37°C.

Knees

Knee components (Genesis II, Smith and Nephew, Inc.) were tested on a 6-station (AMTI, Boston, MA) knee simulator with a 10:1 ratio of gait to stair climbing as the activity patterns. The gait (normal walking) parameters were: 0.69 kN to 2.46 kN axial load, 2.3° to 60° flexion, 2.5° external to 7.5° internal rotation, and 4.9 mm anterior to 7.3 mm posterior translation. The stair climbing parameters were: 0.21 kN to 2.53 kN axial load, 10° to 95° flexion, 0.5° to 5.2° internal rotation and 0.1 mm to 10.8 mm posterior translation. Each knee replacement was immersed in 450 mL of 50% alpha calf serum (Hyclone, Logan, UT with ~22 mg/mL protein) diluted with deionized water and additives of 20mM EDTA and 0.2% sodium azide, which was recirculated and kept at 37°C.

Abrasion Protocol

Abrasion of the femoral components was achieved by tumbling each component individually in a centrifugal barrel mass-finisher (Dia Super Eight Centrifugal Fine Finishing Machine, Nippon Dia Industry Co., LTD, Tokyo, Japan) for 30 seconds. Following tumbling all components were washed and rinsed according to ASTM F 2025. The femoral heads were abraded in the following media: (i) 700 mL of plastic cones embedded with 280 grit silicon carbide particles; (ii) 300 mL of 100 grit (approximately 150 μm) alumina powder; and (iii) water to just cover the powder and cones. Roughness measurements of R_a and R_{pm} were taken after tumbling but before wear testing using a WYKO RST Plus Interferometer (WYCO Corp., Tucson, AZ).

Three measurements (one at the apex, two approximately 30° from the axis of the head pole) were made for each femoral head with a scan size of 1.2 mm x 0.9 mm and magnification of 5.4X. The knee femoral components were abraded in the following media: (i) 1300 mL of plastic cones embedded with 280 grit silicon carbide particles; (ii) 75 mL of 25 µm alumina powder; and (iii) water to just cover the powder and cones. Measurements were performed with the use of a Surfcom 575A Profilometer (Tokyo Seimitsu, Tokyo) with a 2 µm radius stylus tip and a cut-off length of 0.8 mm. Ten roughness measurements were made at pre-selected locations from 0° to 45° of flexion of each condyle of each femoral component. Two parameters: R_a and R_{pm} were used to characterize roughness before and after wear testing. R_a measured the average of all peak heights above the mean line within the assessment length. R_{pm} was an average of the discreet R_p (maximum peak height above the mean surface for each discreet interval) measurements within the assessment length (usually 5 intervals). A scanning electron microscope (SEM; S360, Leica, Inc. Deerfield, IL) was used to view roughness of femoral surfaces.

Results

Hips

Wear was undetectable for the smooth XPE cups. Wear was greater in the abraded condition versus the smooth condition for both XPE and CPE (Fig. 1, Table 2). The CPE wear doubled with abraded CoCr heads in comparison to smooth CoCr heads, and the XPE wear rates increased significantly. Both the smooth and abraded XPE wear rates were lower than CPE in either smooth or abrasive conditions.

FIG. 1-*Volumetric wear from hip simulation study of H-XPE and H-CPE under smooth (S) and abrasive conditions (A).*

TABLE 2-*Hip volumetric wear-rates*

Identification	Wear-rate (mm³/Mc)
H-CPE-S	38.1 $\pm$ 0.58
H-CPE-A	76.0 $\pm$ 3.7
H-XPE-S	-1.19 $\pm$ 0.24
H-XPE-A	15.4 $\pm$ 4.1

The R_a and R_{pm} of the smooth CoCr heads were 0.04 $\pm$0.00µm and 0.58 $\pm$0.10µm, respectively. After tumbling but before wear testing the roughness increased by at least three times, which was a significant increase (p<0.01) and was within clinically reported values for roughened CoCr femoral heads [30-32] (Fig. 2). Upon microscopic examination the tumbled heads appeared similar to retrieved femoral heads (Fig. 3).

Knees

Again as seen in the hips wear of XPE was undetectable in the smooth condition (Fig. 4, Table 3). In addition, wear was greater in the abraded condition for both XPE and CPE. However, in sharp contrast to the hip results, the knee tibial components were much more sensitive to abrasive wear when articulating on XPE. The XPE articulating on abraded femoral components showed the highest wear and was almost two times greater than CPE in the abrasive conditions and over six times higher than the smooth CPE.
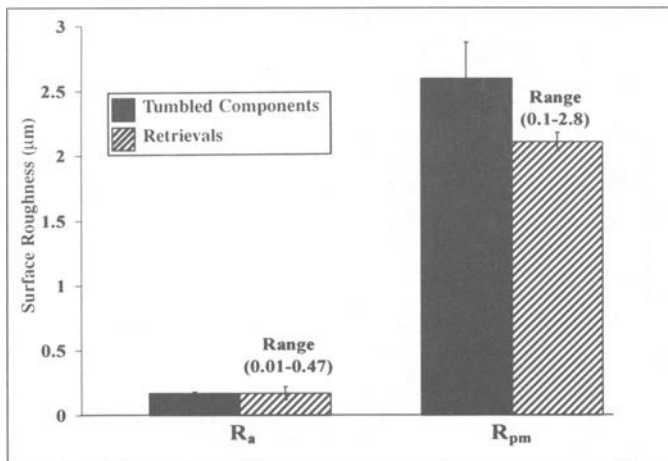
FIG. 2-*Roughness parameters of tumbled and retrieved CoCr femoral heads.*
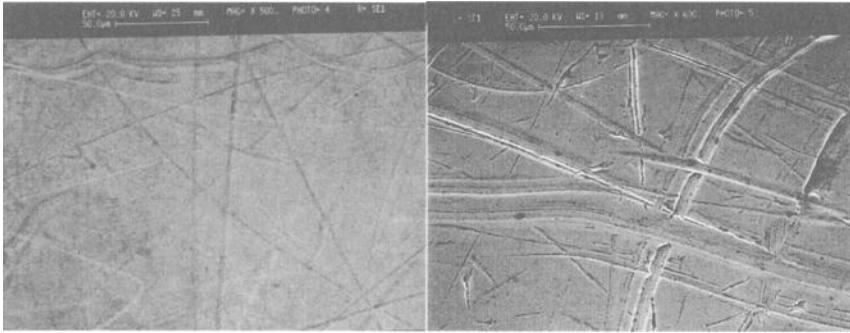
FIG. 3-*SEM of retrieved CoCr head (left) vs. tumbled CoCr head (right).*

The R_a and R_{pm} of the smooth CoCr femoral components were 0.06 ±0.01μm and 0.22 ±0.04μm, respectively.   The tumbling protocol employed in this study significantly increased (min. 2x) the roughness of CoCr femoral components compared to new components (p<0.01). These scratches were similar in shape and orientation to scratches seen on retrievals and had roughness values in the reported range for clinically scratched components (Figs. 5 & 6) [17]. Interestingly, visual inspection with the naked eye showed scratches on the retrievals to be primarily in the direction of motion (flexion/extension); however, under SEM it is clear that the scratches are multi-directional corresponding to internal/external motion of the knee.

Hips vs. Knees

The XPE showed marked improvement with undetectable wear in the smooth condition compared to CPE for both hips and knees. However, when the femoral components were
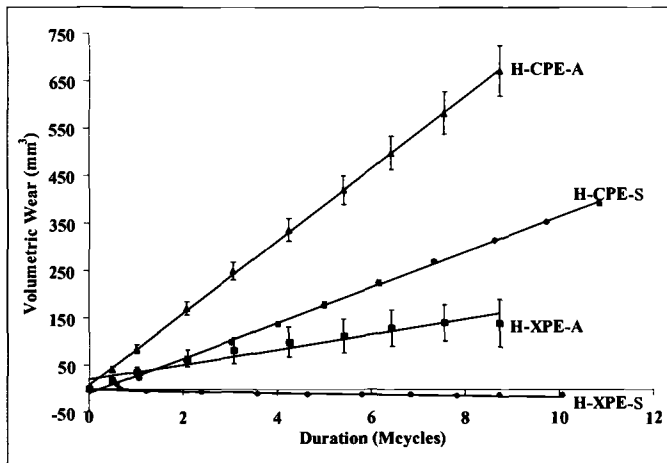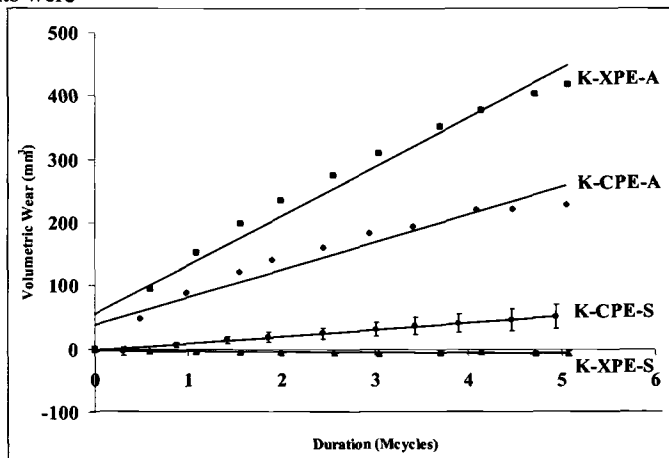

FIG. 4-*Volumetric wear from knee simulator study of K-XPE and K-CPE under smooth (S) and abrasive conditions (A).*

TABLE 3-*Knee volumetric wear rates*

Identification	Wear-rate (mm^3/Mc)
K-CPE-S	11.2 ± 1.04
K-CPE-A	38.8 ± 2.58
K-XPE-S	-0.51 ± 0.20
K-XPE-A	70.4 ± 2.85

abraded, the hips and knees showed divergent results. The hips maintained their wear advantage with XPE whereas; the knees demonstrated a disadvantage (Fig. 7). The XPE hip wear rates were half of the CPE hip wear rates. However, in contrast to abrasive hip testing, the wear-rate of XPE under abrasive knee conditions was two times greater than the CPE knee wear-rate, thus demonstrating that abrasion to the femoral surface from third body debris such as bone cement or chips was more detrimental to knees than hips.

Discussion

Recent total joint replacement demographics show an increase in younger and possibly more active patients [33-35]. In order to evaluate implants for high-demand patients it is necessary to conduct tests in a worst case scenario. The roughened or scratched femoral components are one means of simulating worst case with the assumption that more third body debris such as bone debris, cement etc. is likely to be generated from increased use. Comparison of the tumbled hip and knee femoral components with that of retrieved components shows that quantification of surface roughness is similar (Figs. 2 & 5). The tumbling process uniformly scratches the entire femoral surface; however, only the wear or contact areas affect the wear of the polyethylene. SEM inspection of the wear or contact areas show similar scratching patterns and sizes to retrievals.

Hip simulator wear rates of XPE have been very low or undetectable [1-3]. This study was no exception under smooth conditions. However, it is unlikely that the femoral surfaces of hip implants would remain smooth or unscratched. Studies have shown that retrieved femoral heads show evidence of scratched or roughened surfaces [16,18,19]. Previous hip simulator studies have shown evidence of increased wear with abraded femoral heads [24,25,28,36]. In spite of the increased wear in abrasive conditions XPE acetabular cups continued to have lower wear
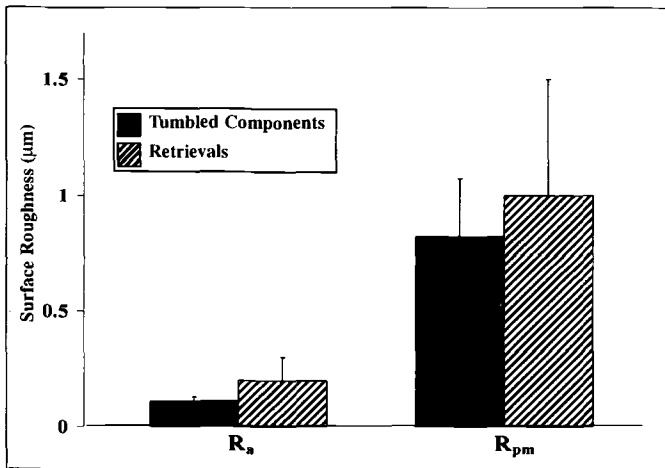
FIG. 5-*Roughness parameters of tumbled and retrieved CoCr femoral knee components.*
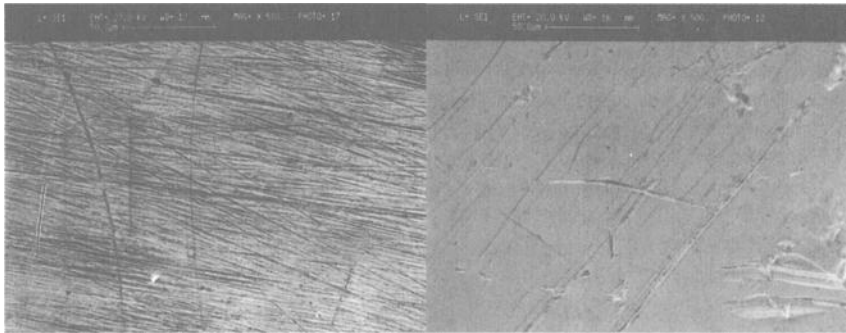
FIG. 6-*SEM of retrieved CoCr knee component (left) vs. tumbled CoCr knee component (right).*

than CPE. This hip study also showed that both forms of UHMWPE were subject to accelerated wear under abrasive conditions, but the wear of XPE continued to be lower than CPE.

This study found similar results to previous studies showing that wear of XPE in knees was also low or undetectable in smooth conditions [4-8]. Again, as in hips, it is highly unlikely that the femoral components would remain smooth in-situ. Studies have shown that retrieved knee femoral components were also susceptible to abrasion [17,20]. However, the issue of abraded femoral components in vitro has only been addressed using CPE [26]. This study showed that XPE was more sensitive to roughening of the femoral component than CPE. In fact, wear rates of XPE knees were twice that of CPE knees in abrasive conditions.

This study confirmed numerous previous studies showing that the wear rates of XPE under smooth conditions are dramatically lower than the wear rates of CPE. These results were in part due to the multiplicity of C-C bonds across adjacent

molecular chains, which retards the ability of the chains to orient in the direction of instantaneous bearing motion [37,38]. Chain orientation of CPE can be of benefit under uni-directional motion; however, any motion across the aligned chains will result in increased wear. It is because the motion patterns in knees are less multi-directional that the wear rates in knee simulators are generally lower than in hip simulators for CPE [39]. The advantage afforded by crosslinked UHMWPE for use in knees is therefore inherently lower than in hips.
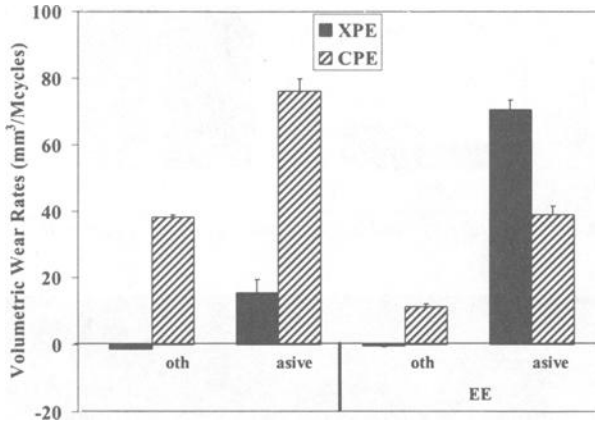
FIG. 7-*Volumetric wear-rates of CPE and XPE in smooth and abrasive conditions for the hip and knee.*

In abrasive conditions two trends were made evident in this study: 1) XPE is significantly more sensitive to abraded counterfaces than CPE, and 2) the heightened sensitivity of XPE to abrasion asserts a greater effect under the load/motion kinematics found in the knee than in the hip.   The net effect of these observations is that for abrasive conditions in a hip, XPE continues to wear at a lower rate than CPE and for knees it is the reverse, XPE wears more than CPE.   The micromechanical phenomenology underlying this behavior remains unknown.   However, it is likely connected to the fundamental material and mechanical property changes brought upon by the crosslinking process, which are: 1) lower toughness, 2) lower impact strength, 3) lower elongation to break, 4) lower tensile strength, 5) lower hardness, 6) lower resistance to fatigue crack propagation, 7) and greater resistance to tractional chain alignment [9-11]. How these changes may manifest as a greater sensitivity to abrasive wear is discussed below.

It can be considered that the crosslinked surface area of the UHMWPE component may be more sensitive to the cutting and ploughing of abrasive wear. Clearly, a material with reduced mechanical properties will be more susceptible to such a wear scenario. This explains why XPE is more sensitive to abrasive wear than CPE. It does not, however, explain why this sensitivity is greater in knees than in hips. A key factor is the fact that XPE, by virtue of the C-C crosslinks across adjacent molecular chains, is resistant to chain alignment under surface traction; however CPE molecules are

more likely to orient themselves in line with the direction of motion through surface traction. The XPE is in a "molecular frozen" state and the CPE is mobile, allowing molecular chains to be more adaptable to directional changes in motion. The likelihood of material removal, i.e., wear, is tied to the chain alignment. Wear is greater when the cutting edges are aligned in a direction oblique to the direction of motion. This scenario is more likely to occur when the scratches are randomly oriented and the motion is mostly linear (knees) than when the motion is multi-directional (hips). Thus, as the sharp asperities of the abraded CoCr components are cutting and plowing through the softer material, XPE molecules do not have enough mobility to align themselves in the direction of the cutting surface.

Conclusions

This was the first study to show that in the application of knees, XPE was highly susceptible to wear in the abraded condition. This study showed that the abrasive to smooth wear ratio was greater for XPE than for CPE in hip and knee simulation. In hip applications XPE wear-rates increased by at least 15-fold from smooth to abraded conditions. However, the XPE wear-rate in the abrasive condition continued to be less than CPE hip wear rates (in either smooth or abrasive conditions). Thus, although sensitive to abrasion, the XPE hips continued to wear less than CPE hips. The XPE knee was definitely more sensitive to abrasion than the hip. In abrasive conditions the XPE knee showed at least a 70-fold increase in wear in comparison to XPE in smooth conditions. In abrasive conditions the XPE knee showed a two-fold increase in wear compared to CPE thus, demonstrating that XPE in the knee was highly sensitive to abrasive wear.

It has been postulated that the high sensitivity to abrasion shown by XPE knees was due to the motion of the knee, the direction of the scratches and the resistance to orientation of the polyethylene chains. Further investigations on the use of crosslinked UHMWPE for tibial bearing components are therefore warranted to determine if the benefit of reduced wear under smooth conditions are outweighed by the risk of accelerated abrasive wear. A cautionary approach to clinical use of crosslinked UHMWPE in TKA is advocated based on these findings.

References

[1] McKellop, H., Shen, F.W., Lu, B., Campbell, P. and Salovey, R., "Development of an Extremely Wear-resistant Ultra High Molecular Weight Polyethylene for Total Hip Replacements". *Journal of Orthopaedic Research*, Vol. 17, No. 2, 1999, pp. 157-167.
[2] Muratoglu, O.K., Perinchief, R.S., Konrad, R. and Harris, W.H. "A Novel Method to Quantify Wear and Creep Deformation on UHMWPE Tibial Knee Inserts". *Orthopaedic Research Society*, 2001, pp. 221.
[3] Ries, M.D., Scott, M.L. and Shilesh, J., "Relationship Between Gravimetric Wear and Particle Generation In Hip Simulators: Conventional Compared With Cross-linked Polyethylene". *The Journal of Bone and Joint Surgery*, Vol. 83-A, No. Sup2-2, 2001, pp. 116-122.
[4] Muratoglu, O.K., Perinchief, R.S. Spiegelberg, S.H., Bragdon, C.R., O'Connor, D.O., Rubash, H. E., Jasty, M. and Harris, W.H. "On the Changes of an Adhesive/Abrasive Wear Mechanism of Polyethylene Tibial Knee Inserts upon

Crosslinking: An In Vitro Simulated Gait Study". *Orthopaedic Research Society*, 2002, pp. 1030.

[5] Schmidig, G., Essner, A. and Wang, A., "Knee Simulator Wear of Cross-Linked UHMWPE". *Society for Biomaterials,* 2000, pp. 860.

[6] Asano, T., Clarke, I., Williams, P., Akagi, M., Shishido, T. and Mizoue, T. "Knee Simulator Wear of Cross-linked UHMWPE with Normal and Mal-rotation Kinematics". *Orthopaedic Research Society*, 2002, pp. 157.

[7] Laurent, M.P., Yao, J.Q., Bhambri, S.K., Gsell, R.A., Gilbertson, L.N., Swarts, D.F. and Crowninshield, R.D. "High Cycle Wear of Highly Crosslinked UHMWPE Acetabular Liners Evaluated in a Hip Simulator". *Orthopaedic Research Society*, 2000, pp. 567.

[8] Essner, A., Wang, A. and Poggie, M. "Crosslinked UHMWPE Subject to Mal-aligned Knee Wear". *Orthopaedic Research Society*, 2002, pp. 1042.

[9] Baker, D.A., Hastings, R.S. and Pruitt, L., "Study of Fatigue Resistance of Chemical and Radiation Crosslinked Medical Grade Ultrahigh Molecular Weight Polyethylene". *Journal Biomedical Material Research*, Vol. 46, No. 1999, pp. 573-581.

[10] Muratoglu, O.K., Bragdon, C.R., O'Connor, D.O., Jasty, M. and Harris, W.H. "A Comparison of 5 Different Types of Highly Crosslinked UHMWPES: Physical Properties and Wear Behavior". *Orthopaedic Research Society*, 1999, pp. 77.

[11] DiMaio, W.G., Saum, K.A., Lilly, W.B. and Moore, W.C. "Effect of Radiation Dose on the Physical Properties of Crosslinked UHMWPE". *Orthopaedic Research Society*, 1999, pp. 100.

[12] Williams, I.R., Mayor, M.B. and Collier, J.P., "The Impact of Sterilization Method on Wear in Knee Arthroplasty". *Clinical Orthopaedics*, No. 356, 1998, pp. 170-180.

[13] Zimlich, R.H., Levesque, M., Jones, W., Del Schutte Jr., H., Livingston, B. J., Sauer, W., H., Spector, M., Weaver, K. "In-Vitro and In-Vivo Effect of Particulate Debris on TKA Articulating Surfaces". *American Academy of Orthopaedic Surgeons*, 1998.

[14] Ries, M., Banks, S., Sauer, W. and Anthony, M. "Abrasive Wear Simulation in Total Knee Arthroplasty". *Orthopaedic Research Society,* 1999, pp. 853.

[15] Jasty, M., Bragdon, C.R., Lee, K., Hanson, A. and Harris, W.H., "Surface Damage to Cobalt-Chrome Femoral Head Prostheses". *Journal of Bone and Joint Surgery (Br)*, Vol. 76-B, No. 1, 1994, pp. 73-7.

[16] Hall, R.M., Siney, P., Unsworth, A. and Wroblewski, B.M. "The Effect of Surface Topography of Retrieved Femoral on the Wear of UHMWPE Sockets". *Medical Engineering Physics*, Vol. 19, No. 8, 1997, pp. 711-719.

[17] Levesque, M., Livinston, B.J., Jones, W.M. and Spector, M. "Scratches on Condyles in Normal Functioning Total Knee Arthroplasty". *Orthopaedic Research Society,* 1998, pp. 247.

[18] Hailey, J.L., Ingham, E., Stone, M., Wroblewski, B.M. and Fisher J. "Quantitative Comparison of Acetabular Cup Wear Rates and Femoral Head Damage in Explanted Charnley Hip Prostheses". *Orthopaedic Research Society*, 1997, pp. 853.

[19] Hall, R.M., Unsworth, A., Siney, P. and Wroblewski, B.M., "Wear in Retrieved Charnley Acetabular Sockets". *IMechE*, Vol. 210, No. 1996, pp. 197-207.

[20] Raab, G.E., Jobe, C.M., Williams, P.A. and Dai, Q.G., "Damage to Cobalt-chromium Surfaces During Arthroscopy of Total Knee Replacements". *Journal of Bone and Joint Surgery*, Vol. 83-A, No. 1, 2001, pp. 46-52.

[21] Essner, A., Schmidig, G. and Wang, A. "Hip Simulator Wear of a Highly Crosslinked UHMWPE Under Clean and Three-Body Conditions". *Society for Biomaterials,* 2000, pp. 854.

[22] Laurent, M.P., Yao, J.W., Gilbertson, L.N., Swarts, D.F. and Crowninsheild, R.D.

"Wear of Highly Crosslinked UHMWPE Acetabular Liners Under Adverse Conditions". *Society for Biomaterials,* 2000, pp. 874.

[23] Taylor, S.K., Serekian, P., Bruchalski, P. and Manley, M. "The Performance of Irradiation-Crosslinked UHMWPE Cups under Abrasive Conditions Throughout Hip Joint Simulation Wear Testing". *Orthopaedic Research Society,* 1999, pp. 252.

[24] McKellop, H.S., Shen, F.W., DiMaio, W. and Lancaster, J.G., "Wear of Gamma-crosslinked Polyethylene Acetabular Cups against Roughened Femoral Balls". *Clinical Orthopaedics and Related Research,* Vol. 369, No. 1999, pp. 73-82.

[25] Saikko, V., Calonius, O. and Keranen, J., "Effect of Counterface Roughness on the Wear of Conventional and Crosslinked Ultra High Molecular Weight Polyethylene Studied with a Multi-Directional Motion Pin-on-Disk Device". *Journal of Biomedical Materials Research,* Vol. 57, No. 2001, pp. 506-512.

[26] Widding, K., Hines, G., Hunter, G. and Salehi, A. "Knee Simulator Protocol for Testing of Oxidized Zirconium and Cobalt Chrome Femoral Components Under Abrasive Conditions". *Orthopaedic Research Society,* 2002, pp. 1009.

[27] Jani, S., Morrison, M., Ries, M., Tsai, S., Scott, M. "Are Ceramic Heads Obsolete in THA with the Advent of Crosslinked UHMWPE?" *Orthopaedic Research Society,* 2002, pp. 49.

[28] Essner, A., Polineni, V.K., Wang, A., Stark, C. and Dumbleton, J.H. "Effect of Femoral Head Surface Roughness and Crosslinking on the Wear of UHMWPE Acetabular Inserts". *Society for Biomaterials.* 1998, pp. 4.

[29] Bergmann, G., Graichein, F. and Rohlmann, A., "Hip Joint Loading During Walking and Running, Measured in Two Patients". *Journal of Biomechanics,* Vol. 26, No. 8, 1993, pp. 969-90.

[30] Bauer, T.W., Taylor, S.K., Jiang, M., and Medendorp, S.V., "An Indirect Comparison of Third-body Wear in Retrieved Hydroxyapatite-coated, Porous, and Cemented Femoral Components." *Clinical Orthopaedics,* Vol. 298, No. 1994, pp. 11-18.

[31] Minakawa, H., Stone, M., Wroblewski, B.M., Ingham, E. and Fisher, J. "Quantification of Third Body Damage, and its Effect on UHMWPE Wear with Different Types of Femoral Heads". *Orthopaedic Research Society,* 1997, pp. 788.

[32] Schmalzried, T.P., Szuszczewiz, E.S., Campbell, P.C. and McKellop, H.A. "Femoral Head Surface Roughness and Patient Activity in the Wear of Hylamer". *Orthopaedic Research Society,* 1997, pp. 787.

[33] Black, J. "Prospects for Alternate Bearing Surfaces in Total Replacement Arthroplasty of the Hip". *Proceedings of 2nd Symposium on Ceramic Wear Couple,* 1997, pp. 2-10.

[34] "The Ortho Factbook: U.S. 1st Edition". 2000, Chagrin Falls, OH: Knowledge Enterprises.

[35] "The Ortho Factbook: U.S. 2nd Edition". 2001, Chagrin Falls, OH: Knowledge Enterprises.

[36] Barbour, P.S., Stone, M.H. and Fisher, J., "A Hip Joint Simulator Study Using New and Physiologically Scratched Femoral Heads with Ultra-High Molecular Weight Polyethylene Acetabular Cups". *Proceedings of the Institution of Mechanical Engineers,* Vol. 214, No. 6, 2000, pp. 569-576.

[37] Wang, A., Polineni, V.K., Essner, A., Sokol, M., Sun, D.C., Stark, C. and Dumbleton, J.H., "The Significance of Nonlinear Motion in the Wear Screening of Orthopaedic Implant Materials". *Journal of Testing and Evaluation,* Vol. 25, No. 2 1997, pp. 239-45.

[38] Wang, A., "A Unified Theory of Wear for Ultra-high Molecular Weight Polyethylene in Multi-directional Sliding". *Wear,* Vol. 248, No. 2001, pp. 38-47.

[39] Andriacchi, T.P., Stanwyck, T.S. and Galante, J.O., "Knee Biomechanics and

Total Knee Replacement". *Journal of Arthroplasty*, Vol. 1, No. 3, 1986, pp. 211-218.

Marta L. Villarraga,[1] Avram A. Edidin,[2] Michael Herr,[3] and Steven M. Kurtz[1]

Multiaxial Fatigue Behavior of Oxidized and Unoxidized UHMWPE During Cyclic Small Punch Testing at Body Temperature

ABSTRACT: We hypothesized that oxidation would influence the resistance to fatigue crack initiation and propagation of Ultra-High molecular weight polyethylene (UHMWPE). We subjected tibial insert surrogates (ram extruded GUR 1050) to accelerated aging protocols following ASTM F 2003-00 (14, 21 and 28 days). Subsurface disc specimens from the control and aged materials at each time period were subjected to cyclic small punch loading to failure (modification of ASTM F 2183-02). A significant decrease in fatigue loading was observed, relative to the un-aged controls, starting at three weeks of accelerated aging. Furthermore, SEM examination of the failed aged specimens revealed a network of multiple secondary initiation sites, which was also confirmed by observation with endoscopy, and microCT. Thus, in contrast to the unoxidized highly crosslinked conventional materials evaluated previously, the oxidized materials failed by the initiation and propagation of cracks from numerous initiation sites with the brittle appearance increasing with oxidation time. These results suggest that oxidized UHMWPE exhibits a different fatigue crack initiation and propagation behavior compared to unoxidized virgin, and crosslinked UHMWPE. Future studies will be needed to increase our understanding of the clinically acceptable fatigue properties for new tibial bearing materials, such as highly crosslinked UHMWPEs.

KEYWORDS: Ultra-high molecular weight polyethylene, UHMWPE, fatigue, crosslinking, oxidative degradation, accelerated aging, cyclic loading, body temperature

Introduction

Although the *in vivo* wear mechanisms of UHMWPE tibial components of total knee arthroplasty can include adhesive/abrasive wear, of greater concern among clinicians is the incidence of fatigue wear, such as pitting or delamination. A variety of UHMWPE factors, such as the presence of fusion defects and post-irradiation aging, have been associated with contributing to fatigue wear of knee replacements [1-8]. Despite the recognition that fatigue resistance of UHMWPE plays an important role in the clinical

[1] Managing Engineer and Principal Engineer, respectively, Exponent, Inc., and Research Associate Professors, Implant Research Center, School of Biomedical Engineering, Science, and Health Systems, Drexel University, 3401 Market St, Suite 300, Philadelphia PA, 19104.
[2] Research Associate Professor, Implant Research Center, School of Biomedical Engineering, Science, and Health Systems, Drexel University, 3141 Chestnut St, Philadelphia PA, 19104.
[3] Senior Engineer, Exponent, and Graduate Student, School of Biomedical Engineering, Science, and Health Systems, Drexel University, 3401 Market St, Suite 300, Philadelphia PA, 19104.

117

performance of knee replacements, a lack of consensus remains among members of the orthopedic research community regarding clinically validated test protocols for assessing the fatigue behavior of UHMWPE. The fatigue crack propagation behavior and fracture resistance of conventional and highly crosslinked UHMWPE have been studied extensively [9-22], yet these properties have not been directly correlated to the clinical incidence of fatigue wear in knee replacements. In particular, the comparatively large size of specimens required for standardized fatigue and fracture tests of polymers effectively limits their application to retrieved UHMWPE components for total knee replacement.

Currently, fatigue wear resistance of UHMWPE materials is assessed by multidirectional joint simulators, that are programmed to duplicate the loading and kinematics of the natural knee joint [23-28]. In addition, manufacturers have developed structural fatigue tests for evaluating candidate UHMWPE materials for knee or patellar replacement. However, insofar as the characterization of fatigue damage is concerned, these complex tests, executed over many millions of loading cycles, are employed as binary, or pass–fail, discriminators for the prevalence of pitting or delamination. For example, researchers have noted that components that have been gamma irradiated in air or nitrogen and aged will exhibit delamination in a contemporary knee simulator, whereas unirradiated components, as well as certain highly crosslinked UHMWPE materials, such as remelted electron-beam irradiated highly crosslinked UHMWPE, show no such fatigue wear damage [4, 29, 30]. Nonetheless, it remains unknown to what extent one can generalize about the incidence of fatigue wear observed in joint simulators to the clinical situation, particularly for new materials, such as highly crosslinked UHMWPE.

Miniature specimen techniques provide an alternate vehicle for assessing mechanical behavior of UHMWPE components at a local scale. We have previously extended the small punch test for UHMWPE, described in ASTM Standard Test Method for Small Punch Testing of Ultra-High Molecular Weight Polyethylene Used in Surgical Implants (F 2183-02), to fatigue loading conditions [31]. Using a "total life" approach, we subjected four types of conventional and highly crosslinked UHMWPE to cyclic loading at 200 N/s and at body temperature in a small punch test apparatus. Cyclic small punch testing under load control was found to be an effective and repeatable method for relative assessment of the fatigue resistance of conventional and highly crosslinked UHMWPE specimens under multiaxial loading conditions. For each of the four conventional and highly crosslinked UHMWPE materials evaluated in this study, fatigue failures were consistently produced according to a power law relationship in the low cycle regime, corresponding to failures below 10000 cycles. No evidence of subcritical crack growth or secondary initiation sites was observed during scanning electron microscopy of the failed specimens after fatigue testing. Consequently, based on scanning electron microscopy examination, the fatigue failures for all four conventional and highly crosslinked materials demonstrated that the fatigue failure initiated from a single initiation site and then propagated in a stable manner before catastrophic fracture. The initiation site was frequently found to be at the surface near the center of the specimen. The results of the fatigue punch study suggested that the low cycle fatigue response of conventional and highly crosslinked UHMWPEs were comparable, in contrast with previous fracture and fatigue crack propagation studies, which ranked highly crosslinked UHMWPE as inferior to conventional materials.

Our initial study of miniature specimen fatigue testing was conducted using unoxidized materials [31]. Based on ample evidence in the literature [32], and our own prior observations of degraded static mechanical behavior in UHMWPE hip and knee components [33-37], we hypothesized that oxidation would also influence the resistance to fatigue crack initiation and propagation. Rather than proceeding directly to characterization of retrievals, we sought to initially test our hypothesis using oxidized UHMWPE produced by accelerated aging. Another objective of our present study was to compare the low cycle fatigue behavior of virgin and oxidized UHMWPE with our previous observations of highly crosslinked UHMWPE under identical loading conditions. A third purpose of our study was to investigate the suitability of two novel techniques for detecting crack initiation in miniature small punch specimens, using either an endoscope or microCT. The long-term goal of this research is to develop further a miniature specimen fatigue testing protocol for characterization of crack initiation and propagation in material obtained from retrieved UHMWPE tibial components.

Materials and Methods

Polyethylene Material Preparation

Test specimens were prepared using the fabrication methods comparable to commercially available orthopaedic components. Ram extruded GUR 1050 UHMWPE resin from the same production batch was utilized in this study. The stock material was machined into approximately 20 square test samples 30 mm in width and 10 mm in thickness, corresponding to the approximate dimensions of a tibial insert. One face of the test samples was specified to have a surface finish comparable to the articulating surface of UHMWPE components. No irradiation was performed on the samples.

The material was subjected to four different aging conditions: no aging (control), and aging in an "oxygen bomb" at 503 kPa (73 psi, 5 atm) O_2 and 70°C for 14 days, 21 days and 28 days. The control material is also referred to as conventional from here forward. Aging in oxygen was conducted in accordance with the ASTM Standard Guide for Accelerated Aging of Ultra High Molecular Weight Polyethylene (F 2003-00). Five of these samples were considered control material, and 15 samples were subjected to artificial aging following the procedures outlined in ASTM F 2003-00 for 14, 21 and 28 days, with five samples aged for each time period.

In previous studies we had evaluated the oxidation level of the same material (un-irradiated ram extruded GUR 1050 from same stock) unaged, and aged to two [36] and four weeks [35], which confirmed that the specimens aged to four weeks were subjected to substantial oxidation in the subsurface regions. This was of importance in order to compare it to oxidation profiles of natural shelf-aged specimens.

Small Punch Testing

Following aging at each period (0, 14, 21, or 28 days), four cylindrical cores were made from each sample and miniature disk specimens (measuring 0.5 mm in thickness and 6.4 mm in diameter) were prepared from locations at a subsurface depth of 1.5 to 2 mm. The subsurface location of the specimens was based on previous natural aging

experiments, which showed peak oxidation levels occurring below the surface at approximately similar locations [35].

To obtain the initial peak load and to provide reference values to establish the loading range for fatigue evaluation, five specimens of each material were loaded monotonically to failure at a rate of 200N/s. Between 11 and 20 specimens of each material condition were then tested in a fatigue mode following a previously established protocol [31]. This cyclic small punch test is an extension of the static small punch test for UHMWPE, described in ASTM F 2183-02. A triangular load waveform at a constant rate of 200N/s was used to fatigue the specimens between a minimum of 2N and up to a maximum load representing a percentage of the mean peak load established during the monotonic testing. Maximum loads ranged from 60% to 94% of the peak loads, which resulted in specimen failure within 10 000 cycles. The low minimum load level results in a nearly constant, near-zero load ratio (minimum/maximum) for all tests. Mechanical testing was performed utilizing a 858 Mini Bionix II closed-loop servo-hydraulic load frame (MTS, Minneapolis, MN), equipped with a 5 kN load cell and tabletop MTS Series 651 environmental chamber. In addition to a factory installed thermocouple that monitored the air temperature of the environmental chamber, a second calibrated thermocouple was inserted into the small punch testing fixture to provide an additional, independent temperature reading of the test device close to the specimen. A voltage signal from the second thermocouple was wired into the servo-hydraulic control module so that testing would commence automatically as soon as the local temperature was within 1°C of the target test temperature of 37°C. For consistency, specimens were preconditioned at the test temperature in a controlled oven for at least 12 hours prior to cyclic testing.

Fracture Surface Evaluation

Following mechanical testing, the specimens were evaluated under light microscopy to describe the morphology of the fracture surfaces. Two specimens from each material condition (one that failed at a low number of cycles, and one that failed at a high number of cycles) were sputter coated with carbon and further evaluated under a scanning electron microscope (SEM) operating at 10kV (JEOL 6300 FV, Peabody, MA) at magnifications of 20× to 800×. SEM evaluation was done to further characterize possible differences in morphology of the fracture surfaces, such as thickness, surface characteristics, and fracture patterns between the material groups.

We conducted a preliminary investigation to compare two nondestructive techniques to characterize the damage initiation and accumulation in the miniature specimens that underwent fatigue punch testing. The first technique evaluated was the use of a surgical endoscope mounted on a custom designed apparatus within the environmental chamber of the materials testing machine to monitor the back surface of the small punch specimen during the cyclic punch testing. A 28-day aged specimen was imaged using the endoscope and optical micrographs were captured from the video during the first 1 000 cycles of loading, and at the moment of fatigue failure.

The second technique evaluated was the use of microCT to detect surface and internal fatigue damage within the miniature specimens. The current (voxel) resolution of microCT systems is on the order of 5 to 10   m. We evaluated one specimen loaded at low loads (high cycles to failure) from each of the aging periods (0, 14, 21, and 28 days) using a commercial microCT scanner (Scanco, Switzerland) with a nominal 9   m voxel resolution. Three-dimensional reconstructions of each specimen and two-dimensional

views of the images taken through the specimens were used to examine the specimens for the presence of surface, through-thickness, and internal cracks.

Data Analysis

The maximum peak loads during single cycle testing to failure were compared using t-tests. A p-value of 0.05 was used as the basis for statistical significance. Power relationships were sought between the applied peak load and the cycles to failure using linear regression analysis (Statview: SAS, Cary, NC). In addition, power relationships were also fit to data normalized with respect to the highest peak load measured in the corresponding single cycle tests. These relationships were evaluated without taking into account the data from the monotonic or single cycle loading conditions for any of the materials. We compared the 95% confidence intervals of the slopes of the power regressions of the raw and normalized peak load versus cycles to failure data to determine if the materials were significantly different in behavior.

Using a customized analysis program, the hysteresis energy (work done in a cycle) for each loading/unloading cycle of each specimen was calculated to allow comparison of the maximum hysteresis energies with the cycles to failure and the corresponding load magnitudes. This allowed the comparison of the amount of hysteresis per loading cycle. In addition, the displacement and hysteresis history throughout loading were compared for all the materials. The relationships between the ultimate displacement (maximum) and the corresponding cycles to failure, and between the ultimate displacement (maximum) and the corresponding load magnitudes were also evaluated for all the materials.

Furthermore, a comparison of the data from this study was done with the results from our previous study which evaluated highly crosslinked UHMWPE and conventional materials subjected to cyclic loading at body temperature [31].

Results

Small Punch Testing

Under monotonic or single cycle loading conditions, the peak loads of the virgin and 14-day aged GUR 1050 EX UHMWPEs were significantly higher than those of the materials aged for 21 and 28 days (p < 0.05, Figure 1, Table 1). In addition, the 21 and 28-day aged GUR 1050 EX materials also had significantly different peak loads during monotonic loading, with the 28-day aged material having the lowest peak load of all the materials evaluated.

For fatigue loading at body temperature, there were no significant differences in the fatigue behavior response curves between the virgin GUR 1050 EX and the 14-day aged GUR 1050 EX UHMWPEs. The 28-day aged material showed the least fatigue resistance of all the materials with consistently lower peak loads at the same cycles to failure when compared to the virgin and the other materials aged for shorter periods (Figure 2, Table 1, p < 0.05). Significant differences were observed when comparing the response curves of the virgin and 14-day aged materials to those of the materials aged for 21 and 28 days (p < 0.05, Figure 2, Table 1).
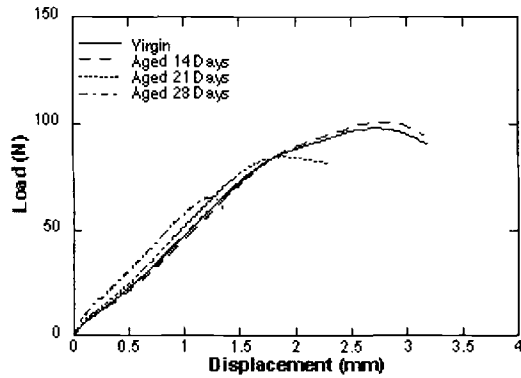
Figure 1— *Load versus displacement data for monotonic (single-cycle) load-controlled tests (200 N/s) at body temperature (37°C) for all materials evaluated (Virgin, 14-day, 21-day and 28-day aged).*
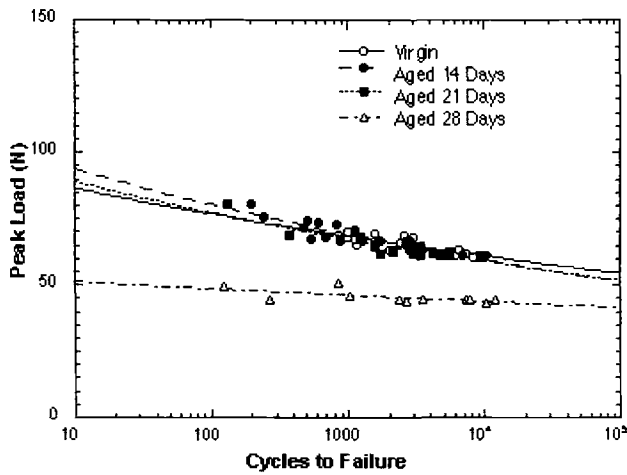
Figure 2— *Peak cyclic load versus cycles to failure for all samples tested.*

Table 1— *Power regression equations for cyclic punch data for each material set for raw data and normalized data, including 95% confidence intervals*

Material GUR 1050	Peak Load (N)	Fatigue Relationship for data[1]	r^2	95% CI for Power Law Exponent for Data
Control (Virgin)	100.8±3.4	$y = 97 x^{-0.050}$	0.67	-0.070 to -0.030
Aged 14 days	101.3±1.2	$y = 109x^{-0.065}$	0.85	-0.082 to -0.048
Aged 21 days	86.2±5.4	$y = 102x^{-0.059}$	0.81	-0.076 to -0.042
Aged 28 days	63.5±4.1	$y = 54x^{-0.022}$	0.42	-0.046 to 0.002[2]

[1]Y defines the load and X defines cycles to failure, as shown in Figure 2.
[2]Significant difference (p<0.05) when compared with all other materials

The hysteresis behavior was distinct between the virgin and the aged materials at both low loads (high cycles to failure) and at high loads (low cycles to failure). The maximum hysteresis values were lower at any given cycle to failure for the 28-day aged material as compared to the other materials in this study (Figure 3A). The 14-day and 21-day aged materials had the highest measured maximum hysteresis values of all the materials evaluated (Figures 3A, 3B), in particular for the samples loaded to higher loads.

The hysteresis history throughout the fatigue tests is shown in Figure 4 for selected samples that were loaded both to low peak loads or high peak loads for each material type. The hysteresis history (Figure 4) and the hysteresis loops (Figure 5) show that amount of hysteresis energy per loading cycle increased gradually as the test advanced for all the materials except for the 28-day aged UHMWPE, when loaded to higher loads (Figures 4A, 4B, 4C, and 4D). In particular, the virgin material displayed saturation in hysteresis magnitude as the test advanced (plateau in curve, Figure 4A) at both low loads and high loads. The samples loaded to lower loads for all the materials showed a sudden increase in hysteresis as the samples were approaching failure, with a more abrupt change in hysteresis magnitude for the most degraded samples (28-day aged, Figures 4A-D).

For all the materials, the sudden or gradual rise in both hysteresis and displacement values occurred simultaneously at the same cycle of loading (Figures 4 and 6, respectively). The amount of hysteresis energy per loading cycle increased during the fatigue tests for all material types (Figures 4 and 5). Similar increases in the hysteresis energy per loading cycle were observed for the virgin, 14-day and 21-day aged material conditions (Figure 4A, 4B, and 4C) with the least amount of increase seen for the 28-day aged material (Figure 4D). The magnitude of displacement recorded throughout the cyclic tests (Figures 6A-D) indicated that the 28-day aged samples deformed the least, mainly due to their advanced state of degradation, and also reflected in the single-cycle load displacement behavior that showed the lowest peak load and displacement, and lowest absorbed energy (area under load-displacement curve). Figure 6 also shows an evident transition in displacement from small to larger displacements with increasing number of cycles for the virgin, 14-day and 21-day aged materials, in comparison to the more abrupt change seen for the 28-day aged material. In general, both the single-cycle (monotonic) test peak load and displacement, and the fatigue hysteresis and the

displacement responses, as measured from the small punch tests, are reflected in the decreased low cycle fatigue resistance for the 28-day aged samples.

(A)

(B)
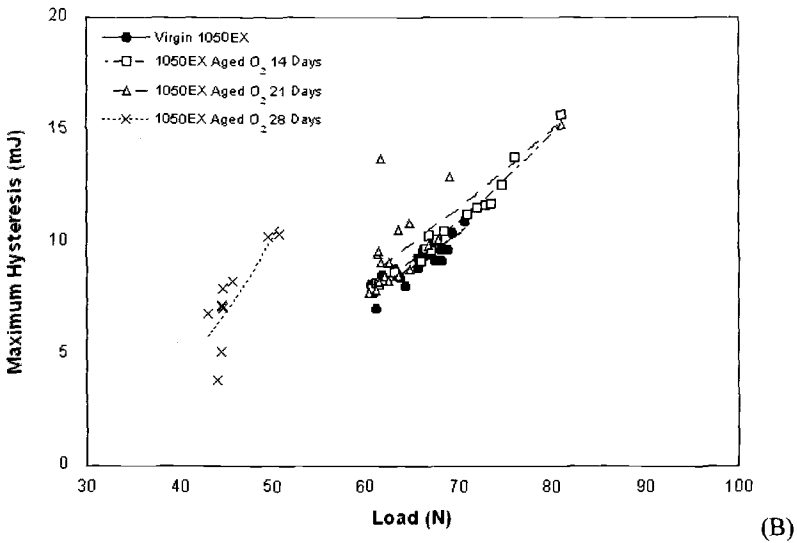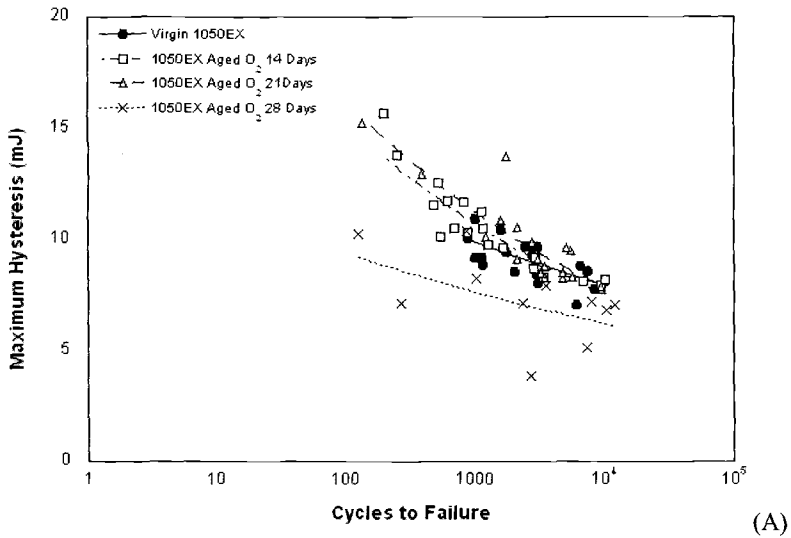
Figure 3— *(A) Maximum hysteresis versus cycles to failure for all samples tested (B) Maximum hysteresis versus peak load for all samples tested.*
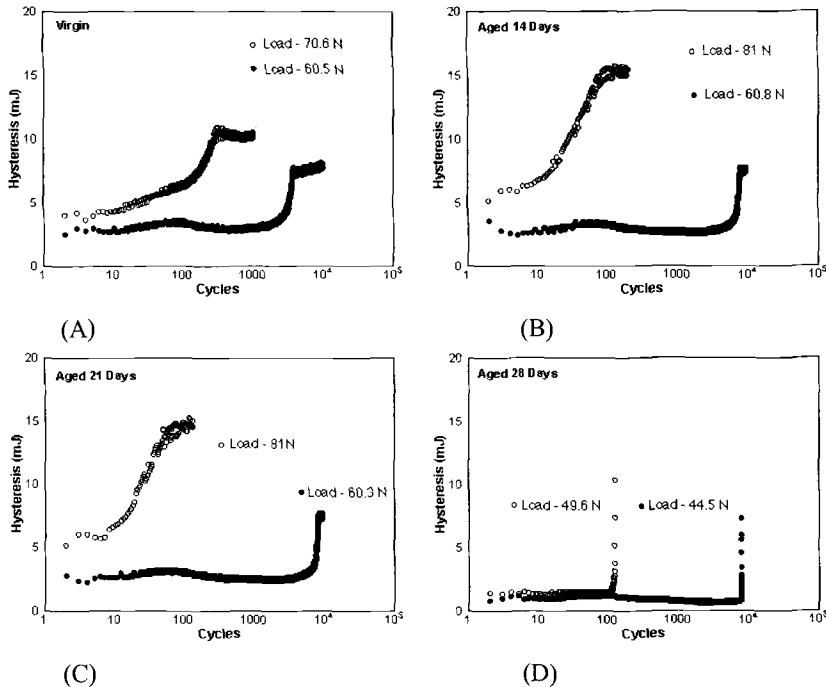
Figure 4 —*Hysteresis history throughout cycles of loading for selected samples at low loads (45-61N) and at high loads (50-81N) for all materials tested: (A) Virgin GUR 1050; (B) GUR-1050 aged 14 days (C) GUR-1050 aged 21 days; (D) GUR-1050 aged 28 days*

Fracture Surface Evaluation

The SEM micrographs (Figure 7 and 8) confirmed that the displacement of the 28-day aged material (Figures 7D and 8D) was much lower than that of the other materials. Evaluation of these micrographs also indicated the difference in the plastic drawing around the punch head, which was more distinctively observed in the virgin material (Figures 7A and 8A) and less evident with increased aging time. The degradation of the 28-day material was clearly observed in the fracture surface observed in the SEM micrographs, both at low (Figure 7D) and high resolution (Figure 8D).

We also utilized the surgical endoscope to characterize the damage initiation and accumulation in a 28-day aged sample that underwent fatigue punch testing. Within the first 1000 cycles of loading, evidence of multiple fatigue crack initiation sites was observed (Figure 9A) at length scales consistent with the granular structure of the UHMWPE (50-100 μm in diameter). The fatigue cracks were observed to develop a communicating network until they propagated through the thickness of the specimen (Figure 9B).

Evaluation of the samples using microCT scanning showed the presence of surface and through thickness cracks in the 28-day aged sample (Figure 10C and 11C). The evaluation of the individual slices through the thickness of the 28-day aged sample (Figure 11C) showed the presence of multiple internal cracks through the thickness of the sample. In comparison, the virgin, and 21-day aged showed a distinct single surface crack in the samples (Figure 10A, 10B, and 11A, 11B).

(A)   (B)   (C)   (D)
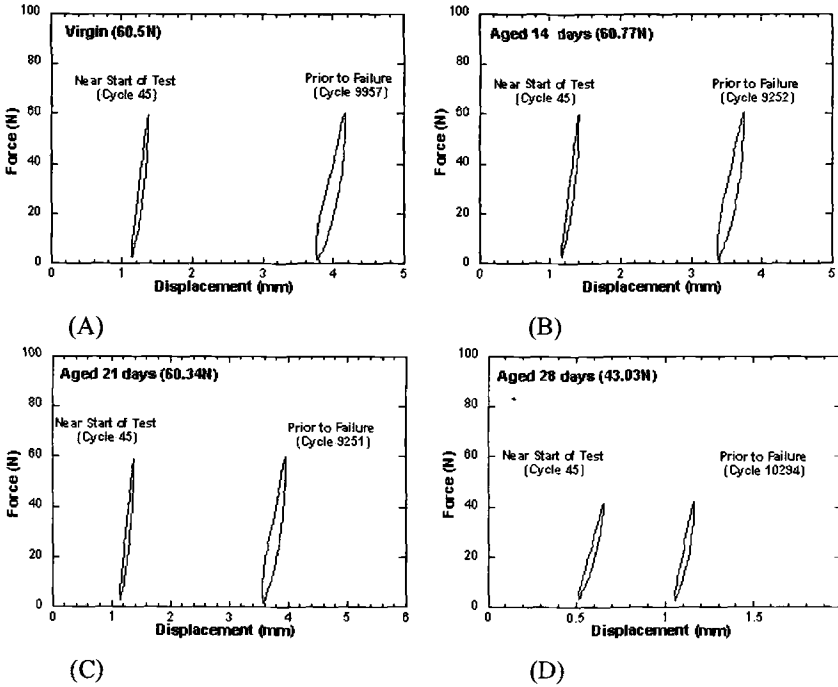
Figure 5 —*Load versus displacement cyclic data (hysteresis loops) for high cycle fatigue samples. Cyclic data shown for near the start of the test and prior to failure. (A) Virgin GUR 1050: loaded to 61 N, 10002 cycles to failure; (B) GUR-1050 aged 14 days: loaded to 61N, 9297 cycles to failure; (C) GUR-1050 aged 21 days: loaded to 60N, 9296 cycles to failure; (D) GUR-1050 aged 28 days: loaded to 43N, 10339 cycles to failure.*
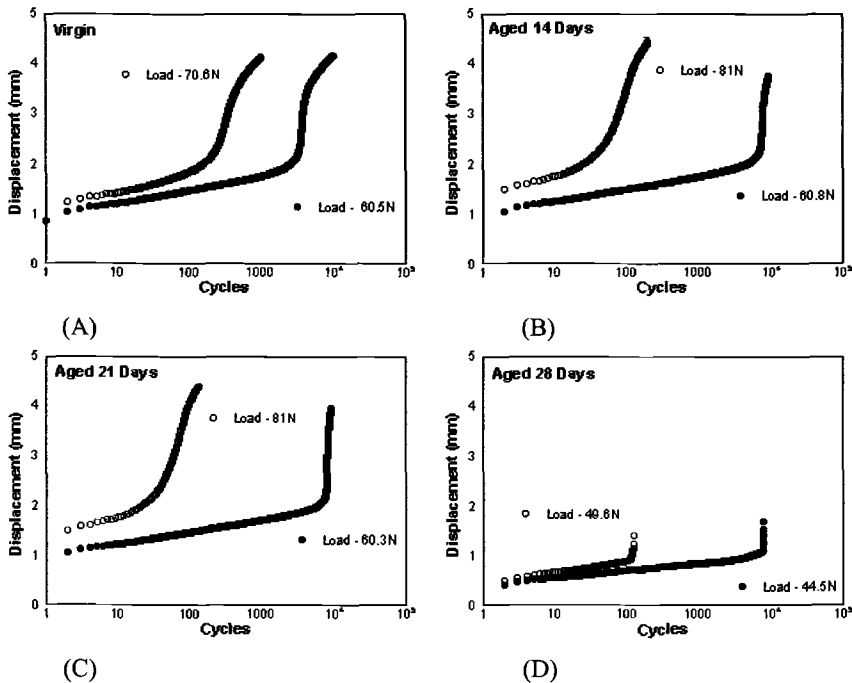
Figure 6 —*Displacement history throughout cycles of loading for selected samples at low loads (45-61N) and at high loads (50-81N) for all materials tested: (A) Virgin GUR 1050; (B) GUR-1050 aged 14 days (C) GUR-1050 aged 21 days; (D) GUR-1050 aged 28 days.*

Comparison to Highly Crosslinked and Conventional Fatigued UHMWPE

The fatigue behavior of the degraded materials in this study was compared to that of the previous series of UHMWPE materials (conventional and crosslinked) that were also tested under cyclic loading. The previous series of materials that had been subjected to fatigue testing included: (1) unirradiated (control); (2) gamma radiation sterilized in nitrogen to 30 kGy; (3) gamma irradiated with a dose of 100 kGy and annealed at 110°C; (4) gamma irradiated with a dose of 100 kGy and remelted at 150°C. The first two material conditions were included to represent conventional UHMWPE materials, whereas the last two conditions were included as representations of contemporary highly crosslinked UHMWPE materials. The crosslinked UHMWPEs had significantly higher peak loads during monotonic loading than the control, conventional and all the oxidized GUR 1050 UHMWPE materials evaluated in this study (p < 0.05) [31]. When evaluating the peak load versus cycles to failure response curves, the 28-day aged material showed an evident decreased fatigue resistance at both low number and high number of cycles as compared to the other oxidized materials and to the conventional, control and the highly crosslinked UHMWPE materials (Figure 12).
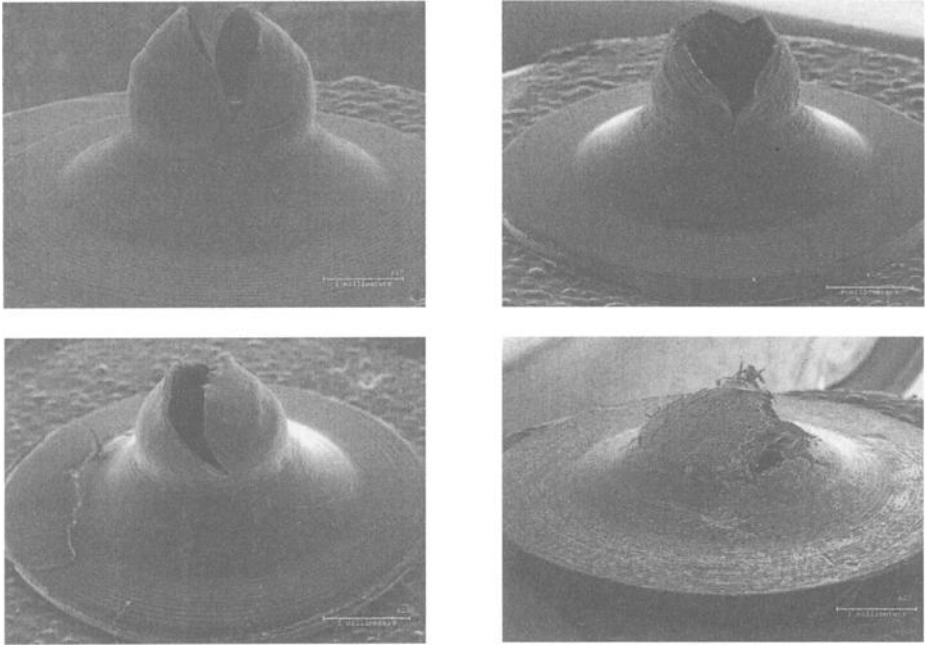
Figure 7 — *Scanning electron micrographs (x20) of failed samples after fatigue testing at high number of cycles: (A) Virgin GUR 1050, 10002 cycles; (B) GUR-1050 aged 14 days, 10220 cycles; (C) GUR-1050 aged 21 days, 9296 cycles; (D) GUR-1050 aged 28 days, 12024 cycles.*

When comparing the maximum hysteresis values for all the samples, the highly crosslinked materials absorbed greater amounts of energy per loading when loaded to higher peak loads, with approximately 11% higher energy levels as compared to the highest values reached for the oxidized materials (14- and 21-day aged).

In terms of the magnitude of total displacement, the materials aged for 14 and 21 days had comparable maximum displacement magnitudes to those of the control and conventional materials that were evaluated previously under cyclic loading. In contrast, the crosslinked materials had much lower maximum displacements than the oxidized materials evaluated in this study.

(A)   (B)   (C)   (D)
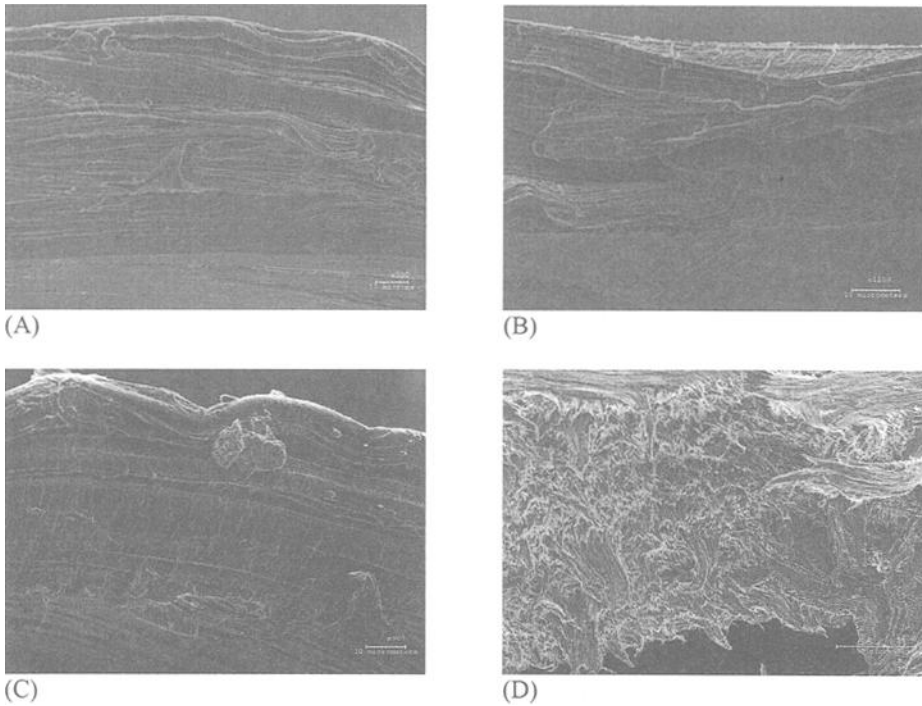
Figure 8 —*Scanning electron micrographs of fracture surfaces of failed samples after fatigue testing at high number of cycles: A) Virgin GUR 1050, 10 002 cycles (x800); (B) GUR-1050 aged 14 days, 10 220 cycles (x1100); (C) GUR-1050 aged 21 days, 9 296 cycles (x900); (D) GUR-1050 aged 28 days, 12 024 cycles (x200).*

(A)   (B)
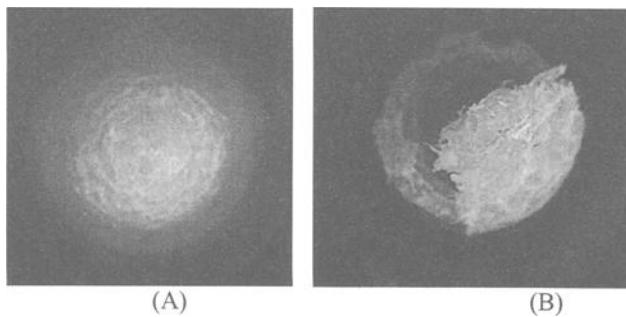
Figure 9 —*Digital optical micrographs of a 28-day aged specimen, observed thorough an endoscope (A) during the first 1 000 loading cycles, note intergranular damage initiation; and (B) at the moment of fatigue failure. For reference, the punch diameter is 2.5 mm.*
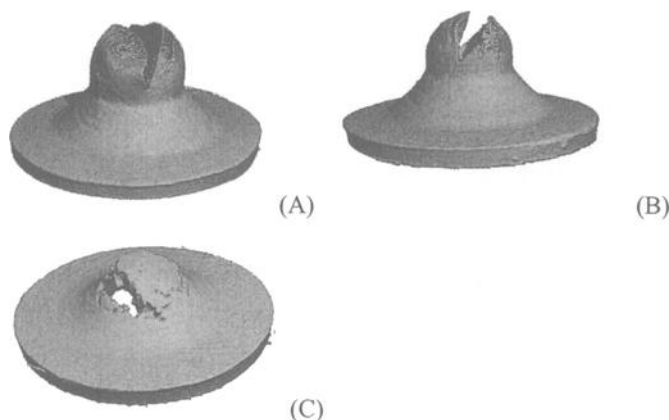
Figure 10 —*Samples tested to low peak cyclic loads lasting larger number of cycles (A) 3D reconstruction of microCT images of a virgin fatigue specimen showing the presence of a single crack on the surface; (B) 3D reconstruction of microCT images of a 21-day aged fatigue specimen showing the presence of a single crack on the surface; (C) 3D reconstruction of microCT images of a 28-day aged fatigue specimen showing the presence of surface, through thickness cracks.*

Discussion

The aged UHMWPE materials all exhibited a power law relationship between the peak cyclic load and the number of cycles to failure, as was observed for the unaged, conventional and highly crosslinked materials. However, a significant decrease in fatigue loading was observed, relative to the unaged controls, starting at about three weeks of aging in the oxygen bomb. Furthermore, examination of the failed, aged specimens using field emission scanning electron microscopy (FE-SEM), digital endoscopy, and micro-CT revealed a network of multiple secondary crack initiation sites. That is, in contrast to the non-oxidized and conventional UHMWPE materials described above, the oxidized material failed by the initiation and propagation of fatigue cracks from numerous initiation sites. These sites appeared to be on or near particle boundaries, consistent with preferential oxidation of the particle boundaries prior to the resin particles themselves, as has been noted by Muratoglu and associates [38]. Our data suggest that oxidized UHMWPE exhibits a fundamentally different fatigue crack initiation and propagation behavior than unoxidized conventional and highly crosslinked UHMWPE. We have previously indicated that the four-week aging protocol for unirradiated polyethylene should not be interpreted as a complete reproduction of all the characteristics associated with natural aging [35]. However, given the subsurface mechanical degradation seen in our previous work, we have suggested that such aged material could provide a realistic model for subsurface mechanical degradation, and as such be suitable for further mechanical testing in venues such as wear simulation.

(A)

(B)

(C)
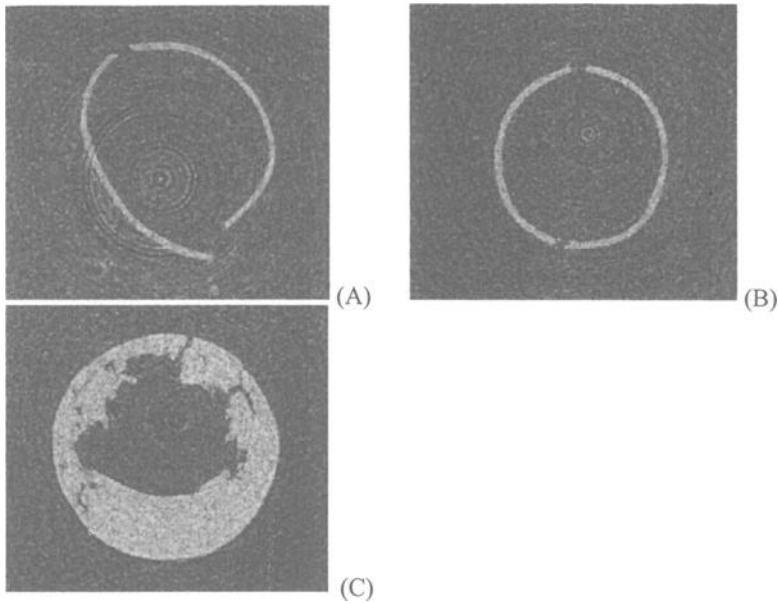
Figure 11—*Samples tested to low peak cyclic loads lasting larger number of cycles. (A) Single 2D microCT slice through virgin fatigue sample to show the single crack present through the thickness of the sample. (B) Single 2D microCT slice through 21-day aged fatigue sample to show the single crack present in the sample. (C) Single 2D microCT slice through 28-day fatigue sample to show the multiple cracks present on a single slice.*
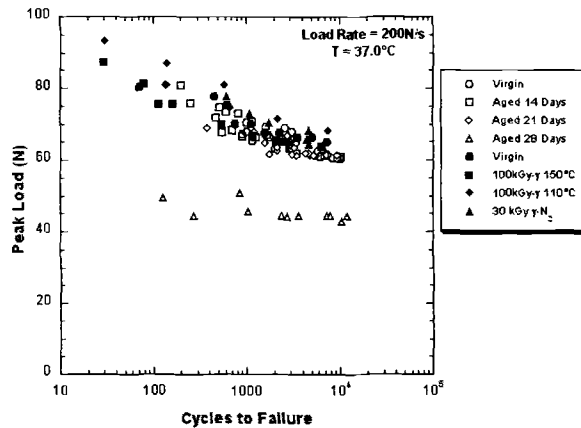
Figure 12— *Peak cyclic load versus cycles to failure for the samples tested in this study and previous set of samples reported, including control, conventional and crosslinked materials.*

In comparison to the findings of Muratoglu *et al.* and Yao *et al.*, which showed that melt annealed highly crosslinked UHMWPE performed better than gamma-air irradiated controls in wear simulations, our work does not compare remelted highly crosslinked UHMWPE to gamma-air controls. Instead we compare highly crosslinked materials (annealed and remelted) to un-irradiated controls which were exposed to accelerated aging conditions. All the samples utilized by Yao *et al.* were exposed to accelerated aging conditions (ASTM F 2003) whereas those by Muratoglu *et al.* were preconditioned in an oven at 80C for 35 days. Gamma-air materials from both previous studies (Yao et al and Muratoglu *et al.)* showed a decrease in mechanical properties due to aging, wheareas the melt-annealed materials showed stability in their mechanical properties despite the aging. In our study, the material that showed the most degradation in mechanical properties was the one aged for 28 days (unirradiated).

Although the results of this study support our hypothesis that oxidation influences the fatigue behavior under the cyclic, multiaxial loading conditions of the fatigue small punch test, it remains difficult to make an association between the accelerated aging conditions and the oxidation states of implanted tibial inserts. It is important to note that accelerated aging conditions have been shown to be consistent with approximately five years of shelf aging for gamma-air components aged for 14 days [39]. Therefore, it remains the subject of future research to determine under what clinical conditions (e.g., combination of shelf life and implantation time), changes in fatigue crack initiation and propagation mechanisms in UHMWPE undergo the transition from apparent "ductile" to "brittle" behavior. This knowledge is critical to our understanding of clinically acceptable fatigue properties for new tibial bearing materials, such as highly crosslinked UHMWPEs, which have already been clinically introduced for total knee replacements.

Cyclic small punch testing was found to be an effective and repeatable method for producing low-cycle fatigue failures in miniature UHMWPE specimens, whether fabricated from conventional (virgin unaged) and aged material, as in the present study, or from highly crosslinked UHMWPE, as shown previously [31]. The testing technique provides information not only about the resistance of UHMWPE materials to low cycle fatigue failure, but also about incremental plastic deformation and hysteresis of the materials under multiaxial cyclic loading. Furthermore, when combined with an imaging technique for such as digital endoscopy or microCT, cyclic small punch testing can address issues of crack initiation as well as propagation in a "total life" approach to fatigue assessment.

At present, it is not known which novel technique (microCT vs. endoscope) will provide the preferred method for detecting initiation in the miniature UHMWPE fatigue specimens. Measurements from the endoscopy have the advantage of being performed *in situ* under live loading conditions, but may not be as high resolution as the microCT images. The latter technique, on the other hand, is likely to be more time consuming and can only be assessed after the completion of testing and removal of the specimen from the test fixtures. Further research will be needed to identify whether one of the new techniques for detecting crack initiation will emerge as clearly superior to the other.

Because of the recent clinical introduction of highly crosslinked polyethylene for total knee arthroplasty, it is critical that the fatigue behavior of UHMWPE tibial inserts be more completely understood so that the information can be used to develop predictive models for the new crosslinked implant materials. However, a major impediment to

studying the fatigue behavior of polyethylene using conventional large specimen techniques, and applying the knowledge to predict clinical fatigue wear performance, relates to the fact that the properties of polyethylene evolve as a function of sterilization, shelf aging, location within the implant, and *in vivo* exposure. It is currently not known whether pitting and delamination of total knee replacements result from compromised mechanical behavior under monotonic loading or cyclic loading conditions, or whether degradation of a combination of static and fatigue polyethylene mechanical properties will lead to fatigue wear *in vivo*. Testing of miniature specimens of UHMWPE from retrieved tibial inserts under both monotonic and fatigue loading conditions is one means by which to gain improved insight into the unique wear damage modes that limit the longevity of knee implants.

Acknowledgements

References

[1] Collier, J. P., Sperling, D. K., Currier, J. H., Sutula, L. C., Saum, K. A., and Mayor, M. B., "Impact of gamma sterilization on clinical performance of polyethylene in the knee," *Journal of Arthroplasty,* 1996, Vol. 11, pp. 377-89.

[2] Currier, B. H., Currier, J. H., Collier, J. P., Mayor, M. B., and Scott, R. D., "Shelf life and in vivo duration. Impacts on performance of tibial bearings," *Clinical Orthopedics,* 1997, Vol. 342, pp. 111-22.

[3] Currier, B. H., Currier, J. H., Collier, J. P., and Mayor, M. B., "Effect of fabrication method and resin type on performance of tibial bearings," *Journal of Biomedical Materials Research,* 2000, Vol. 53, pp. 143-151.

[4] Kennedy, F. E., Currier, J. H., Plumet, S., Duda, J. L., Gestwick, D. P., Collier, J. P., Currier, B. H., and Dubourg, M.-C., "Contact fatigue failure of ultra-high molecular weight polyethylene bearing components of knee prostheses," *Journal of Tribology,* 2000, Vol. 122, pp. 332-339.

[5] Wrona, M., Mayor, M. B., Collier, J. P., and Jensen, R. E., "The correlation between fusion defects and damage in tibial polyethylene bearings," *Clinical Orthopedics,* 1994, Vol. 299, pp. 92-103.

[6] Bostrom, M. P., Bennett, A. P., Rimnac, C. M., and Wright, T. M., "The natural history of ultra high molecular weight polyethylene," *Clinical Orthopedics,* 1994, Vol. 309, pp. 20-8.

[7] Kurtz, S. M., Bartel, D. L., and Rimnac, C. M., "Post-irradiation aging affects the stresses and strains in UHMWPE components for total joint replacement," *Clinical Orthopedics,* 1998, Vol. 350, pp. 209-220.

[8] Bell, C. J., Walker, P. S., Abeysundera, M. R., Simmons, J. M., King, P. M., and Blunn, G. W., "Effect of oxidation on delamination of ultrahigh-molecular-weight polyethylene tibial components," *Journal of Arthroplasty,* 1998, Vol. 13, pp. 280-90.

[9] Baker, D., Hastings, R. S., and Pruitt, L., "Study of fatigue resistance of chemical and radiation crosslinked medical grade ultrahigh molecular weight polyethylene," *Journal of*

Biomedical Materials Research, 1999, Vol. **46**, pp. 573-581.

[10] Baker, D. A., *Macro- and Microscopic Evaluation of Fatigue in Medical Grade Ultra-High Molecular Weight Polyethylene,* Berkeley, CA, Ph.D. Dissertation, University of California at Berkeley, 2001.

[11] Connelly, G. M., Rimnac, C. M., Wright, T. M., Hertzberg, R. W., and Manson, J. A., "Fatigue crack propagation behavior of ultrahigh molecular weight polyethylene," *Journal of Orthopedic Research,* 1984, Vol. 2, pp. 119-25.

[12] Eberhardt, A. W., Cole, J. A., and Lemons, J. E., "The effects of irradiation level and resin on fatigue crack resistance of UHMWPE," *Transactions of the 27th Annual Meeting of the Society for Biomaterials,* 2001, Vol. 24, pp. 480.

[13] Elbert, K. E., Wright, T. M., Rimnac, C. M., Klein, R. W., Ingraffea, A. R., Gunsallus, K., and Bartel, D. L., "Fatigue crack propagation behavior of ultra high molecular weight polyethylene under mixed mode conditions," *Journal of Biomedical Materials Research,* 1994, Vol. 28, pp. 181-7.

[14] Krzypow, D. J., and Rimnac, C. M., "Cyclic steady state stress-strain behavior of UHMW polyethylene [In Process Citation]," *Biomaterials,* 2000, Vol. 21, pp. 2081-7.

[15] Lehman, R. D., Rimnac, C. M., Kershner, J., Sevo, K., Krzypow, D. J., Haggard, W., Parr, J., and Goldberg, V., "Steady-state fatigue and creep response of crosslinked ultra-high molecular weight polyethylenes," *Transactions of the 27th Annual Meeting of the Society for Biomaterials,* 2001, Vol. 24, pp. 477.

[16] Pascaud, R. S., Evans, W. T., McCullagh, P. J., and Fitz Patrick, D. P., "Influence of gamma-irradiation sterilization and temperature on the fracture toughness of ultra-high-molecular-weight polyethylene," *Biomaterials,* 1997, Vol. 18, pp. 727-35.

[17] Pruitt, L., Hermann, R., and Suresh, S., "Fatigue crack growth in polymers subjected to fully compressive cyclic loads," *Journal of Materials Science,* 1992, Vol. 27, pp. 1608-1616.

[18] Pruitt, L., Koo, J., Rimnac, C. M., Suresh, S., and Wright, T. M., "Cyclic compressive loading results in fatigue cracks in ultra high molecular weight polyethylene," *Journal of Orthopedic Research,* 1995, Vol. 13, pp. 143-6.

[19] Pruitt, L., and Bailey, L., "Factors affecting the near-threshold fatigue behavior of surgical grade ultra high molecular weight polyethylene," *Polymer,* 1998, Vol. 39, pp. 1545-1553.

[20] Rimnac, C. M., Wright, T. M., and Klein, R. W., "The effect of waveform on the fatigue crack propagation behavior of ultra high molecular weight polyethylene," *Advances in Fracture Research, Proceedings of the 7th International Conference on Fracture,* 1989, Vol. 1305, pp. 1586-1589.

[21] Sauer, W. L., Weaver, K. D., and Beals, N. B., "Fatigue performance of ultra-high-molecular-weight polyethylene: effect of gamma radiation sterilization," *Biomaterials,* 1996, Vol. 17, pp. 1929-35.

[22] Weightman, B., and Light, D., "A comparison of RCH 1000 and Hi-Fax 1900 ultra-high molecular weight polyethylenes," *Biomaterials,* 1985, Vol. 6, pp. 177-83.

[23] Wang, A., Essner, A., Polineni, V. K., Stark, C., and Dumbleton, J. H., "Lubrication and wear of ultra-high molecular weight polyethylene in total joint replacements," *Tribology International,* 1998, Vol. 31, pp. 17-33.

[24] Burgess, I. C., Kolar, M., Cunningham, J. L., and Unsworth, A., "Development of a six station knee wear simulator and preliminary wear results," *Proceedings of the*

Institute of Mechanical Engineers [H], 1997, Vol. 211, pp. 37-47.

[25] Walker, P. S., Blunn, G. W., Perry, J. P., Bell, C. J., Sathasivam, S., Andriacchi, T. P., Paul, J. P., Haider, H., and Campbell, P. A., "Methodology for long-term wear testing of total knee replacements," *Clinical Orthopedics*, 2000, Issue 372, pp. 290-301.

[26] Walker, P. S., Blunn, G. W., and Lilley, P. A., "Wear testing of materials and surfaces for total knee replacement," *Journal of Biomedical Materials Research*, 1996, Vol. 33, pp. 159-75.

[27] Walker, P. S., Blunn, G. W., Broome, D. R., Perry, J., Watkins, A., Sathasivam, S., Dewar, M. E., and Paul, J. P., "A knee simulating machine for performance evaluation of total knee replacements," *Journal of Biomechanics*, 1997, Vol. 30, pp. 83-9.

[28] Johnson, T. S., Laurent, M. P., Yao, J. Q., and Gilbertson, L. N., "The effect of displacement control input parameters on tibiofemoral prosthetic knee wear," *Wear*, 2001, Vol. 250, pp. 222-226.

[29] Muratoglu, O. K., Bragdon, C. R., O'Connor, D. O., Perinchief, R. S., Travers, J. T., Jasty, M., Rubash, H. E., and Harris, W. H., "Markedly improved adhesive wear and delamination resistance with a highly crosslinked UHMWPE for use in total knee arthoplasty," *Transactions of the 27th Annual Meeting of the Society for Biomaterials*, 2001, Vol. 24, pp. 29.

[30] Yao, J. Q., Gsell, R., Laurent, M. P., Gilbertson, L. N., Swarts, D., Blanchard, C. R., and Crowninshield, R. D., "Improved delamination resistance of melt-annealed electron-beam irradiated highly crosslinked UHMWPE knee inserts," *Transactions of the 28th Annual Meeting of the Society for Biomaterials*, 2002, Vol. 25, pp. 60.

[31] Villarraga, M. L., Kurtz, S. M., Herr, M. P., and Edidin, A. A., "Multiaxial fatigue behavior of conventional and highly crosslinked UHMWPE during small punch testing," *Journal of Biomedical Materials Research*, 2003, Vol. 66A, No. 2, pp. 289-309.

[32] Kurtz, S. M., Muratoglu, O. K., Evans, M., and Edidin, A. A., "Advances in the processing, sterilization, and crosslinking of ultra- high molecular weight polyethylene for total joint arthroplasty," *Biomaterials*, 1999, Vol. 20, pp. 1659-88.

[33] Edidin, A. A., Jewett, C. W., Kwarteng, K., Kalinowski, A., and Kurtz, S. M., "Degradation of mechanical behavior in UHMWPE after natural and accelerated aging," *Biomaterials*, 2000, Vol. 21, pp. 1451-1460.

[34] Edidin, A. A., Villarraga, M. L., Herr, M., Ciccarelli, L., Hozack, W. J., Turner, J., and Kurtz, S. M., "Relationship between clinical performance and mechanical behavior in retrieved UHMWPE acetabular liners," *Transactions of the 28th Society for Biomaterials*, 2002, Vol. 25, pp. 25.

[35] Edidin, A. A., Villarraga, M. L., Herr, M. P., Muth, J., Yau, S. S., and Kurtz, S. M., "Accelerated aging studies of UHMWPE. II. Virgin UHMWPE is not immune to oxidative degradation," *Journal of Biomedical Materials Research*, 2002, Vol. 61, pp. 323-9.

[36] Edidin, A. A., Herr, M. P., Villarraga, M. L., Muth, J., Yau, S. S., and Kurtz, S. M., "Accelerated aging studies of UHMWPE. I. Effect of resin, processing, and radiation environment on resistance to mechanical degradation," *Journal of Biomedical Materials Research*, 2002, Vol. 61, pp. 312-22.

[37] Kurtz, S. M., Rimnac, C. M., Pruitt, L., Jewett, C. W., Goldberg, V., and Edidin, A. A., "The relationship between the clinical performance and large deformation mechanical behavior of retrieved UHMWPE tibial inserts," *Biomaterials*, 2000, Vol. 21, pp. 283-91.

[38] Muratoglu, O. K., Jasty, M., and Harris, W. H., "High resolution synchrotron infrared microscopy of the structure of fusion defects in UHMWPE," *Transactions of the 43rd Orthopedic Research Society,* 1997, Vol. 22, pp. 773.
[39] Sanford, W. M., and Saum, K. A., "Accelerated oxidative aging testing of UHMWPE," *Transactions of the 41st Orthopedic Research Society,* 1995, Vol. 20, pp. 119.

Suzanne A. Maher,[1] Bridgette D. Furman,[1] and Timothy M. Wright[1]

The Effect of Reduced Fracture Toughness on Pitting and Delamination Type Wear of Elevated Cross-Linked Polyethylene

REFERENCE: Maher, S. A., Furman, B. D., and Wright, T. M., "**The Effect of Reduced Fracture Toughness on Pitting and Delamination Type Wear of Elevated Cross-Linked Polyethylene,**" *Crosslinked and Thermally Treated Ultra-High Molecular Weight Polyethylene for Joint Replacements, ASTM STP 1445*, S. M. Kurtz, R. Gsell, and J. Martell, Eds., ASTM International, West Conshohocken, PA, 2003.

ABSTRACT: We hypothesized that the reduced fracture toughness associated with elevated cross-linking of ultra high molecular weight polyethylene would lead to an increase in pitting and delamination in specimens tested in a knee wear apparatus. Two blocks of compression molded polyethylene were electron beam irradiated, one block at 120 kGy, the other at 65 kGy; a third block was not irradiated to serve as a control. The 120 and 65 kGy blocks were post-irradiation heat treated. Wear, J-integral and tensile test specimens were machined from the blocks, and all specimens were sterilized, aged and tested. 65 kGy and 120 kGy irradiated material had significantly lower fracture toughness compared to the control material. Despite the reduced fracture toughness, no evidence of pitting, delamination, or subsurface damage occurred in the corresponding wear specimens after 2 million cycles. In contrast, half of the control specimens exhibited extensive pitting. Our hypothesis was rejected: reduced fracture toughness associated with the elevated cross-linked polyethylene groups was not associated with an increase in pitting and delamination type wear.

KEYWORDS: Polyethylene, fracture toughness, wear, cross-linking

[1]Assistant Scientist, Research Engineer, and Laboratory Director, respectively, Laboratory for Biomedical Mechanics and Materials, Hospital for Special Surgery, 535 East 70th Street, New York, NY, 10021.

Introduction

The ability of elevated cross-linked ultra high molecular weight polyethylene (hereafter simply called polyethylene) to improve implant longevity has yet to be proven *in vivo*. Indeed, its use in orthopaedic implants remains somewhat controversial. It has been shown that for elevated cross-linked polyethylene acetabular liners for total hip replacements, negligible wear rates exist *in vitro* compared to conventional materials [1]. Even against roughened femoral heads, wear rates against aged and un-aged elevated cross-linked polyethylene liners are significantly less than that of conventional polyethylene [2]. However, skeptics cite the change in mechanical properties [3-5] associated with cross-linking as a potential detriment to the long-term functional performance of elevated cross-linked polyethylene articular surfaces.

Polyethylene tibial components from total knee replacements often suffer pitting and delamination damage [6,7]. These damage modes are in turn the result of fatigue fracture mechanisms, caused by the low conformity, high stress environment in which a range of surface stresses are experienced by different locations as the contact area moves across the polyethylene surface [8]. The components of theses stresses parallel to the surface are tensile at the edge of contact and compressive under contact, generating cyclic stress ranges between -40 and 10 MPa [8]. Analytical simulations showed that the large deformation and non-linear, history-dependent response of polyethylene result in surface tensile residual stresses [9]. When these residual stresses are combined with the cyclic stresses in fracture mechanics simulations, crack propagation trajectories consistent with observed pitting and delamination damage are predicted [10]. The decrease in fracture toughness that accompanies cross-linking [11] could, therefore, increase the risk for pitting and delamination in tibial trays by accelerating crack propagation.

In vitro wear testing provides a means for examining the effects of such alterations in material properties on the resulting wear behavior in a controlled setting. We previously developed a wear apparatus [12] to examine the effects of surface geometry, contact load, kinematics, and polyethylene properties on the creation of damage. Studies with this apparatus [13] showed that cracks initially form on the medial-lateral edges of the wear track at less than a million cycles under physiologic loads and frequencies, consistent with the location and magnitude of maximum tensile stresses from analytical studies [10]. With continued testing, the cracks coalesce, forming pits similar to those observed on the bearing surfaces of retrieved implants [14].

The objective of this study was to use our apparatus to determine if alterations in material properties caused by cross-linking would have a detrimental effect on wear behavior. Our working hypothesis was that these alterations, particularly the decrease in fracture toughness, would lead to increased pitting and delamination type wear damage.

Materials and Methods

Specimen Preparation

Specimen preparation began by machining blocks (7.6 x 5.1 x 3.8 cm) from a compression-molded sheet of polyethylene made from GUR 1050 resin (Ticona,

Oberhausen, Germany). The blocks were randomly assigned to three groups. The processing steps for each group are summarized in Figure 1.

GUR 1050 compression molded slab machined into blocks

Blocks randomized to three groups

Preheated and electron beam irradiated

| 65 kGy | 120 kGy | Control |

Melt annealed: heated above melting point and slowly cooled

Machined

| Gas plasma sterilized | Gamma sterilized |

Accelerated aged: presoaked in deionized water at 37°C for 20 days; exposure to flow of O_2 for 10.5 days under 1 atm of pressure

Tested: JAWS, J-integral, tensile tests, depth-density profile.

Figure 1— *Manufacturing processes used on the three groups*

Blocks from two groups were pre-heated and electron beam irradiated at doses of either 65 kGy or 120 kGy. After irradiation, blocks from both groups were melt-annealed to eliminate free radicals. During the melt-annealing process blocks were heated in a forced air oven to a temperature above the melt point of UHMWPE and held to assure that all crystaline was relaxed. Cooling was accomplished over many hours at a very gradual rate in order to control the final material crystalinity. Blocks from the third group were neither irradiated at this stage nor heat treated and served as control material. To eliminate bias, the authors remained blinded throughout the experiment as to the identification of the three groups by the commercial entity (Zimmer, Inc., Warsaw, IN) that performed these procedures.

Specimens for tensile, J integral, and wear tests were machined from the blocks in each group. Tensile test specimens (n = 5 per group) were Type V as defined by ASTM

Standard Test Method for Tensile Properties of Plastics (D638). Three-point bend specimens (n = 10 per group) for J integral testing had W = 16 mm, B = 10 mm, and a = 8 mm, following ASTM Standard Test Method for J_{IC}, A Measure of Fracture Toughness (E813). Wear specimens (n = 4 per group) were 8 mm thick, 43 mm long, and 42 mm wide with a flat articular surface on top and dovetails machined into the bottom to hold the specimen in the apparatus [12].

All specimens were returned to Zimmer, Inc., for sterilization. The two groups of elevated cross-linked polyethylene specimens were sterilized using gas plasma techniques. Specimens from the control group were gamma sterilized to about 2.5 kGy. All specimens were then artificially aged by presoaking in deionized water at 37°C for 20 days, followed by exposure to a continuously bubbling flow of O_2 for 10.5 days under 1 atm pressure in a closed glass chamber filled with deionized water. This protocol creates sub-surface oxidation peaks similar to that found in clinically retrieved components [15].

Wear Tests

Wear tests were conducted on a twelve station, pneumatically controlled wear apparatus [12]. Each station consisted of an air cylinder, cobalt alloy indenter, control rods, and one of the polyethylene specimens mounted in a 3 mm thick metal backing that rested on rollers that allowed freedom of movement in the medial-lateral direction (Figure 2). The air cylinder created a vertical force pushing the cobalt alloy indenter into the polyethylene, while the control rods were connected to a common rotating shaft that created oscillating linear sliding motion. The indenters were 23 mm wide, with an anteroposterior radius of 40 mm and a medial/lateral radius of 19 mm; indenters were polished to an articulating surface finish. The polyethylene specimens were bathed throughout the test in non-iron-supplemented, 100 nm filtered bovine serum (Hyclone, Logan, UT) at room temperature (23°C ± 2°C).

At the beginning of each wear cycle, the indenter was loaded with a 2100 N vertical load and slid anteriorly 20 mm. At the end of anterior travel, the indenter was unloaded to 50 N and slid posteriorly 20 mm. Each station was instrumented with a multi-axis load cell (AMTI, Boston, MA) and an LVDT (Sensotec Inc., Columbus, OH) at the beginning of testing and randomly during the testing to measure the vertical, anteroposterior, and medial-lateral forces and the anteroposterior indenter motion, respectively. Data were collected at 10 Hz with a PC equipped with an analog to digital board and Labtech Notebook (Laboratory Technologies Corp., Wilmington, MA) data acquisition software.

Wear tests were run to 2 million cycles at 0.5 Hz, 24 hours a day. Tests were stopped once a week (corresponding to approximately 250 000 cycles) to examine the wear surfaces macroscopically and under a light stereomicroscope (Wild, Heerbrugg, Switzerland) for surface damage. The projected, two-dimensional wear track and the surface damage areas were visually identified on digital photographs made of the specimen surface and measured using Photoshop (Adobe Systems Inc., Mountain View, CA) and Optimas (BioScan Inc., Edmonds, WA) image analysis software. Damage was characterized into pitting and delamination. Delamination was defined as shallow layers of material removed from the articulating surface; whereas pitting was defined as cavities in the material.
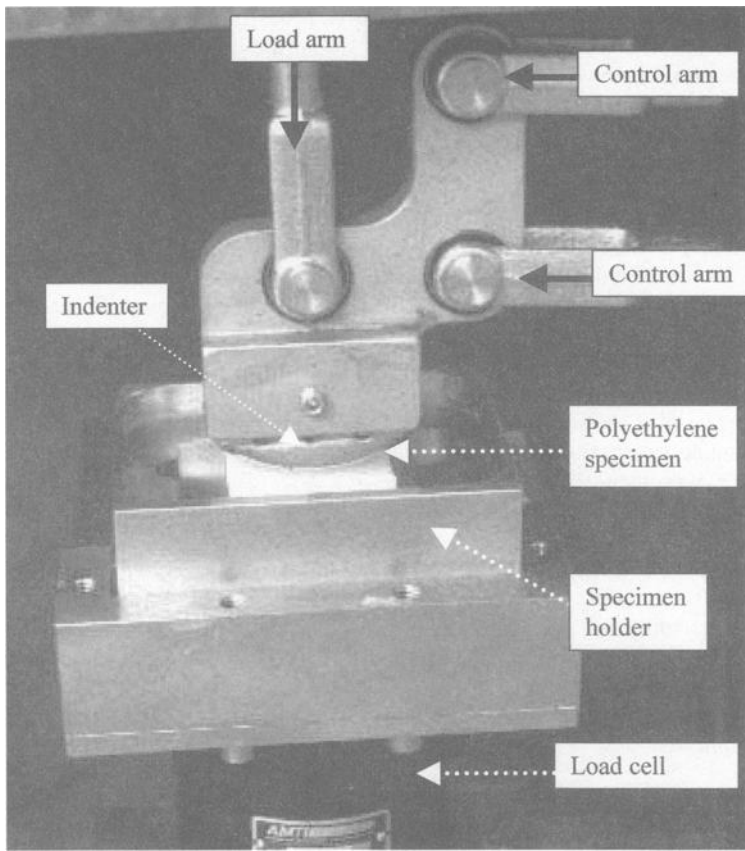
Figure 2— *One of the twelve stations on the wear test apparatus showing the indenter, the polyethylene specimen, the control rods, the load arm, and the load cell.   The control rods move to drag the indenter across the surface (horizontal arrows) while load is applied through the load arm (vertical arrow).*

After inspection, the specimens were randomly replaced on the 12 stations to minimize the effects of individual station characteristics on overall on sample performance, and testing continued. Because of specimen randomization, after every 500 000 cycles, all indentors were polished to prevent specimen specific indenter scuffing from being translated to other specimens. Material wear performance was assessed on the basis of the onset of damage (in 250 000 cycle steps), the worn area, and the percentage of worn area that showed pitting or delamination.

At the completion of 2 million cycles, a 5 mm diameter core was taken through each specimen at a common location away from the wear area. The cores were transversely microtomed into slices approximately 200 microns thick, and the density of each slice was measured using a density gradient column [ASTM Standard Test Method for Density

of Plastics by the Density-Gradient Technique (D1505)], thereby producing a density profile with respect to the articulating surface. From the density profile, the maximum density value and density value of the bulk of the material away from the surface, or bulk density, were determined.

J-integral and Tensile Tests

Following the guidelines of ASTM E813, J-integral tests were performed. Briefly, a sharp crack was created at the base of the notch using a razor, and the specimen was loaded to a pre-defined displacement. The amount of crack extension was measured, and the energy input was computed. A plot of energy versus crack growth for each material was produced [16].

Uniaxial tensile tests were performed according to ASTM D638. Specimens were first instrumented with an extensometer (MTS, Eden Prairie, MN) and tested under strain control at a rate of 2.6%/sec to a strain of 1.5%. Load and specimen dimensions were used to calculate stress. Elastic modulus was calculated from the stress-strain data. The extensometer was then removed, and a second test to failure was conducted at a displacement rate of 50.8 mm/min. Yield stress, ultimate stress, and elongation to break were determined from the data from this second test.

As with the wear tests, data from the J integral and the tensile tests to failure were collected at 10 Hz with a PC equipped with an analog to digital board and Labtech Notebook data acquisition software (Laboratory Technologies Corporation, Wilmington, MA). Data for the first tensile test on each specimen (to determine modulus) were collected at 40 Hz.

Statistical Analysis

Analysis of variance (ANOVA; Zar, 1999) was applied to the data to investigate whether any difference test results existed among the three groups. The significance level was set at 0.05. In cases where ANOVA revealed that intergroup differences existed, Tukey's test at 0.05 level of significance was used to explore exactly how the groups differed [17].

Results

Wear Test Results

After 2 million loading cycles none of the elevated cross-linked polyethylene specimens showed macroscopic or microscopic evidence of pitting or delamination, though the wear areas were burnished and scratched (Figure 3). In contrast, half (2 of 4) of the control specimens showed subsurface damage as early as 750 000 cycles. The damage continued to progress throughout the remainder of the two million cycle test (Figures 4 and 5). The subsurface cracks reached the surface and coalesced, releasing small pieces of polyethylene from the surface and leaving pits behind.
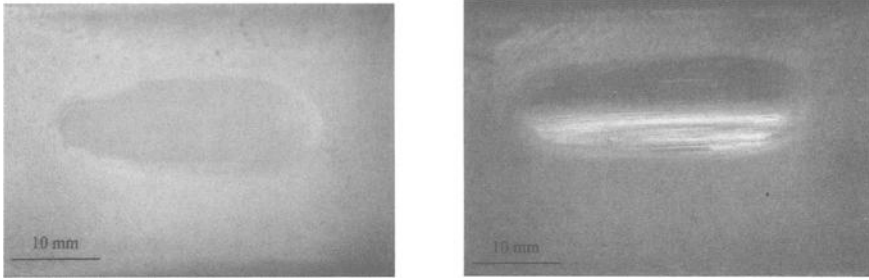
Figure 3— *Wear of a specimen irradiated at 120 kGy after 750 000 cycles and after 2 000 000 cycles.*
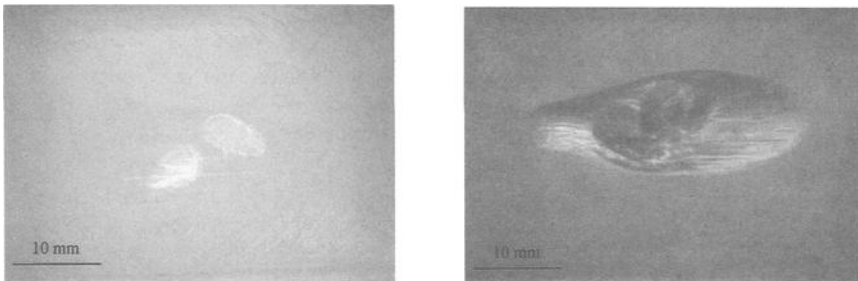
Figure 4— *Wear of a control specimen after 750 000 cycles and after 2 000 000 cycles.*
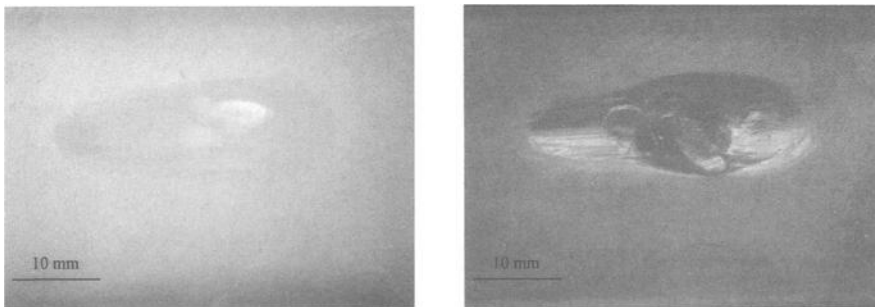
Figure 5— *Wear of a control specimen after 750 000 cycles and after 2 000 000 cycles.*

Pitting occurred at 1 million cycles in one of the control specimens and at 1.25 million cycles in the other (Table 1). By 2 million cycles, significant pitting covered about 40 % of the worn area in the two specimens. The pits averaged approximately 2 mm in width by 6 mm in length.

Table 1— *Summary of damage initiation and progression (including percentage of worn area affected)*

Specimen	250k	500k	750k	1m	1.25m	1.5m	1.75m	2m
Control #1	None	None	Sub-surface damage (18%)	Pitting (29%)	Pitting (29%)	Pitting (45%)	Pitting (45%)	Pitting (45%)
Control #3	None	None	Sub-surface damage (13%)	Sub-surface damage (32%)	Pitting (35%)	Pitting (35%)	Pitting (36%)	Pitting (38%)

Wear track area increased for all groups as the number of cycles increased (Figure 6). On average, the elevated cross-linked groups had larger wear track areas throughout testing. However, this difference was not significant until 1.5 million cycles. At 1.75 million cycles the material irradiated to 120 kGy had a significantly higher wear track area compared to the control group ($p<0.02$, single factor ANOVA); however, no significant difference was found between the two irradiated groups or between the group irradiated at 65 kGy and the control group. At 2 million cycles, both elevated cross-linked groups (65 and 120 kGy) had significantly larger wear track areas compared to the control group ($p<0.02$, single factor ANOVA).
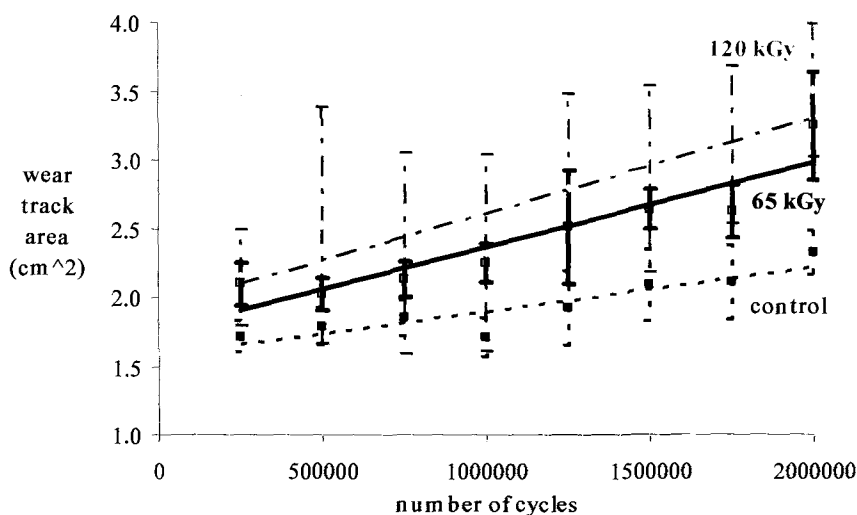
Figure 6— *Wear track area versus number of cycles for all specimens tested. Note: 120 kGy group and 65 kGy have a significantly higher wear track area compared to the control group at 2 million cycles.*

Density Versus Depth Profiles

The peak densities of the control group ranged from 0.945 g/cc to 0.958 g/cc, at depths ranging from 0.794 mm to 1.042 mm below the specimen surface (Figure 7). These sub-surface peaks are similar in both magnitude and position to density peaks found in retrieved components [4,14,15]. The two control specimens that exhibited significant pitting had the highest density peaks of 0.9575 g/cc and 0.9552 g/cc at depths below the surface of 0.794 mm and 0.987 mm, respectively. All elevated cross-linked specimens had depth-density profiles that were without significant sub-surface peaks, and specimen densities were consistently below 0.93 g/cc.

The control group had significantly higher peak density and bulk density (p = 0.05), compared to both irradiated groups. However no significant differences in peak density or cumulative density were found between the two elevated cross-linked groups.
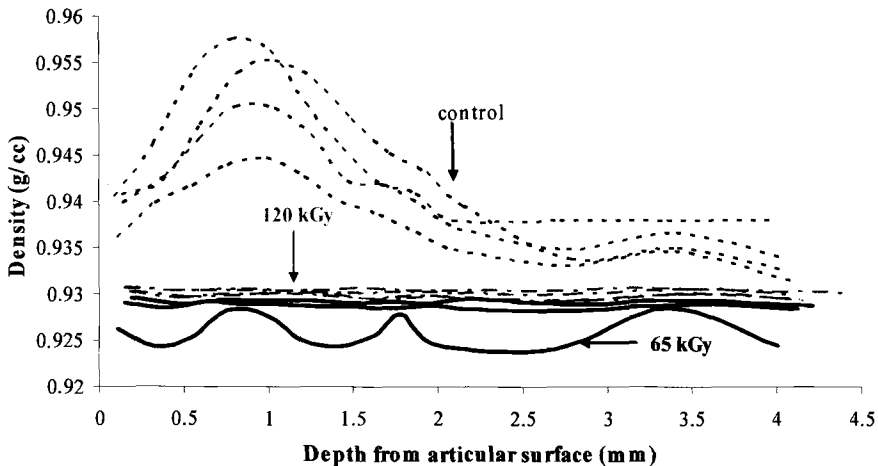
Figure 7— *The density-depth profiles of all specimens that were tested on JAWS. Note: the control groups exhibit a sub-surface peak, similar to that found in retrieved components. The two irradiated groups have a significantly lower density.*

J-integral and Tensile Test Results

The control group specimens exhibited the highest fracture toughness of the three groups – i.e., the highest energy to propagate a crack as denoted by the J-integral curves (Figure 8). Fracture toughness decreased with increasing levels of cross-linking. For example, the energy required to propagate a crack 0.3 mm was 23 kJ/m^2 for the control material, 15 kJ/m^2 for the material irradiated at 65 kGy, and 9 kJ/m^2 for the material irradiated at 120 kGy.
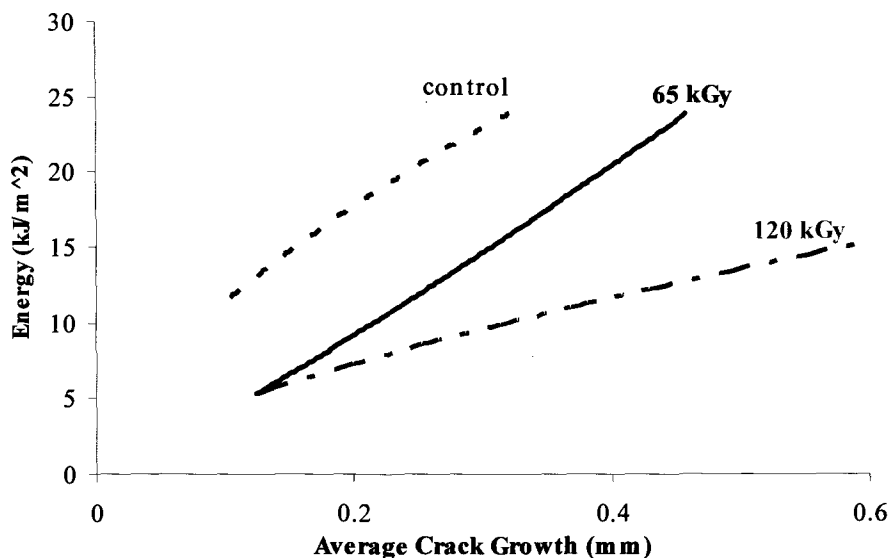
Figure 8— *The J-integral results of the three material groups (following accelerated aging).*

The tensile properties also differed significantly among the three groups (Table 2). Specimens from the control polyethylene had significantly higher elastic moduli and significantly greater yield stresses than specimens from either of the elevated cross-linked polyethylene groups. The 120 kGy polyethylene group had a significantly lower elongation to break than the control group or the 65 kGy group. No other significant differences were found.

Table 2— *Tensile test results for the three material groups (following accelerated aging)*

	Control	65 kGy	120 kGy
Young's Modulus (GPa)	1148.6 ± 94.4[1]	811.6 ± 41.6	849.1 ± 57.7
Yield Strength (MPa)	27.1 ± 2.9[2]	23.0 ± 1.1	24.1 ± 1.0
Ultimate Strength (MPa)	40.8 ± 4.1	53.1 ± 7.1	49.2 ± 8.5
Elongation at break (%)	333.1 ± 23.3	320.0 ± 21.8	206.7 ± 20.3[3]

[1] = significantly higher than the elevated cross-linked groups
[2] = significantly higher than the 65 kGy elevated cross-linked group
[3] = significantly lower than the control and 65 kGy elevated cross-linked groups

Discussion

Elevated cross-linked polyethylene is currently considered an alternate bearing material, and as such, its mechanical properties and their influence on *in vivo* implant performance are still under investigation. For example, the reduced fracture toughness of elevated cross-linked polyethylene [5, 11] has been hypothesized to lead to an increase in the incidence of pitting and delamination type wear. This could offset reported improvements in adhesive/abrasive type wear [1] as have been measured *in vitro* for elevated cross-linked polyethylene [2,18,19].

The objective of this study was to explore whether the changes in mechanical properties (in particular fracture toughness) associated with elevated levels of cross-linking would correlate with increases in pitting and delamination wear in polyethylene specimens tested in a knee wear apparatus. We found that fracture toughness decreased as the level of cross-linking increased (Figure 8) as has been previously reported in the literature [5,11]. However, despite reduced fracture toughness the elevated cross-linked specimens did not exhibit subsurface damage, pitting, or delamination after 2 million loading cycles. On the other hand, 50% of the control specimens – which had a higher fracture toughness – exhibited significant pitting that covered 40% of the wear track area.

The explanation for this finding may lie in the mechanism by which pits are created in the articular surface. Polyethylene pitting can be considered in four stages: crack initiation; crack propagation, crack coalescence, and finally material removal leaving a pit behind. The energy required for crack initiation – the first step in the pitting process – was not measured in the J-integral test used in this study. It is possible that elevated cross-linked polyethylene may have a higher resistance to crack initiation, and thus increased resistance to the onset of pitting type wear.

Other reasons could explain why the control group (with the highest fracture toughness) pitted during wear testing, whereas the elevated cross-linked groups (with reduced fracture toughness) did not pit or delaminate. Consider the mechanical property changes that accompanied the increased cross-linking. For example, the elevated cross-linked groups had a significantly lower elastic modulus compared to the control group (849 MPa for the 120 kGy group compared with 1148 MPa for the control group). This difference in modulus led to a larger average wear track area in the elevated cross-linked specimens throughout testing (Figure 6). The increased contact area for the same applied load meant that the elevated cross-linked materials experienced reduced stresses (as load was carried over a larger area). The wear track area was not significantly larger for the elevated cross-linked specimens until 1 250 000 cycles of testing – by which time, pits were already evident in the control specimens. Of course, the altered elastic and yield properties that occurred in the elevated cross-linked materials might also have influenced the magnitudes of the residual stresses that developed within and near the contact areas in these materials [9,10], a fact that would not necessarily be reflected in our wear and contact area measurements.

As part of the cross-linking process, all elevated cross-linked blocks were melt stabilized after irradiation. The stabilization process eliminates free radicals and gives greater resistance to the oxidative effects of aging [20,21]. Since the control samples were not melt stabilized, when all specimens were subsequently artificially aged, the control group was more degraded by the aging process compared to the elevated cross-

linked specimens. This was apparent in the subsurface peak in density seen in the control specimens, which was not seen in the cross-linked specimens (Figure 7). In effect, by artificially aging all specimens, we are providing an inherent disadvantage to the control group that may not be mirrored in clinical reality.

A subsurface zone of peak density in retrieved implants and in artificially aged polyethylene has been identified as a region of reduced fracture toughness and therefore as a zone where cracks propagate, ultimately leading to delamination [22]. In this study, both control samples that exhibited pitting had distinct sub-surface peaks in density. Whereas, the two control samples which did not pit or delaminate had slightly lower peak densities (Figure 7). This suggests that the variability in performance of the control group may be a result of slight variations in the effects of the aging protocol.

In vitro tests [24] and implant retrieval analyses [14,25] have shown that resin type and manufacture method influence wear behavior. For example, density-depth profiles taken from shelf aged tibial trays have shown that directly molding 1900 resin produces a more oxidation resistant material compared to 4150 and 4120 resin [26]. In an analysis of 23 retrieved Miller-Galante inserts, Won et al. [14] showed that direct compression molded 1900 resin was more resistant to oxidative degradation than ram extruded 4150 resin. A possible limitation of our study therefore is that the influence of resin type and manufacturing method (compression molded vs. extruded) on wear behavior was not investigated; compression molded GUR1050 was the only resin used.

The results of this study cannot be generalized to modes of cross-linking other than that used in this study (electron-beam irradiation), or to elevated cross-linked polyethylene that has not been melt annealed. Indeed, since melt stabilization affects polyethylene modulus, yield strength, elongation to break, viscoelasticity and fracture toughness [11,23] our tests do not allow us to determine whether the cross-linking or the melt-annealing processing step led to the superior wear performance of the cross-linked group. Furthermore, it is not possible to differentiate the effects of manufacturing changes (i.e. cross-linking and heat treating) from those attributable to preconditioning (i.e. accelerated aging).

In summary, lack of information about resistance to crack initiation leaves the possibility that elevated cross-linked polyethylene may be more sensitive to design features that can act as crack initiation sites; however further investigation was outside the scope of this research. It appears that the density-depth profile may create a clearer picture as to whether pitting and delamination type wear is likely to occur or not, whilst interpretation of J-integral data in terms of wear performance is less certain. Nonetheless, the material properties of elevated cross-linked polyethylene did not lead to increased pitting or delamination damage in specimens tested in our knee wear simulator apparatus, when compared to conventional polyethylene.

Our working hypothesis that the alterations in material properties of elevated cross-linked polyethylene, particularly the decrease in fracture toughness, associated with elevated levels of cross-linking would lead to increased wear damage was rejected.

Acknowledgments

References

1. Edidin, A.A., Pruitt, L., Jewett C.W., Crane DJ, Roberts D, Kurtz SM., "Plasticity-Induced Damage Layer is a Precursor to Wear in Radiation-Elevated Cross-Linked UHMWPE Acetabular Components for Total Hip Replacement," Journal of Arthroplasty, Vol. 14, No. 5, 1999, pp. 616-627.
2. McKellop, H., Shen, F.-w., DiMaio, W., Lancaster, J.G., "Wear of Gamma-Elevated Cross-Linked Polyethylene Acetabular Cups Against Roughened Femoral Balls," Clinical Orthopaedics and Related Research, Vol. 369, 1999, pp. 73-82.
3. Lewis, G., "Properties of Crosslinked Ultra-High-Molecular-Weight Polyethylene," Biomaterials, Vol. 22, No. 4, 2001, pp. 371-401.
4. Wright, T.M., Li, S., "Biomaterials," Basic Orthopaedic Science 2nd Edition, Edited by Buckwalter, J.A., Einhorn, T.A., Simon, SR, published by American Academy of Orthopaedic Surgeons, ISSN: 0-89203-177-8, 2000, Chapter 6.
5. Pascaud, R.S., Evans, W.T., McCullage, P.J., Fitzpatrick, D.P., "Influence of Gamma-Irradiation Sterilization and Temperature On The Fracture Toughness of Ultra-High-Molecular-Weight Polyethylene," Biomaterials, Vol. 18, No. 10, 1997, pp. 727-35.
6. Wright, T.M., Rimnac, C.M., Stulberg, D., Mintz, L., Tsao A.K., Klein R.W., McCrae C, "Wear of Polyethylene in Total Joint Replacements," Clinical Orthopaedics and Related Research, Vol. 276, 1992, pp. 126-134.
7. Hood, R.W., Wright, T.M., Burstein, A.H., "Retrieval Analysis of Total Knee Prostheses: A Method and its Application To 48 Total Condylar Prostheses," Journal of Biomedical Materials Research, Vol. 17, No. 5, 1983, pp. 829-42.
8. Bartel, D.L., Bicknell, V.L., Wright, T.M., "The Effect of Conformity, Thickness, and Material on Stresses In Ultra-High Molecular Weight Components for Total Joint Replacement," Journal of Bone and Joint Surgery Am., Vol. 68, No. 7, 1986, pp. 1041-51.
9. Estupinan, J.A., Bartel, D.L., Wright, T.M., "Residual Stresses in Ultra-High Molecular Weight Polyethylene Loaded Cyclically by a Rigid Moving Indenter in Nonconforming Geometries," Journal of Orthopaedic Research, Vol. 16, No. 1, 1998, pp. 80-8.
10. Estupinan, J.A., "Simulation of Macroscopic Surface Damage Mechanisms to UHMWPE Components in Total Knee Replacement," Ph.D. Thesis submitted to Cornell University, 2000.
11. Duus, L.C., Walsh, H.A., Gillis, A.M., Furman, B.D., Li, S., "A Comparison of the Fracture Toughness of Cross Linked UHMWPE made from Different Resins, Manufacturing Methods and Sterilization Conditions," Transactions of the Society for Biomaterials, 2000, pp. 384.
12. Baldini, T.H., Wright, T.M., Estupinan, J.A., Bartel D.L., "An Apparatus for Studying Wear Damage in UHMWPE: Description and Initial Test Results," Proceedings of the American Society of Mechanical Engineers, 1998.
13. Baldini, T., Wright, T., Bartel, D., Estupinan, J., Duus, L., Li, S., "Wear Damage is Affected by Modulus in Knee Joint Geometries," Transactions of 46th Annual Orthopaedic Research Society Meeting, 2000, pp. 0453.

14. Won, C.H., Rohatgi, S., Kraay, M.J., Goldberg, V.M., Rimnac, C.M., "Effect of Resin Type and Manufacturing Method on Wear of Polyethylene Tibial Components," Clinical Orthopedics and Related Research, 376, 2000, 161-171.
15. Walsh, H.A., Furman, B.D., Li, S., "A Protocol to Mimic 5 Year Shelf Aging of UHMWPE," Transactions of the Society for Biomaterials, 6th World Biomaterials transactions, 2000, pp. 421.
16. Rimnac, C.M., Wright, T.M., Klein, R.W., "J Integral Measurements of Ultra High Molecular Weight Polyethylene," Polymer Engineering and Science, Vol. 28, No. 24, 1988, pp. 1586 – 1589.
17. Zar, J.H., "Biostastical Analysis," Fourth Edition, ISBN 0-13-081542-X, Published by Prentice-Hall, Inc. New Jersey, 1999.
18. McKellop, H., Shen, F.W., Lu, B., Campbell, P., Salovey, R., "Development of an Extremely Wear-Resistant Ultra High Molecular Weight Polyethylene for Total Hip Replacements," Journal of Orthopaedic Research, Vol. 17, No. 2, 1999, pp. 157-67.
19. Oonishi, H., Kuno, M., Tsuji, E., Fujisawa, A., "The Optimum Dose of Gamma Radiation-Heavy Doses to Low Wear Polyethylene in Total Hip Prostheses," Journal of Materials Science in Medicine, Vol. 8, 1997, pp. 11-8.
20. Premnath, V., Harris, W.H., Jasty, M., Merrill, E.W., "Gamma Sterilization of UHMWPE Articular Implants: An Analysis of the Oxidation Problem," Biomaterials, Vol. 17, 1996, pp. 1741-1753.
21. Rimnac, C.M., Klein, R.W., Betts, F., Wright, T.M., "Post-Irradiation Aging of Ultra-High Molecular Weight Polyethylene", Journal of Bone and Joint Surgery, 76A, 1994, 105-1056.
22. Bell, C.J., Walker, P.S., Abeysundera, M.R., Simmons, J.M., King, P.M., Blunn, G.W., "Effect of Oxidation on Delamination of Ultrahigh-Molecular-Weight Polyethylene Tibial Components," Journal of Arthroplasty, Vol. 13, No. 3, 1998, pp. 280-90.
23. Furman, B.D., Ryan, D.N., Duus, L.C., Li, S., "Effect Of Radical Quenching On Viscoelastic Properties Of Electron Beam Cross Linked UHMWPE," Transactions of the Society for Biomaterials, 2000, pp. 919.
24. Furman, B.D., Ritter, M.A., Perone, J.B., Furman, G.L., Li, S., "Effect of Resin Type and Manufacturing Method on UHMWPE Oxidation and Quality at Long Aging and Implant Times," Transactions of the Orthopaedic Research Society, 1997, pp. 92.
25. Ritter, M.A., "Direct Compression Molded Polyethylene For Total Hip and Knee Replacements," Clinical Orthopaedics and Related Research, Vol. 393, 2001, pp. 94-100.
26. Gillis, A.M., Furman, B.D., Li, S., "Influence of Ultra High Molecular Weight Polyethylene Resin Type and Manufacturing Method on Real Time Oxidation," Transactions of the Orthopaedic Research Society, 1998, pp. 360.

Aiguo Wang,[1] Michael Manley,[1] and Paul Serekian[1]

Wear and Structural Fatigue Simulation of Crosslinked Ultra-High Molecular Weight Polyethylene For Hip and Knee Bearing Applications

REFERENCE: Wang, A., Manley, M., and Serekian, P., "**Wear and Structural Fatigue Simulation of Crosslinked Ultra-High Molecular Weight Polyethylene For Hip and Knee Bearing Applications**," *Crosslinked and Thermally Treated Ultra-High Molecular Weight Polyethylene for Joint Replacements, ASTM STP 1445*, S. M. Kurtz, R. Gsell, and J. Martell, Eds., ASTM International, West Conshohocken, PA, 2003.

ABSTRACT: There have been increasing concerns about the structural fatigue resistance of crosslinked UHMWPE devices due to deterioration of certain mechanical properties. However, due to the lack of clear correlation between specific mechanical properties and clinical performance, these concerns remain theoretical. In order to evaluate the potential benefits and risks of various crosslinked polyethylene materials for hip and knee bearing applications, two clinically relevant worst-case scenarios were simulated on functional devices. In the first worst-case scenario, cemented all-poly patellar components were tested under simulated stair-climbing conditions with rotational misalignment. In the second worst-case scenario, metal-backed thin acetabular liners were tested in a hip joint simulator under rim-loading conditions. Various types of crosslinked UHMWPE were prepared according to published process descriptions of commercial materials. While significant levels of volumetric wear reduction were confirmed by both the patellar and hip simulator tests, mixed results were obtained on the structural integrity of the devices. The latter was more significantly affected by the post-irradiation thermal treatment history than by the total dose of irradiation. Re-melting following irradiation led to catastrophic fractures of both rim-loaded liners and rotational-malaligned patellar pegs. The key mechanical property that was positively identified to correlate with the structural fatigue performance of crosslinked polyethylene materials was the ultimate tensile strength, whereas tensile elongation within 250% and 400% range had no effect on structural integrity. However, the results presented in this study should not be misconstrued with respect to the potential clinical performance of irradiation crosslinked and re-melted polyethylene liners with proper designs. In fact, the true outcome of all the crosslinked materials can only be revealed by long-term clinical follow-up.

KEYWORDS: Crosslinked Polyethylene, Structural Fatigue, Wear, Annealing, Remelting

Introduction

Recent advances in tribology and polymer technology have led to the development and commercialization of various types of radiation crosslinked ultra-high molecular

[1] Director of Bearing Technology, Chief Scientific Advisor and Vice President of Advanced Technology, respectively, Stryker Howmedica Osteonics, 300 Commerce Ct., Mahwah, NJ 07430.

weight polyethylene (UHMWPE) for acetabular bearing applications in total hip replacement [1-4]. Elevated crosslinking is accomplished by gamma or electron-beam irradiation of a ram-extruded bar or compression-molded sheet at a dose greater than 4 MRads (40kGys). This irradiated bar or sheet is subsequently thermally treated either above (re-melting) or below the melt-temperature (annealing) in order to eliminate or reduce residual free radicals. Acetabular components are then machined from the irradiated and thermally treated rod or sheet. Packaging of the components is done either in air or an inert environment depending upon the terminal sterilization method. Implant manufacturers who prefer re-melting over annealing have chosen ethylene oxide gas (EtO) or gas plasma techniques to sterilize their crosslinked cups while those who prefer annealing over re-melting have decided on conventional gamma sterilization in an inert environment. Table 1 summarizes the general process description of three different types of crosslinked polyethylene acetabular components marketed by three major orthopaedic implant manufacturers. Major variances are the irradiation source (gamma or e-beam), thermal treatment method (re-melting or annealing) and sterilization technique (gas plasma, EtO or gamma-in-nitrogen sterilization).

Table 1 *Process description of three different types of crosslinked materials*

Manufacturer & Tradename [reference]	Base UHMWPE	Radiation Source & Dose	Thermal Treatment	Sterilization Method
DePuy Marathon™ [2]	Ram-Extruded GUR1050 Bar	Gamma 5 MRads	Re-Melt (155°C)	Gas Plasma
Zimmer Longevity™ [3]	Compression Molded GUR1050 Sheet	E-Beam 10 MRads (40°C)	Re-Melt (>136°C)	Gas Plasma
Howmedica Osteonics Crossfire™ [4]	Ram-Extruded GUR1050 Bar	Gamma 7.5 MRads	Anneal (>120°C&<136°C)	3-MRads Gamma in N_2

Numerous hip joint simulator evaluations have shown an exponential drop in volumetric wear rate of polyethylene acetabular components with increasing the total dose of irradiation irrespective of the irradiation source or thermal treatment method [1-4]. Despite the fact that the Longevity™ (Zimmer Holdings, Inc., Warsaw, Indiana) and Crossfire™ (Howmedica Osteonics, Inc., Mahwah, New Jersey) materials are different in irradiation source, thermal treatment history and sterilization method, both achieved an identical 90% wear rate reduction compared to conventional 3-MRads gamma-in-nitrogen sterilized materials in different hip simulator tests [3,4]. The same magnitude of wear reduction is attributed to the same 10-MRads total dose received by both crosslinked materials. The Marathon™ (DePuy, Warsaw, Indiana) material is different from both Longevity and Crossfire in that it receives only 5 MRads of gamma irradiation – one half that of the dose of Longevity or Crossfire. Reported hip simulator test results indicated an 85% wear reduction for Marathon compared to a virgin unirradiated material [2]. Since the unirradiated material wears at a rate twice that of the 3-MRads gamma-in-

nitrogen sterilized material as demonstrated by two independent hip simulator studies [5,6] and clinical comparisons [7], the 85% wear reduction over virgin polyethylene would be reduced to 50% if compared to the 30-MRads gamma-in-nitrogen sterilized polyethylene. However, the achievement of significant wear reductions is not without consequences. Mechanical properties such as elongation (ductility) and toughness are usually compromised [2,8,9]. The extent of the mechanical property reduction depends on the total dose of irradiation as well as the thermal treatment method. Given the same thermal treatment history, the mechanical properties decrease as the total irradiation dose increases [8,9]. Therefore, the 5-MRads-irradiated/re-melted Marathon material is able to maintain its mechanical properties better than the 10-MRads irradiated/re-melted Longevity although the latter possesses better wear resistance.

Historically, intentionally highly crosslinked polyethylene materials had been used clinically in total hip replacement with reported success prior to the general introduction of the contemporary irradiation-crosslinked and thermally treated materials [10-12]. In the 1970s, a group of Japanese surgeons irradiated polyethylene cups to at least 100-MRads in air by gamma rays without any thermal treatment [13]. A three to five-fold wear reduction was reported in clinical follow-ups up to 20 years compared to unirradiated and EtO sterilized cups [10]. During a similar time period, a highly crosslinked polyethylene gamma-irradiated at 12-MRads in the presence of acetylene gas was introduced for clinical use in South Africa [14]. A six-fold wear reduction was reported compared to conventional gamma-in-air sterilized polyethylene in a retrospective clinical study [11]. In the late 1980s, a chemically crosslinked polyethylene was developed for a clinical trial in a small group of patients [15]. All the crosslinked cups were of the cemented Charnley type and coupled with alumina ceramic heads. A prospective clinical study with a mean follow-up period longer than ten years showed a six-fold wear reduction for the crosslinked polyethylene/alumina combination compared to the conventional Charnley polyethylene/stainless low-friction arthroplasty components [12]. In all three cases, the crosslinked materials were not re-melted and the acetabular components were cemented without the use of metal shells. Encouraged by these earlier clinical successes, researchers at Howmedica Osteonics developed the Crossfire highly crosslinked polyethylene for acetabular bearing applications. The rationale for the Crossfire process was to take advantage of the elevated level of crosslinking for wear reduction and the clinically proven gamma-in-nitrogen sterilization for oxidation resistance while preserving the microstructure and consolidation history of the virgin material without re-melting. History has shown that a dramatic change in polyethylene microstructure leads to undesirable and sometimes catastrophic clinical performance. Carbon fiber reinforced polyethylene (Poly II), heat-pressed polyethylene and high-temperature/high-pressure processed Hylamer are typical examples of past clinical failures [16-20].

Entering into the twenty-first century, the demographics of patient populations have changed significantly. Total hip replacement surgeries are being performed in younger and more active patients. Demands for longevity, function and range of motion are increasing along with modularity and cementless fixation. Thin polyethylene liners, metal backing and large femoral heads are becoming popular again. The timely introduction of the various types of highly crosslinked polyethylene is likely to reduce the incidence of wear-debris induced osteolysis and hence potentially increase the longevity and

functional performance of total hip arthroplasty. However, other forms of clinical failures, such as component fracture associated with poor locking mechanisms [21,22], thin liners, insufficient support [23], and impingement related wear and loosening due to incorrect component positioning, and inadequate range of motion [24,25], may become limiting factors for long-term clinical performance. The concerns about the mechanical property compromises of highly crosslinked polyethylene and their effect on structural integrity of total hip replacement devices must be addressed. More important, as crosslinked polyethylene materials are being introduced for total knee applications in which the primary failure modes are fatigue-related delamination and mechanical fracture by over-loading or component mal-alignment [26-30], the concerns for wear debris generation may become secondary whereas the demands for maintaining the structural integrity of the polyethylene tibial or patellar component may become imperative. The present study was designed to address those concerns. The objectives were two-fold. First, a potentially worst-case clinical scenario for a metal-backed polyethylene liner was simulated in a hip joint simulator by using thin polyethylene liners rim-loaded in metal shells without dome-support. This was intended to determine the limiting design factors for potential structural failure of various types of crosslinked polyethylene liners and to compare the relative fracture resistance of those materials given the same compromised design. Second, a worst-case clinical scenario for a cemented all-poly patellar component was simulated in a patello-femoral joint simulator under rotational malalignment while performing simulated stair-climbing activities. In both cases, the performance of crosslinked materials was evaluated with respect to a conventional 3-MRads gamma-in-nitrogen irradiated polyethylene.

Materials and Experimental Methods

Materials and Mechanical Properties

A single-batch of ram-extruded GUR1050 ultra-high molecular weight polyethylene (PerPlas Medical Ltd., Lancashire, U.K.) was used as the base material. Three different types of crosslinked materials were processed according to the published descriptions summarized in Table 1. The first crosslinked material (designated material M) was prepared by irradiating the extruded bars by a Co^{60} gamma source to a total dose of 5 MRads (50 kGys) at room temperature. The irradiated material was subsequently re-melted at 150°C. The second crosslinked material (designated material L) was prepared by irradiating the extruded bars by an electron beam (e-beam) to a total dose of 10 MRads at 40°C. The irradiated material was subsequently re-melted at 150°C. The third crosslinked material (designated material X) was prepared by irradiating the extruded rod by the same ^{60}Co gamma source as in material M to a total dose of 7.5 MRads. The irradiated material was subsequently annealed at 130°C below the melt-temperature. Tensile specimens were machined from all three irradiated and thermally treated bars according to the standard of the American Society For Testing and Materials (ASTM) F648 (type IV specimens). For the 7.5-MRads-gamma-irradiated and annealed material (X), the tensile specimens were packaged under partial vacuum in an air-impermeable barrier package filled with nitrogen and then sterilized by gamma irradiation at 3 MRads. This terminal gamma sterilization yielded a total irradiation dose of 10.5 MRads for

material X. For comparative purposes, tensile specimens were also machined from both virgin ram-extruded GUR1050 and direct molded Montel 1900H (PerPlas Medical, Lancashire, UK), packaged in nitrogen and sterilized by gamma irradiation at 3 MRads (designated material E and material C).

Tensile tests were performed on all materials using an Instron load-frame according to procedures described in ASTM F648. Five identical specimens were tested for each material. Student's t-test was used for testing for statistical significance at the 95% confidence level ($P<0.05$).

Functional Fatigue Simulation Methods

Hip Simulator Test – thin acetabular liners of 32-mm internal diameter and 2.5-mm minimum thickness were machined from the crosslinked and the virgin materials (materials M, L, X and E). All cups went through the same treatments as the corresponding tensile specimens. Cups were seated inside a metal shell. A 4-mm gap was created between the dome of the polyethylene liner and the metal shell so that the liner was supported at the rim only. This liner/shell assembly was modeled after the ACS design that showed an unusually high incidence of liner fracture in-vivo [23]. The metal shell was press-fitted into a cylindrical polyethylene holder for mounting onto a hip joint simulator. Figures 1(a) and 1(b) show an overall view as well as a cross-sectional view of the liner/shell/holder assembly, respectively. Two identical 12-station hip joint simulators (MTS, Eden Prairie, MN) were employed for testing the structural integrity of the rim-loaded liners. All liners were mounted in the upright position against matching 32-mm diameter CoCr femoral heads (Howmedica Osteonics, Mahwah, NJ). A cross-path motion between the liner and the head was created via a rotating inclined bearing block [31]. A physiologic loading pattern with a maximum load of 2450 N and minimum load of 150 N was applied superiorly through the axis of the liner [32]. Motion and loading were synchronized at 1 Hz. A fetal-substitute alpha-calf serum diluted by 50% with deionized water was used as a lubricant. The resulting total protein concentration of the lubricant was 20 g/L, which was within the physiological range of joint fluids in patients after total hip arthroplasty [33]. For each lubricant bath, a total of 450 mL fluid was used. For every 250000 cycles of testing, the liner was removed from the metal shell, ultrasonically cleaned in a soap water solution and then pure deionized water. After drying in partial vacuum, all liners were visually inspected for signs of cracking or fracture. A complete structural failure of the liner was defined as the detection of a through-thickness open crack or cracks by the naked eyes. Once an open crack was detected, the liner was removed from further testing, and a new liner was added to that open station left by the failed liner. All intact liners were weighed using an electronic balance (resolution: 0.01 mg) to determine weight loss. Soak-control cups were used for weight-loss correction due to fluid absorption. Four duplicate liners for each material were tested. Only those liners that survived 1 million cycles were included in the wear calculations.

Patello-femoral Simulator Test – all-poly patellae were machined from a slightly modified version of material L. Instead of e-beam irradiation, gamma irradiation was used to create crosslinking (10 MRads) followed by re-melting at 150°C. The latter

material was designated material **L**-γ. Tensile tests showed that material **L**-γ and material **L** (e-beam) possessed virtually identical mechanical properties (see Table 2 in Experimental Results). A biomechanical model based upon high load and flexion activities such as stair climbing [34], was used to measure wear and structural integrity of aligned and rotationally mal-aligned all-polyethylene patellae. The patellar components were cemented (Simplex® P, Howmedica Osteonics) onto metal fixtures and articulated against "aligned" and "mal-aligned" (6^0 internally rotated) femoral components. The patella were subjected to a constant 2224 N force and articulated against femoral components rotating from 60^0 to 120^0 at 1.33 Hz with serum lubrication (50% alpha-calf serum). For the aligned test, the patellar component remained centered in the patellar track of the femoral component throughout the range of flexion tested. For the mal-aligned test, edge loading of the patella occurred at 60 degrees of flexion and at 120 degrees of flexion, respectively (Figures 2a and 2b). Patellae of identical geometry (Scorpio® Concentric Dome, Howmedica Osteonics, Mahwah, New Jersey) made of conventional GUR1020 UHMWPE (material **E-1020**) and highly crosslinked GUR1050 UHMWPE (material **L**-γ) were tested to one million cycles. Following testing, wear was determined by gravimetric measurement of the patellae relative to cemented soak control specimens at the start and the end of one million cycles.
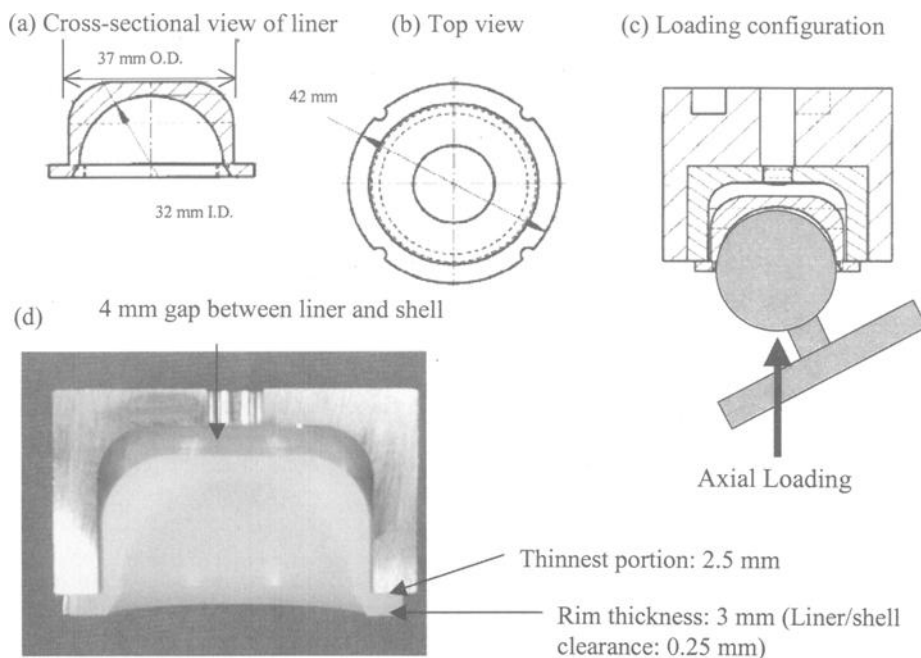

Figure 1 *(a) cross-sectional view of liner, (b) top view of liner with four anti-rotation locking points, (c) loading configuration in the hip simulator, and (d) cross-sectional view of an actual liner/shell assembly.*
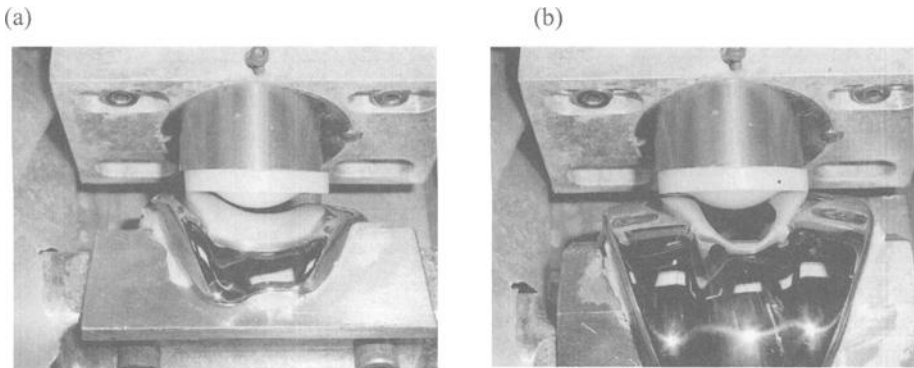
(a)   (b)

Figure 2 *Mal-aligned patello-femoral contact at (a) 60 degrees flexion, and (b) 120 degrees flexion.*

Experimental Results

Mechanical Properties

Uniaxial tensile properties (ASTM F648) of all the materials are summarized in Table 2. Comparisons of the materials for yield stress, ultimate tensile strength (UTS), elongation and tensile toughness are presented in Figures 3(a) to 3(d), respectively. There was no correlation between yield stress and radiation dose. However, re-melting following irradiation caused a 15% drop in yield stress regardless of total irradiation dose, Figure 3(a). For the non-remelted materials (*E*, *C* and *X*), increasing the total dose from 3 MRads to 10.5 MRads had no effect on ultimate tensile strength. However, for the re-melted materials (*M*, *L* and *L*-γ), there was a significant drop in ultimate strength with increasing radiation dose, Figure 3(b). For example, compared to the control material (*E*), UTS decreased by 20% and 30% for the 5-Mrad-γ-remelted (*M*) and the 10-Mrad-ebeam-remelted (*L*) materials, respectively, Figure 3(c). Elongation decreased for all crosslinked materials. Tensile toughness also decreased for all crosslinked materials compared to both the GUR1050 and 1900H controls, Figure 3(d). However, the crosslinked/annealed material (*X*) had significantly greater toughness than all the re-melted materials regardless of the radiation dose (5 or 10 MRads), or radiation source (gamma or e-beam). At the 10 MRads level, radiation source (gamma or e-beam) had no effect on mechanical properties (*L* vs *L*-γ). The compression-molded GUR1050 and the direct-molded 1900H materials showed identical yield stress and ultimate strength values. The elongation and toughness for the 1900H material was, however, significantly lower than those for the GUR1050 material.

Table 2 *ASTM F-648 tensile properties*

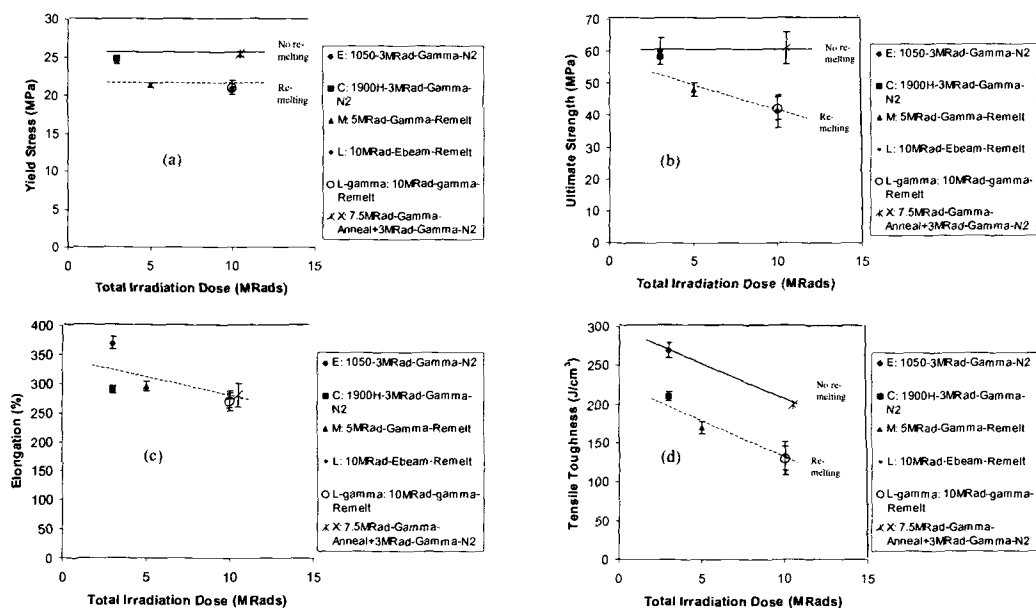| Material	Tensile Property (N=5)			
	Yield Stress (MPa)	UTS (MPa)	Elongation (%)	Toughness (J/cm^3)
E: GUR1050-3Mrad-γ-N$_2$	24.5 ± 0.4	60.0 ± 4.2	370 ± 10	270 ± 30
C: Direct-Molded 1900H-3Mrad- γ–N$_2$	24.8 ± 0.4	58.3 ± 2.4	290 ± 6	210 ± 10
M: 5Mrad-γ-Remelt	21.3 ± 0.3	48.2 ± 2.2	297 ± 8	170 ± 20
L: 10Mrad-ebeam-Remelt	20.9 ± 0.2	41.2 ± 5.1	274 ± 15	130 ± 30
L-γ: 10MRads-γ -Remelt	21.0 ± 0.9	42.2 ± 3.5	270 ± 15	130 ± 25
X: 7.5Mrad-γ-Anneal+3Mrad-γ -N$_2$	25.4 ± 0.4	61.1 ± 5.0	281 ± 21	200 ± 20

Figure 3 *(a) yield stress, (b) ultimate strength, (c) elongation, and (d) toughness.*

Functional Fatigue Simulations

Acetabular Liners – Due to the lack of dome support, all the thin liners exhibited significant deformation or cold-flow in the form of "buckling" of the rim when inspected after the first interval of testing (250000 cycles). All four liners from material *L* (10Mrad-ebem-remelt) showed open cracks at the thinnest portion of the cylindrical wall immediately below the rim, Figure 4(a). Two of four liners from material *M* (5Mrad- γ - remelt) showed similar open cracks, Figure 4(b). The other two liners (*M*) survived one million cycles. None of the liners from either material *E* (3Mrad-γ-N$_2$) or material *X* (7.5Mrad-γ-anneal+3Mrad-γ-N$_2$) exhibited cracking and all of them survived one million cycles, Figures 4(c) and 4(d). The length of the open crack for each of the fractured liners was measured with a digital caliper. This was then divided by the test cycles during which the crack was formed, which gave an average estimation of the crack-opening rate (mm/10^6 cycles). Since all liners from material *L* fractured during the very first interval of testing, wear rate of this material could not be measured. For materials *M*, *E* and *X*, wear rates were measured from the liners that survived one million cycles. Table 3 summarizes the test results.
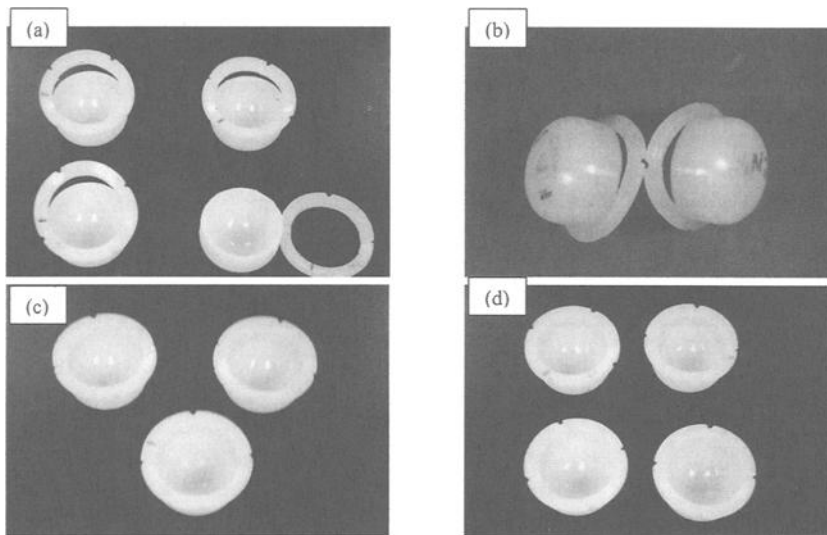

Figure 4 *Photographs of liners taken at one million cycles: (a) material L, (b) material M, (c) material E and (d) material X.*

Table 3 *Summary of the hip simulator wear and structural fatigue results*

Liner Material	Number of Liners Fractured	Crack-Opening Rate $(mm/10^6 \text{ cycles})$[1]	Wear Rate $(mm^3/10^6 \text{ cycles})$
L: 10Mrad-ebeam-remelt	4 of 4 (100%)	394 ± 59 (N=4)	N/A (all fractured)
M: 5Mrad-γ-remelt	2 of 4 (50%)	187 ± 9 (N=2)	22.1 ± 3.2 (N=2)
X: 7.5Mrad-γ-anneal +3Mrad-γ-N$_2$	0 of 4 (0%)	0	5.7 ± 1.1 (N=4)
E: 3Mrad- γ -N$_2$ (control)	0 of 4 (0%)	0	57.1 ± 19.2 (N=4)

[1] Differences between *L* and *M*, *L* and *X*, *L* and *C*, *M* and *X*, *M* and *C* are statistically significant ($P<0.003$).

Figure 5 shows wear-rate comparisons of materials *M*, *X* and *E*. Relative to the control material *E*, material *M* showed 61% wear reduction while material *X* showed 90% wear reduction. When material *X* is compared to material *M*, the former showed 74% less wear. In order to assess the relative importance of the mechanical properties on the structural fatigue resistance, the crack-opening rate data are plotted against each of the tensile properties in Figures 6(a) to 6(d). The best linear correlation was found between the crack-opening rate and the ultimate strength ($R^2=0.97$). Yield stress played a secondary role ($R^2=0.83$) while elongation was of least importance ($R^2=0.31$). Since toughness was a resultant property of ultimate strength and elongation, its correlation to the crack-opening rate reflects the composite effect of ultimate strength and elongation. The lower correlation coefficient for the composite effect ($R^2=0.75$) than that for the ultimate strength alone ($R^2=0.97$) indicates that it is the ultimate strength rather than the tensile toughness that is of primary importance.
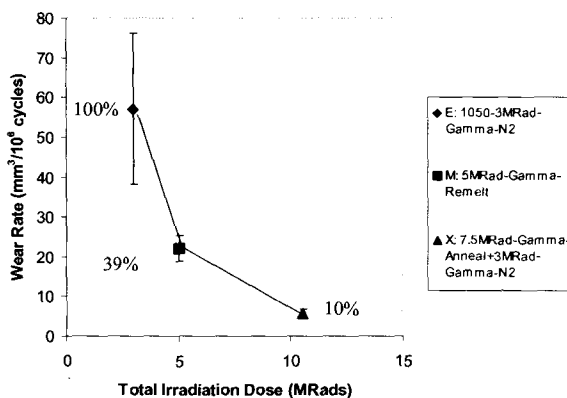

Figure 5 *Average wear rates for liners survived one million cycles of testing (all materials are statistically significantly different from one another in wear rate).*
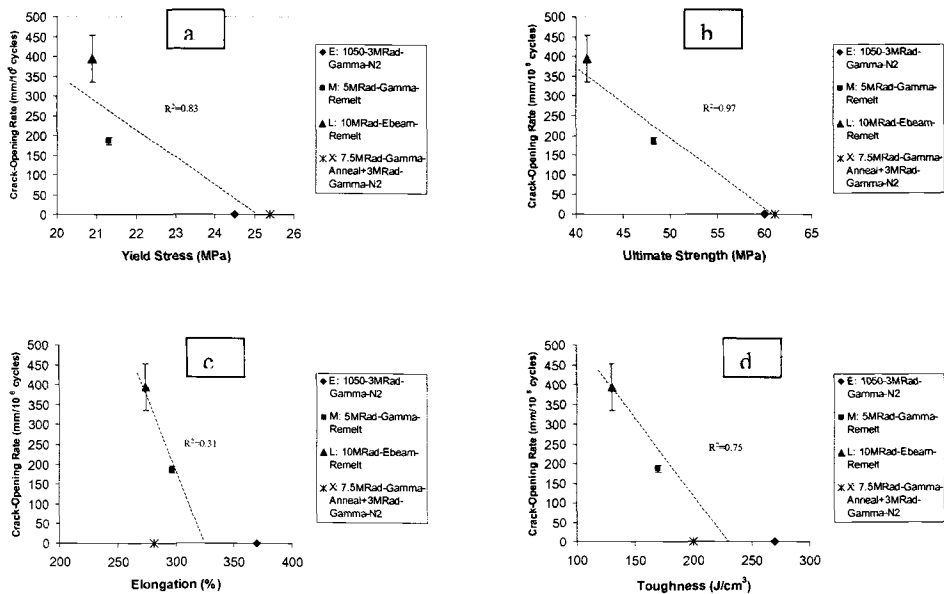
Figure 6 *Crack-opening rate vs. mechanical properties: (a) yield stress, (b) ultimate strength, (c) elongation and (d) toughness.*

Patellar Components – the patello-femoral simulator test was intended to simulate the wear and structural integrity of the control (***E-1020***) and the crosslinked/remelted (***L-γ***) materials under stair climbing conditions. The one million cycles of simulated stair climbing is approximately equivalent to 10 years of in-vivo duration for a typical patient [34]. All patellar components with normal alignment survived one million cycles without fracture of the peg or bone cement debonding. Under mal-alignment conditions, however, all the patellae for the crosslinked/re-melted material fractured at the peg before one million cycles whereas none of the patellae for the control material fractured, Figures 7(a) and (b). For all the intact patellae, wear was measured after all bone cement was removed from the interface. Table 4 summarizes the test results. For the control material, mal-alignment caused a significant increase in the wear rate (110%, P<0.05). Under the normal alignment conditions, the crosslinked/remelted patellae showed 35% less wear than the control. This difference was statistically significant (P<0.05). Because of peg fracture, wear of the crosslinked/re-melted patellae under mal-aligned conditions could not be measured.

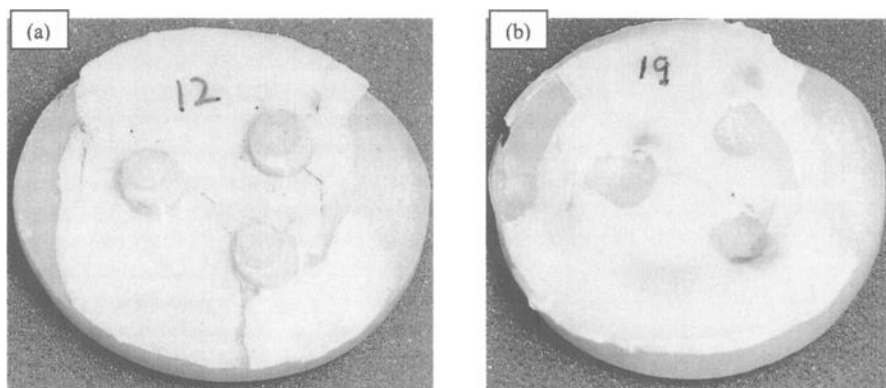Figure 7 *Photographs of representative patellae after one million cycles of simulated stair climbing under mal-alignment conditions: (a) the 3Mrad- γ-N₂ control showing no peg fracture and (b) the crosslinked/re-melted material showing complete fracture of all three pegs.*

Table 4 *Summary of the patellar test results (N=3)*

Patellar Material	Number of Fractured Patellae		Patellar Wear Rate $(mm^3/10^6$ cycles)	
	Aligned	Mal-aligned	Aligned	Mal-aligned
Control (E-1020: 3Mrad-γ-N₂)	0	0	7.67 ± 3.98	16.23 ± 3.45
Crosslinked/Re-melted (L-$γ$: 10Mrad-γ-remelt)	0	4	4.57 ± 1.56	N/A

Discussion

The present investigation again confirmed the benefits of elevated crosslinking for wear reduction in acetabular components as demonstrated in earlier studies [1-4]. The predominant material factor that influences cup wear rate is the total dose of irradiation. Radiation source and thermal treatment method are of secondary importance. Unlike previous studies, the present research focused on two possible worst-case clinical scenarios with the objective of revealing potential limitations of contemporary radiation-crosslinked and thermally treated polyethylene materials for hip and knee bearing applications. Two major observations were made. First, given a compromised acetabular cup design, all the radiation crosslinked and re-melted materials studied here significantly increased the risk for structural failure of the devices, whereas the highly crosslinked and thermally annealed (below melt) material showed no increased risk. This finding was very similar to that of two previous studies by Walsh et al. [35,36] that compared melt-quenched and non-quenched crosslinked materials to virgin polyethylene in a functional

fatigue setup of rim-loaded liners. In the experimental setup of Walsh et al., the rim-loaded liner was loaded axially without motion and a razor notch was created below the rim. Second, given a potentially poor surgical technique, e.g., rotational mal-alignment of a femoral component, all-poly patellar components made of a highly crosslinked and re-melted polyethylene fractured completely at the fixation pegs whereas no failure was seen in any of the components made of a conventional gamma-in-nitrogen sterilized polyethylene.

The liner test results revealed a number of misunderstandings of the effect of crosslinking on structural fatigue behavior of crosslinked polyethylene materials. First, the perception that structural integrity decreases with increasing radiation dose regardless of the post-radiation thermal treatment history is false. In fact, the structural integrity of the rim-loaded thin liners was adversely affected for the irradiated and re-melted materials only. The highly crosslinked and annealed (below melt) material showed equally excellent resistance to liner fracture as the conventional material. Therefore, as far as structural fatigue is concerned, post-irradiation thermal treatment method has a more pronounced effect than the total dose of irradiation. Second, the perception that crosslinking deteriorates mechanical properties because of decreases in tensile elongation is false. Tensile elongation was seen to be the most sensitive property to crosslinking regardless of radiation source or thermal treatment method. However, it is also the least important property that affects the structural fatigue performance of the rim-loaded liners. Ultimate tensile strength and yield stress have far greater correlations. It is strength, not ductility, that determines the structural fatigue resistance of crosslinked polyethylene devices. A good example is the direct-molded 1900H material, which had great strength but poor elongation. Its clinical performance has been excellent [37,38]. Finally, the perception that tensile toughness (area under a stress-strain curve) determines fatigue fracture resistance of crosslinked polyethylene devices is not necessarily true. Since toughness is a composite property that depends on strength and ductility, the use of this parameter as an indication of fatigue performance may mistakenly point to the wrong choice of a material that is low in strength but high in ductility.

The root cause for the drop in ultimate and yield strength of radiation crosslinked polyethylene after re-melting lies in the significant alteration of crystallinity and crystalline morphology [39]. Re-melting forces the occurrence of re-crystallization upon cooling. Once a polyethylene is highly crosslinked, re-crystallization is hindered because of decreased chain mobility. Crystallization from the melt occurs in a smaller domain, resulting in the formation of smaller crystal lamellae and lower crystallinity than that pre-existed in the virgin or as-irradiated state. Therefore, the intention of eliminating free radicals by re-melting has a significant cost attached to it. As the strength drops, the ability of the re-melted materials to sustain higher stresses also decreases. To ensure proper function of an implant device or devices made of re-melted polyethylene, attention must be paid to avoiding stress concentrations and excessive loading situations such as rim-loading of thin liners or mal-alignment of patello-femoral components.

The irradiated/annealed and gamma-in-nitrogen sterilized polyethylene contains free radicals. It is widely accepted that gamma-in-air irradiated polyethylene oxidizes during shelf-storage [40-44]. This oxidation accelerates after five years on the shelf. Several clinical studies have indicated that fatigue-related wear such as delamination in tibial bearing components occurs almost exclusively for those that had had at least one year of

shelf-storage prior to implantation [45,46,47]. Normally four to five years of shelf-storage in air were required before an elevated level of fatigue wear could be detected in long-term clinical follow-ups [47]. In other words, the existence of a significant level of oxidation in the polyethylene prior to implantation is a pre-requisite for delamination wear of gamma-in-air sterilized tibial components in-vivo. Since the mid 1990s, the implant industry has responded to the oxidation challenge by introducing gamma-in-inert sterilization and air-impermeable packaging. To the best of our knowledge, we have not been able to locate a single literature study that links gamma-inert sterilized components to unacceptable levels of wear or fatigue damage in-vivo.

Despite the fact that gamma-in-air sterilized polyethylene oxidizes on the shelf, there has been no clinical evidence correlating in-vivo performance or wear rate to oxidation in total hip replacement [48,49]. There has been plenty of clinical evidence indicating that acetabular cup wear rate decreases with increasing implantation time [50-52]. This implies that either oxidation does not occur in-vivo or occurs at such a slow rate that it has no adverse clinical consequence. A recent clinical study comparing gamma irradiated polyethylene with EtO sterilized polyethylene cups showed that the mean wear rate for the gamma-in-air sterilized cups was only 50% that of the EtO sterilized cups despite the fact that the latter had no free radicals [7]. However, acetabular cups made of Hylamer enhanced polyethylene were an exception. Significantly higher incidence of accelerated wear and osteolysis has been reported for Hylamer liners compared to conventionally processed GUR liners [19,20]. The heightened sensitivity of Hyamler to oxidative degradation was attributed to its unique crystalline structural that resulted from a high-temperature/high-pressure re-melting process [53].

The results presented in this study should not be misconstrued with respect to the potential clinical performance of irradiation crosslinked and re-melted polyethylene liners with proper designs. In fact, the true outcome of all the crosslinked materials can only be revealed by long-term clinical follow-up.

Conclusions

The potential benefits and risks of various radiation crosslinked and thermally treated UHMWPE materials have been evaluated by functional simulations of hip and knee bearing devices under two possible worst-case scenarios. All crosslinked materials exhibited significant levels of wear reduction. However, the irradiated and re-melted materials showed elevated risks for structural failure for thin liners in rim loading and for all-poly patellar components under mal-aligned conditions. The irradiated and annealed material, on the other hand, showed similar structural fatigue resistance to a conventional control material despite the fact that the former received three times the radiation dose of the latter.

Structural fatigue performance of crosslinked polyethylene liners is best correlated to the ultimate tensile strength followed by yield stress. Elongation or ductility above 250% has no effect on structural integrity. It is strength, not ductility, that determines the structural fatigue resistance of crosslinked materials in high stress situations.

References

[1] Wang, A., Essner, A., Polineni, V. K., Stark, C., and Dumbleton, J. H.: "Lubrication and wear of ultra-high molecular weight polyethylene in total joint replacements," *Tribology International*, Vol. 31, Nos. 1-3, 1998, 17-33.

[2] McKellop, H., Shen, F., Dimaio, W., and Lancaster, J. G.: "Wear of gamma-crosslinked polyethylene acetabular cups against roughened femoral balls," *Clinical Orthopaedics and Related Research*, Vol. 369, 1999, 73-82.

[3] Laurent, M. P., Yao, J. Q., Bhambri, S. K., Gsell, R. A., Gilbertson, L. N., Swarts, D. F., and Crowninshield, R. D.: "High cycle wear of highly crosslinked UHMWPE acetabular liners evaluated in a hip simulator," *Trans 46th Orthop Res Soc*, 2002, p. 567.

[4] Taylor, S., Serekian, P., Bruchalski, P., and Manley, M. T.: "The performance of irradiation-crosslinked UHMWPE cups under abrasive conditions throughout hip simulation testing," *Trans 45th Orthop Res Soc*, 1999, p. 252.

[5] Essner, A. and Wang, A.: "Comparison of two different hip wear simulators," *Trans 46th Orthop Res Soc*, 2000, p.217.

[6] Essner, A., Polineni, V. K., Wang, A., Stark, C., and Dumbleton, J. H.: "Effect of femoral head surface roughness and crosslinking on the wear of UHMWPE acetabular inserts," *Trans 24th Soc For Biomaterials*, 1998, p. 4.

[7] Karrholm, J., Digas, G., Nivbrant, B., Rohrl, S., and Thanner, J.: "Increased femoral head penetration using polyethylene sterilized with ethylene oxide," *Trans 47th Orthop Res Soc*, 2001, p. 1025.

[8] McKellop, H., Shen, F. W., Lu, B., Campbell, P., Salovey, R.: "Development of an extremely wear-resistant ultrahigh molecular weight polyethylene for total hip replacements," *J Orthop Res*, Vol., 17, 1999, 157-167.

[9] Muratoglu, O. K., Bragdon, C. R., O'Connor, D. O., Merrill, E. W., Jasty, M., Gul, R., and McGarry, F.: "Unified wear model for highly crosslinked ultra-high molecular weight polyethylenes (UHMWPE)," *Biomaterial*, Vol., 20, 1999, 1463-1470.

[10] Oonishi, H.: "Long term clinical results of THR. Clinical results of THR of an alumina head with a crosslinked UHMWPE cup," *Orthopaedic Surgery and Traumatology*, Vol., 38 (11), 1985, 1255-1264.

[11] Grobelaar, C. J., Weber, F. A., Spirakis, A., Du Plessis, T. A., Cappert, G., and Cakic, J. N.: "Clinical experience with gamma irradiation-crosslinked polyethylene – A 14 to 20 year follow-up report," *S. Africa Bone Joint Surg*, Vol., 11, 1999, p.140.

[12] Wroblewski, B. M., Siney, P. D., and Fleming, P. A.: "Low-friction arthroplasty of the hip using alumina ceramic and crosslinked polyethylene – A ten-year follow-up report," *J Bone Joint Surg*, Vol., 81-B (1), 1999, p.54.

[13] Oonishi, H., Takayama, Y., and Tsuji, E.: "Improvement of polyethylene by irradiation in artificial joints," *Radiat Phys Chem*, Vol., 39, 1992, p.495.

[14] Grobelaar, CJ, Du Plessis, T. A., and Marais, F.: "The radiation improvement of polyethylene prosthesis: A preliminary study," *J Bone Joint Surg,* Vol., 60-B (3), 1978, 370-374.

[15] Wroblewski, B. M., Siney, P. D., Dowson, D., and Colling, S. N.: "Prospective clinical and joint simulator studies of a new total hip arthroplasty using alumina ceramic heads and cross-linked polyethylene cups," *J Bone Joint Surg,* Vol., 78-B (2), 1996, 280-285.

[16] Wright, T. M., Astion, D. J., Bansal, M., Rimnac, C. M., Green, T., Insall, J. N., and Robinson, R. P.: "Failure of carbon fiber-reinforced polyethylene total knee-replacement components," *J Bone Joint Surg,* Vol., 70-A (6), 1988, 926-932.

[17] Wright T. M., Rimnac, C. M., Faris, P. M., and Bansal, M.: "Analysis of surface damage in retrieved carbon fiber-reinforced and plain polyethylene tibial components from posterior stabilized total knee replacements," *J Bone Joint Surg,* Vol., 70-A (9), 1988, 1312-1319.

[18] Kilgus, D. J., Funahashi, T. T., Campbell, P. A.: "Massive femoral osteolysis and early disintegration of polyethylene-bearing surface of a total knee replacement," *J Bone Joint Surg,* Vol., 74-A (5), 1992, 770-774.

[19] Livingston, B. J., Chmell, M.J., Reilly, D. T., Spector, M., Poss, R.: "The wear rate of Hylamer cups is higher than conventional PE and differs with heads from different manufacturers," *Trans 43rd Orthop Res Soc,* 1997, p.141.

[20] Chmell, M. J., Poss, R., Thomas, W. H., and Sledge, C. B.: "Early failure of Hylamer acetabular inserts due to eccebtric wear," *J Arthroplasty,* Vol., 11 (3), 1996, 351-353.

[21] Suh, K. T., Chang, J. W., Suh, Y. H., and Yoo, C. I.: "Catastrophic progression of the disassembly of a modular acetabular component," *J. Arthroplasty,* Vol., 8, 1988, p.950.

[22] Peters, C. L., and Sullivan, C. L.: "Locking mechanism failure in the Harris-Galante porous acetabular component associated with recurrent hip dislocation," *J. Arthroplasty,* Vol., 17 (4), 2002, 507-515.

[23] Bono, J. V., Sanford, L., and Toussaint, J. T.: "Severe polyethylene wear in total hip arthroplasty – Observations from retrieved AML Plus hip implants with an ACS polyethylene liner," *J Arthroplasty,* Vol., 9 (2), 1994, 119-125.

[24] Barrack, R. T., and Schmalzried, T. P.: "Impingement and rim wear associated with early osteolysis after a total hip replacement," *J. Bone Joint Surg,* Vol., 84-A (7), 2002, 1218-1220.

[25] Yamaguchi, M., Hashimoto, Y., Akisue, T., and Bauer, T. W.: "Polyethylene wear vector in vivo: a three-dimensional analysis using retrieved acetabular components and radiographs," *J Orthop Res,* Vol., 17 (5), 1999, 695-702.

[26] Landy, M. M., and Walker, P. S.: "Wear of ultra-high molecular weight polyethylene components of 90 retrieved knee prostheses," *J Arthroplasty,* October 1988 Supplement, S73-85.

[27] Wright, T. M., and Bartel, D. L.: "The problem of surface damage in polyethylene total knee components," *Clinical Orthopaedics and Related Research,* Vol., 205, 1986, 67-74.

[28] Hood, R. W., Wright, T. M., and Burstein, A. H.: "Retrieval analysis of total knee prostheses," *J Biomed Mater Res,* Vol., 18, 1981, 181.

[29] Wasielewski, R. C., Galante, J. O., Leighty, R. M., Natarajan, R. N., and Rosenberg, A. G.: "Wear patterns on retrieved polyethylene tibial inserts and their relationship to technical considerations during total knee arthroplasty," *Clin Orthop Rel Res*, Vol., 299, 1994, 31-43.

[30] Majewski, M., Weining, G., and Friederich, N. F.: "Posterior femoral impingement causing polyethylene failure in total knee arthroplasty," *J Arthroplasty*, Vol., 17 (4), 2002, 524-526.

[31] Wang, A., Sun, D. C., Yau, S. S., Edwards, B., Sokol, M., Essner, A., Polineni, V. K., Stark, C., and Dumbleton, J. H.: "Orientation softening in the deformation and wear of UHMWPE," *Wear*, Vol., 203-204, 1997, 230-241.

[32] Paul, J. P.: "Forces transmitted by joints in the human body," *Proc Instn Mech Engrs*, Vol., 181 (Part 3), 1966, 8-15.

[33] Saari, H., Santavirta, S., Nordstrom, D., Paavolainen, P., and Konttinen, Y. T.: "Hyaluronate in total hip replacement," *J Rheumatol*, Vol., 20, 1993, 87-90.

[34] Hungerford, D. S. and Barry, M.: "Biomechanics of the patellofemoral joint," *Clin Orthop*, Vol., *144*, 1979, 9-15.

[35] Walsh, H. A., Furman, B. D., and Li, S.: "The effects of cross-linking on the fracture and fatigue properties of UHMWPE acetabular cups," *Trans 27th Soc For Biomaterials*, 1999, p.592.

[36] Walsh, H. A., Furman, B. D., Naab, S., and Li, S.: "Determination of the role of oxidation in the clinical and in vitro fracture of acetabular cups," *Trans 25th Soc For Biomaterials*, 1999, p.50.

[37] Emerson, R. H. J., Higgins, L. L., and Head, W. C.: "The AGC total knee prosthesis at average 11 years," *J Arthroplasty*, Vol., 15, 2000, 418-423.

[38] Ritter, M. A., Worland, R., Saliski, J.: "Flat-on-flat, nonconstrained, compression molded polyethylene total knee replacement," *Clin orthop Rel Res*, Vol., 321, 1995, 79-85.

[39] Bassett DC: *Principles of polymer morphology*, Cambridge University Press, 1981.

[40] Roe, R. J., Grood, E., Shastri, R., Gosselin, C., and Noyes, F.: "Effect of radiation sterilization and aging on UHMWPE," *J Biomed Mater Res*, Vol., 15, 1981, 209-230.

[41] Streicher, R.: "Influence of ionizing irradiation in air and nitrogen for sterilization of surgical grade polyethylene implants," *Radiat Phys Chem*, Vol., 31, 1988, 693-698.

[42] Sutula, L. C., Collier, J. P., Saum, K. A., et al.: "Impact of gamma sterilization on clinical performance of polyethylene in the hip," *Clin Orthop Rel Res*, Vol., 319, 1995, 28-40.

[43] Collier, J. P., Sperling, D. K., Currier, J. H., et al.: "Impact of gamma sterilization on clinical performance of polyethylene in the knee," *J Arthroplasty*, Vol., 11 (4), 1996, 377-389.

[44] Furman, B. and Li, S.: "The effect of long-term shelf aging of ultra-high molecular weight polyethylene," *Trans 21st Soc For Biomater*, 1995, p.114.

[45] Currier, B. H., Currier, J. H., Collier, J. P., et al.: "Shelf life and in vivo duration – Impacts on performance of tibial bearings," *Clin Orthop Rel Res*, Vol., 342, 1997, 111-122.

[46] Collier, J. P., Sutula, D. C., Currier, B. H., et al.: "Overview of polyethylene as a bearing material – Comparison of sterilization methods," *Clin Orthop Rel Res*, Vol., 333, 1996, 76-86.

[47] Bohl, J. R., Bohl, W. R., Postak, P. D., Heim, C. S., and Greenwald, A. S.: "The influenced of shelf-storage duration on clinical performance of ultra-high molecular weight polyethylene tibial components following gamma sterilization in air," Scientific Exhibits, AAOS, 1999, Booth No. SE020.

[48] Gomez-Barrena, E., Li, S., Furman, B. S., Masri, B. A., Wright, T. M., and Salvati, E. A.: "Role of polyethylene oxidation and consolidation defects in cup performance," *Clin Orthop Rel Res,* Vol., 352, 1998, 105-117.

[49] James, S. P., Blazka, S., Merrill, E. W., Jasty, M., Lee, K. R., Bragdon, C. R., and Harris, W. H.: "Challenge to the concept that UHMWPE acetabular components oxidize in vivo," *Biomaterials,* Vol., 14 (9), 1993, 643-647.

[50] Charnley, J., and Halley, D. K.: "Rate of wear in total hip replacement," *Clin Orthop Rel Res,* Vol., 112, 1975, 170-179.

[51] Devane, P. A. and Horne, J. G.: "Assessment of polyethylene wear in total hip replacement," *Clin Orthop Rel Res,* Vol., 369, 1999, 59-72.

[52] Dowd, J. E., Sychterz, C. J., Young, A. M., and Engh, C. A.: "Characterization of long-term femoral-head-penetration rates – Association wear and prediction of osteolysis," *J Bone Joint Surg,* Vol., 82-A (8), 2000, 1102-1107.

[53] Sun, D. C., Bellare, A., Yau, S. S., Stark, C., and Dumbleton, J. H.: "Oxidative behavior and morphological change in gamma irradiated Hylamer," *Trans 45th Orthop Res Soc,* 1999, p.834.

Mechanical Properties

S. Bhambri,[1] R.Gsell,[1] L. Kirkpatrick,[1] D. Swarts,[2] C.R. Blanchard,[3] and R.D. Crowninshield [4]

The Effect of Aging on Mechanical Properties of Melt-Annealed Highly Crosslinked UHMWPE

ABSTRACT: Crosslinking has been shown to improve significantly the wear resistance of ultra high molecular weight polyethylene (UHMWPE), both in joint simulator tests and in clinical use. High-energy ion radiation, when used to induce crosslinking in UHMWPE, produces free radicals. In the presence of oxygen, the free radicals have been shown to be responsible for oxidative degradation of polyethylene. A melt-anneal treatment of highly crosslinked UHMWPE substantially eliminates the free radicals to an undetectable low level.

The aim of this study was to determine the effect of accelerated oxidative aging on the mechanical and fracture properties of melt-annealed highly crosslinked UHMWPE. Compression molded GUR 1050 UHMWPE was crosslinked by electron-beam irradiation at 100 ± 10 kGy and was followed by a melt-anneal treatment. Both melt-annealed highly crosslinked and conventional gamma irradiated in nitrogen UHMWPE were exposed to an accelerated oxidative challenge in the laboratory. The tensile mechanical properties and crack growth resistance curves (J-R curves) determined for oxidative aged melt-annealed highly crosslinked UHMWPE were either equivalent or superior to the oxidative aged conventional gamma irradiated UHMWPE. The difference in tensile mechanical properties and J-R curves for non-aged and oxidative aged melt-annealed crosslinked UHMWPE was insignificant, indicating that oxidative aging had no detrimental effect on mechanical and fracture properties of melt-annealed highly crosslinked UHMWPE.

KEYWORDS: UHMWPE, crosslinked, aging, fracture toughness, J-R curve

[1]Principal Engineer, [2]Director, [3]Vice President and [4]Senior Vice President, Research Department, Zimmer, Inc., P.O. Box 708, Warsaw, IN, 46580.

Introduction

UHMWPE has been in use as an articulating surface in total joint replacements for well over three decades. The clinical experience of these implant components is generally considered a success. However, polyethylene wear particles have been observed to generate at the articulating surfaces and have been implicated as a limiting factor in the service life of the implant [1,2]. The wear rate has been found to be dependent on various factors including aging due to oxidative degradation of the UHMWPE material. Aging may occur in UHMWPE by the oxidation reaction of free radicals produced in components during high-energy ion irradiation. The effects of oxidative aging on the physical and mechanical properties of UHMWPE gamma sterilized in air have been studied extensively and significant degradation in these properties have been reported [3,4]. Aging related changes in material properties due to oxidative degradation are now understood to be a significant factor affecting wear of articulating surfaces [5,6].

In recent years, two-fold efforts were made to reduce the wear rates of polyethylene. The first was directed to reduce the oxidative degradation of UHMWPE by packaging the components for gamma sterilization in an inert environment or vacuum, or using alternate sterilization methods such as ethylene oxide or gas plasma. The second approach was to enhance the wear performance of polyethylene through highly crosslinking the material. Crosslinking of the molecular chains has been shown to reduce the wear of UHMWPE significantly in several *in vitro* joint simulator studies [7-13] and has also been demonstrated in limited clinical use [14-18]. It has been hypothesized that crosslinking of polymers enhances the resistance to lamellae alignment at the articulating surface, resulting in higher resistance to wear and a substantial reduction in wear particle generation. The crosslinks are believed to reduce the molecular mobility, resist interlamellar plasticity, and minimize alignment-preceding wear. Polyethylene can be extensively crosslinked utilizing high-energy radiation [7,10] or by chemical treatment [18]. Recent advances in crosslinking have used high energy electron beam (e-beam) irradiation to induce crosslinking in bearing components of total joints [8,13].

Crosslinking of polyethylene inherently alters the material's structure, affecting physical and mechanical properties. Free radicals produced during irradiation, if retained in the component, may render the material susceptible to oxidative degradation induced aging. In the case of high energy e-beam irradiation-induced crosslinking of UHMWPE, the free radicals produced during irradiation can be reduced by a subsequent melt anneal. Reduction in free radicals would make the material less susceptible to oxidative degradation induced aging. The objective of this study was to determine the effect of accelerated laboratory aging on mechanical and fracture properties of e-beam crosslinked and melt-annealed medical grade GUR 1050 UHMWPE.

Materials and Methods

Material

The starting resin material used in this study was compression molded medical grade GUR 1050 UHMWPE. The material was received as compression molded slabs cut into rectangular bars. Highly crosslinked UHMWPE (HXPE) was produced by high energy e-beam irradiation of compression molded GUR 1050 at 100±10 kGy. A melt-annealing process to reduce free radicals followed the e-beam irradiation and all crosslinked specimens were double cycle gas plasma sterilized in air. E-beam irradiation and melt annealing were conducted in air and, therefore, prior to specimen preparation, 4.40 mm of the top surface layers were removed from all sides of the bars. Conventional polyethylene specimens obtained from the same manufacturing lot of compression molded slab of GUR 1050 were gamma irradiated in nitrogen at 37±3 kGy and retained in nitrogen package until testing.

Laboratory Aging

Part of the crosslinked and melt-annealed, and conventional gamma irradiated in nitrogen specimens were subjected to accelerated oxidative challenge in the laboratory following Sanford and Saum technique [19] in pure oxygen at 70° C and 5 atm for 14 days per ASTM Test Method F 2003 Method B (Guide for Accelerated Aging of Ultra-High Molecular Weight Polyethylene). The later were referred to as aged-conventional specimens.

Oxidation Index

The oxidation state for both non-aged and laboratory aged specimens was determined by calculating a specimen's average surface oxidation index (SOI) per ASTM Test Method F 2102 (Guide for Evaluating the extent of Oxidation in Ultra-High-Molecular Weight Polyethylene Fabricated Forms Intended for Surgical Implants). The SOI is defined as the average of the FTIR 1720/1369 cm^{-1} oxidation indices from surface to a depth of 3 mm subsurface. The test specimens were 100 μm thick microtomed films. Five films for each material condition were analyzed for the calculation of a specimen's SOI. Oxidation was measured by using a Nicolet Magna-IR 550 spectrometer coupled to a Nic-Plan FTIR microscope with an automated mapping stage (Thermo Nicolet, Madison,WI). The spectral resolution was 4 cm^{-1} and reflection spectra were collected sequentially from top surface to the bottom surface of each specimen using a 200 μm aperture.

Crystallinity

Crystallinity was measured by Differential Scanning Calorimetry (DSC) techniques per ASTM D 3418 (Test Method for Transition Temperatures of Polymers by Thermal Analysis). A TA Instruments 2920 DSC (TA Instruments, New Castle, DE) was used with a controlled heating ramp rate of 10° C/minute from ambient temperature to 200° C,

followed by an isothermal hold for 10 minutes, and then followed by a controlled cooling ramp of 10° C/minute to ambient temperature. The percent crystallinity was calculated from the total heat (J/gram) absorbed during the melting endotherm observed in the heating ramp portion of the experiment and the standard heat of fusion of crystalline UHMWPE (293 J/gram).

Tensile Mechanical Properties

The tensile properties were measured by testing type IV specimens per ASTM E 8 (Test Method for Tension Testing of Metallic Materials) using ASTM F 648 (Specification for Ultra-High-Molecular-Weight Polyethylene Powder and Fabricated Form for Surgical Implants) and D 638 (Test Method for Tensile Properties of Plastics) Type IV specimens on an Instron 55R1125 universal test machine (Instron Corporation, Canton, MA). The crosshead speed was 50.8 mm/minute. Extension to break was measured with an Instron 2663 video extensometer. Five specimens were tested for each material condition. Single-factor ANOVA was used to test statistical significance of the results.

Fracture Toughness

J-integral fracture toughness evaluation has been used successfully for polymer fracture characterization for three decades. J-integral was therefore selected as basis of fracture toughness evaluation and comparison of material toughness in different conditions. J-integral fracture toughness tests were conducted on 12.7mm thick compact-tension specimens per ASTM Test Method E 1820 (Test Method for Measurement of Fracture Toughness). Three identical specimens were machined for each material condition such that the notch was along the longitudinal direction of the bar. A single specimen test technique and normalization method was used to determine a valid J-R curve and J-integral fracture toughness. Applicability of this test method has been demonstrated for polyethylene using small size compact-tension specimens [20].

A load-displacement plot was recorded as a compact-tension specimen was loaded on the test machine. In each group, specimens were loaded to achieve different crack extension values and then unloaded. The specimens were then immersed in liquid nitrogen until equilibrium temperature was reached and loaded on the Instron to fracture. Crack lengths were measured at nine points and the data analyzed to determine fracture toughness and J-R curves.

Results

The non-aged gamma control specimens showed an average SOI of 0.067. The aged gamma sterilized specimens had an average SOI of 0.27. The melt-annealed cross-linked polyethylene had an SOI of 0.008, which increased to 0.03 upon aging. Figure 1 shows a comparison of oxidation indices for all of the material conditions investigated.
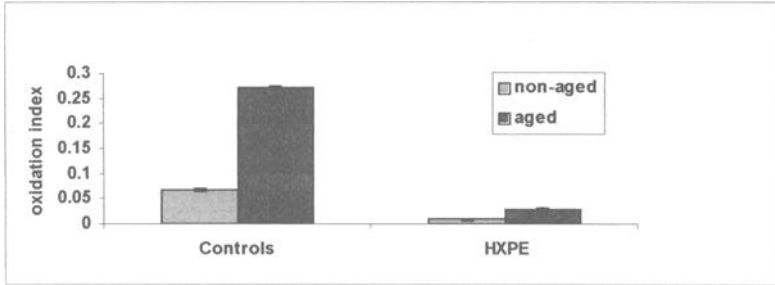

Figure 1- *Surface oxidation index for Control (conventional gamma irradiated) and highly crosslinked UHMWPE in oxidative aged and non-aged conditions.*

Crystallinity and mechanical properties for the four material conditions studied are shown in Table 1. Oxidative aging resulted in a 10% increase in crystallinity (Figure 2) for conventional UHMWPE. The increase in crystallinity for the melt-annealed highly crosslinked UHMWPE was statistically insignificant. The ultimate tensile strength (UTS) of the aged conventional gamma sterilized specimens decreased significantly (by 43%) relative to the non-aged conventional specimens (Figure 3). The yield strength (Figure 3) and elongation (Figure 4) of the conventional UHMWPE increased upon aging by 14% and 16% respectively compared to the non-aged condition. The aged and non-aged crosslinked UHMWPE showed no significant difference in these properties. The oxidative aged crosslinked UHMWPE and the unaged crosslinked UHMWPE demonstrated yield and tensile strength values comparable to the aged conventional polyethylene.

Table 1- *Percent crystallinity and mechanical properties. Standard deviations are shown in parentheses.*

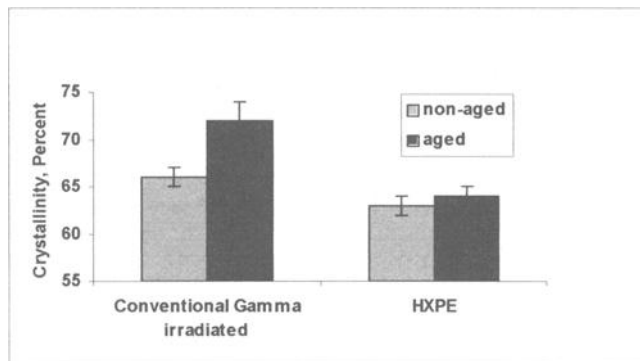| Material GUR 1050	Crystallinity (%)	Tensile strength (MPa)	Yield strength (MPa)	Elongation (%)	Modulus (MPa)	J-Integral Fracture Toughness (kJ/m^2)
Conventional Gamma Sterilized in Nitrogen	66	48.5 (3.2)	20.9 (0.3)	346 (28)	784 (94)	66.4 (2.5)
Conventional Gamma Sterilized, Laboratory aged in oxygen	72	27.7 (1.7)	23.8 (0.4)	401 (28)	1099 (204)	22.9 (1.3)
E-beam highly crosslinked and melt annealed	63	33.3 (3.1)	19.0 (0.2)	233 (14)	642 (109)	30.6 (1.1)
E-beam highly crosslinked and melt annealed, Laboratory aged in oxygen	66	33.0 (1.9)	19.2 (0.2)	235 (5)	681 (124)	34.2 (0.9)

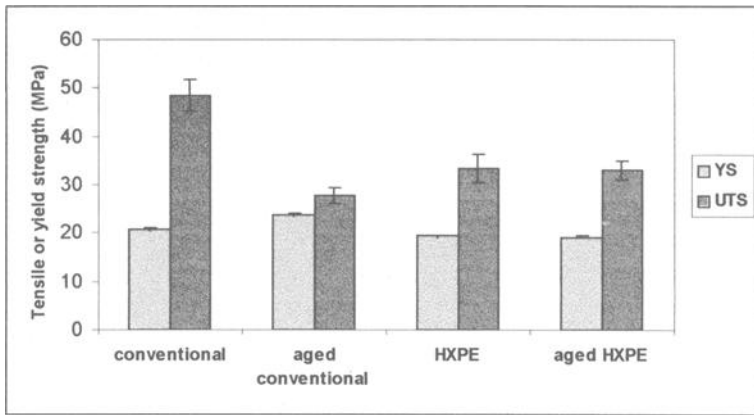Figure 2- *Crystallinity in different material conditions.*

Figure 3- *Tensile strength and yield strength of GUR 1050 in different material conditions.*
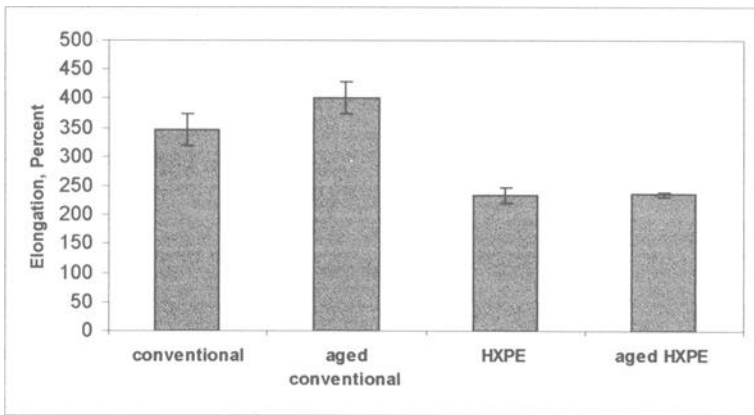

Figure 4- *Percent elongation for materials investigated.*

J-R curves derived from the experimental data are shown in Figures 5 and 6. J-R curves for gamma control specimens (Figure 5) indicated that the crack growth resistance for the aged condition was lower compared to the non-aged condition, while no significant difference in crack growth resistance was observed for melt-annealed crosslinked UHMWPE for the aged and non-aged conditions (Figure 6). The J-integral fracture toughness (J_{IC}) for all material conditions are compared in Figure 7. The J-integral fracture toughness for non-aged gamma control specimens decreased from 66.4 kJ/m^2 to 22.9 kJ/m^2 (by 66%) upon aging. Highly crosslinked UHMWPE showed a slight

increase in fracture toughness from 30.5 to 34.2 kJ/m^2, indicating no detrimental effect of aging on the fracture toughness of crosslinked polyethylene. Fracture toughness for aged crosslinked polyethylene was significantly higher compared to the aged gamma controls. These results indicate that melt annealed highly crosslinked UHMWPE is very resistant to oxidation-induced degradation of material properties associated with aging.
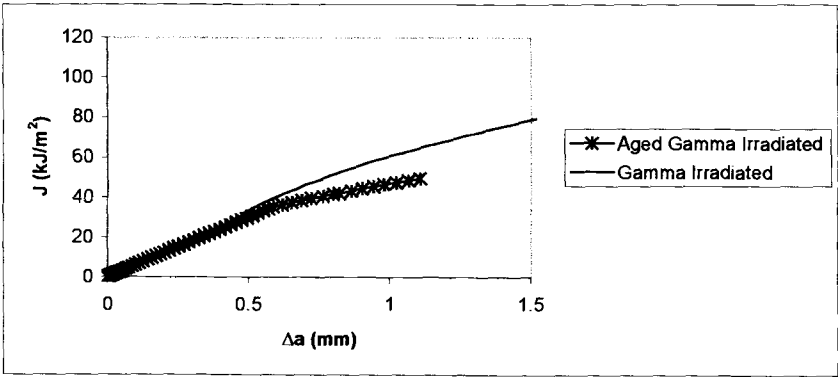
Figure 5- *J-R curves for oxidative aged and non-aged conventional UHMWPE.*
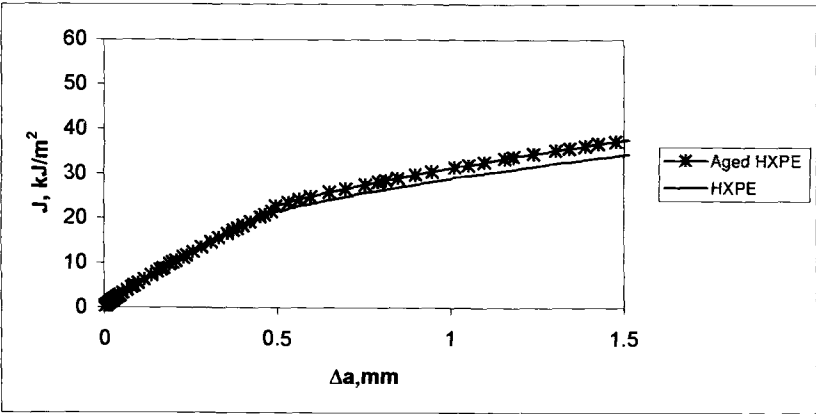
Figure 6- *J-R curves for oxidative aged and non-aged melt-annealed highly crosslinked UHMWPE.*

Discussion

Oxidation indices measured for four material conditions show that both conventional UHMWPE gamma irradiated in nitrogen and melt-annealed highly crosslinked UHMWPE had experienced a change in oxidation level during accelerated oxidative challenge in laboratory aging. However, in oxidative challenged conditions, the melt-annealed highly cross-linked UHMWPE showed a significantly lower average SOI of 0.03 compared to an average SOI of 0.27 for the conventional gamma sterilized material, a difference of almost an order of magnitude. This indicates that melt annealed highly crosslinked UHMWPE material has a significantly lower propensity to oxidative degradation compared to conventional gamma sterilized material. This improved oxidation resistance of highly crosslinked UHMWPE results from the elimination of free radicals during melt annealing, leaving an undetectably low amount of residual free radicals.

Gamma irradiated control specimens had a higher crystallinity compared to the e-beam irradiated and melt-annealed UHMWPE. Oxidative aging resulted in a statistically significant increase in crystallinity for both conventional and highly crosslinked materials. The oxidation induced increase in crystallinity in melt-annealed highly crosslinked polyethylene was relatively small compared to the increase in crystallinity observed for the conventional polyethylene.

The effect of crosslinking and crystallinity on mechanical properties is evident from Table 1. The ultimate tensile strength of the aged conventional specimens decreased significantly, by 43%, relative to the non-aged gamma sterilized conventional specimens. The yield strength of aged conventional specimens was approximately 15% higher compared to non-aged condition. The oxidative aged and non-aged melt annealed highly crosslinked UHMWPE showed no significant difference in any of these properties.

J-R curves for gamma irradiated conventional specimens indicated that the crack growth resistance for the aged condition was lower compared to the non-aged condition while no significant difference in crack growth resistance was observed for melt annealed highly crosslinked UHMWPE for the aged and non-aged conditions. The J-R curves in this study were determined using the single specimen technique and the method of normalization for crack extension measurements. The single specimen technique has been shown to work successfully for other visco-elastic materials such as rubber toughened nylon [21]. Unlike the multiple specimen method, a valid J-R curve can be determined by the single specimen technique [20] using ASTM Method E 1820.

The J-integral fracture toughness concept, J_{IC} has been extensively used to determine fracture toughness or to characterize fracture resistance of UHMWPE. Since there is no standard test protocol for polymers, the J-integral method developed for metals has been critically reviewed and many authors have modified the approach in their work [20,22-24]. The J_{IC} value of 66.4 kJ/ m^2 determined in this study for conventional gamma sterilized in nitrogen GUR 1050 falls within the wide range of fracture toughness values reported for GUR 4150. Rimnac et al. [25] have reported a J_{IC} value of 99.5 kJ/m^2 for unsterilized ram extruded GUR 4150 and Pascaud et al. [23] reported 75.6 kJ/m^2 for the

gamma irradiated in air condition. On the other end of this range, J_{IC} values of 22 and 44.3 kJ/m^2 were reported by Baldini et al. [26] and Lewis and Jeffry [24], also for GUR 4150 gamma sterilized in air. The J_{IC} value of UHMWPE determined in this
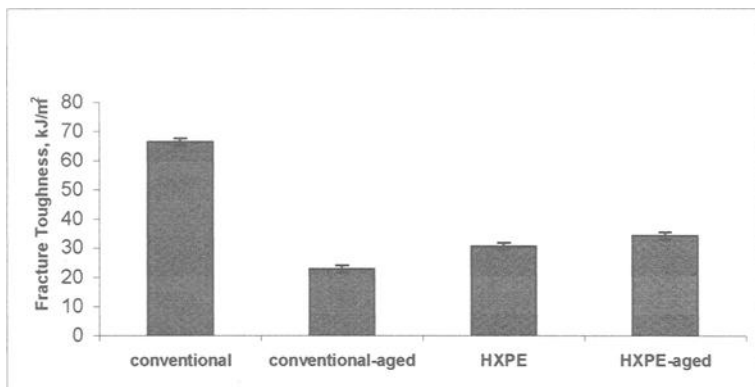

Figure 7- *J-integral fracture toughness for different material conditions.*

study, without using a blunting line in the analysis, is an objective measure of fracture toughness for a material condition on a relative scale, even if absolute numbers are not considered as true values. It may be noted that J_{IC} is not used in the design of devices but only as a measure of a material's relative fracture toughness. Recently, Duus et al. [27] have demonstrated the use of J-R curves in comparing the crack growth resistance of UHMWPE.

Conclusion

E-beam irradiated and melt-annealed highly crosslinked UHMWPE, when challenged with a severe oxidative environment in an accelerated aging treatment in the laboratory, demonstrated an excellent resistance to oxidative degradation. Highly crosslinked melt-annealed UHMWPE had a significantly lower level of oxidation compared to conventional polyethylene gamma sterilized in nitrogen and oxidatively aged following a similar protocol. Oxidative aging of highly crosslinked melt-annealed UHMWPE caused no adverse effects on mechanical and fracture resistance properties. The fracture toughness of highly crosslinked UHMWPE was significantly greater compared to conventional polyethylene when aged under identical oxidative environment.

Acknowledgments

References

[1] Charnley, J., and Hally, D.K., "Rate of Wear in Total Hip Replacement", *Clinical Orthopaedics*, Vol. 112, 1975, pp. 170-179.

[2] Amstutz, H.C., Campbell P., Kossovsky, N., and Clarke, I.C., "Mechanisms and Clinical Significance of Wear Debris-induced Osteolysis," *Clinical Orthopaedics*, Vol. 276, 1992, pp 7–18.

[3] Goldman, M., Gronsky, R., Ranganathan, R., and Pruitt, L., "The Effects of Gamma Radiation Sterilization and Aging on the Structure and Morphology of medical grade Ultra-High-Molecular-Weight Polyethylene", *Polymer*, Vol. 37, 1996, pp. 2909-13.

[4] Premnath , V., Harris, W.H., Jasty, M., and Merrill, E.W., "Gamma Sterilization of UHMWPE Articular Implants: an Analysis of the Oxidation Problem", *Biomaterials*; Vol. 17, 1996, pp. 1741-53.

[5] Li, S., Barrena, E.G., Furman, B.D., Wright, T.M. and Salvati, E.A., "The effect of oxidation and nonconsolidated polyethylene particles on the Wear of Retrieved Acetabular Cups", *5th World Congress in Biomaterials*, 1996, p. 972.

[6] Hardaker, C.S., Fisher, J., Issac, G., Stone, M. and Older, J., "Quantification of the effect of Shelf and *In Vivo* Aging on the *In Vivo* and *In Vitro* Wear Rates of a series of Retrieved Charnley Acetabular Cups", *European Society of Biomaterials*, 2000.

[7] Muratoglu O. K.,Bragdon C.R., O'Connor D.O., Jasty M., and Harris W.H., "A comparison of five different types of Highly Crosslinked UHMWPE: Physical Properties and Wear Behavior", *Transactions of the 45th Annual Meeting of the Orthopedic Research Society*; Anaheim, CA, 1999, p. 77.

[8] Muratoglu, O.K., Bragdon, C.R., O'Connor, D.O., Merrill, E.W., Jasty, M. and Harris, W.H., "Electron beam crosslinking of UHMWPE at room temperature: a candidate bearing material for Total Joint Arthroplasty, *Transactions of the 23rd Society Congress on Biomaterials*, 1997, p. 74.

[9] Muratoglu, O.K., Bragdon, C.R., O'Connor, D.O., Jasty, M. and Harris, W.H, "A novel method of crosslinking ultra-high-molecular-weight polyethylene to Improve Wear, reduce oxidation, and retain mechanical properties", *J. Arthroplasty*, Vol. 16, 2001, pp. 149-160.

[10] McKellop H., Shen F.W., Salovey R., "Extremely low Wear of gamma-crosslinked/remelted UHMWPE Acetabular Cups", *Transactions of the 44th Annual Meeting of the Orthopedic Research Society*; New Orleans, 1998, p. 98.

[11] Jasty M., Bragdon C.R., O'Connor D.O., Muratoglu O. K., Premnath V., Merrill E., and Harris W.H., "Marked improvement in the wear resistance of a new form of UHMWPE in a Physiologic Hip Simulator", Transactions of the 43rd Annual Meeting of the Orthopedic Research Society; San Francisco, CA, 1997, p 785.

[12] Essner A., Polineni V.K., Wang A., Stark C., and Dumbleton J.H., "Effect of Femoral Head surface roughness and crosslinking on the wear of UHMWPE Acetabular Inserts", Transactions *of the 21st Annual Meeting of the Society for Biomaterials*, San Francisco, 1995.

[13] Laurent, M., Yao, J.Q., Bhambri, S.K., Gsell, R.A., Gilbertson, L.N., Swarts, D.F., and Crowninshield, R.D., "High cycle wear of highly crosslinked UHMWPE acetabular liners evaluated in a hip simulator", *46th Annual Meeting of the Orthopedic Research Society*; Orlando, March 12-15, 2000.

[14]Oonishi, H., "Long term clinical results of THR. Clinical results of THR of an alumina head with a crosslinked UHMWPE cup", *Orthopaedic Surgery and Traumatol*, Vol. 38, 1995, pp. 1255-64.

[15]Oonishi, H., Kayoda, Y., and Masuda, S., "Gamma-irradiated cross-linked polyethylene in Total Hip Replacements - analysis of retrieved sockets after long term implantation", *J. Biomedical Materials Research (Applied Biomaterials)*, Vol. 58, 2001, pp. 167-171.

[16]Oonishi, H., Ishimaru, H., and Kato, A., "Effect of cross-linkage by gamma radiation in heavy doses to low wear polyethylene in Total Hip Prostheses", *J Materials Science: Materials in Medicine*, Vol. 7, 1996, pp. 753-763.

[17]Grobbelaar, C.J., du Plessis, T.A., and Marais, F., "The radiation improvement of Polyethylene Prostheses, A preliminary study, *J. Bone and Joint Surgery*, Vol. 60-B, 1978, pp. 370-374.

[18]Wroblewski, B.M., Siney, P.D., Dowson, D., and Collins, S.N., "Prospective clinical and joint simulator studies of a new Total Hip Arthroplasty using alumina ceramic heads and crosslinked cups", *J Bone and Joint Surgery*,; Vol. 78-B, 1996, pp. 280-285.

[19]Sanford, W.M., and Saum, K.A., "Accelerated Oxidative Aging testing of UHMWPE", *Transactions of the 41st Annual Meeting of the Orthopedic Research Society*; Orlando, FL, Feb 13-16, 1995.

[20]Landes, J.D., Bhambri, S.K., and Kang, L., "Fracture Toughness testing of Polymers using small compact specimens and normalization", *J Testing and Evaluation*, Vol. 31, 2003, pp 126-132.

[21]Zhou, Z., Landes, J.D., and Huang, D., "J-R curve calculation with the normalization method for toughened polymers", *Polymer Engineering and Science*, Vol. 34, 1994, pp. 128-134.

[22]Pascaud, R.S. and Evans, W.T., "Critical assessment of methods for evaluating J_{IC} for a medical grade Ultra High Molecular Weight Polyethylene", *Polymer Engineering and Science*, Vol. 37, 1997, pp. 11-17.

[23]Takemori, T.M., and Narisawa, I., "J-integral characterization of impact-modified Polymers", *Advances in Fracture Research*, Pergamon Press, New York, Vol. 4, 1989, pp. 2733-2737.

[24]Lewis G., and Nyman S., "A new method of determining the J-integral fracture toughness of very tough polymers: application to Ultra High Molecular Weight Polyethylene", *Journal of Long-Term Effects of Medical Implants*, Vol. 9, 1999, pp. 289-301.

[25]Rimnac, C.M., Wright, T.M., and Klein, R.W., J-integral measurements of Ultra High Molecular Weight Polyethylene", *Polymer Engineering and Science*, Vol. 28, 1988, pp. 1586-1589.

[26]Baldini, T.H., Rimnac C.M., and Wright, T.M., "The effect of resin type and sterilization method on the static (J integral) Fracture Resistance of UHMW Polyethylene", *Trans. 43rd Annual Meeting, Orthopaedic Research Society*, 1997, p. 780.

[27]Duus, L.C., Walsh, H.A., Gillis, A.M., Noisiez, E., and Li, S., "A comparison of the Toughness of Cross Linked UHMWPE made from different resins, manufacturing methods and sterilization conditions", *Transactions ORS*, Vol. 25, 2000.

Richard S. King,[1] Sarah K. Young,[1] and Keith W. Greer[1]

The Flow Ratio Effect on Oriented, Crosslinked Ultra-High Molecular Weight Polyethylene (UHMWPE)

ABSTRACT: The compression molding process is known to produce UHMWPE components of improved oxidation resistance [1] and quality surface finish. Induction of molecular orientation in non-crosslinked UHMWPE was demonstrated by using a slot drawing process [2]. The objective of this study was to assess the effect of flow ratio on wear and mechanical properties of crosslinked UHMPWE. Pre-irradiated GUR 1020 preforms, corresponding to flow ratios from 1.06 to 1.40, were evaluated in this study. Molecular orientation was shown by Thermal Mechanical Analysis and crossed polarizer microphotographs. Tensile (Type V), double notched Izod and pin on disk wear data were generated. The degree of molecular orientation was correlated with the flow ratio and was reflected by the enhancement of the mechanical properties. Pin on disk wear data show that there was no significant difference in wear resistance between oriented, crosslinked UHMWPE and its machined counterpart.

KEYWORDS: ultra-high molecular weight polyethylene, crosslinking, compression molding, molecular orientation, orthopedic medical devices

Introduction

Consolidation of UHMWPE has been traditionally achieved by ram extrusion and compression molding processes. The latter may be used to produce a slab or a net-shape component. The orthopedic industry routinely machines ram extruded rods or compression molded slabs into a variety of UHMWPE components. The net-shape compression molding process is unique among the manufacturing processes for UHMWPE components. It provides not only a high-quality surface finish but also potential improvement in wear resistance [3] as well.

[1]Principal Scientist, Scientist, and Principal Scientist, respectively, Research Department, DePuy Orthopedics, 700 Orthopedic Drive, Warsaw, IN 46581.

In the last few years, crosslinked UHMWPE implants have been introduced. It has been shown that a crosslinking process followed by a free radical quenching process provides improved wear resistance in hip and knee wear simulation tests [4,5]. However, changes in the UHMWPE structure due to crosslinking have an adverse impact on its mechanical properties, such as tensile elongation, impact resistance [6] and fracture toughness [7].

Molecular orientation has been utilized to improve mechanical properties of a variety of semicrystalline polymers for decades. Linear polyolefins are routinely converted to oriented films or sheets by blow molding and extrusion-tentering processes. Edidin et al used a slot drawing process to prepare oriented UHMWPE [2].

UHMWPE has exceptionally high viscosity in its melt state. After crosslinking, UHMWPE forms a three-dimensional network and its processability deteriorates further. Nevertheless, the feasibility of compression molding pre-irradiated UHMWPE preform has been demonstrated [8]. This process allows for shape forming and free radical quenching to be completed simultaneously.

In this study, our objectives were to assess the effectiveness of compression molding-induced molecular orientation in pre-irradiated UHMWPE preforms and to evaluate the effect of flow ratio on wear and mechanical properties.

Materials and Methods

For processability reason, commercial compression molded GUR 1020 bar was used in this study. Preforms of undersized diameters, in comparison with the mold cavity diameter, were machined from the UHMWPE bar. To facilitate centralization of the undersized puck in the mold, a thin lip of UHMWPE of the diameter of the mold cavity formed the bottom of the preforms (Figure 1L). The ratio of mold cavity diameter to preform diameter was defined as the flow ratio. In this study, flow ratios of 1.06, 1.12, 1.20 and 1.40 were investigated. The preforms were vacuum packaged in aluminum foil bags and gamma irradiated at 50 +5/-0 KGy at Steris Isomedix (Whippany, New Jersey). The gamma-treated packages were stored in a freezer until they were compression molded.

The frozen preforms were defrosted in the vacuum foil packages prior to compression molding. Compression molding was performed in a Wabash vacuum press (Figure 2). A two-stage soak molding cycle was used. A melt soak temperature of 400° – 420° F and a soak duration of twenty to thirty minutes were used. Recrystallization temperature between 260° F and 280° F and recrystallization pressure of 5 000 – 6 000 psi were used with a duration between ten to twenty minutes). The adequacy of the molding cycle was judged by complete filling of the mold without inducing excessive flashing.

There were significant changes in the dimensions of a puck produced by flow molding in comparison with the preform (Figure 1R). The gamma-treated preforms were discolored prior to compression molding. However, the discoloration was eliminated by the molding process. This observation was in agreement with in-house Electron

Paramagnetic Resonance data demonstrating that residual free radicals in flow molded UHMWPE were effectively quenched.

Thermal expansion / contraction data were generated on a TA Instruments 2940 Thermal Mechanical Tester. Tensile test was performed based on ASTM Standard Test Method for Tensile Properties of Plastics (D 638-86) using 400-micron thick type V test specimens and 15.2 mm/min crosshead speed. Double notched Izod impact test was performed based on ASTM Standard Specification for Ultra-High Molecular Weight Polyethylene Powder and Fabricated Form for Surgical Implants (F 648-98). A minimum of five test specimens were used in generating tensile and double notched Izod impact data.

In preparation of tensile test specimens, the horizontal direction is defined as the polymer flow direction while the vertical direction is defined as the compression direction. In double notched Izod impact test specimens, the crack propagation direction is perpendicular to the coupon direction. In other words, for horizontal direction coupons, the impact testing was performed in the vertical direction (Figure 3).

The wear data were generated on an AMTI Ortho-POD wear tester (Figure 4). The Ortho-POD has six stations, multidirectional, programmable motion and load. The test was developed to simulate conditions on the articulating surface of a hip prosthesis. The motion profile was a 5 by 10 mm rectangle with a lift of the pin off the disk once per cycle. The rectangular motion resulted in cross shear of the PE, shown to be necessary to produce clinically relevant wear [9-11], and the lift allowed lubricant to enter the interface.

Pins were machined from cylindrical blocks of PE material, similarly to the Izod impact test specimens (Figure 3). A vertical pin's articular surface was oriented toward the top of the material block similarly, with respect to flow direction, to the articulating surface of tibial inserts made from material processed by this method. Three pins of each material were tested and three were used as unloaded soak controls to account for fluid absorption during the test. They articulated against wrought CoCr disks with starting surface finish values of less than 0.01 μ m Ra, measured with a Form Talysurf Series II contact profilometer.

The Pin-On-Disk test was conducted at 1.3 Hz, resulting in an average linear velocity of 52 mm/sec (the lift consumed approximately 23% of each cycle). The Paul loading curve, with a peak load of 320 N (peak stress ~4.5 MPa) was synchronized with this motion pattern. Ninety percent bovine serum, treated with EDTA and sodium azide, was used as the lubricant. The six test stations were contained within a single reservoir which held 500 mL of serum that was replaced at each data collection interval. The test duration was 2 million cycles with data collection at 500 000 cycle intervals. Gravimetric measurements of the pins were conducted at each data collection interval. Wear rates were calculated by finding the slope of the weight loss versus cycle count for each sample using a least squares fit.
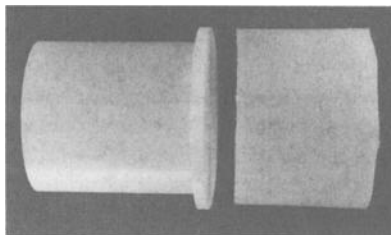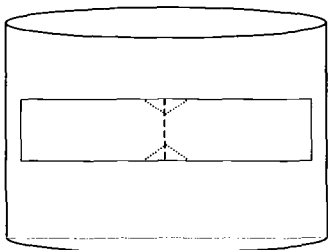
Figure 1 Machined Preform (Left), after Molding (Right)

Figure 2   Wabash Vacuum Press

Horizontal direction coupon (vertical break)   Vertical direction coupon (horizontal break)
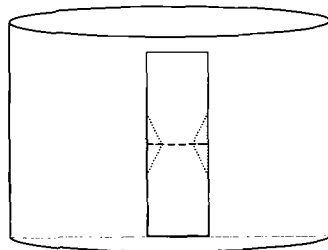

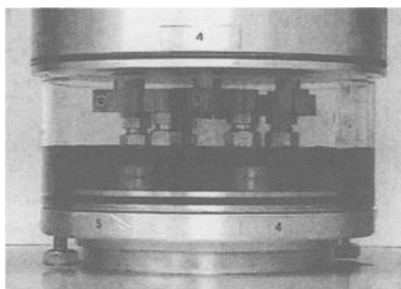Figure 3   Double Notched Izod Impact Test Specimens

Figure 4   Ortho Pin-On-Disk Tester

Results

Biaxial orientation in crosslinked UHMWPE was achieved by a flow molding process during the melt soak stage.   The evidence of molecular orientation in the horizontal direction of molded, crosslinked UHMWPE was demonstrated by a Thermal Mechanical Analysis thermogram (Figure 5).   On melting, the oriented UHMWPE contracted significantly in the horizontal direction of molecular orientation.   In contrast, there was no noticeable shrinkage in the vertical direction, a characteristic of an isotropic material.

The anisotropy of flow-molded, crosslinked UHMWPE was confirmed by intense coloration in the crossed polarizer microphotographs (Figure 6).   In general, there is a direct correlation between the intensity of coloration and the flow ratio.   The higher the flow ratio, the more intense the coloration.   A low level of coloration was observed under crossed polarized light for a non-flow molded UHMWPE.   This is interpreted by the low level of surface orientation induced by film preparation using a microtome.

Table 1 shows that as the degree of molecular orientation (flow ratio) is increased, the mechanical properties are enhanced.   Crosslinked, melt stabilized GUR 1050 material is included for comparison.   Molecular orientation has beneficial effects on tensile strength and impact resistance in the horizontal direction and tensile elongation in the vertical direction.   Nevertheless, high flow ratio has an adverse effect on tensile strength in the direction lacking molecular orientation.

The wear rates for the conventional crosslinked material and the oriented, molded materials are given in Figure 7 with non-crosslinked material included for comparison. The difference in wear rate between the uncrosslinked material and each of the crosslinked materials was statistically significant ($p<0.05$) while the differences between the crosslinked materials were not significant.   The lack of a significant difference between crosslinked materials may be due to the small sample size.
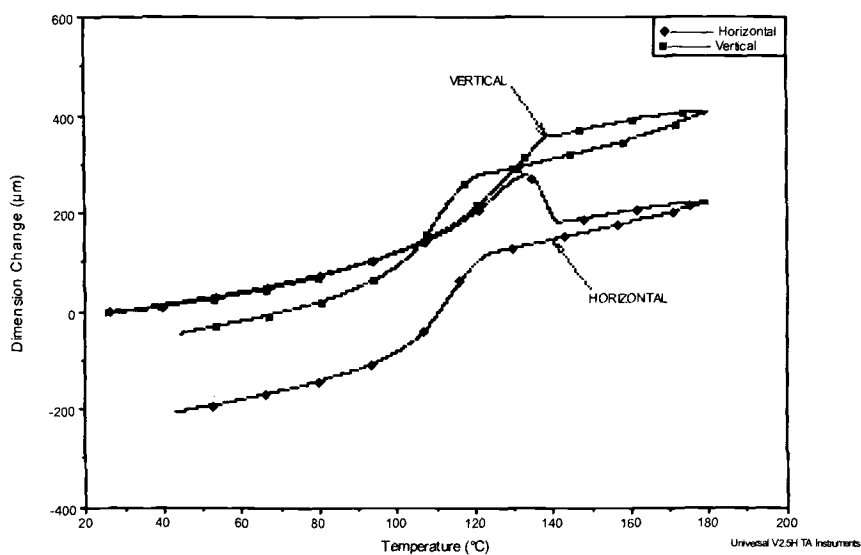
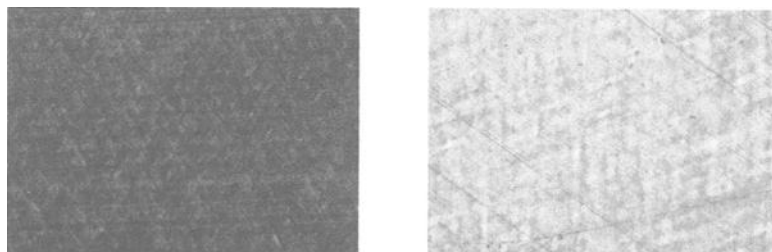Figure 5   Thermal Mechanical Analysis Thermogram of Oriented, Crosslinked
UHMWPE

Figure 6   Crossed Polarizer Microphotographs of Crosslinked UHMWPE
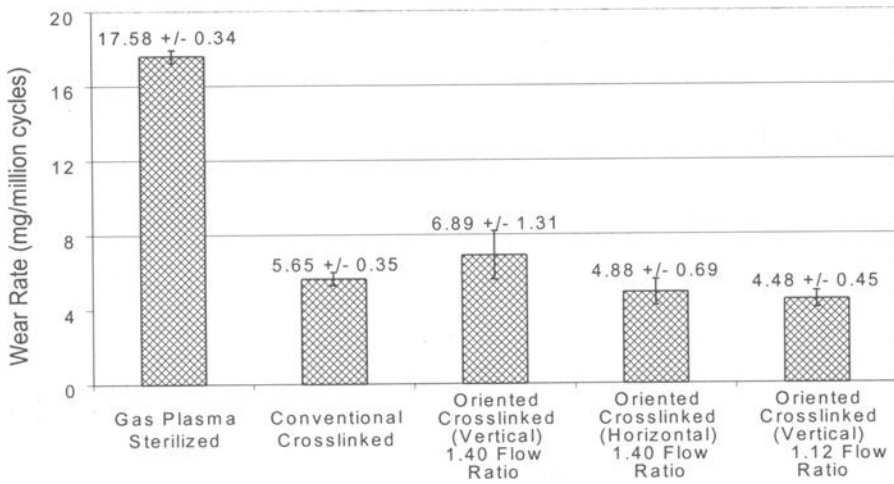showing (Left) Lack of Orientation (Right) with Molecular Orientation

Figure 7   Wear Test Results for Oriented, Crosslinked UHMWPE

	Ultimate Tensile Strength, MPa	Elongation at Break, %	Fracture Energy, MPa	Double Notched Izod Impact, KJ/m²
Conventional	47.2 +/- 6.8	308 +/- 38	71.7 +/- 13.1	71 +/- 1
Flow Ratio 1.06 Horizontal	58.5 +/- 3.0	280 +/- 33	88.9 +/- 11.7	76 +/- 2
Flow Ratio 1.06 Vertical	49.0 +/- 3.2	332 +/- 27	86.9 +/- 9.0	81 +/- 5
Flow Ratio 1.12 Horizontal	55.8 +/- 3.2	283 +/- 18	86.9 +/- 7.6	78 +/- 1
Flow Ratio 1.12 Vertical	47.4 +/- 1.6	435 +/- 25	104.1 +/- 8.3	94 +/- 8
Flow Ratio 1.20 Horizontal	59.8 +/- 4.6	280 +/- 24	90.3 +/- 11.0	74 +/- 2
Flow Ratio 1.20 Vertical	44.6 +/- 2.7	607 +/- 244	108.9 +/- 13.1	110 +/- 13
Flow Ratio 1.40 Horizontal	62.9 +/- 2.1	261 +/- 37	86.2 +/- 12.4	75 +/- 3
Flow Ratio 1.40 Vertical	32.5 +/- 0.9	671 +/- 75	115.1 +/- 14.5	141 +/- 14

Table 1   *Flow Ratio Effects on Mechanical Properties of 50-KGy Crosslinked UHMWPE*

Discussion

Crosslinked UHMWPE deforms and flows under more rigorous conditions than its non-crosslinked counterpart. During the flow molding process, deformation was

completed at the melt soak stage, and molecular orientation was retained by adequate pressurization at the recrystallization soak stage. In comparison with non-crosslinked UHMWPE, the crosslinked structure may facilitate the retention of molecular orientation. Like the compression molding process for pre-irradiated UHMWPE, the flow molding process also induces free radical combination and thus stabilizes the crosslinked UHMWPE.

One molding cycle was used in this study for both low and high flow ratio moldings. The relatively high pressurization during the molding cycle may induce chain scission in UHMWPE, especially in the high flow ratio case. Because the optimal flow ratio lies between 1.12 and 1.20, a reduction in pressurization during flow molding is possible and recommended.

The flow molding process induces biaxial orientation in molded components of crosslinked UHMWPE. The degree of molecular orientation is related to the flow ratio. This is reflected in the extent of enhancement of mechanical properties. Oriented, crosslinked UHMWPE retains the desirable characteristics of conventional crosslinked UHMWPE: wear resistance and oxidation resistance. It also provides improved ductility and tensile strength, which are considered crucial in reducing the incidence of fatigue wear. Based on this study, it may be concluded that oriented, crosslinked UHMWPE is a suitable biomaterial candidate for the demanding articulating surface applications in total joint arthroplasty.

References

[1]   Walsh, H., Gillis, A., Furman, B., and Li, S., "Factors that determine the Oxidation Resistance of Molded 1900: is it the Resin or the Molding," Proceedings, 46th Annual Meeting of Orthopedic Research Society, Vol. 25, 543, 2000.

[2]   Edidin, A., Fisher, J., Dharmastiti, R., Barton, D.C., Doyle, C., and Kurtz, S., "Enhancement of Multiaxial Mechanical Behavior by Slot Drawing of UHMWPE: A Candidate Biomaterial for Total Knee Arthroplasty," Proceedings, 46th Annual Meeting of Orthopedic Research Society, Vol. 23, 563, 2000.

[3]   Furman, B., Lai, S., Li, S., "A Comparison of Knee Simulator Wear Rates Between Directly Molded and Extruded UHMWPE," Proceedings, 27th Annual Meeting of Society for Biomaterials, Vol. 24, 32, 2001.

[4]   McKellop, H., DiMaio, W., Shen, F-W., Lu, B., "Wear of Gamma Radiation Cosslinked PE Acetabular Cups after Aging and Against Roughened Femoral Heads," Proceedings, 45th Annual Meeting of Orthopedic Research Society, Vol. 24, 76, 1999.

[5]   McNulty, D., King, R., Liao, Y-S., Smith, T., Greer, K., Hanes, M., "Wear Rates for a Fixed Bearing Knee System Using Crosslinked UHMWPE Materials," Proceedings, 28th Annual Meeting of Society for Biomaterials, Vol. 25, 382, 2002.

[6]   Greer, K.W., King, R.S., Chan, F.W. "The Effects of Raw Material, Irradiation
        Dose, and Irradiation Source on Crosslinking of UHMWPE," Crosslinked and
        Thermally Treated Ultra-high Molecular Weight Polyethylene for Joint
        Replacements, ASTM STP 1445, S.M. Kurtz, R. Gsell, and J. Martell, Eds.,
        ASTM International, West Conshohocken, PA. 2003
[7]   Duus, L.C., Walsh, H.A., Gillis, A.M., Noisiez, E., Li, S., "The Effect of Resin
        Grade, Manufacturing Method and Crosslinking on the Fracture Toughness of
        Commercially available UHMWPE," Proceedings, 46th Annual Meeting of
        Orthopedic Research Society, Vol. 25, 544, 2000.
[8]   McNulty, D., Smith, T., US Patent 6245276.
[9]   McKellop, H., Campbell, P., Park, S-H., Schmalzried, T., Grigoris, P.,
        Amstutz, H., Sarmiento, A., "The Origin of Submicron Polyethylene Wear
        Debris in Total Hip Arthroplasty," Clin. Orthop., 311, 3-20, 1995.
[10]   Wang, A., Stark, C., Dumbleton, J.H, "Mechanistic and Morphological Origins of
        Ultra-High Molecular Weight Polyethylene Wear Debris in Total Joint
        Replacement Prostheses," J. Eng. Med., 210, 141-155, 1996.
[11]   Saikko, V., Ahlroos, T., "Wear Simulation of UHMWPE for Total Hip
        Replacement with a Multidirectional Motion Pin-on-Disk Device: Effects of
        Counterface Material, Contact Area, and Lubricant," J. of Biomed. Mater. Res.,
        29, 147-154, 2000.

Steven M. Kurtz,[1] Michael Herr,[2] and Avram A. Edidin[3]

The Effect of Specimen Thickness on the Mechanical Behavior of UHMWPE Characterized by the Small Punch Test

---

ABSTRACT: The small punch test has been validated for Ultra High Molecular Weight Polyethylene (UHMWPE) in ASTM F 2183-02. Because only a limited volume of material may be available from retrieved components, reducing the specimen size may increase the number of test specimens. It is unknown if the reduction in specimen thickness will affect the small punch metrics. Therefore, the goal of this study was to examine the relationship between the small punch specimen thickness and the test metrics. Ram extruded GUR 1050 UHMWPE was used to make 5 small punch specimens (diameter 6.35 mm) for each of four different thicknesses: 0.25 mm, 0.33 mm, 0.43 mm, and 0.5 mm. Specimens were tested following ASTM F 2183-02. Power law-based scaling relationships were observed between normalized specimen thickness and the normalized peak load, ultimate load, and work-to-failure of the small punch test ($R^2 = 0.99$, $R^2 = 0.99$, and $R^2 = 0.94$, respectively). A nearly cubic relationship was observed between the normalized specimen thickness and the normalized initial stiffness, which was proportional to the elastic modulus of the UHMWPE, and was predicted based on beam theory ($R^2 = 0.99$). The results of this study provide indication of a reliable means for normalizing small punch test measurements to account for variations in specimen thickness.

KEYWORDS: Small punch test, mechanical properties, ultra-high molecular weight polyethylene, UHMWPE

Introduction

The small punch test, also referred to as the "miniature disk bend test" (MDBT), has its origins during the 1970s from research conducted at MIT for the nuclear power

---

[1] Principal Engineer, Exponent, Inc., and Research Associate Professor, School of Biomedical Engineering, Science, and Health Systems, Drexel University, 3401 Market Street, Suite 300, Philadelphia PA, 19104;

[2] Senior Engineer, Exponent, and Graduate Student, Drexel University, Drexel University, 3401 Market Street, Suite 300, Philadelphia PA, 19104; and

[3] Research Associate Professor, School of Biomedical Engineering, Science, and Health Systems, Drexel University, 3141 Chestnut St, Philadelphia PA, 19104.

industry. [1, 2] Miniature specimen test techniques evolved for metals in the power industry from the need to evaluate mechanical behavior from a small volume of available material. During the past three decades, a mature body of scientific literature has developed regarding the experimental and analytical aspects of the small punch test as related to metallic materials. Over the years, a variety of specimen sizes have been proposed for the small punch test, but most typically the specimen for metallic materials is on the order of 0.1 to 0.5 mm in thickness. [3-5] More recently, the small punch test has been applied to a wide range of polymeric materials, including high-density polyethylene (HDPE), UHMWPE, polyacetal, polytetrafluoroethylene (PTFE), polypropylene (PP), and polymethylmethacrylate (PMMA) bone cements. [6-9]

The specimen size used in the small punch test is highly relevant to the size scale of orthopedic implants and biomaterials. [10] For orthopedic components fabricated from conventional or highly crosslinked UHMWPE, the implant thickness is on the order of 10 mm, but inhomogeneous changes in the physical and chemical properties of UHMWPE are known to occur following gamma irradiation in air. [11-14] In shelf-aged components, the maximum change in physical and mechanical properties evolves below the surface at a depth of 1 to 2 mm. [11, 12] The small punch test has been shown to characterize effectively the inhomogeneous distributions of mechanical behavior in UHMWPE after natural and accelerated aging. [15-17] In addition, the anisotropic behavior of drawn, oriented UHMWPE has been characterized by the small punch test, [18] and the effects of chemical and radiation crosslinking of UHMWPE explored using the technique. [19] Finally, the small punch test has been applied to characterize UHMWPE components after hip simulator testing [7, 20] and after implantation into the human body. [21, 22] Thus, over the past five years, the small punch test has proven to be a versatile tool for evaluating a wide range of UHMWPE materials in as-manufactured, as-sterilized, and as-retrieved conditions. In 2002, ASTM International published the Standard Method for Small Punch Testing of UHMWPE Used in Surgical Implants (ASTM F 2183-02).

The small punch test for UHMWPE consists of an elastic bending phase, a plastic bending phase, and a drawing or stretching phase. During the initial bending phase, the specimen deforms elastically, and the initial stiffness of the specimen (k) is proportional to the elastic modulus (E) of the UHMWPE material[6]

$$E = Ak \tag{1}$$

where the constant of proportionality, A, for the 0.5 mm-thick specimen is found to be 13.5 1/mm.[6] During the plastic bending phase, the plastic deformation is initially localized near the specimen under the center of contact, but as the test progresses, the region of plastic deformation expands until it encompasses the entire thickness of the specimen. For plastic materials, the culmination of the plastic bending phase is accompanied by an initial peak load on the load-displacement curve during the test (Figure 1). During the third phase of the small punch test, the specimen is drawn in biaxial tension around the head of the punch. Tensile rupture of the specimen, characterized by the ultimate load and displacement, is accompanied by an abrupt drop on the load-deflection curve (Figure 1). The work to failure provides a metric related to the toughness of the UHMWPE and has been related to wear performance in hip simulator studies,[21, 22] as well as in retrieval studies.[22]
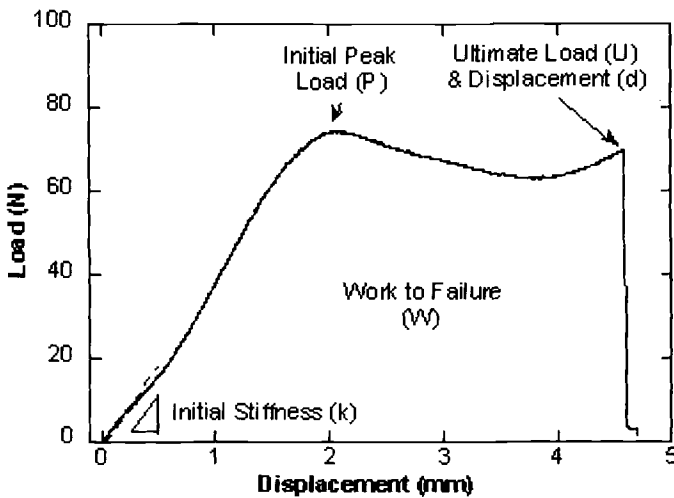
Figure. 1—*Features of the load-displacement curve for UHMWPE, illustrating the initial stiffness (k), initial peak load (P), ultimate displacement (d), ultimate load (U), and work to failure (W, computed as the area under the load-displacement curve).*

For UHMWPE materials, an extensive body of experimental data is available for a specimen thickness of 0.5 mm,[23] and the ASTM standard has been based on a reference specimen thickness of 0.5 mm (0.020 in.). Because only a limited volume of material may be available for characterization in retrieved components, however, reducing the specimen size may be useful to increase the number of possible test specimens from a particular implant. However, it remains to be established how the reduction in specimen thickness would affect the metrics of the small punch test for UHMWPE, complicating comparison with the data published in the literature. As an example of thickness effects, bending theory for a circular-shaped plate of thickness, t, predicts, for plane stress conditions, that [24]

$$E = 12(1 - v^2)\frac{k}{t^3},\qquad(2)$$

where v is the Poisson's ratio and k is the bending stiffness. This suggests that for a generic small punch test apparatus and specimen, the elastic modulus will be proportional to the ratio of the bending stiffness to the specimen thickness-cubed

$$E = a\frac{k}{t^3}\qquad(3)$$

The constant a in the above equation is a function of the geometry for the small punch test apparatus, Poisson's ratio of the specimen material, and coefficient of friction between the punch and the specimen. Theoretical solutions have not yet been established to predict the effect of specimen thickness on the remaining parameters of the small punch test (e.g., initial peak load, ultimate load, ultimate displacement). Consequently, it remains unknown to what extent the metrics of the small punch test reflect fundamental

material properties of UHMWPE versus the geometry. Therefore, the goal of this study was to experimentally determine the relationships between the small punch specimen thickness and the metrics of the small punch test. A secondary goal was to determine the effect of specimen thickness variation, deliberate or random, on the dependability of the results.

Materials and Methods

A lot-controlled, ram-extruded GUR 1050 rod was used to make a total of 20 small punch specimens. The GUR 1050 rod stock used in the present study conformed to applicable national and international standards for implant grade UHMWPE (Standard Specification for Ultra-High-Molecular-Weight Polyethylene Powder and Fabricated Form for Surgical Implants ASTM F 648 and Implants for surgery – Ultra-high molecular weight polyethylene – Part 2: Molded forms ISO 5834-2) used in the manufacture of orthopedic components. The particular lot of UHMWPE selected for the current study was characterized in a previous series of experiments,[25] as summarized in Table 1.

Table 1—*Summary of Physical and Uniaxial Tensile Mechanical Properties for GUR 1050 Extruded Rod used in the Current Study.* [25]

Property	Mean ± SD
Density (g/cc)	0.933 ± 0.001
Degree of Crystallinity (%)[1]	50.4 ± 3.3
Peak Melting Temperature (°C)[1]	136.5 ± 0.8
Elastic Modulus (MPa)[2]	833 ± 9
Yield Stress (MPa)[3]	23.5 ± 0.30
Yield Strain (%)[3]	14.4 ± 0.6
Ultimate Tensile Stress (MPa)[3]	50.2 ± 1.6
Elongation to Failure (%)[3]	421 ± 11

[1]Measured by differential scanning calorimetry. Specimens were heated in nitrogen from 30°C to 170°C at a rate of 10°C/min.
[2]Uniaxial compression testing was conducted at 20°C and at a rate of 0.02 1/s.
[3]Uniaxial tensile testing was conducted at room temperature and at a rate of 30 mm/min.

For the present study, four (4) groups of small punch test specimens were prepared, with specimens from each group having a different thickness: 0.25 mm (0.010"), 0.33 mm (0.013"), 0.43 mm (0.017"), and 0.50 mm (0.020"). For each group, five (5) specimens of each thickness were machined. All the machining operations were performed by a single operator to limit the amount to intraspecimen and interspecimen variability. The 20 specimens were manufactured in random order and each manufacturing operation was completed for all specimens before subsequent operations were executed.   Manufacturing operations were accomplished with precision, temperature-controlled equipment, and specimen thickness measurements were
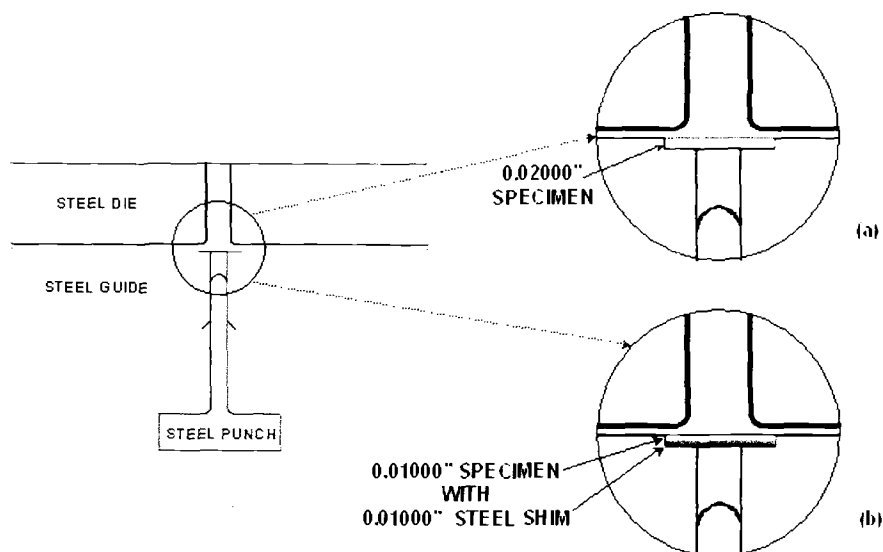
Figure. 2—*Detail of Small Punch Apparatus with 0.50 mm (0.020")thick specimen (a) and with 0.25 mm (0.010")thick specimen with 0.25 mm (0.010") stainless steel shim (b).*

performed immediately after manufacture using calibrated micrometers with 2.0 mm diameter anvils.

Mechanical testing was performed using a closed-loop servo-hydraulic test system (MTS, Model 859 Mini Bionix, Eden Prairie, MN) equipped with an environmental chamber, which was maintained at 21.0°C ± 1°C. Specimens were placed in the environmental chamber for at least 10 minutes prior to testing to achieve thermal equilibrium. All the specimens were tested in random order by one technician following our established protocol that uses indentation with a standard, hemispherical-head punch at a constant displacement rate of 0.5 mm/min.

Specimens were placed in a small punch test die fitted with precision shims that accommodated the various specimen thicknesses (Figure 2). For example, the 0.5-mm specimens were tested in the standard small punch test apparatus following the standard protocol (ASTM F 2183-02). However, the 0.25-mm specimens were tested in the standard small punch test apparatus with a 0.25-mm stainless steel shim placed below it. The shims were custom manufactured from stainless steel by a precision machinist and were sized at 0.08 mm (0.003"), 0.18 mm (0.007"), and 0.25 mm (0.010") to fill the gap in the die that resulted when using the 0.43-mm (0.017"), 0.33-mm (0.013"), 0.25-mm (0.010") thick specimens, respectively.

After assembling the test fixture with a specimen and an appropriately sized shim, the small punch test die was secured to the test system with cap screws and tightened. A thermocouple was inserted into the die to monitor the temperature of the specimen, and a surgical endoscope (Stryker Endoscopy, Santa Clara, CA) with a custom-mounting

fixture was used to view the test specimen in real time. Load and displacement data were collected for all 20 specimens until specimen failure.

Mathematica 4.0 (Wolfram Research, Champaign, IL) was used to post-process the data and to calculate the small punch metrics including initial stiffness, peak load, ultimate load, ultimate displacement, and work-to-failure. Statistical analyses were performed using Statview 5.0 (SAS Institute, Cary, NC) on a personal computer, and regression analyses were used to examine the influence of specimen thickness on the mechanical behavior. Specifically, we sought power law relationships between the normalized thickness and normalized metrics of the small punch test (e.g., initial stiffness, k), of the form

$$\frac{k}{k_0} = (\frac{t}{t_0})^n,$$ (4)

where n is the scaling coefficient, and k_0 and t_0 represent the average initial stiffness and specimen thickness, respectively, in the standard reference condition (corresponding to a specimen thickness of $t_0 = 0.5$ mm, as specified in ASTM F 2183).

The standard relative uncertainty, defined as the estimated standard deviation divided by the mean, was used to quantify the experimental errors associated with the measurements. Relationships between the specimen thickness and standard relative uncertainty were evaluated for each small punch test metric using linear regression.

Results

Systematic changes in the small punch test load-displacement curve were observed as the specimen thickness was decreased (Figure 3, Table 2). A power-law scaling relationship was found to be accurate for predicting the initial stiffness (Figure 4A), peak load (Figure 4B), ultimate load, and work to failure. For initial stiffness, peak load, and ultimate load, the scaling relationship predicted 99% of the variation in the data based on r^2 (Figures 4ABC, Table 2). The scaling relationship for work to failure predicted 94% of the variation in the data (Figure 4D, Table 2). Compared with the other metrics of the small punch test, ultimate displacement was relatively insensitive to changes in specimen thickness (Figure 4E). The scaling coefficients are summarized in Table 3.
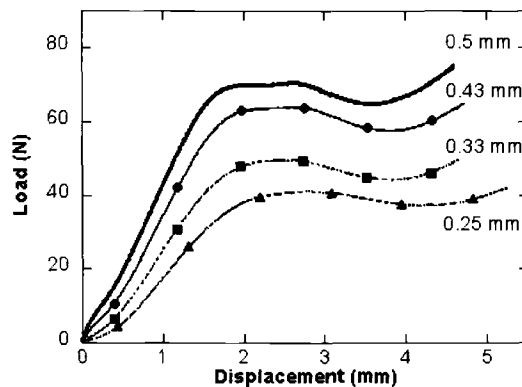

Figure. 3—*Effect of specimen thickness on the small punch test load-displacement curves. Representative curves of each specimen thickness are displayed.*
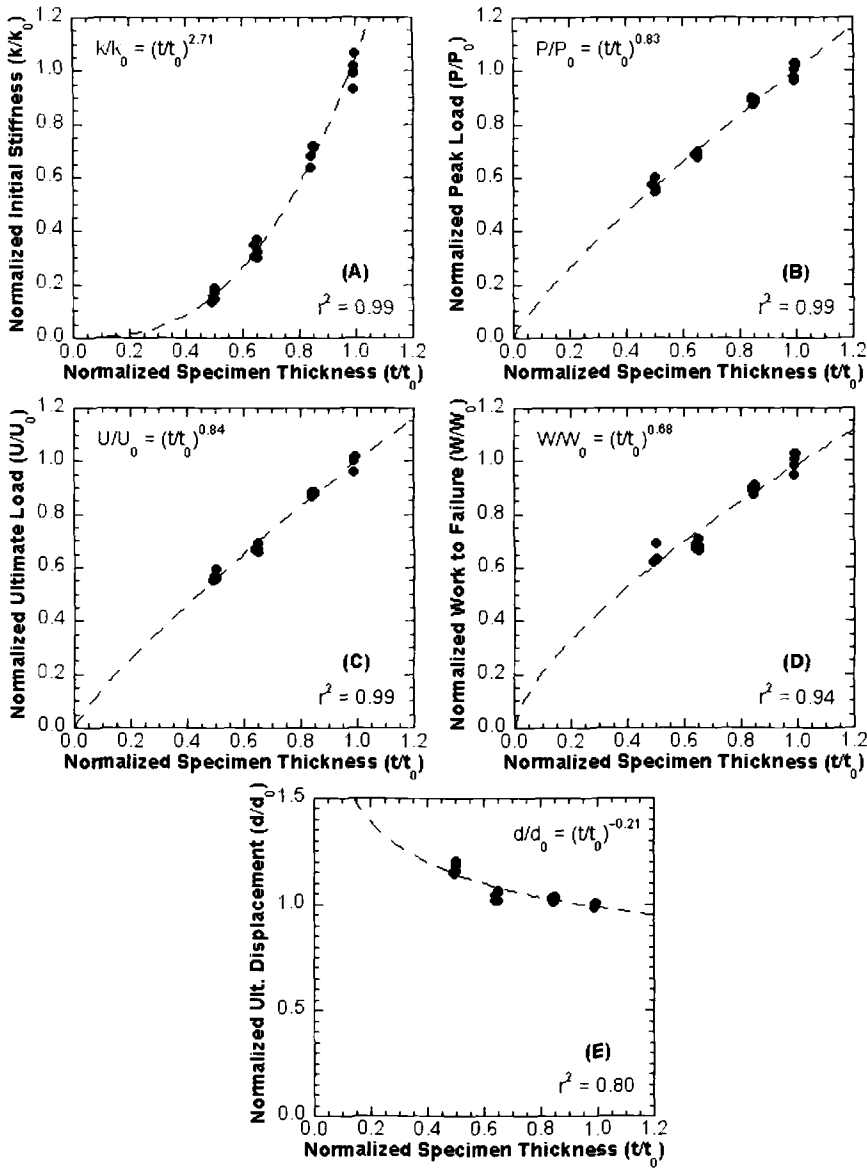
Figure. 4—*Power law scaling relationships for the normalized initial stiffness (A), peak load (B), ultimate load (C), work to failure (D), and ultimate displacement (E) as a function of the normalized specimen thickness. Data are normalized with respect to the average values obtained with a standard-sized (0.50 mm-thickness) specimen.*

Table 2—*Summary of Small Punch Test Results for Varying Thickness (Mean ± SD)*

Specimen Thickness (mm)	Initial Stiffness (N/mm)	Peak Load (N)	Ultimate Load (N)	Ultimate Displacement (mm)	Work to Failure (mJ)
0.25	9.2 ± 1.3	41.4 ± 1.4	42.5 ± 1.3	5.38 ± 0.12	169 ± 8
0.33	19.1 ± 1.7	49.7 ± 0.6	50.1 ± 0.9	4.79 ± 0.10	179 ± 5
0.43	40.3 ± 2.0	64.3 ± 0.7	65.6 ± 0.5	4.72 ± 0.04	235 ± 4
0.50[1]	58.1 ± 2.8	72.4 ±2.2	74.8 ± 1.8	4.60 ± 0.04	263 ± 9

[1]Standard specimen thickness specified in ASTM F 2183

Table 3—*Summary of Thickness Scaling Relationships for the Small Punch Test*

Small Punch Test Metric	Scaling Coefficient,[1] (n)
Initial Stiffness, k	2.71 ± 0.07
Peak Load, P	0.83 ± 0.02
Ultimate Load, U	0.84 ± 0.03
Ultimate Displacement, d	−0.21 ± 0.03
Work to Failure, W	0.68 ± 0.05

[1]Fitted value ± standard error.

Table 4—*Summary of Standard Relative Uncertainty (SD/Mean) for the Small Punch Test Results with Specimens of Varying Thickness*

Specimen Thickness (mm)	Relative Uncertainty, Initial Stiffness (%)	Relative Uncertainty, Peak Load (%)	Relative Uncertainty, Ultimate Load (%)	Relative Uncertainty, Ultimate Displacement (%)	Relative Uncertainty, Work to Failure (%)
0.25	14.1	3.4	3.1	2.2	4.7
0.33	8.9	1.2	1.8	2.1	2.8
0.43	5.0	1.1	0.8	0.9	1.7
0.50[1]	4.8	3.0	2.4	0.9	3.4

[1]Standard specimen thickness specified in ASTM F 2183

The relative uncertainty in the initial stiffness ranged between 4.8 and 14.1% (Table 4). A significant correlation was observed between specimen thickness and the relative uncertainty in the initial stiffness ($p < 0.05$, Table 4). However, for the remainder of the small punch test metrics, no significant relationship was observed with the specimen thickness ($p > 0.05$, Table 4). Overall, the relative uncertainty in the peak load, ultimate load, ultimate displacement, and work to failure ranged between 0.8 and 4.7% (Table 4).

No unusual test behavior was observed during real-time observation of each specimen with the endoscope that was mounted above the test specimens. No indication of

specimen slippage within the die was visible at any time during the tests, and specimen failure appeared to result from a single source of rupture.

Discussion

The approach of previous researchers,[9] as well as the approach adopted for the ASTM method for small punch testing of UHMWPE (F 2183), has been to discard specimens with a thickness that falls outside an acceptable range of values. Discarding nonstandard specimens may be feasible for the evaluation of stock materials, which are in plentiful supply, but when characterizing retrieved UHMWPE components, which are unique and irreplaceable, the discarding of any specimen is undesirable. Our data from the current study indicate that the metrics of the small punch test may be scaled based on the sample thickness, provided that the apparatus is modified such that the initial conformity between the specimen and the die is preserved. The shims employed in the present study were found to be an effective means for maintaining the conformity between the specimen and the die in the small punch test fixture. This suggests, overall, that pragmatically, one might make up a set of spacers, in 0.025 mm increments, from 0.025 to perhaps 0.1 mm, and use them to adjust for sample thickness variations. An alternative but more costly approach would be to machine new specimen holders to accommodate the different sized specimens.

From bending theory, [24] the initial stiffness of the load-displacement curve during the small punch test is predicted to be proportional to t^3 (i.e., corresponding to a scaling coefficient of 3). In the current experiment, we measured that the scaling coefficient for the initial stiffness was roughly 2.7 (Table 3). Thus, the agreement between the initial stiffness data and the expected t^3 relationship is consistent with previous analytical solutions of the miniature disk bend test given in the literature.

Our findings may be used to reliably predict the elastic modulus for specimens of varying thickness using Eq 1, which was validated in previous experiments for UHMWPE.[6] Rearranging Eq 4 and substituting the expression for k_o into Eq 1 for the 0.5 mm thickness, t_0, one obtains

$$E = (At_0^n)\frac{k}{t^n} \qquad (5)$$

Plugging in the values of A from our previous experiment (13.5 1/mm[6]), t_0 (0.5 mm), and n (2.71 from Table 3), we arrive at

$$E = 2.06\frac{k}{t^{2.71}} \qquad (6)$$

for 0.25-mm to 0.5-mm specimens. Since k is predicted to be proportional to $t^{2.71}$ (Eq 4), Eq 6 should produce a measured k-based E that is independent of specimen thickness, t. Indeed, using the specimen thickness and initial stiffness data from our current study, the elastic modulus predicted by Eq 6 is found to be thickness-invariant ($r^2 = 0.00$, Figure 5), with an average ($\pm$SD) value of 792 $\pm$ 65 MPa. This is in close agreement with elastic modulus of 833 $\pm$ 9 MPa (Table 1) measured using large (bulk) specimens prepared from the identical GUR 1050 material.

The experimental uncertainty associated with the elastic modulus predictions is sensitive to specimen thickness (Figure 5, Table 5). Aside from initial stiffness measurements and elastic modulus predictions, the random uncertainties associated with the other metrics of the small punch test (e.g., initial peak load, ultimate load, etc.) appear insensitive to specimen thickness (Table 4). Assuming that the absolute uncertainties in

measuring the stiffness (U_k) and thickness (U_t) are independent and random, the absolute uncertainty in the elastic modulus (U_E) is given by the following expression.[26]

Table 5—*Summary of Absolute Uncertainty in the Elastic Modulus (MPa) with Specimens of Varying Thickness, Estimated by Standard Deviation and Eq 9.*

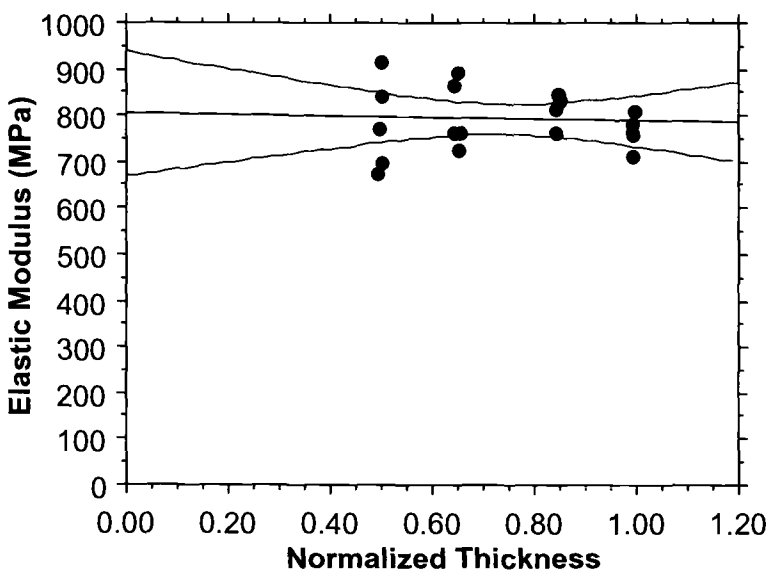| Specimen Thickness (mm)	Standard Deviation (MPa)	Absolute Uncertainty, Equation 9 (MPa)	Absolute Uncertainty, Equation 9 with $U_t = 0$ (MPa)	Absolute Uncertainty, Equation 9 with $U_k = 0$ (MPa)
0.25	100	117	115	22
0.33	73	73	71	17
0.43	34	43	41	13
0.50	36	39	38	11

FIG. 5—*Effect of specimen thickness on elastic modulus predicted by Eq 6.*

$$U_E = \sqrt{\left(\frac{\delta E}{\delta t} U_t\right)^2 + \left(\frac{\delta E}{\delta k} U_k\right)^2} \qquad (7)$$

where, based on Eq 6

$$\frac{\delta E}{\delta t} = -5.58 \frac{k}{t^{3.71}} \text{ and } \frac{\delta E}{\delta k} = \frac{2.06}{t^{2.71}} .$$

(8)

Substituting (8) into (7), we arrive at

$$U_E = \sqrt{\left(5.58 \frac{kU_t}{t^{3.71}}\right)^2 + \left(2.06 \frac{U_k}{t^{2.71}}\right)^2}$$

(9)

We calculated the absolute uncertainty in the elastic modulus as a function of the four sample thicknesses studied using Eq 9 by substituting the mean stiffness (k) and estimated standard deviation (U_k) for each thickness (t) from Table 2. The absolute uncertainty in thickness (U_t) was taken as 0.0025 mm, based on the thickness measurements. As shown in Table 5, Eq 9 provides a reasonable prediction for the absolute uncertainty in the elastic modulus, quantified by the estimated standard deviation. Our analysis further shows that the uncertainty in the stiffness provides the greatest contribution to the overall uncertainty in the elastic modulus (Table 5). Consequently, for the purposes of our uncertainty analysis, we find it reasonable to approximate $U_t = 0$ and thereby simplify Equation (9) as follows

$$U_E = 2.06 \frac{U_k}{t^{2.71}} .$$

(10)

Our analysis therefore indicates that the absolute uncertainty in elastic modulus is proportional to the absolute uncertainty in stiffness measurement and is also a nonlinear function of the specimen thickness.

The usefulness of a test method is greatly enhanced by the ability to generalize the test results across a wide range of specimen and apparatus configurations. When test results are independent of specimen geometry and apparatus, then they are considered to reflect a material property, as opposed to a structural parameter of the test specimen in a particular experiment condition. For example, the yield stress in a uniaxial tensile test is considered a material property, whereas the wear rate of UHMWPE in a hip simulator is a test parameter that is dependent upon a wide range of test conditions. Thus, both material and structural types of tests can provide useful information about the behavior of UHMWPE for preclinical evaluation as well as research purposes. Most of the research conducted on small punch testing of UHMWPE has focused on evaluating different materials using a single apparatus design, described in the ASTM standard F 2183, for a fixed specimen geometry and testing rate.[23] On one hand, this has resulted in an extensive body of test data for a wide range of conventional, highly crosslinked, and retrieved UHMWPE samples. However, methodological questions related to changes in the standard small punch testing configuration have not been addressed in previous studies.

As the results of our study have shown, the metrics of the small punch test for UHMWPE can be generalized across a range of specimen sizes. Due to the complexity of the loading mechanisms in the small punch test, which incorporate bending as well as biaxial deformation, a finite element analysis incorporating a validated constitutive model is necessary to relate the experimental conditions of the test (e.g., applied displacement and resultant load) to predict localized stresses and strains in the UHMWPE specimen. Research is currently underway at our institution to develop improved methods for determining the constitutive behavior of UHMWPE based on interpretation of the measured load-displacement curve from the small punch test.[27] Until improved methods for interpreting the small punch test results are developed, the scaling relationships

derived for the present study provide an initial basis for exploring changes in test configuration on the metrics of the small punch test for UHMWPE. Generalized determination of the potential dependence of the power law coefficients on material will require the rigorous analytical interpretation currently being researched.

Acknowledgement

References

1. Manahan, M. P., Argon, A. S. and Harling, O. K., "The Development of a Miniaturized Disk Bend Test for the Determination of Postirradiation Mechanical Properties," *Journal of Nuclear Materials*, Vol. 104, 1981, pp. 1545-1550.
2. Manahan, M. P., "The Development of a Miniaturized Disk Bend Test for the Determination of Post-Irradiation Mechanical Behavior.," Ph.D. Dissertation. Massachussetts Institute of Technology, Boston, MA, 1982.
3. Mao, X., Saito, M. and Takahashi, H., "Small Punch Test to Predict Ductile Fracture Toughness JIc and Brittle Fracture Toughness KIc," *Scripta Metallurgica et Materialia*, Vol. 25, 1987, pp. 2481-2485.
4. Mao, X., Shoji, T. and Takahashi, H., "Characterization of fracture behavior in small punch test by combined recrystallization-etch method and rigid plastic analysis," *Journal of Testing and Evaluation*, Vol. 15, 1987, pp. 30-37.
5. Foulds, J. R., Woytowitz, P. J., Parnell, T. K. and Jewett, C. W., "Fracture Toughness by Small Punch Testing," *Journal of Testing and Evaluation*, Vol. 23, 1995, pp. 3-10.
6. Kurtz, S. M., Foulds, J. R., Jewett, C. W., Srivastav, S. and Edidin, A. A., "Validation of a Small Punch Testing Technique to Characterize the Mechanical Behavior of Ultra-high Molecular Weight Polyethylene," *Biomaterials*, Vol. 18, 1997, pp. 1659-1663.
7. Edidin, A. A. and Kurtz, S. M., "The Influence of Mechanical Behavior on the Wear of Four Clinically Relevant Polymeric Biomaterials in a Hip Simulator," *Journal of Arthroplasty*, Vol. 15, 2000, pp. 321-331.
8. Giddings, V. L., Kurtz, S. M., Jewett, C. W., Foulds, J. R. and Edidin, A. A., "A Small Punch Test technique for Characterizing the Elastic Modulus and Fracture Behavior of PMMA Bone Cement Used in Total Joint Replacement," *Biomaterials*, Vol. 22, 2001, pp. 1875-1881.
9. Arnold, J. C. and Keeble, J. M., "The Use of Miniature Disc Bend Tests with Plastic Materials," *Polymer Testing*, Vol. 17, 1998, pp. 597-611.
10. Kurtz, S. M., Jewett, C. W., Foulds, J. R. and Edidin, A. A., "A Miniature-Specimen Mechanical Testing Technique Scaled to the Articulating Surface of Polyethylene Components for Total Joint Arthroplasty," *Journal Biomedical Materials Research (Applied Biomaterials)*, Vol. 48, 1999, pp. 75-81.
11. Bostrom, M. P., Bennett, A. P., Rimnac, C. M. and Wright, T. M., "The Natural History of Ultra High Molecular Weight Polyethylene," *Clinical Orthopedics*, Vol. 309, 1994, pp. 20-8.

12. Rimnac, C. M., Klein, R. W., Betts, F. and Wright, T. M., "Post-irradiation Aging of Ultra-high Molecular Weight Polyethylene," *Journal of Bone & Joint Surgery*, Vol. 76A, 1994, pp. 1052-1056.

13. Eyerer, P. and Ke, Y. C., "Property Changes of UHMW Polyethylene Hip Cup Endoprostheses During Implantation," *Journal of Biomedical Materials Research*, Vol. 18, 1984, pp. 1137-51.

14. Roe, R. J., Grood, E. S., Shastri, R., Gosselin, C. A. and Noyes, F. R., "Effect of Radiation Sterilization and Aging on Ultrahigh Molecular Weight Polyethylene," *Journal of Biomedical Materials Research*, Vol. 15, 1981, pp. 209-30.

15. Edidin, A. A., Villarraga, M. L., Herr, M. P., Muth, J., Yau, S. S. and Kurtz, S. M., "Accelerated Aging Studies of UHMWPE. II. Virgin UHMWPE is Not Immune to Oxidative Degradation," *Journal of Biomedical Materials Research*, Vol. 61, 2002, pp. 323-9.

16. Edidin, A. A., Herr, M. P., Villarraga, M. L., Muth, J., Yau, S. S. and Kurtz, S. M., "Accelerated Aging Studies of UHMWPE. I. Effect of Resin, Processing, and Radiation Environment on Resistance to Mechanical Degradation," *Journal of Biomedical Materials Research*, Vol. 61, 2002, pp. 312-22.

17. Edidin, A. A., Jewett, C. W., Kwarteng, K., Kalinowski, A. and Kurtz, S. M., "Degradation of Mechanical Behavior in UHMWPE After Natural and Accelerated Aging," *Biomaterials*, Vol. 21, 2000, pp. 1451-1460.

18. Dharmastiti, R., Barton, D. C., Fisher, J., Edidin, A. and Kurtz, S., "The Wear of Oriented UHMWPE Under Isotropically Rough and Scratched Counterface Test Conditions," *Biomedical Materials and Engineering*, Vol. 11, 2001, pp. 241-56.

19. Kurtz, S. M., Pruitt, L. A., Jewett, C. W., Foulds, J. R. and Edidin, A. A., "Radiation and Peroxide Crosslinking Promote Strain Hardening Behavior and Molecular Alignment in UHMWPE During Multiaxial Loading Conditions," *Biomaterials*, Vol. 20, 1999, pp. 1449-1462.

20. Edidin, A. A., Pruitt, L., Jewett, C. W., Crane, D. J., Roberts, D. and Kurtz, S. M., "Plasticity-induced Damage Layer is a Precursor to Wear in Radiation- cross-linked UHMWPE Acetabular Components for Total Hip Replacement. Ultra-high-molecular-weight Polyethylene," *Journal of Arthroplasty*, Vol. 14, 1999, pp. 616-27.

21. Edidin, A. A., Rimnac, C. M., Goldberg, V. and Kurtz, S. M., "Mechanical Behavior, Wear Surface Morphology, and Clinical Performance of UHMWPE Acetabular Components After 10 Years of Implantation," *Wear*, Vol. 250, 2001, pp. 152-158.

22. Kurtz, S. M., Rimnac, C. M., Pruitt, L., Jewett, C. W., Goldberg, V. and Edidin, A. A., "The Relationship Between the Clinical Performance and Large Deformation Mechanical Behavior of Retrieved UHMWPE Tibial Inserts," *Biomaterials*, Vol. 21, 2000, pp. 283-91.

23. Edidin, A. A. and Kurtz, S. M., "Development and Validation of the Small Punch Test for UHMWPE Used in Total Joint Replacements," *Journal/Functional Biomaterials*, 2001, pp. 1-40.

24. Hoffmann, M. and Birringer, R., "Quantitative Measurements of Young's Modulus Using the Miniaturized Disk-bend Test," *Materials Science and Engineering*, Vol. A202, 1995, pp. 18-25.

25. Kurtz, S. M., Villarraga, M. L., Herr, M. P., Bergström, J. S., Rimnac, C. M. and Edidin, A. A., "Thermomechanical Behavior of Virgin and Highly Crosslinked Ultra-high Molecular Weight Polyethylene Used in Total Joint Replacements," *Biomaterials*, Vol. In Press, 2002, pp.

26. Taylor, J. R., "An Introduction to Error Analysis: The Study of Uncertainties in Physical Measurements," 1997, pp. 45-92.

27. Bergström, J. S. and Boyce, M. C., "Constitutive Modelling of the Large Strain Time-Dependent Behavior of Elastomers," *Journal of Mechanical and Physical Solids*, Vol. 46, 1998, pp. 931-954.

In-Vitro Testing

Keith W. Greer,[1] Richard S. King,[1] and Frank W. Chan[1]

The Effects of Raw Material, Irradiation Dose, and Irradiation Source on Crosslinking of UHMWPE

ABSTRACT: Four Ultra-High Molecular Weight Polyethylene (UHMWPE) materials were evaluated after various irradiation crosslinking processes to determine the effects of the materials and processes on their properties for orthopaedic applications. The materials and processes included two molecular weight materials (GUR 1020 and GUR 1050), two fabricated forms (ram extruded bar and compression-molded sheet), two irradiation sources (gamma and e-beam) and multiple irradiation doses ranging from 30-120 kGy. Increasing irradiation dose led to increased crosslinking, decreased wear, and decreased toughness. The molecular weight of the starting material and the irradiation source both had effects on the final properties while the fabricated form did not. Wear testing of selected groups indicated that there was a direct correlation with irradiation dose but not with the crosslink density (as calculated from the swell ratio).

KEYWORDS: ultra-high molecular weight polyethylene, gamma irradiation, e-beam irradiation, crosslinking, Fourier-Transform infrared analysis, density, tensile properties, Izod impact, wear testing, orthopaedic medical devices, total joint replacement

Introduction

"Highly crosslinked" Ultra-High Molecular Weight Polyethylene (UHMWPE) is currently being sold for total hip and total knee replacement bearings with the expectation of reduced clinical wear and thus improved clinical outcomes. The crosslinking of these materials has been achieved by either gamma or e-beam irradiation with increased irradiation dose leading to increased crosslinking and reduced wear [1,2]. However, increased crosslinking also reduces mechanical properties, particularly toughness, thus there is a trade-off between wear and mechanical properties [1-5]. Much of the debate in the orthopaedic community has been about the proper level of crosslinking for a given application that will reduce wear while maintaining mechanical properties necessary for proper *in vivo* function.

---

[1]Principal Scientist, Principal Scientist, and Team Leader, respectively, Research Department, DePuy Orthopaedics, 700 Orthopaedic Drive, Warsaw, IN, 46581.

Currently manufacturers are using different raw materials, different irradiation processes, and different irradiation doses to produce these "highly crosslinked" UHMWPE products [1-2, 6-9]. It was the objective of this study to determine the effects of irradiation source (gamma vs. e-beam) and irradiation dose on the mechanical, physical, and wear properties of UHMWPE materials produced from two molecular weight resins (GUR 1020 and GUR 1050) and by two fabrication methods (ram extrusion and compression molding).

Materials and Methods

Materials

The four materials chosen for this investigation were GUR 1020 compression-molded sheet (CMS) from Perplas (Bacup, UK), GUR 1020 ram extruded bar (REB) from Perplas, GUR 1050 CMS from Poly Hi (Fort Wayne, IN), and GUR 1050 REB from Poly Hi. The 1020 material is reported to have an average molecular weight of 3-4 million while the 1050 is reported to have a molecular weight of 5-6 million. A single lot of each material was used throughout the study.

Gamma irradiated groups were produced by starting with 76 mm diameter bars of each of the four materials. For the two molded sheet materials, the bars were machined from the molded sheet. Five bars of each material (0.76 m long) were vacuum packaged in a foil bag and subjected to gamma irradiation (Steris Isomedix, Whippany, NJ) in five groups (four materials per group). The nominal irradiation doses were 40, 50, 60, 80, and 120 kGy.

The e-beam irradiated groups were produced by starting with blocks that were 64 mm by 152 mm by 40 mm thick. The blocks were vacuum packaged in foil and subjected to e-beam irradiation using a 10 MeV source (Titan Scan Systems, San Diego, CA). In order to obtain an even irradiation dose through each bar, the blocks were first irradiated from one side and then irradiated from the second side in a second pass through the e-beam. The 1050 REB and 1050 CMS materials were irradiated at nominal doses of 30, 50, 60, 80, and 120 kGy. The 1020 REB and 1020 CMS materials were irradiated only at 60 kGy.

After irradiation, all bars and blocks were heated in argon to a temperature of 155° C and held for 24 hours to quench free radicals by crosslinking, then held for 24 hours at 120° C and cooled to room temperature. As-received samples of all four materials were also evaluated for comparison.

Mechanical Testing

Tensile and impact tests were conducted to evaluate the mechanical properties and toughness of all the groups. Tensile testing was performed on five samples per group per ASTM Test Method for Tensile Properties of Plastics (D 638) using a Type 4 tensile bar and a crosshead speed of 5.08 cm/min. Double-notched Izod impact tests were performed on five samples per group per ASTM Specification for Ultra-High-Molecular-Weight Polyethylene Powder and Fabricated Form for Surgical Implants (F 648).

Physical Properties

The physical properties evaluated included density, swell ratio, and trans-vinylene index (TVI). Density was evaluated on at least three samples from each material using a density gradient column per ASTM Test Method for Density of Plastics by the Density-Gradient Technique (D 1505). The swell ratio was evaluated on at least two samples per group using an SRT-1™ swell ratio tester (Cambridge Polymer Group, Somerville, MA) at 130° C. Samples were 6 mm diameter by 6 mm high cylinders. The swell ratio was subsequently converted to crosslink density [10]. A Nicolet Magna 550 Fourier Transform Infrared (FTIR) spectrometer (Thermo Nicolet, Madison, WI) with a Spectra Tech IR-Plan microscope (Thermo Spectra-Tech, Shelton, CT) and a 50 μm by 200 μm aperture was used for the TVI evaluation. Cross-sections were taken from each of the bars or blocks. From these, 200 μm thin sections were microtomed. Each thin section was then evaluated in 1 mm steps to a depth of either 30 mm (e-beam samples) or 38 mm (gamma samples) starting at the outside edge to determine if there was a trans-vinylene gradient. The TVI was calculated by taking the area under the trans-vinyl vibration at 964 cm^{-1} and dividing it by the area under the 1900 cm^{-1} peak as has been reported in the literature [11]. The average TVI was calculated by averaging the individual TVI measurements through the depth of each sample.

Wear Properties

Hip simulator wear testing was performed on seven of the gamma-irradiated groups to determine if the wear rate was a function of the irradiation dose or the swell ratio (an indication of crosslink density). These seven groups were chosen to include all four materials at 80 kGy, the 1050 CMS material at 40 kGy which had the same swell ratio/crosslink density as the 1020 REB at 80 kGy, a second material at 40 kGy (1020 REB), and a 1020 material with an intermediate dose and swell ratio/crosslink density (1020 CMS at 60 kGy). Either two or three samples per group were tested.

Wear testing was carried out for eight million cycles using an eight-station hip simulator (MTS, Eden Prairie, MN). Test specimens were mounted in the inverted orientation (cup below the head) at 23° to the horizontal plane and rotated about a vertical axis. A load simulating normal gait was applied axially through the acetabular cup base assembly with a peak load of 2000 N [12]. Both the load and rotation were synchronized at approximately 0.95 Hz. The lubricant was 90% bovine serum (HyClone Laboratories, Inc., Logan, UT), with 20 mM EDTA and 0.2% NaN_3 added. The serum was changed every quarter million cycles and gravimetric wear was measured every half million cycles with correction for fluid absorption from soak controls. Wear rates were determined by linear regression and compared using a non-parametric ANOVA.

Results

Irradiation Doses

The actual irradiation doses received by the groups are shown in Table 1. The average dose for the gamma irradiated groups came from the average of ten dosimeters

per bar. The average dose for the e-beam groups was based on the average of the maximum (center of block) and minimum (front of block) doses as calculated from 3-6 dosimeters and a correlation run on a block where dosimeters were placed both on the front and in the middle of the block. The correlation run showed that the inside of a block would receive a 30% higher dose than the front of the block.

Table 1-*Average Irradiation Doses and Dose Ranges*

	Gamma Irradiation		e-beam Irradiation	
Nominal Dose (kGy)	Average Dose (kGy)	Dose Range (kGy)	Average Dose (kGy)	Dose Range (kGy)
30	NA	NA	30	26-34
40	43	40-45	NA	NA
50	51	49-53	50	44-57
60	63	60-66	61	53-69
80	83	78-88	81	70-92
120	124	120-130	121	104-137

Tensile Properties

Even though the yield strength and ultimate tensile strength of the as-received materials were decreased by crosslinking, all groups maintained values above the ASTM F 648 minimums of 19 and 27 MPa respectively (Table 2).

The effects of irradiation dose on the elongation to break are shown in Figure 1 for the gamma materials and in Figure 2 for the e-beam materials. While all four materials showed decreases in elongation with increasing irradiation dose, the two lower molecular weight 1020 materials (CMS and REB) have similar elongation at the same dose, and for gamma irradiation they have about 15% higher elongation for all doses compared to both 1050 materials (CMS and REB). This difference was significant (student's t-test, $p<0.05$). For equal materials and doses, the e-beam process gave higher elongation than the gamma process, although there was more variation for most groups. All the tensile data are given in Table 2.
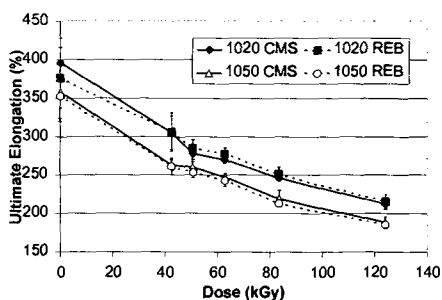

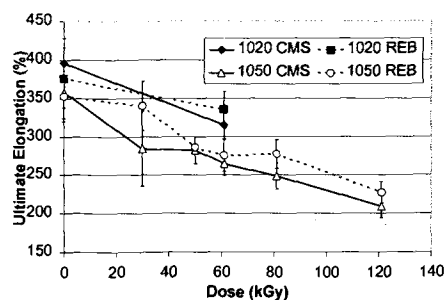Figure 1-*Ultimate elongation of gamma irradiated materials*

Figure 2-*Ultimate elongation of e-beam irradiated materials*

Table 2-*Tensile Properties*

Nominal Dose (kGy)	Irradiation Source	Material	Form	Yield Strength (MPa)		UTS (MPa)		Ultimate Elongation (%)	
				Avg.	StDev	Avg.	StDev	Avg.	StDev
0	None	1020	CMS	23.6	0.1	42.1	2.7	396	20
			REB	23.6	0.1	37.2	6.4	376	52
		1050	CMS	22.5	0.1	43.8	3.5	358	20
			REB	22.3	0.4	40.0	5.0	353	33
30	e-beam	1050	CMS	20.4	0.1	36.7	5.8	284	49
			REB	21.0	0.1	43.6	6.8	340	32
40	gamma	1020	CMS	21.4	0.1	38.9	4.2	305	22
			REB	21.3	0.2	36.5	4.1	306	25
		1050	CMS	20.0	0.2	32.4	1.5	263	7
			REB	20.8	0.3	32.5	1.1	261	11
50	gamma	1020	CMS	21.1	0.2	35.1	2.6	278	11
			REB	21.4	0.2	33.4	2.3	285	11
	e-beam	1050	CMS	20.4	0.1	37.6	3.3	282	18
			REB	21.1	0.1	35.4	1.0	286	3
	gamma	1050	CMS	20.2	0.3	34.5	2.1	260	10
			REB	22.3	0.1	33.5	1.0	253	7
60	e-beam	1020	CMS	21.3	0.0	41.6	3.7	315	18
			REB	23.5	0.2	45.3	5.0	335	24
	gamma	1020	CMS	23.1	0.1	36.7	0.7	270	5
			REB	23.1	0.2	35.4	0.8	278	8
	e-beam	1050	CMS	20.4	0.1	36.9	3.8	264	15
			REB	21.2	0.2	39.5	3.1	275	21
	gamma	1050	CMS	20.1	0.1	33.2	1.2	247	5
			REB	20.6	0.1	31.6	1.0	243	8
80	gamma	1020	CMS	22.9	0.0	35.5	0.4	246	3
			REB	23.2	0.1	34.0	1.2	251	9
	e-beam	1050	CMS	20.5	0.1	35.6	3.2	248	17
			REB	22.8	0.2	42.5	5.1	277	19
	gamma	1050	CMS	20.3	0.1	32.3	1.4	219	11
			REB	20.8	0.1	30.2	0.6	213	5
120	gamma	1020	CMS	21.4	0.1	33.3	1.7	212	7
			REB	21.3	0.3	31.1	2.1	215	9
	e-beam	1050	CMS	20.6	0.2	34.1	4.0	209	15
			REB	21.2	0.2	36.6	3.2	227	14
	gamma	1050	CMS	20.0	0.1	30.2	1.6	188	7
			REB	21.0	0.1	29.2	1.0	185	5

Impact Properties

The effects of irradiation dose on impact strength are shown in Figures 3 and 4 for the gamma and e-beam materials respectively. The lower molecular weight 1020 material generally showed higher toughness at the same dose compared to the higher molecular weight 1050 material, although the differences were small from 60-80 kGy for the gamma materials. The fabrication method (i.e. REB vs. CMS) had little effect on the impact strength for either 1020 or 1050. Under the same conditions, the e-beam process showed higher impact strength than the gamma process (except for 1050 REB at 60 kGy). The differences were significant ($p < 0.05$) for 1050 REB and for 1050 CMS at all doses except 60 kGy. The impact data are included in Table 3.
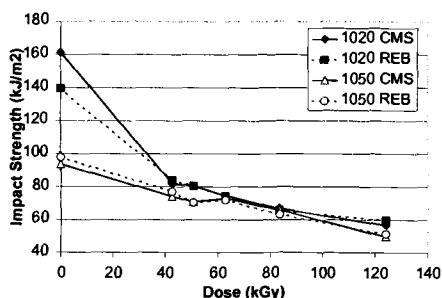
Figure 3-*Impact strength of gamma irradiated materials*
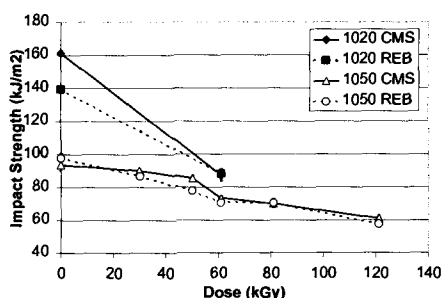
Figure 4-*Impact strength of e-beam irradiated materials*

Density Evaluation

The density values as a function of dose are shown in Figures 5 and 6 for gamma and e-beam materials, respectively. The as-received materials have the highest densities while doses of 30-60 kGy produce the lowest densities for all materials with densities slightly increasing at the higher doses (80-120 kGy). The lower molecular weight 1020 materials have the higher densities at all doses.
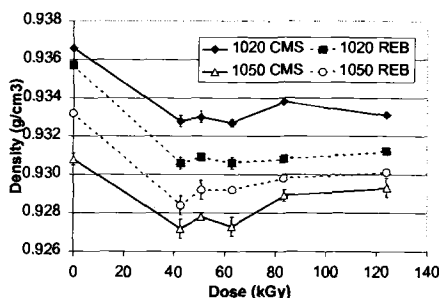

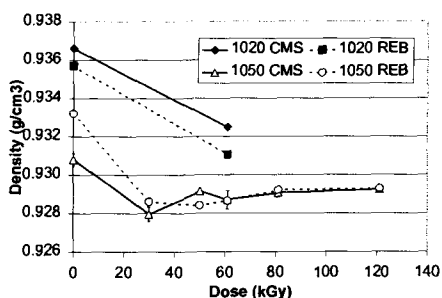Figure 5-*Density values for gamma irradiated materials*

Figure 6-*Density values for e-beam irradiated materials*

Table 3-*Impact and Swelling Properties*

Nominal Dose (kGy)	Irradiation Source	Material	Form	Impact (kJ/m^2)		Swell Ratio		Apparent XLD	
				Avg.	StDev	Avg.	StDev	Avg.	StDev
0	None	1020	CMS	161.3	1.9	NA	NA	NA	NA
			REB	139.5	1.4	NA	NA	NA	NA
		1050	CMS	93.7	3.4	NA	NA	NA	NA
			REB	97.9	2.9	NA	NA	NA	NA
30	e-beam	1050	CMS	90.1	1.2	3.38	0.00	0.130	0.000
			REB	86.8	1.0	3.41	0.03	0.129	0.002
40	gamma	1020	CMS	81.8	0.8	3.85	0.26	0.105	0.011
			REB	84.0	0.3	3.83	0.12	0.106	0.006
		1050	CMS	74.1	1.1	3.28	0.04	0.137	0.003
			REB	77.0	0.4	3.80	0.31	0.108	0.013
50	gamma	1020	CMS	80.5	1.4	3.77	0.08	0.109	0.004
			REB	80.4	1.5	3.88	0.13	0.105	0.007
	e-beam	1050	CMS	85.4	1.6	3.07	0.12	0.154	0.010
			REB	77.7	2.2	3.18	0.01	0.144	0.001
	gamma	1050	CMS	70.8	1.4	3.31	0.06	0.135	0.005
			REB	70.4	0.5	3.39	0.10	0.130	0.006
60	e-beam	1020	CMS	87.4	3.6	3.27	0.02	0.138	0.001
			REB	88.1	3.2	3.28	0.05	0.138	0.004
	gamma	1020	CMS	74.6	2.0	3.37	0.01	0.131	0.000
			REB	74.3	1.0	3.52	0.02	0.122	0.001
	e-beam	1050	CMS	73.3	1.2	2.88	0.04	0.172	0.004
			REB	70.6	1.5	2.91	0.18	0.170	0.019
	gamma	1050	CMS	73.0	1.6	3.02	0.06	0.158	0.006
			REB	72.0	0.4	3.33	0.05	0.134	0.004
80	gamma	1020	CMS	66.6	2.4	3.10	0.05	0.152	0.005
			REB	65.7	0.9	3.28	0.03	0.137	0.003
	e-beam	1050	CMS	70.1	2.9	2.77	0.23	0.189	0.023
			REB	70.4	2.6	2.81	0.05	0.181	0.006
	gamma	1050	CMS	65.6	0.5	2.94	0.05	0.166	0.004
			REB	63.1	1.2	3.01	0.04	0.160	0.004
120	gamma	1020	CMS	56.7	0.2	3.08	0.29	0.156	0.024
			REB	59.6	1.2	3.17	0.19	0.146	0.015
	e-beam	1050	CMS	60.9	2.0	2.47	0.03	0.234	0.005
			REB	57.5	2.1	2.58	0.00	0.214	0.001
	gamma	1050	CMS	49.9	1.7	2.65	0.01	0.202	0.001
			REB	51.4	0.6	2.79	0.03	0.183	0.004

Swell Ratio/Crosslink Density

The swell ratio, which is expected to be an indicator of crosslink density (XLD), is shown as a function of dose for the gamma materials in Figure 7 and for the e-beam materials in Figure 8. In general, increasing irradiation dose led to decreased swell ratio for all materials. The 1050 materials have a lower swell ratio than the 1020 materials for almost all doses while for the same dose and material, the e-beam materials have a lower swell ratio. This appears to indicate that the 1050 materials have higher crosslink densities than the 1020 materials at the same doses; however, the swell ratio may also be affected by chain entanglements, which are directly related to molecular weight [*13*]. If so, the 1050 materials, with their higher molecular weight, will have more entanglements that may produce a lower swell ratio than 1020 materials, even if their actual crosslink density is the same. Because of the possible contribution of entanglements to the swell ratio, the crosslink density was not plotted as a function of dose. However, the crosslink density was calculated and labeled as apparent XLD and is given in Table 3.
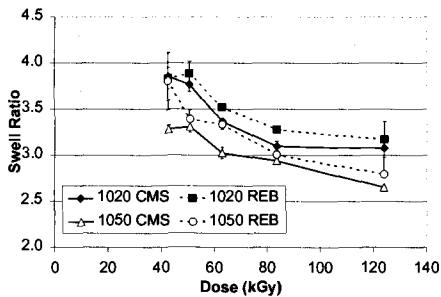
Figure 7-*Swell Ratio for gamma irradiated materials*
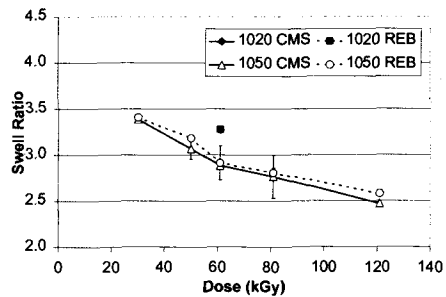
Figure 8-*Swell Ratio for e-beam irradiated materials*

Trans-Vinylene Index

The effect of irradiation dose on the trans-vinylene index (TVI) is shown in Figure 9 for the gamma materials and in Figure 10 for the e-beam materials.
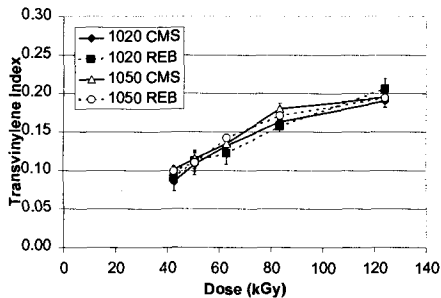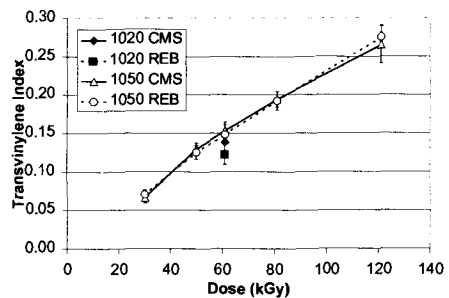

Figure 9-*TVI for gamma irradiated materials*

Figure 10-*TVI for e-beam irradiated materials*

The gamma materials show similar levels of trans-vinylene formation for both 1020 and both 1050 materials at all doses, although in many cases the differences are statistically significant. When compared to the gamma 1050 materials, the e-beam 1050 materials show a more linear response with a similar TVI at lower doses (30-50 kGy) and a higher TVI at higher doses (60-120 kGy). Muratoglu et al. [11] found similar responses for 1050 REB. One characteristic of the e-beam samples was a gradient in TVI through the thickness as shown in Figure 11 with the lowest TVI at the surface and a higher TVI in the center of the irradiated block. For the 1050 CMS material at 121 kGy, the center was about 48% higher than the surface.

Wear Properties

Wear test results for the seven groups are shown in Figure 12. Figure 13 (wear vs. swell ratio) shows there is no correlation between wear and swell ratio because the two groups with the same swell ratio (1050 CMS at 43 kGy and 1020 REB at 83 kGy) have significantly different wear rates (p=0.01). Figure 14 shows that there is a very good linear correlation (R = -0.98) between wear rate and dose, despite differences in materials and processing conditions. It also shows that the 1020 REB samples had the same wear rate as the 1050 CMS samples at both 43 kGy (p=0.999) and 83 kGy (p=0.99). These
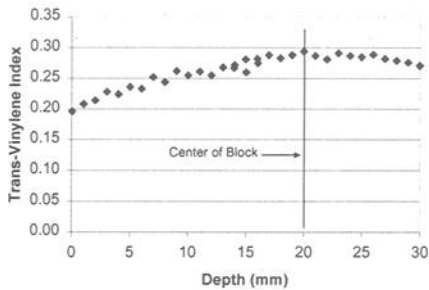

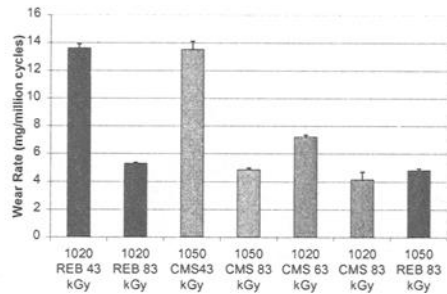Figure 11-*TVI through the thickness for 1050 CMS e-beam irradiated material at 121 kGy.*

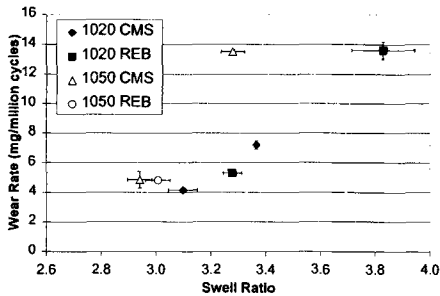Figure 12-*Hip simulator wear rates for gamma irradiated groups*

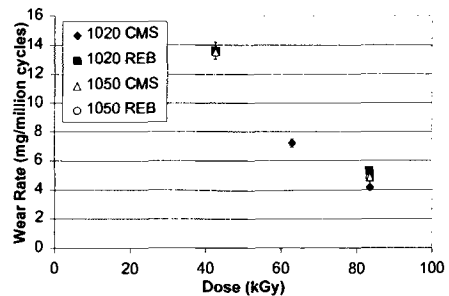Figure 13-*Wear rate as a function of swell ratio*

Figure 14-*Wear rate as a function of dose*

results suggest that the wear rate is a function of dose for 1020 and 1050 material fabricated as either CMS or REB.

Discussion

This study indicates that the choice of starting material, fabrication form and irradiation method can affect the crosslinking and subsequent mechanical properties of UHMWPE in the range of doses from 30-120 kGy.

Because irradiation of UHMWPE causes crosslinking of the material, the range of doses evaluated produced major changes in most of the properties. These dose effects were irrespective of the molecular weight of the starting material (e.g., 1020 or 1050), fabricated form (CMS or REB), or irradiation source (gamma or e-beam). In particular, increasing the dose increased the crosslinking level (as noted by the decrease in swell ratio), reduced the tensile elongation, reduced the impact strength, increased the trans-vinylene index, and ultimately reduced the wear rate.

The choice of fabricated form, either CMS or REB, had very little effect on most of the properties reported here while the molecular weight of the resin did. When compared under the same irradiation conditions, the lower molecular weight 1020 material had higher tensile elongation, higher impact strength, and higher swell ratio. However, for the gamma irradiated groups, the trans-vinylene index and hip simulator wear rates were similar for the 1020 and 1050 materials.

The choice of e-beam or gamma irradiation also affected the final properties of the crosslinked material. When the same materials, forms and doses were compared, the e-beam material had higher elongation, higher impact strength, and lower swell ratio and higher TVI. However, there was generally more variation in properties for the e-beam materials, which probably is a result of the uneven irradiation dose through the thickness as shown by the TVI results and the irradiation dosimeters. With regard to reporting on the toughness of irradiation crosslinked materials, it should be noted that the higher impact toughness of e-beam materials reported here is in contrast to the lower fracture toughness of e-beam irradiated materials reported by Duus et al. [4].

The finding of this study that wear of irradiated UHMWPE is not solely a function of the crosslink density appears to be in conflict with previous reports [1-3]. However, these reports were based only on GUR 4150 REB and did not compare different raw materials. If the gamma irradiated 1020 and 1050 materials are considered separately, then wear rate is directly related to swell ratio as can be seen in Figure 13. However, when the materials are considered together, it is the dose that determines the wear rate as shown in Figure 14.

One explanation for why the wear results are not correlated with crosslink density is that the swell ratio is not just a measure of crosslink density but also includes the effects of chain entanglements in the material. Since chain entanglements in a material increase as molecular weight increases, 1050 materials would have more entanglements than 1020 materials [13]. The hypothesis would be that when 1020 and 1050 are irradiated at the same dose, the amount of crosslinking is essentially the same while the swell ratio is different because the higher molecular weight 1050 material has more entanglements that inhibit the swelling of the material.

References

[1] McKellop, H., Shen, F., Lu, B., Campbell, P., and Salovey, R., "Development of an Extremely Wear-Resistant Ultra High Molecular Weight Polyethylene for Total Hip Replacements," *Journal of Orthopaedic Research*, Vol. 17, No. 2, 1999, pp. 157-167.

[2] Muratoglu, O. K., Bragdon, C. R., O'Connor, D. O., Jasty, M., and Harris, W. H., "A Novel Method of Cross-Linking Ultra-High-Molecular-Weight Polyethylene to Improve Wear, Reduce Oxidation, and Retain Mechanical Properties," *The Journal of Arthroplasty*, Vol. 16, No. 2, 2001, pp. 149-160.

[3] Muratoglu, O. K., Bragdon, C. R., O'Connor, D. O., Jasty, M., Harris, W. H, Gul, R., and McGarry, F., "Unified Wear Model for Highly Crosslinked Ultra-High Molecular Weight Polyethylenes (UHMWPE)," *Biomaterials*, Vol. 20, 1999, pp. 1463-1470.

[4] Duus, L. C., Walsh, H. A., Gillis, A. M., Noisiez, W., and Li, S., "The Effect of Resin Grade, Manufacturing Method, and Cross Linking on the Fracture Toughness of Commercially Available UHMWPE," *Transactions of the Orthopaedic Research Society,* Vol. 25, 2000, p. 544.

[5] DiMaio, W. G., Saum, K. A., Lilly, W. B., and Moore, W. C., "Effect of Radiation Dose on the Physical Properties of Crosslinked UHMWPE," *Transactions of the Orthopaedic Research Society*, Vol. 24, 1999, p. 100.

[6] Greenwald, A. S., Bauer, T. W., and Ries, M. D., "New Polys for Old: Contribution or Caveat?" *69th Annual meeting of the American Academy of Orthopedic Surgeons*, Dallas, Texas, 2002.

[7] Manley, M. T., Capello, W. N., D'Antonio, J. A., and Edidin, A. A., "Highly Crosslinked Polyethylene Acetabular Liners for Reduction in Wear in Total Hip Replacement," Scientific Exhibit SE022, *67th Annual Meeting of the American Academy of Orthopaedic Surgeons*, Orlando, Florida, 2000.

[8] Furman, B. D., Bhattacharyya, S., Hernoux, C., Ranawat, C. S., and Li, S., "Independent Evaluation of Wear Properties of Commercially Available Cross Linked UHMWPE," *Transactions of the Society for Biomaterials*, Vol. 24, 2001, p. 33.

[9] Furman, B., Agner, S., and Li, S., "Is There a Difference in Wear Properties of Commercially Available Crosslinked UHMWPE?," *Transactions of the Orthopaedic Research Society*, Vol. 27, 2002, p. 1038.

[10] Spiegelberg, S. H., Kurtz, S. M., and Edidin, A. A., "Effects of Molecular Weight Distribution on the Network Properties of Radiation- and Chemically-Crosslinked Ultra High Molecular Weight Polyethylene," *Transactions of the Society for Biomaterials*, Vol. 22, 1999, p. 215.

[11] Muratoglu, O. K., and Harris, W. H., "Identification and Quantification of Irradiation in UHMWPE Through Trans-Vinylene Yield," *Journal of Biomedical Materials Research*, Vol. 56, 2001, pp. 584-592.

[12] Paul, J.P., "Forces Transmitted by Joints in the Human Body," *Proceedings of the Institution of Mechanical Engineers*, Vol. 181F, 1967, pp. 8-15.

[13] Ferry, J.D., *Viscoelastic Properties of Polymers*, 3rd Edition, John Wiley and Sons, New York, 1980, pp 241-247.

Kenneth R. St. John[1] and Robert A. Poggie[2]

Characterization of the Wear Performance of Crosslinked UHMWPE and Relationship to Molding Procedures

Abstract: Using an eight-station hip wear simulator, radiation-crosslinked polyethylenes were tested for their resistance to wear-related weight loss and the results compared to results for studies conducted on the same machine using polyethylene that was being implanted at the time. The testing results showed that the wear rate of crosslinked (60 kGy) Slab Compression Molded (SCM) polymer was about 63% lower than standard (30 kGy) SCM cups and 69% less than Ram Extruded 4150 (30 kGy) cups. The Near-net Final Shape molded (NFS) crosslinked (60 kGy) specimens had an 89% reduction in wear rate over the standard (30 kGy) NFS cups, regardless of whether GUR 1020 or GUR 1050 crosslinked cups were tested. All wear rates for nitrogen packaged materials were significantly superior to those for cups sterilized in air and for earlier generation GUR 4150 products sterilized and stored in contact with oxygen.

The results confirm that both the SCM and NFS molding processes produce acetabular cups with excellent wear properties as compared to previous processes. The additional crosslinking process, described herein, provided a major improvement in the wear resistance with either molding process with greater improvement occurring in the NFS specimens.

Keywords: wear, crosslink, compression molding, extrusion, orthopaedics, tribology, final shape molding

Introduction

Over the last 10 to 15 years, there has been a continuous effort in many research laboratories around the country to improve the wear properties of ultra-high molecular weight polyethylene. Improvements in manufacturing, packaging, and sterilization techniques have yielded as much as a 90% reduction in the wear rates of polyethylene bearing components [1]. The objectives of this research were to evaluate the effects of raw

[1] Associate Professor, Department of Orthopaedics and Rehabilitation, University of Mississippi Medical Center, 2500 North State Street, Jackson, MS 39216-4505.
[2] Director, Applied Research, Implex Corp., 80 Commerce Drive, Allendale, NJ 07401-1600.

material identity, consolidation process, packaging condition, radiation dose, and temperature during sterilization on the wear properties of polyethylene tested in a hip simulator.

Materials and Methods

The polymer specimens (28 mm acetabular inserts or cups) and test conditions that were used are shown in Table 1. UHMWPE resins utilized were GUR 4150 (equivalent to GUR 1150), GUR 1020, and GUR 1050, which differ in the molecular weight and whether calcium stearate was added to the polyethylene resin before consolidation [1]. Specimens were Ram Extruded (RE) (Poly-Hi Solidur), Slab Compression Molded (SCM) (Perplas Medical Ltd.), or near net-final-shape molded (NFS) (PPD Meditech). All specimens were packaged under vacuum at the time of sterilization except for the aged samples. The aged samples were SCM GUR 1120 cups that had been sterilized in air and stored in inventory for five years before testing. All heads were unused or repolished 28 mm cobalt chromium alloy heads taken from product inventory.

Specimens were either sterilized using gamma irradiation to approximately 30 kGy by standard methods or were subjected to a crosslinking process in that the specimens were maintained at a temperature of 190°F while being irradiated to a level of approximately 60 kGy [2]. The mechanical and physical properties of the crosslinked polymers have been reported previously [3,4].

Table 1 - *Characteristics of Specimens Tested*

Designation	Raw Material	Molding Process	Irradiation
4150 RE	GUR 4150	Ram Extruded (RE)	31 kGy
1020 SCM	GUR 1020	Slab Compression Molded (SCM)	31 kGy
1120 SCMA	GUR 1120	Slab Compression Molded (SCM)	~30 kGy in Air Shelf Aged Five Years
1020 SCMX1	GUR 1020	Slab Compression Molded (SCM)	50 kGy, 190F
1020 SCMX2	GUR 1020	Slab Compression Molded (SCM)	60 kGy, 190F
1020 NFS	GUR 1020	Near Net Final Shape (NFS)	30 kGy
1020 NFSX	GUR 1020	Near Net Final Shape (NFS)	64 kGy, 190F
1050 NFSX	GUR 1050	Near Net Final Shape (NFS)	64 kGy, 190F

Testing was conducted on an eight-station hip simulator (MTS, Eden Prairie, MN) that had been constructed with the addition of load cells and torque cells on every testing station. All samples were mounted with the head on top (anatomic position) and testing was conducted at a loading rate of one cycle per second using a Paul curve [5] with a maximum load of 3 000N. The specimens were immersed in filtered, undiluted bovine calf serum, to

which had been added 20mM EDTA (disodium EDTA dihydrate, Sigma, St. Louis, MO). The serum lubricant was removed and frozen and the specimens cleaned, dried, and weighed every 500 000 cycles, in accordance with ASTM Guide for Gravimetric Wear Assessment of Prosthetic Hip-Designs in Simulator Devices (F1714) to quantify losses due to wear. This method accounts for fluid uptake of the polyethylene through the use of fluid soak controls. The total length of testing varied between 3 000 000 and 6 000 000 cycles.

In comparing the results of wear rates, the Mann-Whitney U (Rank Sum) test was used to compare the individual results for each separate sample tested. The nature of the data, in which different samples sizes for each of the groups existed, this test was the most suitable.

Results

Table 2 shows the wear rate data in milligrams per million cycles (mg/mc) for each of the types of polyethylene tested. The results are then plotted to show the relative rates of wear that were observed for each polymer species and specimen condition. In each figure in which error bars appear, they represent one standard deviation from the mean.

Table 2 - *Wear Testing Results*

Designation	n	Wear Rate (mg/mc) First 2,000,000 Cycles	Wear Rate (mg/mc) After 2,000,000 Cycles
4150 RE	3	23.7 ± 3.0	18.6 ± 1.8
1020 SCM	3	21.8 ± 1.5	15.6 ± 0.4
1120 SCMA	3	49.2 ± 8.4	28.2 ± 6.2
1020 SCMX1	5	7.8 ± 2.4	5.8 ± 1.4
1020 SCMX2	2	5.9 ± 0.6	5.7 ± 0.1
1020 NFS	2	17.5 ± 0.0	17.0 ± 0.7
1020 NFSX	4	3.1 ± 0.2	1.9 ± 0.1
1050 NFSX	2	2.6 ± 0.6	1.9 ± 0.2

The initial results of testing of the GUR 4150 RE cups and the GUR 1020 SCM cups are plotted in Figure 1, along with results adapted from a report by McKellop [6] for GUR 1020 cups packaged and sterilized in the same manner. In Figure 2, the results for all compression molded polymers without calcium stearate (GUR 1020, GUR 1050) are displayed graphically. On a different scale, Figure 3 shows the results for the crosslinked polymers in greater detail. Figure 4 compares four different conditions of SCM polymer for resistance to wear in a hip simulator. The aged GUR 1120 cups (Hoechst AG) were three samples from two different manufacturing lots.

Statistical analysis of the wear rates from each of the studies showed 4150 RE to be significantly different from 1020 SCM (p=0.05). 1020 SCM was significantly different from 1020 SCMX and 1020 NFSX specimens (p<0.05). Type 1020 SCMX wear rates were significantly different from 1020 NFSX (p<0.05). Because of the small sample size (n=2), no significant difference was found between 1020NFS and any other group. There was no difference between 1050 NFSX and 1020 NFSX wear rates.
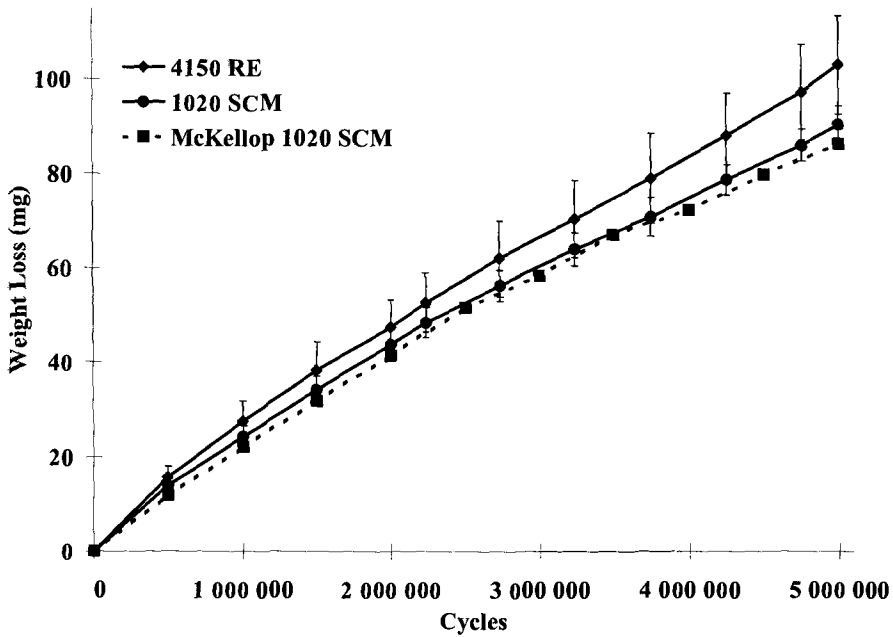
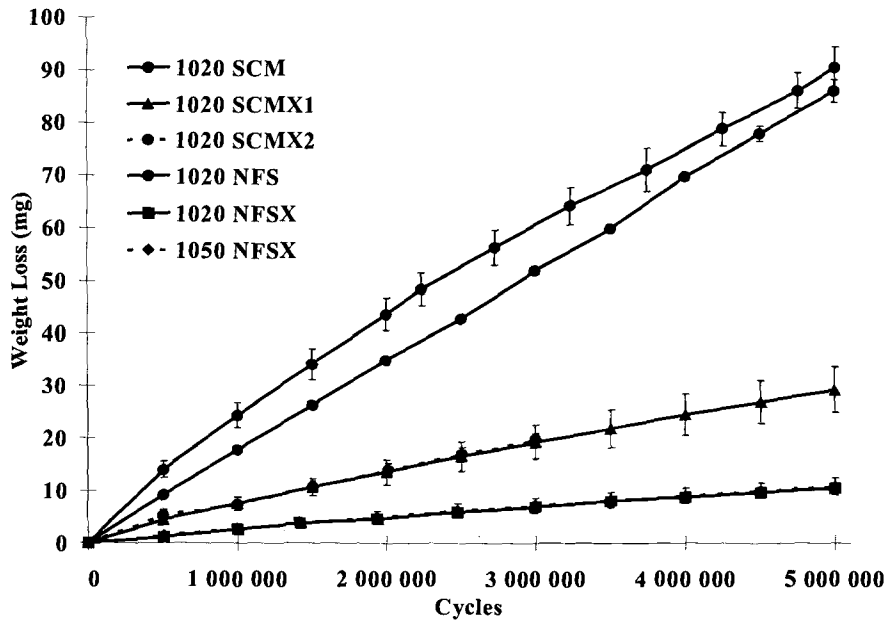Figure 1 - *Comparison of Wear Rates - Standard Sterilization*

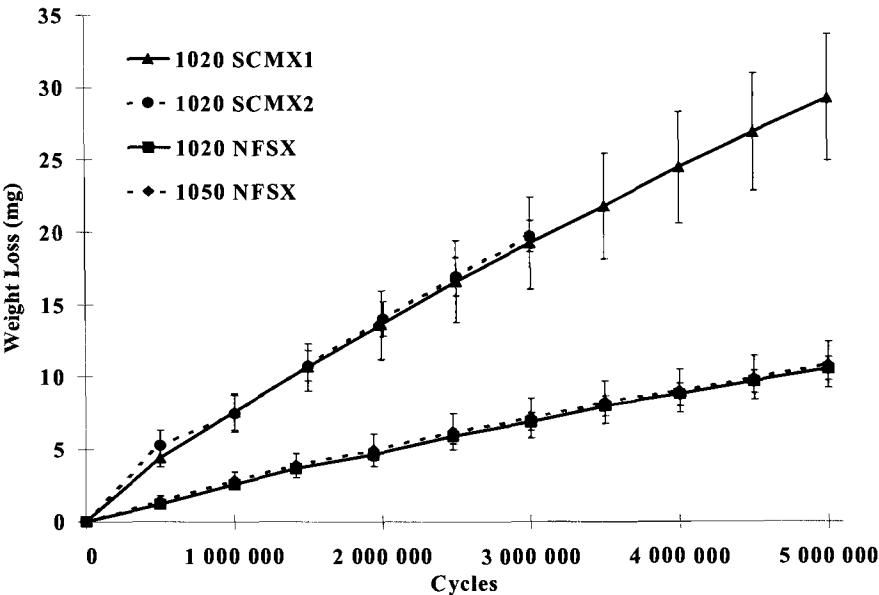Figure 2 - *Comparison of the Wear of Polymers Without Calcium Stearate*

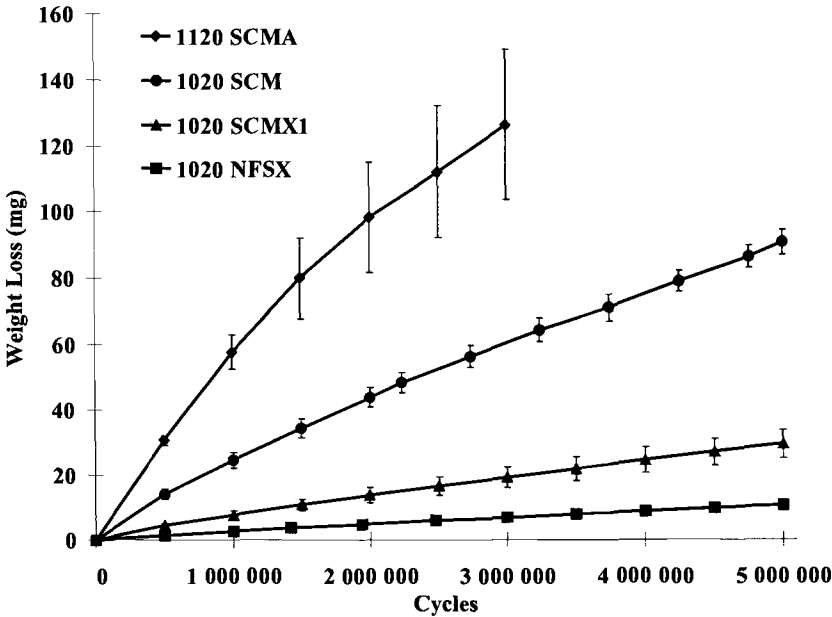Figure 3 - *Wear Performance of Crosslinked Polyethylene*

Figure 4 - *Effects of Packaging, Molding Process, and Crosslinking*

Discussion

The results of the wear testing of the 1020 SCM material were nearly identical to those reported by Harry McKellop for material from the same source, packaged and sterilized in a similar manner by a different manufacturer.[6] This similarity suggests that the wear results being reported here may be compared to other published results from that research group. This study showed that the specimens that were ram extruded, had a higher molecular weight, and contained calcium stearate (4150 RE) exhibited a higher wear rate than those that were slab compression molded, had a lower molecular weight, and contained no calcium stearate (1020 SCM).

The crosslinking process as described provided a 63% reduction in wear (1020 SCMX1 and 1020 SCMX2) over the material that was sterilized without the additional crosslinking process. Additionally, a further 67% reduction in wear occurred when the specimens were near-net-final-shape molded (1020 NFSX). The overall reduction in wear of the 1020 NFSX samples over the 1020 SCM specimens was 88%. These data suggest that, in addition to the effects of crosslinking, the process parameters of time, temperature, and pressure used for the consolidation of the polymer resin play a major role in the wear properties of the finished product and its response to crosslinking. The specific reason for this improvement was not determined, but may be related to differences in the temperature profile used in the molding processes and resultant improvements in the consolidation of the raw material from the powder form, which controls the percentage and size of the crystalline domains.

Comparison of the results for specimens 1020 NFSX to specimens 1050 NFSX shows that the earlier differences between the wear of 4150 RE and 1020 SCM were not likely to have been due to differences in molecular weight but were due to either molding process or calcium stearate content. McKellop [6] found that neither molecular weight nor calcium stearate content had an affect on wear rate, whereas Schmidt [7] found a large effect due to calcium stearate. Schmidt studied the fusion defects in the specimens and found that those containing the additive had more molding defects. It would appear that the presence of calcium stearate may inhibit complete consolidation of the polyethylene during formation, and that in the absence of consolidation defects, calcium stearate may have little effect on wear. It is therefore likely that disagreements in the literature about the effect of calcium stearate may be more appropriately considered to be related to differences in molding processes in that some specimens were fully consolidated despite the presence of calcium stearate while others were not. It would appear that the differences seen in this study were likely due to differences in process parameters during consolidation, which are controlled by the consolidators of the polyethylene.

Because of the small sample sizes, some of the differences between wear curves that appear to be highly significant in the figures had p values of about 0.05, and it is likely that larger sample sizes would have increased the statistical significance of this study.

Conclusions

This study has shown that the process of molding, packaging and sterilizing a polyethylene hip cup plays a major role in the resultant wear properties of the material. It

would appear that molecular weight of the resin and content of calcium stearate do not play a measurable part so long as complete consolidation of the polymer has occurred.

The process of near net final shape molding of ultra high molecular weight polyethylene appears to enhance the wear resistance of the polymers tested, when crosslinked. This finding has important implications in the development of new hip systems since back side wear of inserts against metallic acetabular components might be solved by molding the polyethylene directly into the metallic component.

References

[1]   Kurtz, S. M., Muratoglu, O. K., Evans, M., and Edidin, A. A., "Advances in the Processing, Sterilization, and Crosslinking of Ultra-High Molecular Weight Polyethylene for Total Joint Arthroplasty," *Biomaterials,* Vol. 20, 1999, pp. 1659-1688.

[2]   Poggie, R., Averill, R., and Afflitto, R., "Wear-Resistant Olefinic Medical Implant and Thermal Treatment Container Therefor," United State Patent # 6,355,215, March 12, 2002.

[3]   Stiehl, J. B., St. John, K. R., Afflitto, R., and Poggie, R. A., "Improved Wear Resistance of Compression Molded Cross-Linked Polyethylene," Scientific Exhibit, American Academy of Orthopaedic Surgeons, San Francisco, CA, February 28-March 4, 2001.

[4]   St. John, K. R., Afflitto R. M., Averill, R. G., and Poggie, R. A., "Comparison of the Wear Resistance of Two Cross-linked Polyethylene Materials," 25th Annual Meeting of the Society for Biomaterials, Providence, RI, April 28- May 2, 1999.

[5]   Paul, J. P., "Forces Transmitted by Joints in the Human Body. Lubrication and Wear in Living and Artificial Human Joints," *Proceedings of the Institution of Mechanical Engineers,* Vol 181J, 1966, pp. 8-15.

[6]   McKellop, H. A., Shen, F.-W., Campbell, P., and Ota, T., "The Effect of Molecular Weight, Calcium Stearate, and Sterilization Methods on the Wear of Ultra High Molecular Weight Polyethylene Acetabular Cups in a Hip Joint Simulator," *Journal of Orthopaedic Research,* Vol. 17, 1999, pp. 329-339.

[7]   Schmidt, M. B., and Hamilton, J. V., "The Effects of Calcium Stearate on the Properties of UHMWPE," *Transactions of the Orthopaedic Research Society,* Vol. 21, 1999, p.22.

Niels A. Abt,[1] Werner Schneider,[1] Rolf Schön,[1] and Claude B. Rieker[1]

Influence of Electron Beam Irradiation Dose on the Properties of Crosslinked UHMWPE

ABSTRACT: The purpose of this study was to investigate the influence of a dose of e-beam irradiation on the mechanical and tribological properties of crosslinked UHMWPE.

Specimens of UHMWPE were irradiated at different dose levels between 0 and 110 kGy using the WIAM e-beam process. Irradiation was followed by melt annealing and slow cooling.

In general, the mechanical properties of irradiated UHMWPE decrease with increasing irradiation dose. Increasing the irradiation dose from 50 to 95 kGy results in a loss of 4% yield strength, 16% elongation, 15% tensile strength and 18% impact strength. Crystallinity does not change significantly.

In comparison with conventional material, irradiation with 50 kGy reduces the wear rate by 73%. A further reduction of 56% can be realized by increasing the dose from 50 to 95 kGy.

KEYWORDS: polyethylene, ultra-high molecular weight polyethylene, beta irradiation, electron beam, crosslinking, wear testing, orthopedic medical devices

Introduction

Ultra-high molecular weight polyethylene (UHMWPE) has been used for bearing components in total joint replacement since the 1960s. Although joint arthroplasty is one of the most successful surgical interventions, wear debris of the UHMWPE components resulting from articulation has been a problem, because such debris is associated with bone resorption, subsequent aseptic loosening, and implant failure [1-3].

---

[1] Research Scientists, Centerpulse Orthopedics, PO Box 65, CH-8404 Winterthur, Switzerland.

Low wear solutions, e.g. metal-metal and ceramic-ceramic, were developed to solve the problem of aseptic loosening. Pioneer work was already made by Grobbelaar [4], Oonishi [5] and Wroblewski [6] in the 70s and 80s to improve the wear behavior with highly crosslinked UHMWPE by means of irradiation. A second generation of highly crosslinked UHMWPE developed in the mid-90s produced remarkable in-vitro results, with almost no measurable wear in hip-simulator studies [7, 8]. Following extensive, further investigations, these highly crosslinked UHMWPE solutions were implanted from the late nineties on and have shown good early performance up to now [9].

Although theoretical explanations endeavor to improve the comprehension of the observed effects, they still have to be validated as well through experiments.

The object of this study was to show how the properties of UHMWPE specimen Warm-Irradiated by means of the Adiabatic Melted (WIAM) process are influenced by the irradiation dose, with the focus on the mechanical properties and tribological screening tests.

Material and Methods

Raw Material

The resin type investigated was compression-molded GUR 1050. The plate was sectioned into bars of 3 x 6.5 x 50 cm. For comparison, a conventional UHMWPE was used as reference. The material was compression-molded GUR 1020, gamma-irradiated under N_2 with a dose between 25 and 40 kGy.

Irradiation

The specimens were irradiated with a 10 MeV Rhodotron electron beam accelerator. The material was heated to 120°C, and irradiated at different dose levels. The specimens were exposed to 0, 20, 35, 50, 65, 80, 95, 110 kGy. The conveyor-belt speed was constant in consideration of the appropriate selected dose rate (Table 1). After irradiation, all specimens were thermally treated for 5 hours at a temperature of 150°C to eradicate the free radicals, and then cooled slowly.

Trans-Vinylene Index

Two microtome slices with a thickness of 300 μm were taken 10 mm below the e-beam incidence surface from each specimen. IR spectra were collected in transmission on microtomed sections using a BioRad FTS-45 with a resolution of 4 cm^{-1}. The values presented here are the averages of the two IR spectra. The trans-vinylene index (TVI)

was calculated by normalizing the area under the trans-vinylene vibration at 965 cm^{-1} to that under the 1900 cm^{-1} vibration [10].

Table 1 - *Process parameter and TVI of radiation-crosslinked UHMWPE (WIAM) as a function of the radiation dose.*

Sample ID	Dose, kGy	Dose Rate, mA*m^{-1}*min^{-1}	TVI
WIAM-0	0	--	--
WIAM-20	20	1.37	0.037
WIAM-35	35	2.39	0.092
WIAM-50	50	3.25	0.130
WIAM-65	65	4.22	0.186
WIAM-80	80	5.20	0.237
WIAM-95	95	6.50	0.293
WIAM-110	110	7.53	0.321

Crystallinity

The crystallinity of the test samples was determined using a Perkin Elmer DSC7 at a heating rate of 10°C/min. The specimen were taken from the core of the irradiated bars. The heat of fusion was calculated by integrating the DSC endotherm in the first heat-up with subtraction of the baseline. The crystallinity was calculated using the heat of fusion of 100% crystalline polyethylene (291 J/g) [11]. For the qualitative comparison of the endothermic curves, the data was manually corrected to a flat base, but not normalized by the specimen's weight.

Tensile Properties

The variation in the mechanical properties as a function of absorbed radiation dose for the radiation-crosslinked specimen was determined by applying Dumbell specimen type V prepared according to the Standard for Determination of Tensile Properties (ISO 527). The specimen were machined from the crosslinked bars, rectangular to the direction of the e-beam (*n=10* for each absorbed dose level). A sample thickness of 1.5 ± 0.5 mm and test speed of 100 ± 10 mm/min has been used as specified in the Standard for Implants for Surgery - Ultra-high molecular weight polyethylene - Part 2 : Molded forms (ISO 5834/2-98).

Impact Strength

The variation in the impact strength as a function of absorbed irradiation dose for the radiation-crosslinked specimen was determined using double-notched specimen for

Charpy impact strength, prepared according to the Standard for Ultra-high-molecular-weight polyethylene (PE-UHMW) molding and extrusion materials (ISO 11542). The specimen were machined from the crosslinked bars, $n=10$ for each absorbed dose level.

Pin-on-Disc Experiment

The pins used in the pin-on-disc (POD) experiments were machined from the crosslinked test samples ($n=6$) so as to have the articulation surfaces of the pins 3 mm below the free surfaces. During the radiation crosslinking, oxidation takes place near free surfaces with a depth of penetration of about 1 mm [12-14]. To be able to investigate the wear behavior of the crosslinked polymer, the oxidized surface layers had therefore be machined away. The counterfaces used in the POD experiments were wrought CoCrMo alloy discs with implant surface finish (Ra=0.059 ± 0.121 μm). The multi-directional motions were obtained by a rotating pin on a rotating disc. With one disc rotation, the pin rotates four times, which leads to four changes in the wear direction. Table 2 shows the parameters of the wear testing.

Table 2 – *Wear Parameters of the Pin-on-Disc experiment*

Parameter	Value
Load	3.45 MPa
Lubricant	33 % calf serum – 67 % Ringer's solution
Temperature	37°C
Speed	27 mm*s^{-1}
Frequency	1 Hz
Number of cycles	1 Million

The wear factor was measured on-line by the dimensional change in the height of the pin and by the gravimetric method [15]. Wear is a function of the load on the pin and the distance the pin travels on the disc, multiplied by the wear factor. The wear factor k is defined by the following equation [16]:

$$k = \frac{V}{W \cdot l} \tag{1}$$

where
k = wear factor [mm^3/Nm]
V = volume of wear [mm^3]
W = load [N]
l = the distance displaced [m]

The POD wear tester used in this study was developed in our laboratory [17] according to the guidelines of Practice for Reciprocating Pin-on-Flat Evaluation of

Friction and Wear Properties of Polymeric Materials for Use in Total Joint Prostheses (ASTM F 732). A conventional UHMWPE was also tested.

Results

Table 1 presents the irradiation dose with the associated dose rate and the TVI for each specimen. The dose rate was specified appropriately so that every specimen was irradiated at the same conveyor belt speed. Absorbed dose and TVI exhibit linear correlation (Figure 1) as reported elsewhere [10].
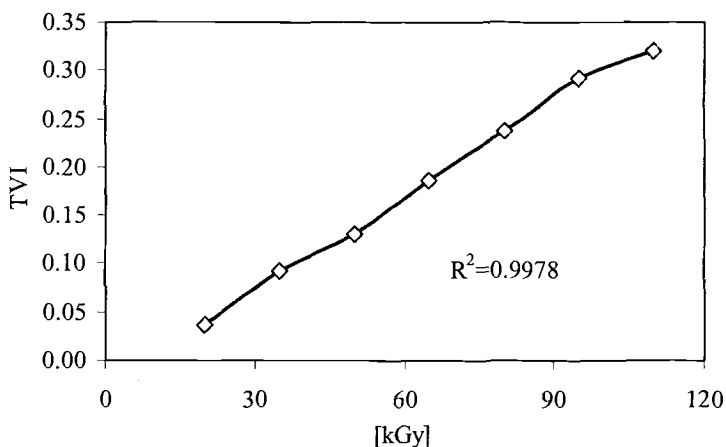

Figure 1 - *Trans-vinylene index vs. irradiation dose of e-beam irradiated WIAM.*

Crystallinity

With the DSC, no significant change can be observed in the crystallinity (Figure 2) with an increasing irradiation dose. The data suggest a slight decrease, but could not be confirmed. Although the degree of crystallinity remains constant, our data suggest a change in the crystalline morphology. With an increasing dose, the onset of melting displaces towards lower temperatures, indicating a reduction in the size of crystallites (Figure 3).

Mechanical Properties

Table 3 shows how the mechanical properties of the irradiated UHMWPE are affected by irradiation dose. All the values from the tensile testing and the impact strength

decrease with increased irradiation dose. For comparison, Table 4 presents typical values of untreated GUR 1050. These values are the averages of data taken from the delivery certificates of the raw material.
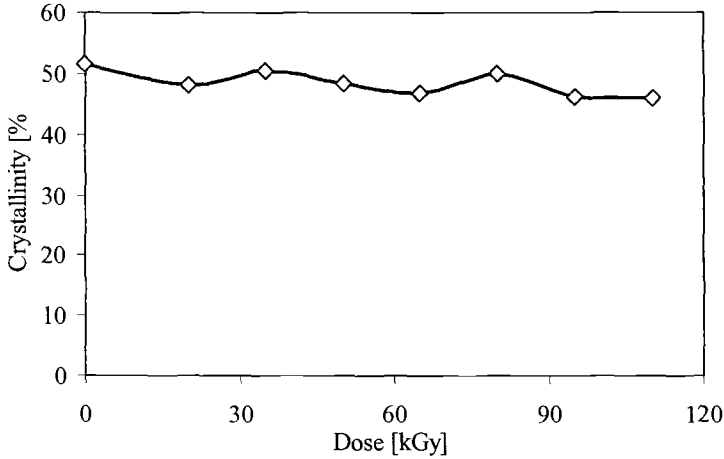

Figure 2 - *Crystallinity of WIAM vs. irradiation dose, measured with DSC in the first heat-up.*
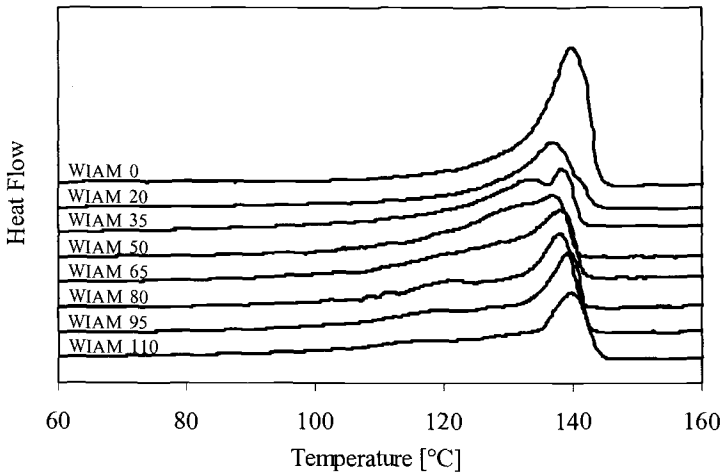

Figure 3 - *DSC curves show the change in morphology*

The ultimate tensile strength reduces by 21.4 % for the first increase from GUR 1050 to 50 kGy and by another 14.6 % from 50 to 95 kGy (Figure 4). The impact strength shows a similar behavior with a loss of 19.4 % between GUR 1050 and WIAM-50, and a

further loss of 14.3 % when increasing the dose from 50 to 95 kGy (Figure 5). Compared with the elongation at break, it can be seen that the reduction of the elongation is more sensitive at higher dose levels. The elongation at break reduces 9.3 % between GUR 1050 and WIAM-50, and 14.3 % by increasing the dose from 50 to 95 kGy.

Table 3 - *Properties of radiation-crosslinked UHMWPE (WIAM) as a function of irradiation dose.*

Sample ID	Cryst.	Yield Strength	Tensile Strength	Elongation	Impact Strength	Wear Factor
	%	MPa	MPa	%	kJ/m^2	mm^3/Nm
Sulene-PE	54.4	25.6 ± 0.4	57.8 ± 5.2	432 ± 15	143.0 ± 1.9	3.88 ± 1.94
WIAM-0	46.9	21.8 ± 0.4	54.9 ± 1.8	371 ± 7	77.7 ± 1.6	10.44 ± 1.56
WIAM-20	46.3	19.6 ± 0.4	46.9 ± 2.2	341 ± 7	81.8 ± 1.1	3.25 ± 0.67
WIAM-35	46.1	19.9 ± 0.3	41.6 ± 1.6	328 ± 10	85.0 ± 2.0	1.53 ± 0.15
WIAM-50	46.5	20.3 ± 0.2	37.2 ± 1.2	330 ± 7	83.8 ± 5.2	1.02 ± 0.53
WIAM-65	45.0	19.8 ± 0.2	36.8 ± 2.1	324 ± 9	77.9 ± 6.2	0.77 ± 0.27
WIAM-80	46.1	19.4 ± 0.2	33.5 ± 2.5	317 ± 9	77.8 ± 3.7	0.63 ± 0.60
WIAM-95	45.6	19.7 ± 0.2	31.6 ± 3.5	278 ± 15	69.0 ± 4.6	0.46 ± 0.17
WIAM-110	44.7	19.0 ± 0.3	31.9 ± 0.9	273 ± 3	67.0 ± 1.5	0.35 ± 0.18

Least affected is the yield strength. Comparing GUR 1050 with WIAM-50, a loss of 0.5 % can be established and a increase of the dose up to 95 kGy leads to a loss of 4.4 % in total (Figure 4).
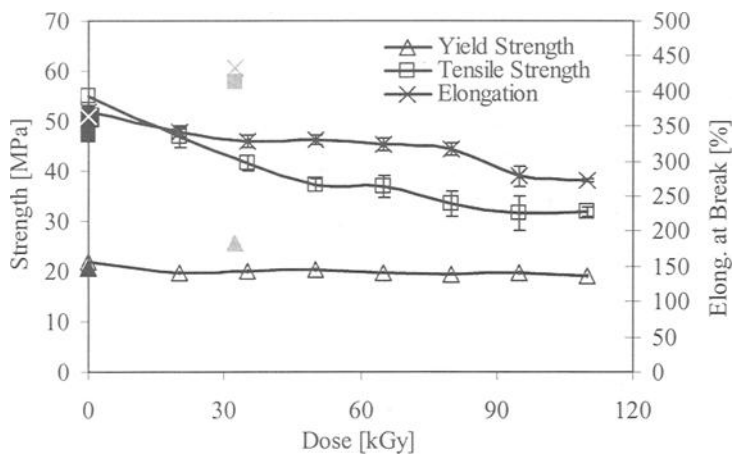

Figure 4 - *Tensile properties of WIAM vs. irradiation dose. Conventional UHMWPE (gamma in N$_2$) (⊛) and raw material (■) is included for reference purposes.*

Table 4 - *Typical values of untreated GUR 1050.*

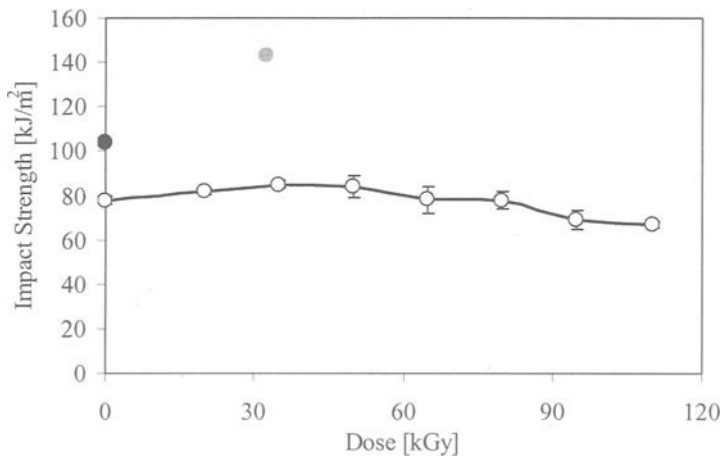|	Yield Strength (MPa)	Tensile Strength (MPa)	Elongation (%)	Impact Strength (kJ/m^2)
Typical	20.7	47.3	364	104
ISO 5834-2	> 19	> 27	> 250	> 30

Figure 5 - *Charpy impact strength of WIAM vs. irradiation dose. Conventional UHMWPE (gamma in N₂) ( ) and raw material (●) is included for reference purposes.*

Pin-on-Disc Experiment

The measured wear factors (Table 3) show how wear behavior is affected by the irradiation dose. A conventional UHMWPE (gamma in N_2) is added to the chart to establish a comparable reference (Figure 6). WIAM-50 shows a reduction in wear factor at a factor of 3.8 compared to the conventional UHMWPE. Increasing the dose from 50 to 95 kGy, leads to a further 50% reduction in the wear factor.

Discussion

The loss of the mechanical properties for irradiated UHMWPE is known and well-documented for gamma-irradiated UHMWPE [18]. Since this reduction under certain methods used to produce crosslinking has been the cause for concern, finding the optimal

process and the optimal process parameters for crosslinking has become a important field of research [18, 7]. Although it is reported by Muratoglu et al. [7] that using electron beam with the WIAM process results in retained mechanical properties, it is important to acquire more data.
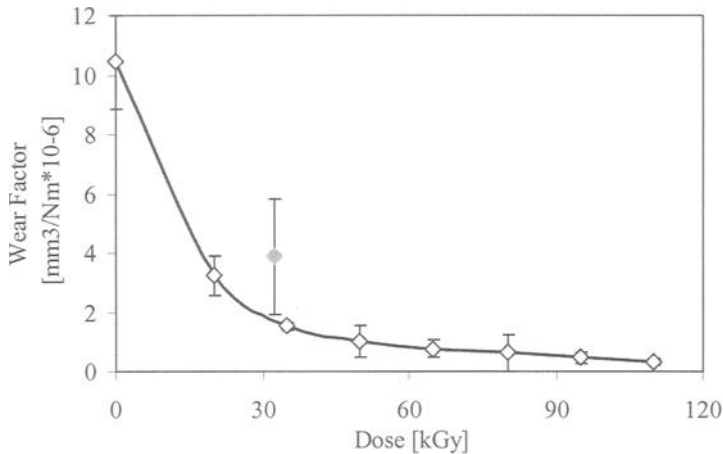

Figure 6 - *Wear factor vs. irradiation dose, measured with multi-directional pin-on-disc apparatus. Conventional UHMWPE (gamma in N_2) is included (⊕) for reference purposes.*

We therefore investigated the mechanical properties and the wear behavior of electron beam irradiated WIAM-UHMWPE as a function of absorbed dose in the present work.

It is said that crosslinking results in a loss of 30-40 % ultimate tensile strength and elongation at break [18]. Compared with the data from this study, it can be shown that using an electron beam with the WIAM process it only results in a loss of 23 % (elongation) and 33 % (UTS) with an irradiation dose of 95 kGy. These findings, except for the preserved yield strength and crystallinity, do not support the theory of Muratoglu [19], which proposes stable mechanical properties for higher doses (Figures 4,5).

Hubbard [20] showed for gamma-irradiated UHMWPE, that the mechanical properties depend on the crystallinity of the material. Since with WIAM, the crystallinity stays constant, another mechanism must be responsible in WIAM for the observed loss of the mechanical properties. We believe that the answer can be found in the change of the crystal morphology (Figure 3). Reducing the size of the crystallites reduces the mechanical properties, but not as much as when the crystallinity decreases itself. Further investigation will be needed to confirm this.

An estimation of the load in artificial hips, based on the reported worst case of 870% body weight for stumbling [21] and the equation for Herzian contact stress with the smallest head (22 mm) results in stresses of 50% of the yield strength. Consequently, the reduction of the mechanical properties should not be estimated too critically, since yield

strength is the least affected value. As to the higher loads in artificial knees extensive testing will be appropriate.

It is well known that crosslinking UHMWPE results in extremely low wear [7, 22]. With regard to the wear factor, it can be easily seen that the standard deviation of the conventional UHMWPE is much higher than for e-beam irradiated material. The reason is the accuracy of the gamma irradiation: Depending on where the product is placed in the gamma carrier, the dose can vary between 25 and 40 kGy.

Conclusions

Since it is known that highly crosslinking of UHMWPE reduces the mechanical properties and improves the wear behavior, it is important to take this into account when designing products of highly crosslinked materials and choosing the right crosslinking process with the appropriate parameters. The study shows that the usage of electron beam-WIAM at higher doses to crosslink UHMWPE is a good way to drastically improve wear properties and achieve effective implants, if the decrease in strength can be compensated appropriately. Studies about wear particle distributions of different crosslinked UHMWPEs [23, 24] suggest that this extremely low wear solution seems to be optimal not only in its wear behavior, but also promise good results with regard to the particle generation rate and the resulting biological reaction.

Acknowledgments

References

[1]   Willert, H. G., "Reactions of the Articular Capsule to Wear Products of Artificial Joint
Prostheses," *Journal of Biomedical Materials Research*, Vol. II, No. 2, March 1977, pp. 157-164.

[2]   Harris, W. H., "The problem is Osteolysis," *Clinical Orthopaedics and Related Research*, Vol. 311, Feb. 1995, pp. 46-53.

[3]   Dumbleton, J. H., Manley, M. T. and Edidin, A. A., "A Literature Review of the Association between Wear Rate and Osteolysis in Total Hip Arthroplasty," *Journal of Arthroplasty*, Vol. 17, No. 5, Aug. 2002, pp.649-61.

[4]   Grobbelaar, C. J., du Plessis, T. A. and Marais F., "The Radiation Improvement of Polyethylene Prostheses. A Preliminary Study," *Journal of Bone and Joint Surgery. British Volume*, Vol. 60-B, No. 3, Aug. 1978, pp.370-4.

[5]   Oonishi, H., Takayama Y. and Tsuji E., "Improvement of Polyethylene by Irradiation in Artificials Joints," *Radiation Physics and Chemistry*, Vol. 39, 1992, pp. 495-504

[6]   Wroblewski, B. M., Siney, P. D., Dowson, D. and Collins S. N., "Prospective Clinical and Joint Simulator Studies of a New Total Hip Arthroplasty using Alumina Ceramic Heads and Cross-Linked Polyethylene Cups," *Journal of Bone and Joint Surgery. British volume*, Vol. 78, No. 2, March 1996, pp. 280-285.

[7]   Muratoglu, O. K., Bragdon, C. R., O'Connor, D. O., Jasty, M. and Harris W. H., "A Novel Method of Cross-Linking Ultra-High-Molecular-Weight Polyethylene to Improve Wear, Reduce Oxidation, and Retain Mechanical Properties. Recipient of the 1999 HAP Paul Award," *Journal of Arthroplasty*, Vol. 16, No. 2, Feb. 2001, pp. 149-160.

[8]   McKellop, H., Shen, F. W., Lu, B., Campbell, P. and Salovey, R., "Development of an Extremely Wear-Resistant Ultra High Molecular Weight Polyethylene for Total Hip Replacements." *Journal of Orthopaedic Research*, Vol. 17, No. 2, March 1999, pp. 157-167.

[9]   Muratoglu, O. K., Greenbaum, E., Larson, S., Jasty, M., Freiberg, A. A., Burke D. and Harris W. H., "Surface Analysis of Early Retrieved Acetabular Polyethylene Liners: a Comparison of Standard and Highly Crosslinked Polyethylenes," *48th Annual Meeting of the Orthopaedic Research Society*, Feb. 2002, poster No. 1029.

[10] Muratoglu, O. K. and Harris, W. H., "Identification and Quantification of Irradiation in UHMWPE through Trans-Vinylene Yield," *Journal of Biomedical Materials Research*, Vol. 56, No. 4, Sep. 2001, pp.584-592.

[11] Brandup, J. and Immergut, E. H., "Polymer Handbook. 3rd ed.," Wiley, New York, 1989.

[12] Muratoglu, O. K., Bragdon, C. R., O'Connor, D. O., Merrill, E. W., Jasty, M. and Harris W. H., "Electron Beam Crosslinking of UHMWPE at Room Temperature, a Candidate Bearing Material for Total Joint Arthroplasty," *23rd Annual Meeting of the Society for Biomaterials*, April 1997, paper 74.

[13] Gul, R., "Improved UHMWPE for Use in Total Joint Replacement," *Materials Science and Engineering*. Cambridge, Massachusetts Institute of Technology, 1997. p. 232.

[14] McKellop, H., Shen F. W. and Salovey, R., "Extremly Low Wear of Gamma-Crosslinked / Remelted UHMWPE Acetabular Cups," Proc Orthopaedic Research Society, 1998, paper 98-17.

[15] Muratoglu, O. K., Bragdon, C. R., O'Connor, D. O., Jasty, M., Harris, W. H., Gul, R. and McGarry, F., "Unified Wear Model for Highly Crosslinked Ultra-High Molecular Weight Polyethylenes (UHMWPE)," *Biomaterials*, Vol. 20, Nr. 16, Aug. 1999, pp. 1463-1470.

[16] Walker, P. S., "Human Joints and their Artificial Replacements," Charles C Thomas Publisher, Springfield, Illinois, 1977, p. 373.

[17] Rieker, C. B., Schaffner, S., Schön, R., Konrad, R., "Bi-Directional Screening Wear Test with Clinical Validation," *European Orthopaedic Research Society*, Oct. 2000.

[18] Lewis, G., "Properties of Crosslinked Ultra-High-Molecular-Weight Polyethylene," *Biomaterials*, Vol. 22, No. 4, Feb. 2001, pp. 371-401.

[19] Muratoglu, O. K., "Crosslinked Polyethylene. A Promising Technology for Total Joint Replacement in the 21th Century," *47th Annual Meeting of the Orthopaedic Research Society, Polyethylene Workshop*, Feb. 2001.

[20] Hubbard, N. T. and Cooper, C. A., "Dose Rate Affects the Mechanical Properties of Gamma Crosslinked UHMWPE," *28th Annual Meeting of the Society for Biomaterials*, April, 2002, paper 59.

[21] Bergmann, G., Graichen, F. and Rohlmann, A., "Hip Joint Loading during Walking and Running, Measured in Two Patients." *Journal of Biomechanics*, Vol. 26, No. 8, Aug. 1993, pp. 969-990.

[22] Greer, K., Chan, F., Liao, Y., McNulty, D. and King, R., "Hip Simulator Wear of Crosslinked UHMWPE as a Function of Irradiation Dose and Crosslink Density," *28th Annual Meeting of the Society for Biomaterials*, 2002, poster 713.

[23] Ries, M. D., Scott, M.L. and Jani, S., "Relationship between Gravimetric Wear and Particle Generation in Hip Simulators: Conventional Compared with Cross-Linked Polyethylene." *Journal of Bone and Joint Surgery. American Volume*, Vol. 83-A, No. 2, 2001, pp. 116-122.

[24] Illgen, R. L., Laurent, M. P., Watanuki, M., Hagenauer, M. E., Bhambri, S. K., Pike, J. W., Blanchard, C. R. and Forsythe, T. M., " Highly Crosslinked vs. Conventional Polyethylene Particles—an In Vitro Comparison of Biologic Activities" *49th Annual Meeting of the Orthopaedic Research Society*, Feb. 2003, poster 1438.

Charles R. Bragdon, B.S.,[1] *Daniel O'Connor,*[1] *Orhun K. Muratoglu, Ph.D.,*[1] *William H. Harris, M.D.*[1]

Development of a Model for Testing Third Body Wear of UHMWPE Acetabular Components

ABSTRACT: The purpose of this paper is to describe the development of a new wear test protocol utilizing third body particulate debris in order to assess conventional and highly cross-linked polyethylene components. A series of tests were performed using the Boston Hip Simulator to evaluate different types of particles for possible use. Modifications to the simulator are described which ensure that the third body particles can be maintained in suspension. In this series of studies, alumina particles in a concentration of 0.15mg/cc appeared to provide the most effective challenge to the wear resistance of UHMWPE while at the same time not creating unrealistic destruction to the femoral head. In all of the experiments, under all conditions, the WIAM highly crosslinked polyethylene acetabular components resisted the effects of the third body particles and the concomitant changes in the femoral heads distinctly better than the conventional UHMWPE.

KEYWORDS: Polyethylene, Crosslinked, Wear, Third body, Simulator, Debris

Introduction

Bragdon et al. have shown a correlation of the type and magnitude of wear of ultra-high molecular weight polyethylene (UHMWPE) generated using the Boston AMTI hip simulator to that found in well functioning arthroplasties retrieved at autopsy [1]. To date, however, no relevant model exists for evaluating polyethylene wear in the presence of hard third body particles which have access to the articulation. No standard test exists. Only one report of any such test has been published. McKellop et al. reported runaway polyethylene wear after as little as 400000 cycles when titanium particles are sandwiched between the ball and cup using a PM-Med inverted, biaxial rocking motion wear tester [2]. The titanium femoral heads used in these tests showed massive erosion. The particle load, the inability of the particles to leave the articulation, the severe damage to the titanium head and the aggressive nature of the test, raise some questions about the clinical relevance of this model in studying artificial hip bearing couples of cobalt chrome and polyethylene. Other researchers have chosen to study the effects of third body wear indirectly by using scratches counterfaces [3, 4]. Though this approach addresses the

[1]Orthopaedic Biomechanics and Biomaterials Laboratory, Massachusetts General Hospital, 55 Fruit Street, GRJ 1206, Boston, MA 02114, cbragdon@partners.org.

secondary effect of third body debris, namely resulting changes in the surface roughness of the metal articular surface, it does not include the more complex interaction of particulate debris entering and leaving the articulation between a hard and plastic bearing couple.

Studies of components retrieved after clinical use during revision cases give some insight into the expected surface morphologies which might result from third body abrasive wear [2, 5-8]. A retrieval study by Jasty et al. reported on damage of retrieved CoCr femoral head, but only in the form of fine scratches and an increase in surface roughness (Ra) in localized area of the heads. The appearance of the articular surface of the majority of retrieved polyethylene acetabular surfaces showed a highly polished wear surface in the absence of third body wear. In contrast, the wear surfaces of polyethylene components subjected to relatively large amounts of third body, such as when particles of cement become trapped in the articulation or when so much metal debris was present that it discolored the surrounding tissue, had a dull appearance due to the much coarser wear features on the surface. This is a reflection that the wear mechanism of the polyethylene had changed.

Another complicating issue is the dynamic nature of third body damage in vivo with varying amounts of third bodies present in the articulation at any one time, and in the case of CoCr heads, the indication by some research groups that polishing or "healing" of this damage over time can offset damage to the femoral head [9].

The issue of establishing a third body wear model is particularly complicated because of the multiplicity of the variables involved. The matrix of possible models is high. Consider the following variables. The first is the nature of the potential third bodies which may be generated from any one of the materials used in the hip reconstruction as well as the manufacturing process. This list includes PMMA, Ti, CoCr, Si 02, Ba, Zirconia, alumina, chromium three ortho phosphate, stainless steel and others. Next are issues within each of these materials in terms of particle size and particle concentration. Should the particles be put in the serum or into the articulation or both? Should the serum be circulated? Should the articulation be upright as in the body or upside down? If upside down, are the particles trapped? Will the particles be imbedded in the polyethylene? How severe should the scratching of the femoral head be? Will the progressive damage to the head complicate interpretation of the third body wear?

The purpose of this study was to evaluate a wide variety of potential third body wear models in a hip simulator and then, after selecting the preferred conditions, to study highly crosslinked (WIAM) material in contrast with conventional UHMWPE.

Materials and Methods

We elected to study third body wear in a hip simulator in the upright position with the acetabular component above the femoral component since this position more closely represents the in vivo human condition.

Using 32mm internal diameter by 62mm outer diameter conventional polyethylene acetabular components articulating against implant quality chrome cobalt head in the Boston hip simulator, two series of wear tests were performed. Conventional polyethylene acetabular components are defined as having been sterilized using 2.5megarads of gamma radiation in an ambient air environment. In the first series, different amounts of several types of third body debris were added to the usual 400cc of

circulating 100% bovine serum which was used as a lubricant. The goal of this first series of tests was to identify which type of third body particle would be most appropriate to use in an in vitro model, and to see how well the particles stayed in suspension over time. Tests included:

A) 0.5 gm of 1-2μ chromium particles;

B) 0.5 or 1.0 gm of PMMA power without barium sulfate added in the serum;

C) PMMA powder without barium sulfate initially sandwiched between the head and cup;

D) Barium sulfate particles 1μ in size added to the serum in four different amounts 0.135, 0.25, 0.5, 1.0 gm;

E) 0.5 gm of 1μ barium sulfate initially sandwiched between the head and cup; and

F) Aluminum oxide particles 1μ in size in amounts of 0.063, 0.135, 0.25, 0.50 gm placed in the serum or 0.5 gm sandwiched initially between the head and cup.

In order to sandwich the particles between the head and cup, the cup was held upside down, particles were placed into the cup, and then the femoral head was held firmly in place while the chamber was assembled with the joint in the upright position and filled with serum. In this way the particles remained in the articulation until after the machine was started. Thereafter, they were free to enter and leave the articulation.

In this first series of experiments, it was noticed that the third body particles tended to settle and collect at the bottom of the reservoir over time despite the circulation of the serum. As a temporary solution to this problem in the first series of experiments, the serum was stirred manually three times each day in order to maintain the particles partially in circulation.

Before the second series of experiments was conducted, a modification in the way the bovine serum was recirculated through the test chambers was made to eliminate the settling of the debris in the serum reservoir. To accomplish this, the cylindrical reservoir was replaced with a cylindrical tube with the entry port on top and the return port on the bottom. This eliminated the settling zone present in the original configuration and when coupled with the agitation present in the test chamber due to the motion of the components, the circulating particles were maintained in suspension. This change also reduced the amount of serum used for each chamber to about 250cc. With these specific modifications to the serum recirculation, a known concentration of particles could be maintained in uniform suspension with the particles free to enter and leave the articulation.

Based on the wear results and changes in the surface morphology of the articular surface of the first series of studies, barium sulfate and aluminum oxide particles were selected for further detailed study. With the modifications to eliminate settling of the particles complete, a longer-term study was performed of 0.5gm, (2.5mg/cc), of barium sulfate particles in the serum and five different concentrations (0.15, 0.30, 0.42, .83 or 1.67 mg/cc), of alumina particles in the serum.

In all studies, weight loss was measured to determine the wear rate of the polyethylene. Were rates were measured every 0.5 million cycles. Wear rates were reported two ways. The average total wear rate reflects the total weight change divided by the total number of cycles and was reported as wear per million cycles. The incremental wear rate was determined for each individual 0.5 million cycles and reported for that specific test interval as wear per million cycles. This is done to show more clearly the change in wear rate over time, which may occur during such testing. Also the

surface morphological features of the wear area were studied using optical and scanning electron microscopy.   During the second series of wear tests, the highly crosslinked WIAM UHMWPE was studied in parallel to the conventional UHMWPE. New polyethylene components and femoral heads were used for each phase of testing described above.

Results

The first series of experiments showed that the wear rates and surface morphologies of the conventional UHMWPE were not significantly affected by the addition of the chromium or PMMA particles in the concentrations used, with the wear rates measured being similar to the control cups without added particles.   Neither the PMMA particles without barium nor the chromium particles caused much scratching of the femoral head, increased wear of the polyethylene, or changed the appearance of the wear surface, even when they were placed directly in the articulation.

The wear rate of conventional UHMWPE increased moderately with increasing amounts of barium sulfate particles in the first series of experiments, resulting in a 54% increase in polyethylene wear rate after one million cycles when 2.5 mg/cc of barium sulfate particles were added to the serum. A localized area of fine scratches was apparent on the CoCr femoral heads along with a corresponding buffed, non-polished area on the polyethylene surface characteristic of the surface of retrieved human acetabular components that contained third bodies.   The results were similar when the barium particles were initially sandwiched between the head and cup.

The most striking increase in polyethylene wear rate occurred with the use of aluminum oxide particles, with wear rates ranging from a high of 85 mg of wear /million cycles with 0.5 gram of particles placed directly in the articulation to a low wear rate of 20 mg/million with 0.135 mg of alumina oxide were placed in the serum. The severity of the wear as judged by the darkening of the serum, damage to the head, and increase in wear rate was dependent on the concentration of the particles.   Interestingly, when the damaged femoral head from the most severe case was reused without any third bodies present, the polyethylene wear rate remained high but decreased over time, possibly as the damage to the head was smoothed out over time.   Such polishing of damaged heads by UHMWPE has been seen before [9].

Surprisingly, in the second series of studies, the initially higher wear rates which were achieved with the 2.5mg/cc concentration of barium sulfate particles decreased over time from a high of 45.6±2.44mg/million cycles during the first million cycles until it approached the wear rate of about that of the controls, 26.5±2.11 during the third million cycles (Figure 1). The femoral heads were only mildly scratched and the wear surface of the polyethylene, which had been buffed when the initial wear rate was high, became glossy.

When the highly cross-linked WIAM polyethylene was challenged with 2.5mg/cc of barium sulfate particles, no effect on wear rates could be measured. The wear rate of the highly cross-linked WIAM treated polyethylene components remained at undetectable levels out to three million cycles (Figure 1).
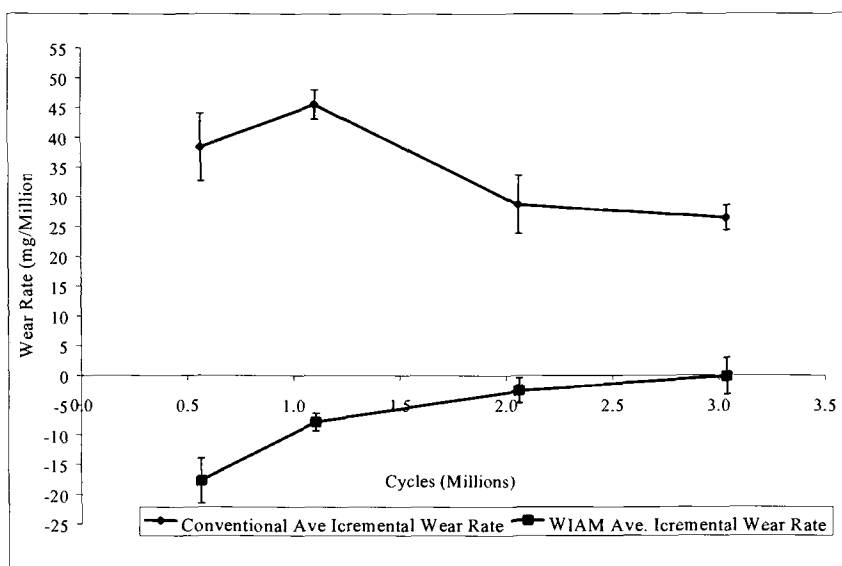
Figure 1 Average Incremental Wear Rate of Conventional and WIAM Components with 2.5mg/cc Barium Sulfate Particles added to the Serum

Attention was turned to the more aggressive third body test, that which used 1.0 micrometer alumina particles. The conventional cups studied with different concentrations of alumina particles added to the serum all had higher wear rates than the control components without particles added to the serum. Concentrations of aluminum oxide particles of 0.42, 0.85 and 1.67 mg/cc led, in some instances, to wear rates as high as 280 mg/million cycles and severe eccentric wear of the CoCr femoral head. This severe wear resulted in metal debris being accumulated on the femoral head. Since this result is clearly outside the bound of any known clinical experience, concentrations in excess of 0.30mg/cc were deemed unrealistic. The next study was performed to determine which concentration, 0.30 or 0.15mg/cc, would give more representative results using conventional UHMWPE. This comparison was also made against the highly cross-linked WIAM polyethylene components.

The incremental wear rate of the conventional and WIAM treated acetabular components for each concentration of Alumina particles is shown in Figure 2. As before, the bovine serum was changed every 0.5 million cycles in order to minimize the buildup of metal debris on the femoral head. Charting the incremental wear rates shows more clearly how the wear rates change over time as the heads are continually damaged.

As seen in Figure 2, the incremental wear rate increases over time at each concentration for both the conventional and WIAM treated components. With the conventional UHMWPE components and 0.15mg/cc of aluminum oxide particles, the initial wear rate was only 25mg/million cycles for the first million cycles, which is similar to the control rates without any third bodies present. However, over longer time the wear rate increased to 159 mg/million cycles during the third million cycles of wear.
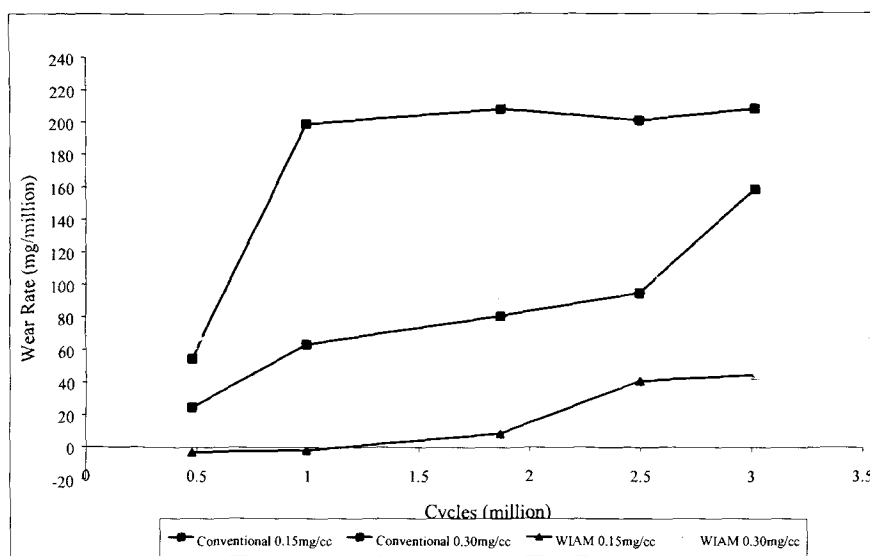
Figure 2 Third Body Average Incremental Wear Rate Using 1μ Alumina Particles added to the serum in Concentrations of 0.30 and 0.15mg/cc N=2 each

With the higher concentration of 0.3 mg/cc alumina particles, the incremental wear rate of the conventional material increased from 55 mg/million cycles for the first million cycles to 208 mg/million cycles during the third million cycles. These increases in polyethylene wear rate were associated with progressive increases in damage to the femoral head in the form of scratching and material removal.

For all corresponding tests with alumina particles, the incremental wear rate of the WIAM components were always lower than that of the conventional material subjected to the same particle load. With 0.15mg/cc of alumina particles, the incremental wear rate of the WIAM components increased from the undetectable rate of –2.78/million cycle during the first million cycles to a maximum of 45 mg/million cycles during the third million cycles. With the higher dose of 0.3mg/cc of alumina particles, the incremental wear rate of the WIAM components varied between a low of 45mg/million cycles and a high of 115. These variations were associated with variable amount of metallic deposits accumulating on the femoral head at this concentration.

The surface appearance of all the polyethylene components exposed to alumina third body particles was similar, having a dull, non-reflective appearance, similar to clinical cases with severe third body load and/or damage to the femoral head.

All femoral heads subjected to the alumina particle concentration of 0.3mg/cc had considerable metal films deposited on the surface, even when the serum was changed every 0.5 million cycles. Therefore, it appears that the use of 1.0μ alumina particles in a concentration of 0.15mg/cc using the Boston AMTI hip simulator is a significantly harsh third body wear challenge for evaluating polyethylene acetabular components.

Conclusion

In defining our recommended third body wear model, we elected to not put the hard third body particles directly into the articulation because we and McKellop et al. [2] showed that the particles became embedded into the polyethylene and this technique can produce severe disruption of the femoral heads in short time periods. Similarly, we chose to concentrate our efforts on developing a test protocol which utilized third body debris rather than using scratched metal counterfaces as described by Fisher et al [3, 4].

We concentrated our efforts on using third body particles which would be likely to readily migrate into the joint. We studied four types of particles. In this series of experiments the highest wear rates, the most damage to the CoCr femoral head, and the greatest change to the polyethylene wear morphologies, occurred with the use of aluminum oxide particles, which were chosen to represent the hard oxide layer which can be abraded from the surface of metal alloy components. Although barium sulfate particles have been implicated in third body wear in vivo, the damage created by these particles even in the relatively high concentration used here was neither as severe nor as consistent as compared to the use of alumina particles. Even in concentrations of barium sulfate that did increase the polyethylene wear rates of conventional UHMWPE, there was no increase in wear of the WIAM material. Of special interest was the decrease in wear rate over time in the experiments with barium sulfate in the serum.

While any model for "third body" wear will perforce, be arbitrary and to a degree artificial, the alumina particles in a concentration of 0.15mg/cc appeared to provide the most effective challenge to the wear resistance of UHMWPE while at the same time not creating unrealistic destruction to the femoral head.

In all of the experiments, under all conditions, the WIAM highly crosslinked polyethylene acetabular components resisted the effects of the third body particles and the concomitant changes in the femoral heads distinctly better than the conventional UHMWPE.

Bibliography:

1.   Bragdon, C.R., O'Connor, D.O., Lowenstein, J.D., Jasty, M., Harris, W.H.,. *Comparison of Polyethylene Wear and Polyethylene Wear Debris Generated on a New Hip Simulator Versus Direct Measurements of In Vivo Wear.* in *Orthopaedic Research Society.* 1997. San Francisco, California.

2.   McKellop, H.A. and T.V. Rostlund, *The wear behavior of ion-implanted Ti-6Al-4V against UHMW polyethylene.* Journal of Biomedical Materials Research, 1990. **24**(11): p. 1413-25.

3.   Endo, M., et al., *Comparison of wear, wear debris and functional biological activity of moderately crosslinked and non-crosslinked polyethylenes in hip prostheses.* Proceedings of the Institution of Mechanical Engineers. Part H - Journal of Engineering in Medicine, 2002. **216**(2): p. 111-22.

4.   Fisher, J., et al., *The influence of scratches to metallic counterfaces on the wear of ultra-high molecular weight polyethylene.* Proceedings of the Institution of Mechanical Engineers. Part H - Journal of Engineering in Medicine, 1995. **209**(4): p. 263-4.

5.   Buly, R.L., et al., *Titanium wear debris in failed cemented total hip arthroplasty. An analysis of 71 cases.* Journal of Arthroplasty, 1992. **7**(3): p. 315-23.

6.   Jasty, M., et al., *Surface damage to cobalt-chrome femoral head prostheses.* J Bone Joint Surg Br, 1994. **76**: p. 73-77.

7.   Jasty, M., et al., *Wear of polyethylene in total joint replacement.* Seminars in Arthroplasty, 1994. **5**(1): p. 41-44.

8.   Isaac, G.H., et al., *The Role of Acrylic Cement in Determining the Penetration Rate of the Femoral Heads in the Polyethylene Sockets of Charnley Hip Prostheses.* 1991.

9.   McKellop, H., et al., *Wear of gamma-crosslinked polyethylene acetabular cups against roughened femoral balls.* Clin. Orthop. and Related Res., 1999. **369**: p. 73-82.

Bridgette D. Furman,[1] *Suzanne A. Maher,*[1] *Timothy G. Morgan,*[2] *and Timothy M. Wright*[1]

Elevated Crosslinking Alone Does Not Explain Polyethylene Wear Resistance

---

ABSTRACT: New ultra high molecular weight polyethylene (UHMWPE) materials have been introduced that utilize elevated radiation doses combined with post-irradiation heat treatments. The elevated radiation dose creates higher levels of crosslinking and is reported to cause improved abrasive wear resistance. The heat treatment quenches free radicals that result from irradiation, thus preventing oxidative degradation. Although abrasive wear occurs between conforming bearing surfaces, macroscopic wear damage is more commonly cited than abrasive wear as a limiting factor with non-conforming surfaces such as occur in knee replacements. Though these new materials demonstrate reduced mechanical properties compared to conventional UHMWPE gamma irradiated in air, recent studies revealed that some of these materials performed well under non-conforming *in vitro* wear conditions. Our aim was to understand why materials with reduced fracture toughness and yield strength would be more resistant to wear damage.

Polyethylene materials with varying radiation doses and heat treatments were examined. We compared modulus, yield strength, ultimate stress, and ductility, J-integral fracture toughness, density and wear. Crystalline morphology was evaluated using transmission electron microscopy. A relation was found between modulus, morphology and wear behavior. Materials with modulus equal to or less than *850 MPa* and the majority of lamellae measuring less than 200 nm demonstrated no pitting, delamination or cracking in wear tests, regardless of the level of crosslinking. Even though elevated crosslinked materials showed reduced toughness, they demonstrated good damage resistance, but elevated crosslinking alone does not explain wear damage resistance.

KEYWORDS: polyethylene, wear, morphology, mechanical properties

---

[1] Research Engineer, Assistant Scientist, and Laboratory Director, respectively, Laboratory for Biomedical Mechanics and Materials, Hospital for Special Surgery, 535 East 70th Street, New York, NY 10021.

[2] Graduate Research Assistant, Sibley School of Mechanical and Aerospace Engineering, Cornell University, 130 Upson Hall, Ithaca, NY, 14853.

Introduction

Recently, new polyethylene materials have been introduced that demonstrate reduced *in vitro* wear rates in acetabular components for total hip replacement (THR) compared to rates measured for components made from conventional UHMWPE gamma irradiated in at historical range of 25 to 40 kGy[1-3]. These new materials are created by exposing conventional UHMWPE to elevated levels of irradiation that in turn create elevated levels of crosslinking . Irradiation has long been used to sterilize orthopaedic devices. Gamma irradiation of UHMWPE results in both crosslinking and the formation of free radicals associated with subsequent oxidative degradation. In an attempt to prevent or limit oxidative degradation, manufacturers first began sterilizing devices made from conventional polyethylene in oxygen free or reduced oxygen environments [4]. This process also moderately increased the amount of crosslinking in the material, resulting in moderately reduced *in vitro* wear rates [5]. The new elevated crosslinked polyethylenes use irradiation doses of either gamma or electron beam irradiation typically between 50 and 100 kGy, markedly greater than the historical range of 25 to 40 kGy. Oxidation of the polyethylene is a much greater risk at these higher irradiation doses. Therefore, post-irradiation heat treatments were introduced in an effort to quench the free radicals that are created as a result of the irradiation and that directly lead to oxidation. These treatments involve heating the material above the melting point following the irradiation process [2-3,6].

Though the elevated crosslinked materials demonstrate reduced *in vitro* hip simulation wear rates over conventional polyethylene, they also demonstrate reduced mechanical properties and fracture toughness [7,8]. This reduction in properties may not be as important a factor with abrasive wear, which dominates between conforming bearing surfaces. However, in wear between non-conforming surfaces, such as occurs in knee replacements, macroscopic wear damage in the form of pitting and delamination is more commonly cited than abrasive wear as a limiting factor. Pitting and delamination are directly related to fracture and fatigue processes that in turn depend on the mechanical properties such as toughness, ductility, and strength. A clear hypothesis that emerges from this argument is that elevated crosslinked materials would be less resistant than conventional polyethylene to this type of damage. Nonetheless, recent studies in our laboratory revealed that some of these materials performed well under non-conforming (total knee-type) wear conditions [9]. Our current aim was to understand why materials with reduced fracture toughness and yield strength would be more resistant to damage. We retrospectively reviewed wear, tensile and fracture results from three tests in an attempt to understand the relationship between mechanical and physical properties and wear behavior.

Materials

We compiled all of our results from tests conducted on a custom test apparatus [9-12]. In total, six materials were examined in this study, three made from GUR 4150 resin and three from GUR 1050 resin (Hoechst, Houston, TX). Two control materials, one from each resin, were machined from unirradiated stock and then gamma irradiated in air to 25 kGy.

In addition to the GUR 4150 control (Reference polyethylene [13]), two additional GUR 4150 materials were evaluated, a high elastic modulus material (modulus greater

than 2 GPa [14]) and a low modulus material (less than 0.8 GPa [15]). The high modulus material was fabricated by subjecting ram extruded 76 mm diameter rods (PolyHi Solidur, Ft. Wayne, IN) to high temperature and pressure [14]. The low modulus material was compression molded [15]. All GUR 4150 materials were gamma irradiated to 25 kGy. Specimens were then accelerated aged in air at 74°C, 100% humidity, for 14 days.

The final two materials were made from GUR 1050 resin that had been treated to obtain elevated levels of crosslinking. Blocks (7.6 x 5.1 x 3.8 cm) were machined from stock GUR 1050 material, pre-heated, and then electron beam irradiated at doses of 65 and 120 kGy. After irradiation, the blocks were heated in a forced air oven to a temperature above the melt point of UHMWPE and held to assure that all crystalline was relaxed. Cooling was accomplished over many hours at a very gradual rate in order to control the final material crystallinity. Specimens were then machined from the blocks, sterilized using a gas plasma technique, and accelerated aged in water at 80°C, at 1 atm O_2, for 14 days.

Specimens for tensile, J-integral, and wear tests were machined for each material. Tensile test samples (n = 5 per group) were Type V as defined by Standard Test Method for Tensile Properties of Plastics (ASTM D638). Three-point bend specimens (n = 10 per group) for J-integral testing had W = 16 mm, B = 10 mm, and a = 8 mm, following Standard Test Method for Measurement of Fracture Toughness (ASTM E1820). Wear samples (n = 4 per group) were 8 mm thick, 43 mm long, and 42 mm wide with a flat articular surface on top and dovetails machined into the bottom to hold the specimen in the apparatus [16]. All samples were artificially aged to simulate the effects of oxidative degradation of approximately five years of shelf aging [17-18].

Methods

Wear tests were conducted on a 12-station, pneumatically controlled wear apparatus as previously described [16]. Each station consisted of an air cylinder, cobalt alloy indenter, control rods, and a polyethylene specimen mounted in a 3 mm thick metal backing that rested on rollers allowing freedom of movement in the medial-lateral direction. The air cylinder created a vertical force pushing the indenter into the polyethylene, while the control rods were connected to a common rotating shaft that created oscillating linear sliding motion. The indenters were 23 mm wide, with an anteroposterior radius of 40 mm and a medial/lateral radius of 19 mm; indenters were polished to an implant grade mirror-like finish. Specimens were bathed throughout the test in 100% bovine serum, non-iron-supplemented, 100 nm filtered (Hyclone, Logan, UT) at room temperature (23°C ± 2°C).

At the beginning of each wear cycle, the indenter was loaded with a 2100 N vertical load and slid anteriorly 20 mm. At the end of anterior travel, the indenter was unloaded to 50 N and slid posteriorly 20 mm. Wear tests were run to 2 million cycles at 0.5 Hz, 24 hours a day. Tests were stopped once a week, approximately 250 000 cycles, to examine the wear surfaces macroscopically and under a light stereomicroscope (Wild, Heerbrugg, Switzerland) for surface damage.

Material wear performance was assessed on the basis of the onset of damage (in 250 000 cycle steps), specifically pitting and cracking. At the completion of 2 million cycles, a 5 mm diameter core was taken through each sample at a common location away from the wear area. The cores were transversely microtomed into slices approximately 200

microns thick, and the density of each slice was measured using a Standard Test Method for Density of Plastics by the Density-Gradient Technique (ASTM D1505), thereby producing a density profile from the articulating surface into the depth of the specimen. From the density profile, the maximum density value of the material and its location were determined.

Uniaxial tensile tests were performed according to ASTM D638. Specimens were first instrumented with an extensometer (Model 632.26C-20, MTS, Eden Prairie, MN) and tested under strain control at a rate of 2.6%/sec to a strain of 1.5%. J-integral tests were performed following the guidelines of ASTM E1820. Briefly, a sharp crack was created at the base of the notch in the center of the three-point bend specimen using a razor, and the specimen was loaded to a pre-defined displacement. The amount of crack propagation was measured, and the energy input was computed. A plot of energy versus crack growth for each material was produced [19].

Morphology of each of the six UHMWPE materials was determined using transmission electron microscopy (TEM). Small slivers were sliced from the test specimens with a razor blade and immersed in chlorosulfonic acid for six hours at 60°C. The slivers were then washed in two baths of sulfuric acid and two baths of water. After drying, they were embedded in epoxy, which was allowed to cure overnight. The slivers were ultra-microtomed at room temperature to a thickness of approximately 70nm. The resulting sections were collected using 300 mesh copper grids and stained with an aqueous solution of uranyl acetate. The sections were imaged in a TEM at 100 kV.

Morphology measurements were determined from prints taken at a magnification of 63 500 times. Photographs of the TEM prints were scanned and saved in TIFF format. Length measurements of the crystalline lamellae were made within a randomly selected 420x300 pixel (2.21x1.58 micron) area of interest. The lamellae were identified in the scans automatically using Matlab 6.1, by thresholding on the basis of image intensity after the background variation was normalized and then smoothed with a 3x3 pixel median filter on the original TEM image.

Lamellar length was determined by skeletonizing the lamellae and then measuring the length of the resulting midline. The skeletonization process sequentially removed pixels from the edge of the lamellae until no more pixels could be removed without disconnecting the structure. Remaining pixels represented the midline across the lamellae.

Statistical Analysis

Differences among the test results and the morphologies from the six UHMWPE materials were investigated using analysis of variance (ANOVA; [20]). In cases where ANOVA revealed that intergroup differences existed, Tukey's test was used to explore differences between groups [20]. Spearman's rank correlation, ρ, was used to examine the relationship between mechanical properties and progression of damage with wear testing. All analyses used a significance level of 0.05.

Results
Wear Test Results: 0 – 1 Million Cycles

After 250,000 cycles, all specimens showed burnished wear tracks. After 330 000 cycles, two of four 4150 control specimens showed a small amount of pitting and cracks

initiating at the surface along both the medial and lateral edges of the wear track (Table 1). At 750 000 cycles, two of four 1050 control specimens showed subsurface cracks. All other specimens demonstrated only burnished wear tracks.

Table 1. *Summary of damage initiation and progression (n = 4 per condition)*
Number of wear specimens exhibiting pitting and cracking at 250,000 through 2.2 million cycles.

Sample	250k	500k	750k	1m	1.25m	2m	2.2m+
4150 Control	None	2 pits/cracks	2 pits/cracks	4 pits/cracks	4 pits/cracks	4 pits/cracks	4 pits/cracks
1050 Control	None	None	2 cracks	1 pitting 1 cracks	2 pitting	2 pitting	2 pitting
4150 High Modulus	None	None	None	None	2 pits/cracks	2 pits/cracks	4 pits/cracks
4150 Low Modulus	None	None	None	None	None	None	None
1050 – 65 kGy	None	None	None	None	None	None	None
1050 – 120 kGy	None	None	None	None	None	None	None

Wear Test Results: 1 – 2 Million Cycles

After 1 million cycles, all four 4150 control specimens showed pitting and cracking along the medial and lateral edges of the wear track. In addition, the two specimens that initially showed pitting formed more pits, and large cracks began to form along the medial and lateral edges of the wear track (Figure 1a). In the 1050 control specimens, pitting occurred at 1 million and 1.25 million cycles in the two specimens that had previously shown subsurface cracks (Figure 1d). By 1.25 million cycles, two of the high modulus 4150 specimens also had pits and cracks at the edge of the wear track (Figure 1b). The two remaining 1050 control specimens, all eight 1050 elevated crosslinked specimens (65 kGy and 120 kGy), two remaining high modulus specimens, and all four low modulus specimens continued to show only burnishing within the wear track.

Wear Test Results: 2+ Million Cycles

After 2 million loading cycles none of the 1050 elevated crosslinked (65 kGy and 120 kGy) or 4150 low modulus specimens showed macroscopic or microscopic evidence of pitting or delamination, though the wear areas were burnished and scratched (Figures 1 c,e,f). After 2.2 million cycles, the two 4150 control specimens that had experienced cracking along the medial and lateral edges of their wear tracks began to form additional cracks in the center of the wear track. By the conclusion of the tests, all four 4150 control specimens showed pitting and cracks, two of four 1050 control specimens showed pitting and cracking, and three of four 4150 high modulus specimens demonstrated pitting. All 4150 low modulus specimens, all 1050 elevated crosslinked specimens (65 kGy and 120 kGy), two 1050 controls, and one 4150 high modulus demonstrated only burnishing and scratching of the wear track.

Figure 1. *Wear Test Specimens at 2 million cycles*

a. 4150 Control

d. 1050 Control

b. 4150 High Modulus

e. 1050 - 65 kGy

c. 4150 Low Modulus

f. 1050 - 120 kGy
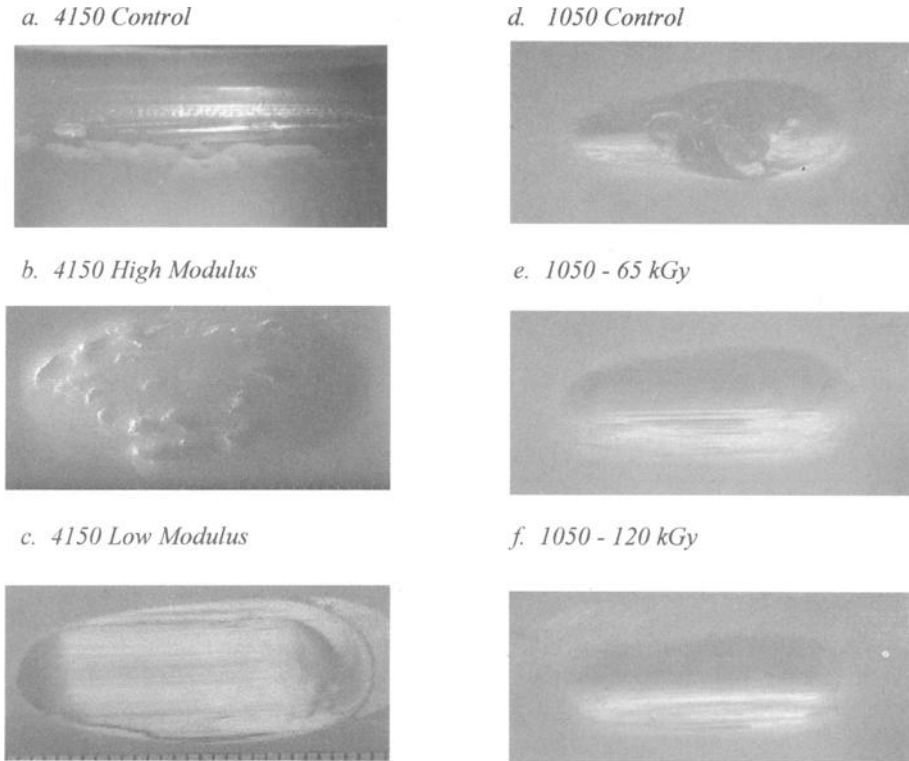
Compiled Mechanical Test Results

No difference in elastic modulus was found between the 4150 and 1050 control materials (Table 2). Significant differences were found, however, between the two control materials and the other four materials. The 4150 low modulus and the elevated crosslinked 1050 materials (65 and 120 kGy) had significantly lower moduli than the other UHMWPE materials.

The 1050 control material had a significantly higher yield strength than the 4150 control and both elevated crosslinked 1050 materials (65 and 120 kGy). No other significant differences in yield strength were found.

Differences were found in ultimate tensile strength between the two control materials, with the 4150 control being significantly stronger than the 1050 control. The 4150 control material was also significantly stronger than the 4150 low modulus material, while the 1050 control material was significantly weaker than the 1050-65 kGy elevated crosslinked material. The ultimate tensile strength of the 1050-65 kGy elevated crosslinked material was also significantly stronger than the 4150 low modulus material.

Table 2. *Mechanical Properties and Density of Materials*

Material	Modulus (GPa)	Yield Strength (MPa)	UTS (MPa)	Elongation to Break (%)	Peak Density (g/cc)
4150 Control	0.94 ± 0.08	24.0 ± 0.4	51.7 ± 3.7	376 ± 20	0.9650 ± 0.0010
1050 Control	1.15 ± 0.09	27.1 ± 2.9	40.8 ± 4.1	333 ± 23	0.9520 ± 0.0056
4150 Low Modulus	0.74 ± 0.09	24.5 ± 0.7	42.2 ± 4.0	332 ± 49	0.9448 ± 0.0020
4150 High Modulus	2.80 ± 0.13	NA	NA	NA	0.9684 ± 0.0009
1050-65 kGy	0.81 ± 0.04	23.0 ± 1.1	53.1 ± 7.1	320 ± 22	0.9293 ± 0.0005
1050-120 kGy	0.85 ± 0.06	24.1 ± 1.0	49.2 ± 8.5	207 ± 20	0.9305 ± 0.0003

NA-data was not collected for indicated property

The elongation to break of the 4150 control material was significantly greater than all other materials. The 1050-120 kGy material had a significantly lower elongation to break than any of the other materials.

The 4150 control material and 4150 low modulus material had the highest J-integral fracture toughness, followed by 1050 control material, 65 kGy irradiated 1050 and 120 kGy irradiated 1050 elevated crosslinked materials (Figure 2).

Compiled Density Results

The average maximum density values for each material are listed in Table 2. The two control materials (1050 and 4150) and the 4150 high modulus material had significantly higher peak densities than the other three materials. The location of the maximum density for the materials with higher oxidation levels was at the surface for the 4150 control and subsurface between 0.1 and 1.0 mm below the articular surface for the 1050 control and 4150 high modulus material. The other materials had relatively flat density profiles.

Wear-Material Property Relationships

Correlations of mechanical properties and progression of damage from wear tests for all materials showed a relationship between modulus and elongation to break and the development of pitting and delamination. As modulus increased and elongation to break (measured in the tensile tests) decreased, the probability for pitting and delamination to occur in the wear tests increased. Maximum density also directly related to the development of pitting and delamination; as density increased, the development of pitting and delamination was more probable.

Figure 2. *J-Integral Fracture Data of Materials*
(Note: 4150-high modulus data not available)
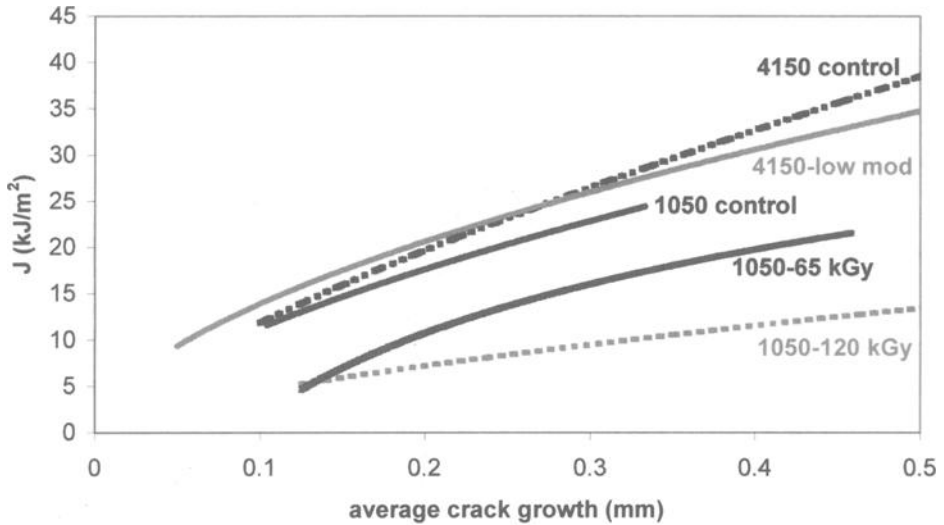
Morphology Results

The two control materials showed similar crystalline morphologies and lamellar length size distributions (Figures 3 and 4, respectively). A difference in length distribution was noted between the three GUR 4150 materials (Figure 4a). The greatest percentage of lamellar lengths for the 4150 control material was found between 125 and 150 nm, while the low modulus 4150 material had the greatest percentage between 150 and 200 nm. The high modulus 4150 material had a smaller but still marked percentage of lamellar lengths between 125 and 200 nm, but also had a large percentage of lamellae that were more than 500 nm in length. The GUR 1050 materials showed similar lamellar length distributions (Figure 4b) to each other. Lamellar size distributions for the three materials that showed no pitting, cracking or delamination at the end of the wear tests (4150 low modulus, 1050-65kGy, 1050-120kGy) were also similar (Figure 4c).

Figure 3. *TEM images for all materials (magnification 63,500x)*

a. *4150 Control*   b. *4150 High Modulus*   c. *4150 Low Modulus*

d. *1050 Control*   e. *1050 - 65 kGy*   f. *1050 - 120 kGy*
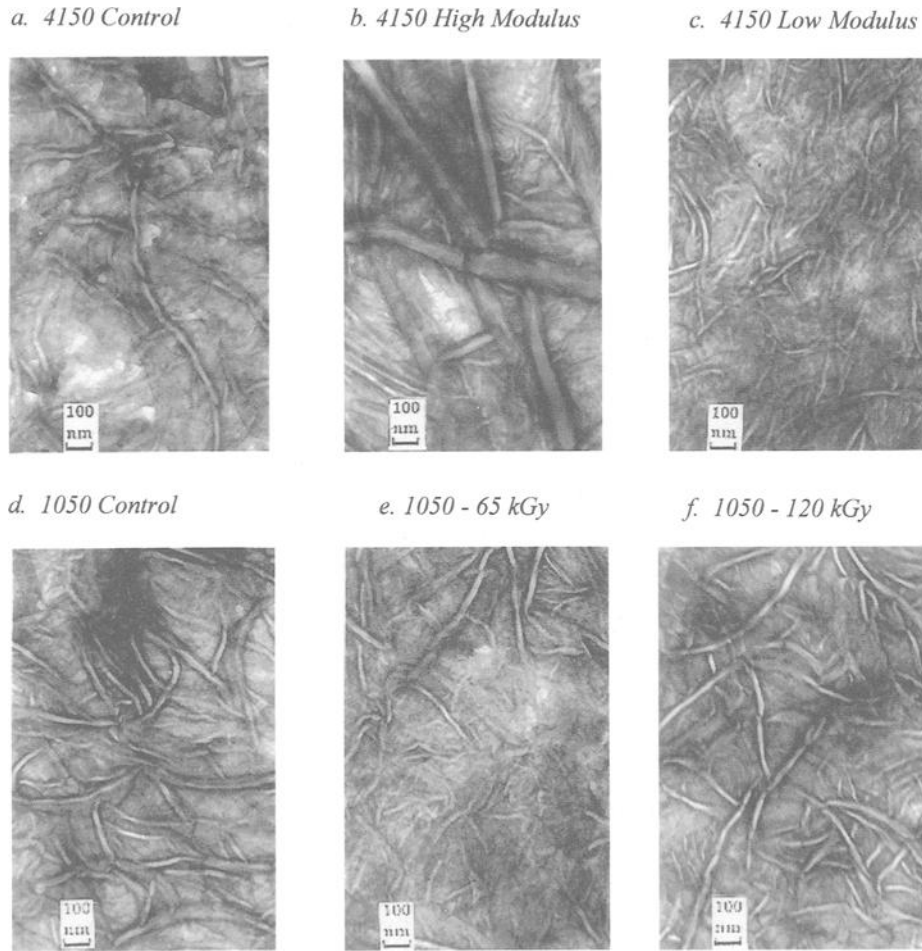
Figure 4. *Histograms of Lamellar Size Distribution*
a.   GUR 4150 materials
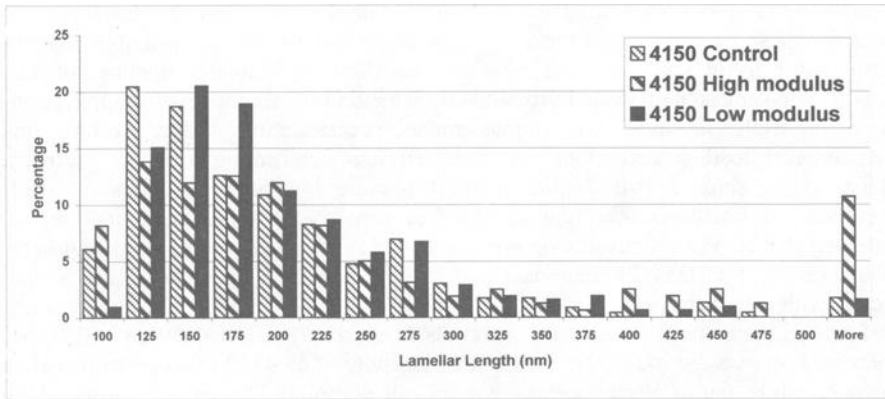
b.   GUR 1050 materials
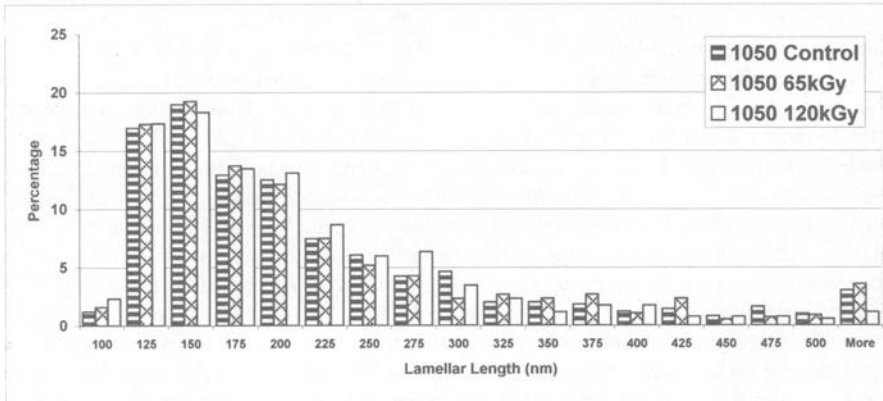
c.   Materials with no pitting, cracking or delamination at 2 million cycles
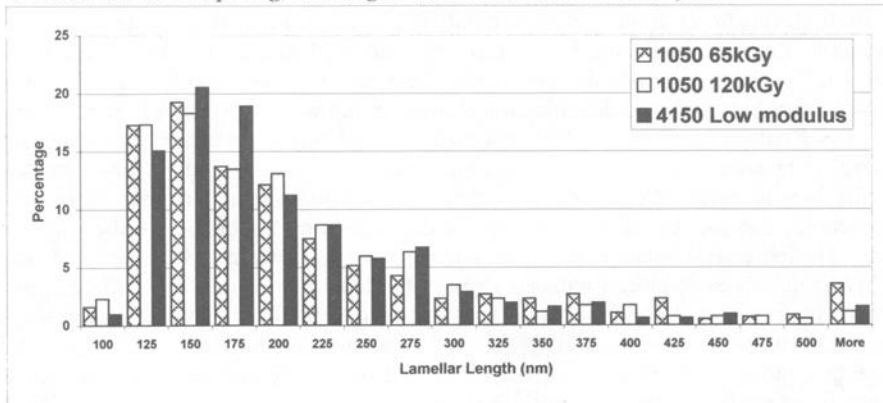
Discussion

Elevated crosslinked materials have shown superior wear resistance over conventional UHMWPE in laboratory testing using hip joint simulators. Clinical measurements of wear for these new materials remains too short as yet to determine if this advantage carries over to *in vivo* use. The reported reduction in J-integral fracture toughness demonstrated for some elevated crosslinked materials raises concerns for application of these materials in total knee replacements, necessitating further testing under physiological loading conditions and between less conforming articular geometries. Maher et al. showed that despite reduced fracture toughness compared to control materials, no fracture related damage modes, such as pitting or delamination, were observed [9,12]. We sought to examine mechanical properties, morphology and density of six different UHMWPE materials and to correlate these mechanical and material factors with wear behavior.

The two resins used to form the materials in our study, GUR 4150 and GUR 1050, both have an average molecular weight of 5 million. The 4150 resin contains calcium stearate, while the 1050 resin does not. Both control materials demonstrated high subsurface oxidation levels following artificial aging (as demonstrated by the high subsurface peak density values (Table 2) and pitting and delamination during wear testing (Table 1). The high modulus 4150 material also demonstrated subsurface oxidation and pitting and delamination wear damage. This result is consistent with clinical results. Ahn reported for three cases, large areas of pitting and delamination of enhanced polyethylene spacers from retrieved total knee replacements [21]. The compression molded low modulus 4150 material, on the other hand, did not show elevated oxidation levels and did not experience pitting or delamination wear damage. This latter finding is consistent with clinical results for directly molded polyethylene inserts. Ritter reported on a series of more than 540 total hip replacements at more than 22 years of follow-up and more than 4 500 total knee replacements all at more than five years of follow-up. All of the acetabular and tibial components were manufactured by direct compression molding. Wear and osteolysis related failures were minimal, with osteolysis noted in only two acetabula and no tibia [22]. Won et al., also showed in retrieved Miller Galante knees that direct compression molded 1900 resin was more resistant to oxidative degradation than ram extruded 4150 resin [23].

Both elevated crosslinked 1050 materials (65 and 120 kGy) were subjected to melt-annealing aimed at quenching free radicals that can lead to oxidative degradation. Not surprisingly, these materials did not demonstrate elevated oxidation levels. They were also resistant to pitting and delamination damage in the wear tests. Maher et al. reported that the 1050 elevated crosslinked materials showed larger wear areas than the 1050 control wear specimens, consistent with these materials demonstrating a lower modulus in the tensile tests. Wear area was determined using image analysis software to characterize damage into areas of pitting and delamination as a function of the total worn area. The increased contact area for the same applied load meant that the elevated cross-linked materials experienced reduced stresses (as load was carried over a larger area). Others have reported that melt-annealing alone can affect modulus, yield strength, elongation to break, viscoelasticity and fracture toughness, but the effects of the melt-annealing process versus those of the elevated crosslinking on wear resistance of the material can not be determined from this study.

The three materials that showed the greatest fracture damage resistance on *in vitro* wear tests had similar lamellar size distribution and tensile elastic modulus. The low modulus in the 4150 material was achieved by controlling pressure, temperature, and cooling rate during the molding process. This process produced a material with more crystalline lamellae with shorter lengths than extruded rods of the same resin. Based on our results, the melt-annealed elevated crosslinked materials showed lamellar size distributions similar to the 1050 control material that was not melt-annealed. However, the elevated crosslinked materials had significantly lower elastic moduli than the standard crosslinked 1050 control. This difference in modulus can only be attributed to either the elevated irradiation dose or the melt-annealing process. We are currently undergoing further controlled studies to determine which of the two processes provides the reduced elastic moduli for the elevated crosslinked materials.

In summary, for the six UHMWPE materials examined in our study, the low modulus 4150 directly molded material and the melt-annealed elevated crosslinked 1050 materials were the most resistant to pitting and delamination. This resistance was significantly correlated with lower modulus. Surprisingly, J-integral fracture toughness did not directly correlate with wear damage under knee-like loading conditions. The role of crystalline lamellar size distribution on mechanical and wear performance of polyethylene remains poorly understood. The problem, and a limitation of our study as well, is that the current methodology for examining lamellae relies on thin slices of material in which the lamellae are viewed as two-dimensional, thereby giving only a limited view of the structure. To further investigate the connection between morphology and performance, we plan on measuring lamellar width at higher magnifications and also attempting to reconstruct three-dimensional representations of the lamellae using S-TEM.

References

[1] McKellop H, Shen F-w, DiMaio W, Lancaster JG, "Wear of gamma-elevated cross-linked polyethylene acetabular cups against roughened femoral balls", *Clinical Orthopaedics and Related Research*, 369: 73-82, Dec 1999.

[2] McKellop H, Shen FW, Lu B, Campbell P, Salovey R, "Development of an extremely wear-resistant ultra high molecular weight polyethylene for total hip replacements", *Journal of Orthopaedic Research*, 17(2), 157-67, 1999b.

[3] Muratoglu OK, Bragdon CR, O'Connor DO, Jasty M. Harris WH, "A novel method of cross-linking ultra-high-molecular-weight polyethylene to improve wear, reduce oxidation, and retain mechanical properties", *Journal of Arthroplasty*, 16(2):149-60, Feb 2001.

[4] Bargmann LS, Bargmann BC, Collier JP, Currier BH, Mayor MB, "Current sterilization and packaging methods for polyethylene", *Clinical Orthopaedics & Related Research*. (369):49-58, Dec 1999.

[5] McKellop HA, Shen FW, Campbell P, Ota T, "Effect of molecular weight, calcium stearate, and sterilization methods on the wear of ultra high molecular weight polyethylene acetabular cups in a hip joint simulator", *Journal of Orthopaedic Research*, 17(3):329-39, May 1999.

[6] Sun DC, Stark CF, "Non-oxidizing polymeric medical implant". U.S. Patent 5,414,049, 9 May 1995.

[7] Duus LC, Walsh HA, Gillis AM, et al., "A comparison of the fracture toughness of cross linked UHMWPE made from different resins, manufacturing methods and sterilization conditions", *Transactions of 26th Society for Biomaterials*, 384, 2000.

[8] Pascaud RS, Evans WT, McCullage PJ, Fitzpatrick DP, "Influence of gamma-irradiation sterilization and temperature on the fracture toughness of ultra-high-molecular-weight polyethylene", *Biomaterials*, 18(10):727-35, 1997.

[9] Maher, S.A., Furman, B.D., and Wright, T.M., "The Reduced Fracture Toughness that Accompanies Elevated Cross-Linking of Polyethylene is not associated with an Increase in Pitting and Delamination Type Wear", *Crosslinked and Thermally Treated Ultra-High Molecular Weight Polyethylene for Joint Replacements ASTM STP 1445*, S.M. Kurtz, R. Gsell, and J. Martell, Eds., ASTM International, West Conshohocken, PA, 2003.

[10] Baldini T, Wright T, Bartel D, Estupinan J, "Wear Damage is affected by conformity in knee joint geometries", *Transactions of 25th Society for Biomaterials*, 131,1999.

[11] Baldini T, Wright T, Bartel D, Estupinan J, Duus L, Li S, "Wear Damage is affected by modulus in knee joint geometries", *Transactions of 46th ORS*, 0453, 2000.

[12] Maher SA, Furman BD, Wright TM, "Reduced Fracture Toughness of Enhanced Cross-Linked Polyethylene is Not Associated with Increased Wear Damage", *Transactions of 28th Society for Biomaterials*, 542, 2002.

[13] Bennett AP, Wright TM, Li S, "Global reference UHMWPE: characterization and comparison to commercial UHMWPE", *Transactions of 42nd ORS*, 472, 1996.

[14] Li S, Howard EG, "Process of Manufacturing Ultrahigh Molecular Weight Linear Polyethylene Shaped Articles". U.S. Patent 5,037,928, 6 Aug 1991.

[15] Burstein AH, Li S, "Process for producing ultra-high molecular weight low modulus polyethylene shaped articles via controlled pressure and temperature and compositions and articles produced there from". U.S. Patent 5,721,334, 24 Feb 1998.

[16] Baldini TH, Wright TM, Estupinan JA, Bartel DL, "An Apparatus for studying wear damage in UHMWPE: description and initial test results", ASME, 1998.

[17] Furman BD, Lelas J, McNulty D, Smith T, Li S, "Kinetics, Chemistry, and Calibration of UHMWPE Accelerated Aging Methods", *Transactions of the 44th ORS* 23:102, 1998.

[18] Walsh HA, Furman BD, Li S, "A protocol to mimic 5 year shelf aging of UHMWPE", *Transactions of the 6th World Biomaterials*, 421, 2000.

[19] Rimnac CM, Wright TM, Klein RW, "J integral measurements of ultra high molecular weight polyethylene", *Polymer engineering and Science*, 28 (24), 1586 – 1589, 1988.

[20] Zar JH, <u>Biostastical Analysis</u>, Fourth Edition, ISBN 0-13-081542-X, Published by Prentice-Hall, Inc. New Jersey, 1999.

[21] Ahn NU, Nallamshetty L, Ahn UM, Buchowski JM, Rose PS, Lemma MA, Wenz JF, "Early failure associated with the use of Hylamer-M spacers in three primary AMK total knee arthroplasties", *Journal of Arthroplasty*, 16(1):136-9, Jan 2001.

[22] Ritter MA., "Direct compression molded polyethylene for total hip and knee replacements", *Clinical Orthopaedics and Related Research.*, 393, 94-100, 2001.

[23] Won CH, Rohatgi S, Kraay MJ, Goldberg VM, Rimnac CM, "Effect of resin type and manufacturing method on wear of polyethylene tibial components", *Clinical Orthopaedics and Related Research*, 376, 161-171, 2000.

AUTHOR INDEX